Modulation of the Hippo signalling pathway by a novel miRNA to enhance cardiac regenerative capacity

A thesis submitted to the University of Manchester for the degree of Doctor of Philosophy in the Faculty of Biology, Medicine and Health

2020

Ardiansah Bayu Nugroho

School of Medical Sciences
Division of Cardiovascular Sciences

Contents

Word count: 50,179

List of Figures

List of Tables

Abbreviations

3'UTR	3' untranslated region
5-HT	5-hydroxytriptamine
5-HTT	5-hydroxytriptamine transporter
AAV	Adeno-associated virus
ACE	Angiotensin converting enzyme
ADS	Artificial digestion solution
AGO	Argonaute
AJ	Adherens junction
AMOT	Angiomotin
AMOTL1	Angiomotin-like protein 1
AMPK	5' adenosine monophosphate-activated protein kinase
ANKRD1	Ankyrin repeat domain 1
ARB	Angiotensin receptor blocker
BMP	Bone morphogenetic protein
BrdU	5-bromo-2'-deoxyuridine
BSA	Bovine serum albumin
BSF	Biological services facility
cAMP	Cyclic adenosine monophosphate
CCNA2	Cyclin A2
CCNB1	Cyclin B1
CCNE1	Cyclin E1
CDK	Cyclin-dependent kinase
CDX2	Caudal type homeobox 2
ChIP	Chromatin immunoprecipitation
CK1δ/ε	Casein kinase 1 isoform δ or ε
cKO	Cardiomyocyte-specific knockout
Crb	Crumbs
CRT	Cardia resynchronisation therapy
CT	Cycle threshold
cTG	Cardiomyocyte-specific transgenic
CTGF	Connective tissue growth factor
cTnI	Cardiac troponin I
CVD	Cardiovascular disease
CYR61	Cysteine-rich angiogenic inducer 61
d/sLVD	Left vetricular diameter at diastole or systole
DAB2	Disabled homolog 2
DAPI	4',6-diamidino-2-phenylindole
DGCR8	DiGeorge syndrome critical region 8
dIVS	Interventricular septum diastolic thickness
DMEM	Dulbecco's modified Eagle media
DNA	Deoxyribonucleic acid

DPBS	Dulbecco's phosphate buffered saline
dPW	Posterior wall diastolic thickness
E2F	E2 factor
ECL	Enhance chemiluminescence
ECM	Extracellular matrix
EdU	5-ethynil-2'-deoxyuridine
EDV	End diastolic volume
ELISA	Enzyme-linked immunosorbent assay
ERBB	Epidermal growth factor receptor family
ERK	Extracellular signal-regulated kinases
ESC	Embryonic stem cell
ESV	End systolic volume
FBS	Fetal bovine serum
FFPE	Formalin fixed paraffin embedded
FOXO1	Forkhead box protein O1
FSTL1	Follistatin-like 1
GAPDH	Glyceraldehide-3-phosphate dehydrogenase
GPCR	G protein-coupled receptor
GPER	G protein-coupled estrogen receptor
GRB2	Growth factor receptor bound protein 2
HECT	Homologous to the E6-AP carboxyl terminus
HF	Heart failure
HGF	Hepatocyte growth factor
HIF-1α	Hypoxia inducible factor 1α
HOMER1	HOMER scaffold protein 1
Hpo	Hippo
HW	Heart weight
I/R	Ischemia reperfusion
ICD	Implantable cardioverter defibrillator
ICM	Inner-cell mass
IdU	Iododeoxyuridine
IGF	Insulin-like growth factor
IL8	Interleukin 8
IMS	Industrial methylated spirit
iPSC	Induced pluripotent stem cell
ITCH	Itchy E3 ubiquitin protein ligase
Kbr	Kibra
KPNA2	Karyopherin alpha 2
LAD	Left anterior descendens coronary artery
LATS	Large tumour suppressor kinase
LPA	Lysophosphatidic acid
LW	Lung weight
MAPK	Mitogen activate protein kinase
MAPKKK	Mitogen activated protein kinase kinase kinase

Mats	MOB kinase activator-like 1
MCS	Multiple cloning sites
MI	Myocardial infarction
miRNA	Micro ribonucleic acid
MLLT11	MLLT11 transcription factor 7 cofactor
	Myeloid/lymphoid or mixed-lineage leukemia translocated to 11
MMP3	Matrix metalloproteinase 3
MnSOD	Manganese superoxide dismutase
mRNA	Messenger ribonucleic acid
MST	Mammalian STE20-like protein kinase 1
MTSS1	Metastasis suppressor protein 1
MYH7	Myosin heavy chain
NEDD4	Neural precursor cell expressed developmentally down-regulated 4
NF2	Neurofibromatosis 2
NFAT	Nuclear factor of activated T-cells
NPPA	Natriuretic peptide A
NPPB	Natriuretic peptide B
NRCM	Neonatal rat cardiomyocyte
NRG	Neuregulin
OCT4	Octamer-binding transcription factor 4
PAX3	Paired box gene 3
PBS	Phosphate buffered saline
PCI	Percutaneous coronary intervention
PCR	Polymerase chain reaction
PEI	Polyethylenimine
PFA	Paraformaldehyde
pHH3	Phosphorylated histone H3
PI3K	Phosphoinositide-3-kinase
PIK3CB	Phosphatidylinositol-4,5-bisphosphate 3-kinase catalytic subunit beta
PIK3R3	Phosphoinositide-3-kinase regulatory subunit 3
POU4F1	POU Class 4 Homeobox 1
PTEN	Phosphatase and tensin homolog
qPCR	Quantitative polymerase chain reaction
RAA	Renin angiotensin aldosteron
RASSF1A	Ras association domain family 1 isoform A
RIPA	Radioimmunoprecipitation assay
RISC	RNA-induced silencing complex
RNA	Ribonucleic acid
ROCK	Rho-associated protein kinase
ROS	Reactive oxygen species
RUNX1	Runt-related transcription factor

RWT	Relative wall thickness
S1P	Sphingosine-1-phosphate
SAV	Salvador family WW domain containing protein 1
SEM	Standard error of means
SERT	Serotonin transporter
SETD6	SET domain containing 6
siRNA	Small interfering RNA
SIRT1	Sirtuin 1
SLC6A4	Solute carrier family 6 member 4
SMAD	sMothers against decapentaplegic homolog
SOCS1	Suppressor of cytokine signalling 1
SPRY4	Sprouty RTK signalling antagonist 4
STAT3	Signal transducer and activator of transcription 3
TAC	Transverse aortic constriction
TBST	Tris buffered saline with Tween 20
TBX	T-box transcription factor
TE	Trophoectoderm
TEAD	TEA domain transcription factor
TGFβ1	Tranforming growth factor β1
TJ	Tight junction
TL	Tibia length
TMB	Tetramethylbenzidine
TXNIP	Thioredoxin interacting protein
UAS	Upstream activating sequence
UV	Ultraviolet
Vgll	Vestigial like family
Wnt	Wingless & integration-1
Wts	Warts
ZEB2	Zinc Finger E-Box Binding Homeobox
ZnT1	Zinc transporter 1
α-MHC	α myosin heavy chain

Abstract

A thesis submitted to the University of Manchester by Ardiansah Bayu Nugroho for the degree of Doctor of Philosophy entitled

"Modulation of the Hippo signalling pathway by a novel miRNA to enhance cardiac regenerative capacity"

June 2019

Recent studies have revealed that postnatal human hearts possess a marked ability for renewal, raising hope for a new therapeutic approach for cardiac repair through stimulating endogenous cardiomyocyte proliferation. Modulation of the Hippo pathway, a key regulator of cardiomyocyte proliferation and survival, has been shown to improve cardiac structure and function post-MI. However, targeting the core components of the pathway for therapeutic purpose is difficult due to the limited understanding on its upstream regulatory mechanism. MicroRNAs (miRNAs), small non-coding ribonucleic acids (RNAs), are considered potential therapeutic targets because of their ability to modulate the expression of genes, including those related to the Hippo pathway. The aim of this study is to identify novel miRNA(s) that can modulate the Hippo pathway and enhance cardiac regenerative capacity.

First, we performed literature review, bioinformatics study, and Yes-associated protein (YAP) luciferase assay to screen candidate miRNAs for their ability to enhance the activity of YAP, the main effector of the Hippo pathway, and identified miR-411 as a potential Hippo regulator. Overexpression of miR-411 can significantly induce cardiomyocyte proliferation by reducing phosphorylation of Hippo component large tumour suppressor kinase 1 (LATS1) and YAP. To test the effects of miR-411 *in vivo*, we overexpress miR-411 by injecting miR-411 mimics resuspended with non-viral vector polyethilenimine directly into the myocardium of a normal heart or following myocardial infarction (MI). Overexpression of miR-411 can induce cardiomyocyte cell cycle re-entry in the adult heart and improve cardiac structures and functions at four weeks post-MI.

To investigate miR-411 target genes in cardiomyocytes, the expression of 30 candidate target genes was examined following *in vitro* and *in vivo* overexpression of miR-411. The expression of the serotonin transporter gene (SERT) was found to be significantly downregulated and the interaction between miR-411 and the 3' untranslated region (3'UTR) of SERT messenger RNA (mRNA) was confirmed by luciferase assay, indicating that SERT is a direct target of miR-411. Interestingly, small interfering RNA (siRNA)-mediated knockdown of SERT resulted in a significant reduction in LATS1 phosphorylation and an increase in YAP activity, a phenotype similar to that of miR-411 treated neonatal rat cardiomyocytes (NRCMs). In addition, experiments using serotonin receptor antagonist supported the finding that miR-411 mediated Hippo modulation was linked with SERT-dependent signalling. However, the exact mechanism is yet to be investigated. In conclusion, miR-411 enhances cardiac regeneration and improves cardiac function post-MI by modulating the Hippo pathway. The mechanism is likely through the inhibition of SERT expression.

Declaration

I declare that no portion of the work referred to in this thesis has been submitted in support of an application for another degree or qualification of this or any other university or other institute of learning.

Ardiansah Bayu Nugroho

Division of Cardiovascular Sciences
School of Medicine
Faculty of Biology, Medicine and Health

Copyright statement

List of conference presentations and publications

CONFERENCES

- Division of Cardiovascular Sciences Showcase 2016, Faculty of Biology, Medicine, and Health, University of Manchester, UK
- Division of Cardiovascular Sciences Showcase 2017 (poster), Faculty of Biology, Medicine, and Health, University of Manchester, UK
- Doctoral Academy Graduate Society (DAGS) Conference 2017 (poster), University of Manchester, UK
- British Society of Cardiovascular Research (BSCR) Conference 2017 (participant), Manchester, UK
- BSCR Conference 2018 (poster), Manchester, UK
- Northern Cardiovascular Research Group (NCRG) Conference 2018 (poster), Newcastle, UK
- EMBO Conference on the Hippo Signalling Pathway 2018 (poster), Rome, Italy
- Manchester Regenerative Medicine Network (MaRMN) Mini Symposium 2019 (speaker), University of Manchester, UK

AWARD & PUBLICATION

Award:

- 2nd Best Poster in the Division of Cardiovascular Sciences Postgraduate Showcase 2017, University of Manchester
- The BSCR/BAS (British Society for Cardiovascular Research/ British Atherosclerosis Society) Poster Prize, BSCR Conference 2018

Publication:

- Triastuti, E, **Nugroho, AB**, Zi, M, et al. Pharmacological Inhibition of Hippo Pathway using XMU-MP-1 Protects The Heart Against Adverse Effects during Pressure Overload. *Br J Pharmacol*. 2019

Acknowledgments

I would like to take this opportunity to thank my inspirational supervisor Dr Delvac Oceandy for his consistent support throughout my PhD programme. I have learned a lot from Delvac who has helped me in not only improving my lab skills but also my personal development as a researcher.

I would also like to thank my co-supervisor Dr Elizabeth Cartwright for her support and advice throughout my PhD and her assistance especially for animal projects.

I would also like to extend my gratitude to LPDP (Indonesia Endowment Fund for Education) and the Indonesian Ministry of Finance for the PhD funding support.

My thanks also goes to the Oceandy and Cartwright Lab which has been very welcoming and extremely helpful. I am especially grateful to Dr Nicholas Stafford, Dr Min Zi, and Mr Sukhpal Prehar for their expertise and help with the animal experiments. I am grateful to have found friends in Yulia, Efta, Farrah, and Thuy.

I am incredibly lucky to have the unwavering support from my wonderful wife Lita. Thank you for being the best company during those sleepless nights. Love you always.

Finally, I give all my gratitude and massive thanks to my mom, my dad, my sister and my brother who are always be there for me. Thanks for sparing me from problems back at home so I can focus on doing my PhD. I owe you everything.

CHAPTER 1

Introduction

Chapter 1 - Introduction

1.1 General overview of ischemic heart disease

Cardiovascular diseases (CVDs) remain the leading cause of morbidity and mortality in the world with an estimated 17.5 million people dying annually due to the diseases (Mendis et al., 2011; Mendis et al., 2014). In the United Kingdom alone, CVDs affect approximately 7.4 million people and contribute to more than a quarter of all deaths annually (Townsend et al., 2015). Ischemic heart disease, including myocardial infarction (MI) and the resulting heart failure (HF), is the biggest contributor of global cardiovascular death, followed by cerebrovascular disease, hypertensive heart disease, inflammatory heart disease, and other types of CVDs (Mendis et al., 2014).

Ischemic heart disease, also known as coronary heart disease, is a chronic inflammatory disease of the coronary arteries leading to the formation of atherosclerotic plaque and the narrowing of the arterial lumen (Yamada et al., 2002). Acute MI, on the other hand, is initiated by the rupture or erosion of an unstable atherosclerotic plaque leading to total occlusion of the coronary arteries that are located distal to the plaque (Anderson and Morrow, 2017). The ensuing cessation of oxygen and nutrient supply results in the loss of cardiomyocytes, which is caused by apoptosis and necrosis. The extent of the resulting infarction depends upon the size of the occluded artery (the bigger the artery, the bigger the area at risk), duration and intermittency of the occlusion, and the presence of collateral blood circulation (Heusch and Gersh, 2017). In the recent decades, the improvement in the treatment and management of MI has successfully reduced the time needed between patients arriving at the hospital and the reperfusion therapy, resulting in the limitation of infarct size and a steady decline in acute MI-related deaths (Briffa et al., 2009). Nevertheless, infarcted myocardium, regardless of the size, can trigger chronic remodelling and subsequent HF in the long-term.

1.1.1 Cardiac remodelling and development of HF post-MI

The development of HF in post-MI patients arises from a complex, slowly-progressing structural and functional transformation of the heart after MI, called cardiac remodelling (French and Kramer, 2007). This process (Figure 1.1) involves changes in heart shape, size, cellular composition, and function as a response to acute loss of cardiomyocytes, and it is governed by mechanical, neurohormonal, and genetic factors (Sutton and Sharpe, 2000). The extent of post-MI remodelling is a major determinant of the survival and clinical outcomes of the patients during recovery following MI, and thus is often used as a primary endpoint in evaluating treatment strategies (Bhatt et al., 2017; Sutton and Sharpe, 2000).

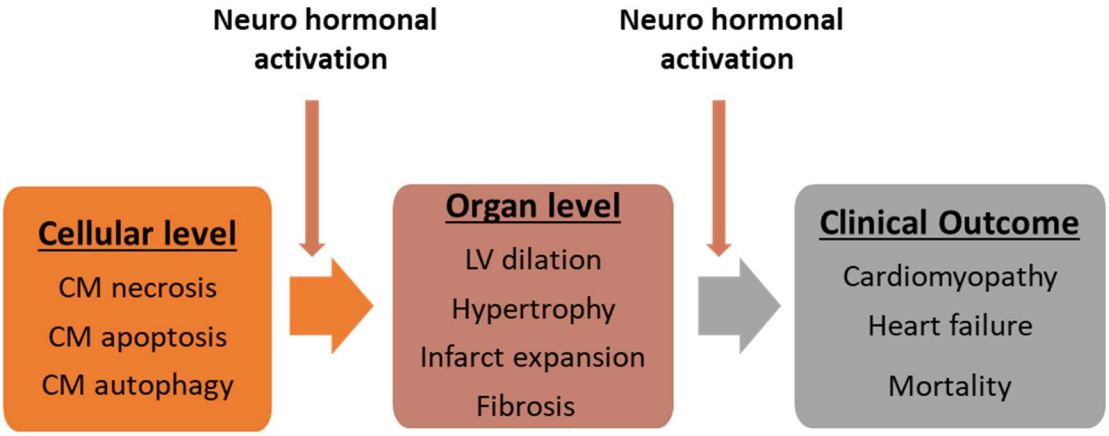

Figure 1.1 The mechanism of cardiac remodelling post-MI. Changes at cellular and organ levels during the remodelling process will determine clinical outcomes post-MI (CM: cardiomyocyte, LV: left ventricle).

Post-MI remodelling can be seen within hours to days of an initial ischemic insult (an early phase) and can continue over the following weeks to months (a late phase). The early phase of post-MI remodelling occurs mainly in the infarct area and is characterised by infarct expansion (French and Kramer, 2007; Sutton and Sharpe, 2000). Infarct expansion is initially caused by the stretching and permanent rearrangement of damaged cardiomyocytes in the ischemic area. As the remodelling goes on, recruited inflammatory cells secrete serine proteases and matrix metalloproteinases which degrade the necrotic tissue and extracellular matrix. This eventually leads to wall thinning and ventricular dilation of the infarcted segment. The extent of the infarct expansion is largely dependent on the size, severity, and

location of the infarct (Bhatt et al., 2017; French and Kramer, 2007; Sutton and Sharpe, 2000; Weisman and Healy, 1987). Reperfusion therapy, either by primary percutaneous coronary intervention (PCI) or thrombolysis, is crucial to salvage the injured peri infarct border region and thus minimise the infarct area (Heusch and Gersh, 2017).

Changes in the ventricular shape due to infarct expansion result in increased wall stress and impaired cardiac systolic and diastolic function. In response, the body activates two neurohormonal mechanisms: the renin-angiotensin-aldosterone system (RAAs) and the adrenergic/sympathoadrenal system to compensate for the decreased cardiac function (Rouleau et al., 1993). Angiotensin II and aldosterone cause systemic vasoconstriction and increased water retention whilst catecholamines, mediators of the adrenergic nervous system, similarly cause vasoconstriction in addition to increased heart rate (Bhatt et al., 2017; Rouleau et al., 1993). In the heart, both RAAS and the adrenergic nervous system, together with local paracrine/autocrine factors, modulate the development of cardiac hypertrophy - the main feature of the late phase of post-MI remodelling (Sutton and Sharpe, 2000). Angiotensin II and catecholamines can bind to G protein coupled receptors (GPCRs) and activate pro-hypertrophy signals, such as MAPK and NFAT/Calcineurin, to stimulate cardiomyocyte growth (Nakamura and Sadoshima, 2018) (Figure 1.2). As a result, the ventricular wall along the non-infarcted segment becomes thicker, which subsequently reduces wall stress. Both neurohormonal modulators can also increase cardiac contractility through increasing the cytosolic Ca^{2+} (Bhatt et al., 2017; Sutton and Sharpe, 2000). Initially, these collective changes can compensate for diminished cardiac function post-MI. In the long-term, however, sustained pathological stimuli due to the persistence of the infarcted segment will lead to the deterioration of cardiac function and heart failure (Diwan and Dorn, 2007).

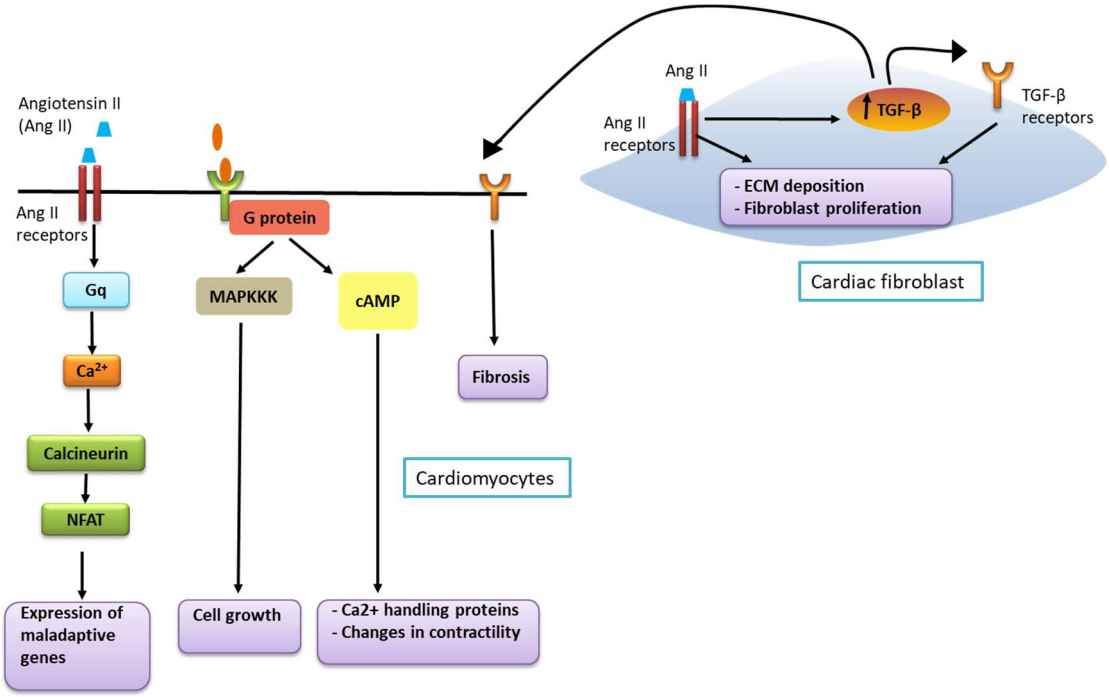

Figure 1.2 Pathways involved in cardiac remodelling post-MI. Activation of angiotensin II receptors by Angiotensin II induces the expression of maladaptive genes via Calcineurin/NFAT signalling. β-adrenergic receptor activation induces the MAPK pathway to induce cell growth and cAMP to increase contractility. Excessive β-adrenergic stimulation, however, is associated with receptor desensitisation, hypertrophy, cell death, and mitochondrial dysfunction. Angiotensin II stimulates TGF-β production which subsequently activates TGF-β receptors in cardiac fibroblasts and cardiomyocytes to induce fibrosis. MAPKKK: mitogen-activated protein kinase kinase kinase, cAMP: cyclic adenosine monophosphate, Ang II: angiotensin II, NFAT: nuclear factor of activated T-cells, TGF-β: transforming growth factor β.

Whilst RAAS and the adrenergic nervous system are crucial for compensation responses, they also contribute to the maladaptive changes that result in the transition from compensated to decompensated remodelling (Diwan and Dorn, 2007). These include interstitial fibrosis, the loss of β-adrenergic receptor responsiveness, and progressive and irreversible cardiomyocyte deaths (Sutton and Sharpe, 2000). One of the key mediators of interstitial fibrosis in the heart is TGFβ1 signalling. The activation of TGFβ1 signalling by angiotensin II results in the phosphorylation of Smad2/3 which, when bound with Smad4, can facilitate the proliferation of cardiac fibroblasts and the deposition of the extracellular matrix (Dobaczewski et al., 2010). It has also been reported that the Angiotensin II/TGFβ1 axis can activate β-adrenergic receptors and thus may contribute to excessive

adrenergic stimulation during the transition from stable hypertrophy to heart failure (Schultz et al., 2002). The deleterious effects of chronic and excessive adrenergic drive in heart failure have been reported in both animal and human studies (Böhm et al., 1998; Lymperopoulos et al., 2013; Osadchii et al., 2007). As discussed above, adrenergic stimulation is initially required due to its inotropic properties; however, chronic stimulation of β-adrenergic receptors can lead to pathological hypertrophy and reduced β-adrenergic responsiveness (Dorn and Brown, 1999). In addition, both angiotensin II and β-adrenergic stimulation have been shown to induce progressive cardiomyocyte death, which contributes to ventricular dilation and wall thinning (Hartupee and Mann, 2017). In summary, altered cellular compositions of the heart due to increased fibrosis and progressive cell death, combined with significant impairment in cardiac contractility, will ultimately lead to the development of end-stage heart failure.

1.1.2 Current HF management

HF is considered a long-term condition that can be managed but cannot be cured. The key aims of therapy in HF patients are to alleviate symptoms and prolong survival. Current treatments for HF involve several strategies, including pharmacological and device-based therapies (Krum and Driscoll, 2013). Drugs to treat HF mainly target neurohormonal activation, such as angiotensin converting enzyme (ACE) inhibitor, angiotensin receptor blockers (ARBs), and β-blocker (Fang, 2005; Krum and Driscoll, 2013). Both ACE inhibitors and ARBs block the RAAS by inhibiting the production of angiotensin II and the activation of angiotensin receptors, respectively, whilst β-blockers block the activation of β-adrenergic receptors (Gheorghiade and Goldstein, 2002; Sweitzer, 2003). The primary mechanism of action of these drugs is to inhibit excessive neurohormonal activation and thus prevent cardiac remodelling. In addition, ACE inhibitors and ARBs can lower blood pressure by inducing peripheral vasodilation, which in turn helps to reduce the amount of contractile force needed by the left ventricle to produce cardiac output (Krum and Driscoll, 2013; Sweitzer, 2003). β-blockers, on the other hand, can lower the heart

rate by reducing the sympathetic drive. This allows the left ventricle to fill more completely and thereby increase cardiac output (Gheorghiade and Goldstein, 2002).

Device-based therapies are increasingly used in HF management, especially for patients with severe or end-stage HF (Krum and Driscoll, 2013). There are two main device-based therapies commonly used in HF patients: the implantable cardioverter defibrillator (ICD) and cardiac resynchronisation therapy (CRT). Both devices are often implanted together in patients with an increased risk of sudden death due to fatal arrhythmia and ventricular dyssynchrony (Bardy et al., 2005; Moss et al., 2009; Tang et al., 2010).

Current HF therapies have been shown to significantly alleviate symptoms and prolong survival (Krum and Driscoll, 2013). However, these therapies are unable to reverse adverse cardiac remodelling and cannot overcome the fundamental cause of HF, which is the loss of cardiomyocytes (Lin and Pu, 2014). Due to poor cardiac regenerative capacity, new therapeutic strategies are needed to substitute the loss of cardiomyocytes during and after MI. Cell therapy has recently emerged as one of the potential therapeutic strategies to treat HF. The aim of this strategy is to transplant externally-derived progenitor cells in the hope that these cells can differentiate into cardiomyocytes and replace the lost cardiomyocytes. Previous clinical trials using different types of progenitor cells such as adult progenitor cells (mesenchymal stem cells and bone-marrow-derived stem cells) and pluripotent stem cells (induced pluripotent stem cells/iPSCs and embryonic stem cells/ESCs) have demonstrated good safety records (Sanganalmath and Bolli, 2013). However, the improvements reported after cell therapies are often modest and direct lineage tracing studies fail to show that the majority of the implanted cells differentiate into cardiomyocytes *in vivo* (Balsam et al., 2004; Nygren et al., 2004). Moreover, additional concerns such as poor integration with the host myocardium, increased risk of arrhythmic events, and teratoma formation have been reported when ESC or iPSC are used (Sanganalmath and Bolli, 2013).

Cardiomyocytes are believed to be terminally differentiated and mitotically inactive cells with no capacity to regenerate. However, multiple lines of evidence have shown that new cardiomyocytes are generated in adult hearts during their lifetime (Bergmann et al., 2009; Bergmann et al., 2015). This highlights the possibility of inducing the endogenous regenerative capacity of the heart as a novel therapeutic approach to replace the cardiomyocyte loss in MI.

1.1.3 Cardiac regenerative potential

Complete cardiac regeneration is well-documented in lower vertebrates such as amphibians and fish (Bettencourt-Dias et al., 2003; Jopling et al., 2010; Kikuchi et al., 2010; Laube et al., 2006; Oberpriller and Oberpriller, 1974; Poss et al., 2002; Rumiantsev and Shmantsar, 1968). After varying degrees of resection in three species of amphibians (newt, salamander, and frog), deoxyribonucleic acid (DNA) synthesis and cardiomyocyte proliferation are evident at the site of injury. In zebrafish, complete heart regeneration after a 20% ventricular resection is achieved after 2 months (Poss et al., 2002). In mammals, a similar robust regeneration is observed in mice. However, this phenomenon is only evident in neonatal (1-day old) mice. When a similar procedure was conducted in 7-day old mice, significant fibrosis instead of cardiomyocyte proliferation was observed at the injury site, indicating that cardiomyocytes have exited the cell-cycle and thus no longer have the capacity to regenerate (Porrello et al., 2011b; Rumyantsev, 1977). It appears that the heart's regenerative capacity is decreased as the organism ages or becomes more evolutionarily advanced.

While it is clear that neonatal mammalian hearts have robust regenerative capacity, the concept of cardiomyocyte renewal in adult mammals and humans is hugely contested. It is commonly believed that the adult heart is not capable of regeneration, although there is evidence of DNA synthesis in the adult mammalian heart, which dates back decades ago (Rumyantsev, 1977). Initially, cardiomyocyte proliferation was measured indirectly by incorporating labelled nucleosides that integrate with newly synthesised DNA. However, the rates of cardiomyocyte

proliferation measured by this method are variable. Earlier studies reported that the cardiomyocyte labelling indexes range from 0 – 0.45% (Bergmann et al., 2009; Soonpaa and Field, 1997; Walsh et al., 2010). In injured rat hearts following MI and coronary artery narrowing, cardiomyocyte labelling indexes were reported to be approximately 1-2% (Senyo et al., 2013). In humans, evidence of postnatal cardiomyocyte proliferation was presented by two studies with varying results. Instead of administering exogenous nucleosides, the first group exploited the peak carbon-14 isotope concentration in the atmosphere, which was due to the aboveground nuclear bomb tests from the 1950s until the early 1960s. After the Limited Nuclear Test Ban Treaty was signed in 1963, the concentration of carbon-14 isotope (^{14}C) in the atmosphere decreased exponentially. ^{14}C in the atmosphere reacts with oxygen to form $^{14}CO_2$, which can be absorbed by plants via photosynthesis. Through food webs, ^{14}C isotope can end up being incorporated into the DNA of dividing cells in humans. Consequently, the cellular ^{14}C concentration in humans born around or after the nuclear bomb tests corresponds to that of the atmosphere at any given time. The time at which the cells divide can be inferred by plotting the concentration of ^{14}C in the cells on a graph depicting the fluctuation of the atmospheric ^{14}C concentration over the years. The researchers found that the samples (human cardiomyocytes) were younger than the respective subjects' age, indicating that cardiomyocytes are able to divide years after the subjects were born. By using a mathematical model of ^{14}C data from both subjects born before and after the nuclear bomb tests, they were able to further determine the rate of cardiomyocyte turnover in the subjects. The results suggest that the annual cardiomyocyte turnover rate is between 0.2 – 2% and there is a negative correlation between the cardiomyocyte turnover rate and the age of the subjects. The cardiomyocyte turnover rate decreases from 1% at the age of 25 to 0.45% at the age of 75 (Bergmann et al., 2009).

The second group measured dividing cardiomyocytes indirectly by detecting iododeoxyuridine (IdU)-positive cardiomyocytes from deceased cancer patients who had been treated with IdU. IdU is a nucleoside analogue which will incorporate into

newly synthesised DNA *in vivo*. The researchers were able to determine that, on average, 22% new cardiomyocytes are generated every year (Kajstura et al., 2010). This number is much higher than what was found in the previous study. These findings, however, must be interpreted with caution. The first thing to consider is that adult cardiomyocytes are capable of DNA synthesis without undergoing cell division. This is the reason why most adult cardiomyocytes are diploid or polyploid. In addition, DNA synthesis can also be contributed to by DNA repair mechanisms. This is particularly relevant in cancer patients as DNA repair is upregulated after chemotherapy and radiation therapy. Secondly, there are other cell populations in the heart, such as fibroblasts, endothelial cells, and vascular smooth muscle cells, which proliferate more than cardiomyocytes. Both of these factors may lead to an overestimation of the cardiomyocyte proliferation rate.

To address this problem, researchers use a combination of several techniques including the typical labelled nucleoside incorporation technique with genetic lineage tracing and/or more advanced methods such as multi-isotope imaging mass spectrophotometry. These techniques allow us to detect the dividing cells more accurately and to trace the origin of newly dividing cells. A study by Senyo *et al.* using these methods reported that the cardiomyocyte proliferation rate is less than 1% (0.76%), which is similar to what was found in previous studies (Bergmann et al., 2009; Senyo et al., 2013). Furthermore, the aforementioned study also described that most of the newly-generated cardiomyocytes are from pre-existing cardiomyocytes, instead of from progenitor cells as initially thought (Senyo et al., 2013). Similar findings are reported in zebrafish and neonatal mouse studies (Ali et al., 2014; Jopling et al., 2010; Kikuchi et al., 2010). These findings are crucial because they have shifted the paradigm that progenitor cells are the main source of heart regeneration and thus further highlight the potential of augmenting cardiac endogenous regenerative capacity rather than relying on the transplantation of exogenous progenitor cells to replace myocardial loss during MI.

1.1.4 Mechanisms of cardiac regeneration

To be able to manipulate the endogenous capacity of the heart, sufficient understanding of how heart tissue can regenerate is crucial. Embryonic cardiomyocytes in mammalian hearts can freely divide and the resulting increase in cardiomyocyte number largely accounts for embryonic heart growth (Galdos et al., 2017). Embryonic cardiomyocytes thrive in the relatively hypoxic intrauterine environment and rely on glycolytic metabolism to acquire energy. Soon after birth, however, the vast majority of cardiomyocytes exit the cell cycle and undergo dramatic changes linked to the greater need for robust ventricular pump function and greater availability of oxygen relative to the intrauterine environment (Galdos et al., 2017; Jacot et al., 2008). They switch from glycolytic metabolism to oxidative phosphorylation as their primary energy source and undergo structural and functional maturation to improve contraction efficiency (Ellen Kreipke et al., 2016; Galdos et al., 2017; Schiaffino et al., 1993). As cardiomyocyte cell cycle withdrawal happens at around the same time as cardiomyocyte transformation for efficient contraction, it is postulated that these two events are linked.

The cardiomyocyte maturation that accompanies cardiomyocyte cell cycle withdrawal involves extensive changes in cardiomyocyte cytoarchitecture, which include, but are not limited to, an increase in cardiomyocyte size, multinucleation and polyploidisation of cardiomyocyte nuclei, t-tubule formation, electrical coupling, and increased sarcomere prominence (Galdos et al., 2017). However, these changes have been reported to pose significant barriers to adult cardiomyocyte proliferation (Gonzalez-Rosa et al., 2018; Y. Zhang et al., 2010). To overcome these barriers, several studies have reported that proliferating adult cardiomyocytes in the infarct border zone dedifferentiate to less mature phenotypes to allow proliferation (Senyo et al., 2013; Y. Zhang et al., 2019). The dedifferentiation process is characterised by profound sarcomere disassembly and altered gene expression profiles with a downregulation of the genes involved in cardiac hypertrophy, electrical, and

contractile function, and an upregulation in genes involved in cell cycle, proliferation, and survival (Galdos et al., 2017; Jopling et al., 2010; Y. Zhang et al., 2010).

In recent years, the understanding of cellular mechanisms that underlie cardiomyocyte dedifferentiation and proliferation has increased dramatically. A number of groups have identified several molecular signals that can stimulate cardiomyocyte proliferation. For example, the modulation of cell cycle signals has been shown to induce cardiomyocyte proliferation in adult mice. During a normal cell cycle, Cyclin A2 is required for progression from G1 to S and G2 to M phase, whilst cyclin D2 positively regulates G1/S transitions (Ahuja et al., 2007). Several studies have reported that the overexpression of these genes promotes adult cardiomyocyte proliferation. The expression of constitutively active cyclin A2 in mice since embryonic day 8 results in cardiomegaly due to increased cardiomyocyte proliferation (Chaudhry et al., 2004). After MI, transgenic mice overexpressing cyclin A2 have significantly less cardiac dilation and improved cardiac function, accompanied by increased cell cycle re-entry in the border zone (Cheng et al., 2007). Adenovirus-mediated delivery of cyclin A2 in rat and swine models of MI has been shown to protect the heart against MI by increasing cardiomyocyte mitoses, decreasing fibrosis, and improving cardiac function (Shapiro et al., 2014; Woo et al., 2006). Similarly, cardiac-specific overexpression of cyclin D2 in MI promotes cardiomyocyte proliferation and reduces infarct size (Pasumarthi et al., 2005). Recently, Mohamed *et al.* used *in vivo* lineage tracing to show that combinatorial overexpression of cyclin-dependent kinase 1 (CDK1), CDK4, cyclin B1, and cyclin D1 in MI mouse models can efficiently induce the proliferation of adult cardiomyocytes with significant improvement in cardiac function after acute or sub-acute MI. They also found that CDK1 and cyclin B can be replaced by TGF-β and Wee1 inhibitors with the same results (Mohamed et al., 2018). This suggests that direct cell cycle reactivation can be a viable therapeutic strategy for cardiac repair if used carefully.

In addition to cell cycle regulators, several signalling networks that regulate heart development have been reported to also regulate cardiomyocyte proliferation. One such example is the network consisting of Neuregulin (NRG1) and its receptors -

Erb-B2 receptor tyrosine kinase 2 (ERBB2) and ERBB4 (Citri and Yarden, 2006). Reduced NRG1 signalling by ERBB4 and ERBB2 inactivation results in mice being born with dilated cardiomyopathy and with increased vulnerability to stresses such as pressure overload or cardiotoxic antibiotic anthracycline (Fukazawa et al., 2003; Heallen et al., 2019). Contrarily, exogenous administration of NRG1 has been reported to induced cardiomyocyte dedifferentiation and proliferation, leading to a marked improvement in cardiac function post-MI (Bersell et al., 2009). Moreover, D'Uva *et al.* found that the transient induction of constitutively active ERBB2 after MI promoted cardiomyocyte dedifferentiation, proliferation, and redifferentiation, leading to reduced infarct size and enhanced cardiac function (D'uva et al., 2015). Further investigations revealed that the ERK and AKT pathways act as downstream mediators of NRG1/ERBB2 signalling to induce cardiomyocyte proliferation (D'uva et al., 2015).

Studies conducted during the past decade have indicated the importance of epicardium (the visceral layer of pericardium) in heart development and regeneration (Cao and Poss, 2018). Epicardium-derived growth factors, such as follistatin like-1 (FSTL1) and insulin-like growth factor 2 (IGF2), are reported to modulate cardiomyocyte proliferation. Wei *et al.* reported that the level of epicardial FSTL1 decreases following MI and that administration of human epicardial FSTL1 via an epicardial patch can induce proliferation of pre-existing cardiomyocytes, as well as improve cardiac function and survival in murine and porcine models of MI (Wei et al., 2015). Similarly, epicardial IGF2 was found to be crucial in cardiomyocyte proliferation in the developing heart (Wei et al., 2015) . Other growth factors of non-epicardial origin, such as IGF1 and hepatocyte growth factor (HGF), have also been found to stimulate cardiomyocyte proliferation, angiogenesis, as well as improve cardiac function when injected together into a pig heart post-MI (Koudstaal et al., 2014).

As discussed above, the manipulation of developmental signalling pathways can often be beneficial for heart regeneration after injury. Several studies have identified a number of intrinsic cardiac developmental signals and manipulated their

expression in MI models. T-box 20 (TBX20), a critical transcription factor for heart development, is perhaps one of the more extensively studied developmental signals in the heart (Greulich et al., 2011). Genetic mutations in the human TBX20 gene are associated with a wide spectrum of developmental anomalies, including defects in septation and valvulogenesis, and cardiomyopathy (Posch et al., 2010). Studies in mice revealed that TBX20 knockout in the developing heart resulted in a severely hypoplastic heart and midgestational lethality, whilst TBX20 gain of function led to increased cardiomyocyte proliferation and myocardial thickness (Cai et al., 2005; Chakraborty and Yutzey, 2012). Xiang *et al.* demonstrated that inducible, cardiac-specific TBX20 overexpression in adult mice reduced infarct size and markedly improved survival and cardiac function (Xiang et al., 2016). They found that TBX20 overexpression induced the activity of several proproliferative pathways, including PI3K/AKT,YAP, BMP/SMAD1/5/8 and repressed the transcription of antiproliferative genes p21 and Meis1 (Xiang et al., 2016). Mahmoud *et al.* subsequently showed that Meis1 deletion in mice results in the downregulation of cell cycle inhibitors p15 and p16, which in turn induces cardiomyocyte cell cycle re-entry and proliferation without any damaging effects on cardiac function (Mahmoud et al., 2013).

Accumulating evidence has demonstrated that cardiomyocyte proliferation is also regulated by miRNA networks (Eulalio et al., 2012; Porrello et al., 2013). These miRNAs can modulate the expression of the genes involved in cardiomyocyte proliferation, such as cell cycle inhibitor Check 1 and oncogene YAP (Porrello et al., 2013; Tian et al., 2015). YAP, one of the proteins targeted by TBX20 and a strong proliferation inducer, has been identified as the main effector of a pathway called the Hippo signalling pathway. The Hippo-YAP pathway is an established protein kinase cascade that regulates tissue growth and development through the modulation of cell proliferation and survival. Recently, the Hippo pathway has been shown to modulate cardiomyocyte proliferation and thus can be targeted to enhance cardiac regeneration.

1.2 The Hippo Signalling Pathway

Firstly discovered in Drosophila, the Hippo signalling pathway is an important regulator of organ size control, tissue regeneration, and stem cell renewal. Due to its ability to modulate the proliferative response of adult cardiomyocytes, the Hippo pathway can be a promising target in cardiac regeneration. This section will summarise the core components of the Hippo pathway, the effects of Hippo pathway modulation in the heart, as well as recent developments in Hippo pathway regulatory mechanisms.

1.2.1 The components of the Hippo pathway

The core components of the Hippo pathway were discovered through genetic screening for tumour suppressor genes in Drosophila. Amongst the initially identified members of this pathway are four genes: Warts (Wts), Salvador protein (Sav), protein kinase Hippo (Hpo), and MOB kinase activator-like 1 (Mats) (Halder and Johnson, 2011). Protein kinase Hpo forms a complex with Sav and subsequently activates the Wts-Mats complex. The Wts-Mats complex then phosphorylates a transcriptional co-activator Yorkie (Yki), resulting in its exclusion from the nucleus. Intranuclear Yki forms a complex with transcription factors Scalloped, which then induces the expression of genes that promote cell proliferation and growth (Harvey and Tapon, 2007; Pantalacci et al., 2003; Tapon et al., 2002; Udan et al., 2003).

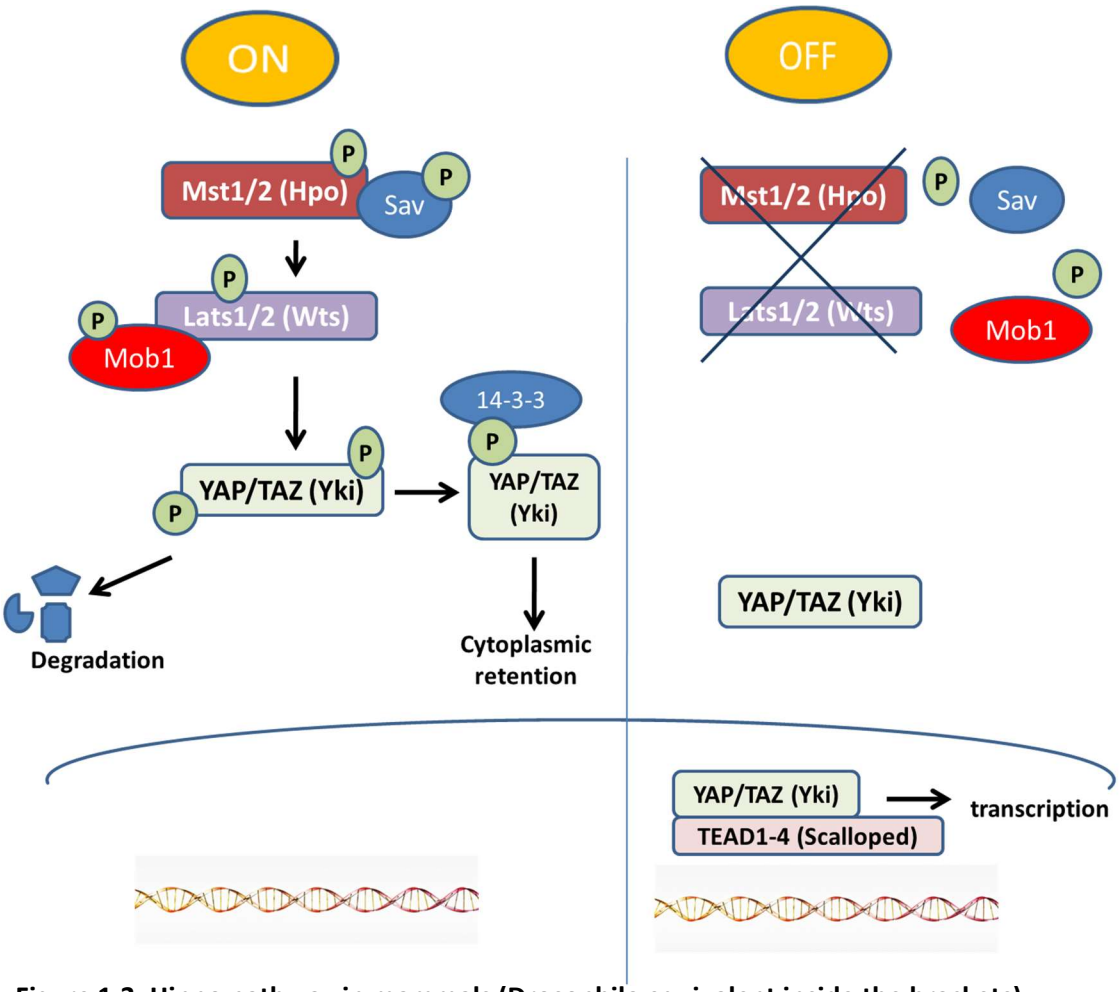

Figure 1.3. Hippo pathway in mammals (Drosophila equivalent inside the brackets).

The core components of the Hippo pathway are highly conserved across species in the eukaryotic kingdom (Table 1.1, Fig.1.3). Similar to what is observed in Drosophila, Hippo pathway activation in mammals is initiated by the activation of two Hpo homologs, MST1 and MST2, by upstream regulators. The activated MST1/2 then form a complex with the Sav homolog, SAV1, to phosphorylates two Wts homologs, LATS1 and LATS2 (Chan et al., 2011; Tapon et al., 2002). LATS1/2 interacts physically with two Mats homologs (MOB1A and MOB1B) to form a complex which phosphorylates the Yki homologs, YAP and TAZ (Hirabayashi et al., 2008; J. Zhang et al., 2008). The phosphorylation of YAP and TAZ leads to the degradation and/or cytoplasmic retention of YAP/TAZ and hence makes them unable to bind to the Scalloped homolog, TEAD (TEA domain-containing transcription factors), and prevent

the activation of their target genes (Vassilev et al., 2001; L. Zhang et al., 2008; Zhao et al., 2008). In summary, the Hippo pathway regulates the cytoplasmic/nuclear localisation of YAP/TAZ.

Table 1.1 Core components of the Hippo pathway in mammals and their Drosophila homologs

Mammalian protein	Abbreviation	Drosophila homolog
Mammalian STE-20-like kinase 1 and 2	MST1/2	Hippo
Salvador homologue 1	SAV1	Salvador
Large tumour suppressor kinase 1 and 2	LATS1/2	Warts
Mps one binder e activator-like 1	MOB1	Mats
Yes-associated protein 1	YAP	Yorkie
Transcriptional co-activator with PDZ-binding domain	TAZ	
TEA domain-containing transcription factors 1-4	TEAD 1-4	Scalloped

YAP and its paralog, TAZ, are the main effectors of the Hippo pathway. Although YAP and TAZ are structurally very similar, with approximately 60% similarity in their protein sequences (Varelas, 2014), there are a few differences between them as well (Figure 1.4). First, although both have WW domains that mediate protein – protein interactions, such as interaction with LATS1/2, YAP has two WW domains separated by between 20-23 amino acids, whilst TAZ only has one (Kanai et al., 2000; Webb et al., 2011). Furthermore, YAP contains a SH3-binding domain and a proline-rich region needed for mRNA processing at its N-terminus, both of which are absent in TAZ (Varelas, 2014). Finally, although most residues in the TEAD binding domain are conserved between YAP and TAZ, the YAP protein has a PxxΦP motif (x is any amino acid and Φ is a hydrophobic residue), whilst TAZ does not (Webb et al., 2011). Whether or not these differences have any implications on their biological activity is yet to be investigated.

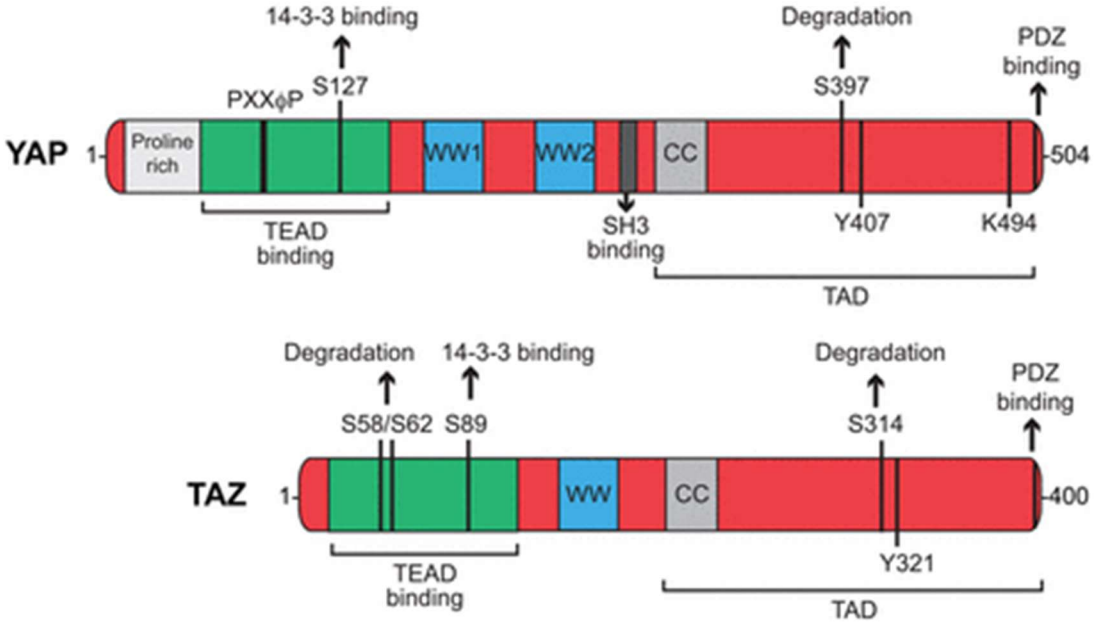

Figure 1.4 Regulatory domains of the Hippo effectors YAP/TAZ. Important domains and regulatory modifications within YAP and TAZ. Prominent regions include the WW domain(s), the coiled-coil (CC) domain, the SH3-binding domain, the TEAD transcription factor-binding domain, the transcriptional activation domain (TAD) and the PDZ-binding motif. Taken from Varelas (Varelas, 2014).

The Hippo pathway inhibits YAP/TAZ mainly via two mechanisms, cytoplasmic retention and degradation. YAP retention in the cytoplasm can be induced by: (i) binding between the phosphorylated Ser 127 region and the 14-3-3 protein and (ii) interaction between the WW domain and the PPxY region of the angiomotin (AMOT) protein (Kanai et al., 2000; Zhao et al., 2011). These mechanisms are conserved in TAZ except for a slight difference in the phosphorylation target (Ser 127 in YAP *vs*. Ser 89 in TAZ) (Chan et al., 2011). The degradation of YAP/TAZ by the Hippo pathway is initiated by the phosphorylation of the Ser 381 region by phosphorylated LATS1/2. This subsequently leads to further phosphorylation by casein kinase 1 (CK1δ/ε) and ultimately activates the phosphorylation-dependent degradation process (Zhao et al., 2010).

When the Hippo pathway is turned off, YAP/TAZ can accumulate in the nucleus and bind to the transcriptional coactivators TEAD protein family, which have 4 homologous members, TEAD1-4. TEAD proteins have a transactivation domain

which can bind with activating factors such as YAP/TAZ and a TEA domain which can bind to the specific DNA elements and thus activate gene expression. In addition to Yap/TAZ, TEAD proteins also interact with other activating factors such as vestigial-like (Vgll) proteins and p160s (Belandia and Parker, 2000; Pobbati et al., 2012; Vaudin et al., 1999). TEAD proteins on their own are incapable of inducing any biological effects and thus require coactivators to exert their roles. Each coactivator is capable of exerting different biological effects. The biological effects of TEAD proteins which are mediated by the Hippo pathway (YAP/TAZ) will be discussed below.

1.2.2 General roles of the Hippo pathway

The biological roles of the Hippo signalling pathway in animals and humans can be summarised in three major points: (a) early development and stem cell regulation, (b) cell proliferation and cancer, and (c) organ size control (Fig 1.5). Each point will be discussed in more detail below.

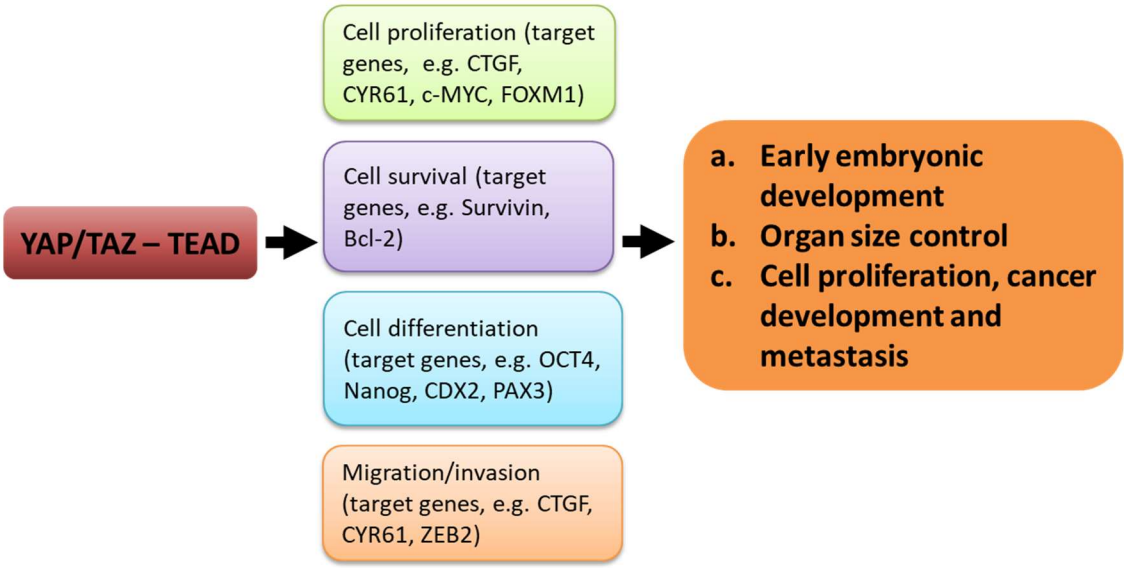

Figure 1.5 Schematic diagram of Hippo pathway roles in regulating biological function. Activated YAP/TAZ binds to TEAD and facilitates the transcription of several genes involved in cell proliferation, differentiation, survival, and migration.

1.2.2.1 Early development and stem cell regulation

In mice, the Hippo pathway plays a significant role in embryonic development such as cell fate determination during the pre-implantation stage and the maintenance of normal embryonic growth. Shortly before implantation, the cells in a mouse blastocyst will develop into two cell lineages: The trophoectoderm (TE) and the inner cell mass (ICM). TE is normally derived from the outer cells of a mouse blastocyst and will give rise to extraembryonic tissue. ICM, on the other hand, is derived from the inner cells and will differentiate into embryonal layers (Cockburn and Rossant, 2010). In outer cells, an inactivated Hippo pathway means higher nuclear YAP activity, which can bind to and activate TEAD proteins. In contrast, higher YAP cytoplasmic sequestration is found in the inner cells, indicating an active state of the Hippo pathway and an inability to bind to TEAD proteins inside the nucleus (Nishioka et al., 2009). One of the TEAD homologs, TEAD4, is pivotal in determining TE/ ICM fate (Home et al., 2012; Nishioka et al., 2009). TEAD4 knockout embryos have been shown to exhibit significantly reduced TE markers, CDX2 (caudal type homeobox 2) and GATA3, and all their cells transformed into ICM (Home et al., 2009; Nishioka et al., 2009; Ralston et al., 2010). Moreover, the inner cells of a mouse with deficient Hippo signalling due to complete LATS1/2 knockout displays similar YAP localisation profiles to the outer cells, i.e. higher nuclear YAP accumulation and TE markers expression (Lorthongpanich et al., 2013).

A study using YAP-deficient mice suggests that YAP is critical in overall embryonic development. YAP-/- embryos fail to develop an organised yolk sac vascular plexus and show a series of developmental anomalies, including failed chorioallantoic fusion, caudal dysgenesis, and a shortened body axis (Morin-Kensicki et al., 2006).

In embryonic stem cells (ESCs), the Hippo pathway interacts with the transforming growth fator β (TGFβ) pathway to maintain the cell pluripotency. The effector of the Hippo pathway, YAP/TAZ, forms a complex with the effector of the TGFβ pathway, transcription factor SMAD2/3, and subsequently binds to TEAD and a

core stem cell regulator, OCT4. The result is the modulation of genes that regulate pluripotency, such as Nanog, OCT4, and SOX2 (Tamm et al., 2011). Complete knockout of YAP in mice results in the loss of pluripotency as indicated by reduced expression of OCT4 and SOX2. Ectopic YAP expression can reverse this effect and thus maintains the ESC phenotypes (Lian et al., 2010). In human induced pluripotent stem cells (iPSCs), MST1 and LATS2 knockdown has been shown to increase the efficiency of iPSC reprogramming via the upregulation of nuclear YAP/TAZ (Qin et al., 2012; Robertson et al., 2017). This finding further highlights the importance of Hippo signalling in modulating stem cell phenotypes.

1.2.2.2 Organ size control

Organ size control is a very complex process which requires a delicate balance between the internal proliferative capacity of an organism, and the physiological signal from the surrounding environment. The mechanism that controls organ size is not yet fully understood, but extensive research has led to the identification of the Hippo pathway as a key component in organ size control. Gain or loss of function studies in Drosophila provide the initial clue that the Hippo pathway can regulate organ size. Complete knockout of Wts, for example, leads to the excessive apical growth of imaginal disc epithelial cells (Justice et al., 1995). The complete loss of another main component the of Hippo pathway, Hpo, leads to faulty apoptosis and increased tissue growth and proliferation. This effect is mediated by higher nuclear Yki, which subsequently increases the target gene expression, such as cell cycle regulator cyclin E and the Drosophila inhibitor of apoptosis protein Diap1 (Harvey et al., 2003; Jia et al., 2003; Pantalacci et al., 2003; Udan et al., 2003). The overexpression of Yki has also been shown to induce tissue overgrowth (Verghese et al., 2012). On the other hand, gain of function studies have shown that the overexpression of several Hippo pathway components, including Sav, Hpo, Mats, and Wts, leads to increased apoptosis and smaller organs (Tapon et al., 2002; Udan et al., 2003; Wu et al., 2003).

In mammals, however, the findings from several studies using similar techniques led to a different conclusion regarding the role of the Hippo pathway in organ size control. YAP overexpression in mice has been shown to increase the size of the liver up to three to four times the normal size (Camargo et al., 2007; Dong et al., 2007). This overgrowth phenotype results from an increase in proliferation and not in size, which is suggestive of the role of YAP in cell proliferation. However, this effect appears to be organ- or context-specific. Specific deletion of MST1/2 in mouse limb bud tissue, and SAV1 in various mouse epithelial tissues, resulted in a mild anomaly of growth plate development and differentiation failure, respectively, without substantial changes in organ size (Lee et al., 2008; Song et al., 2010). Moreover, a YAP overexpression study on the small intestines of mice reported a differentiation abnormality without an apparent increase in organ size (Camargo et al., 2007). Taken together, these findings suggest that the organ size control mechanism in mammals may be more complex than that in Drosophila. The abnormality in differentiation as a result of Hippo signalling modulation suggests that the primary role of the Hippo pathway in mammals may be to regulate cell cycle exit.

Physiological cues upstream of the Hippo pathway, which are crucial for organ size determination are not yet well understood. Contact inhibition of proliferation is thought to be one of the important factors in controlling tissue growth. Contact inhibition is activated when cells in an organ or in a monolayer culture come into contact with each other or the surrounding environment upon reaching a certain density. Changes in cell size, shape, mechanical force, and tissue organisation as a result of contact will activate various signals, such as α-catenin and E-cadherin, which subsequently activate the Hippo pathway to restrict cell proliferation. The other signals involved in tissue growth control will be discussed in more detail in section 1.2.4.

1.2.2.3 Cell proliferation and cancer

As mentioned in the previous section, the core components of the Hippo pathway are tumour suppressor genes, which control the activity of oncogene YAP.

Therefore, the loss of Hippo signalling can result in increased cell proliferation and cancer risks. In humans, an elevated level of nuclear YAP/TAZ is commonly found in several cancer types, suggesting an anomaly in Hippo modulation. In neurofibromatosis and malignant mesothelioma, for example, the mechanisms which lead to increased nuclear YAP/TAZ are NF2 and LATS2/SAV1 mutation, respectively (Hamaratoglu et al., 2006; Murakami et al., 2011). The NF2 gene encodes the tumour suppressor gene Merlin, which is an upstream regulator of LATS kinases (N. Zhang et al., 2010). Mutations in SAV1 and MOB1 have also been reported in human renal carcinoma cell line and melanomas (Tapon et al., 2002). However, in other types of cancers, it is not always clear how nuclear YAP/TAZ is elevated. In hepatocellular carcinoma, one study reported that YAP overexpression is found in 50% of 177 samples (Xu et al., 2009). Another study investigating human breast cancer found that TAZ overexpression was found in 80% of the analysed samples (Cordenonsi et al., 2011). Interestingly, these studies did not describe any mutation in the core components of the Hippo pathway. This suggests that there are other modulators, either upstream or downstream, which allow YAP/TAZ to escape Hippo signalling inhibition. This finding can be put into consideration when choosing the appropriate strategy to target the Hippo pathway in cancer.

1.2.3 The role of Hippo pathway in the heart

1.2.3.1 Hippo pathway in heart development

Genetic deletion and overexpression studies in animal models have provided a very useful insight on the role of the Hippo pathway in heart development (summarised in Table 1.2). The vital role of the Hippo pathway in controlling organ size is also observed in the heart. Heallen *et al*. created a mouse model with conditional deletion of SAV1 by a knockin Nkx2.5^{Cre} (Heallen et al., 2011). Nkx2.5 is a crucial regulator of heart development which drives the SAV1 deletion at embryonic day 7.5 (E7.5) (Moses et al., 2001). Mice lacking the SAV1 gene display heart enlargement and myocardial expansion due to increased YAP and cardiomyocyte proliferation (Heallen et al., 2011). The conditional knockout of other genes, such as

MST1/2 and LATS1/2, results in similar phenotypes: cardiomegaly and myocardial expansion with preserved general architecture of the heart (Heallen et al., 2013; Moses et al., 2001). By using the same Nkx2.5^{Cre} strain to create a mouse model with YAP conditional knockout, Xin *et al.* showed that the absence of YAP produces embryonic lethality due to a hypoplastic heart and an abnormally thin myocardium (Xin et al., 2011). The number of cardiomyocytes decreases by approximately 50% due to the significant reduction in cardiomyocyte proliferation (Xin et al., 2011). Similarly, conditional inactivation of the YAP allele, specifically in cardiomyocytes using Tnnt2^{Cre}, results in embryonic lethality at E16.5 due to severe cardiac hypoplasia (Von Gise et al., 2012). On the other hand, cardiac-specific overexpression of YAP in mice results in hepatic congestion and cardiomegaly (Von Gise et al., 2012). Further examinations revealed a dramatic increase in cardiomyocyte proliferation, resulting in profound myocardial overgrowth with marked hypertrabeculation. Collectively, these results demonstrate that the Hippo signalling pathway modulates YAP to regulate cardiomyocyte proliferation during cardiac development. In adult mice, impaired Hippo signalling promotes several pathological changes in the heart, such as increased apoptosis, fibrosis, and hypertrophy.

Table 1.2 Summary of cardiac phenotypes of the Hippo pathway in mouse models

Gene	Mouse model	Phenotypes
MST1	cTG (cardiomyocyte-specific transgenic)	Premature death, dilated cardiomyopathy, ventricular wall thinning, increased cardiomyocyte apoptosis, fibrosis, no hypertrophy (Yamamoto et al., 2003)
	cTG of MST1 dominant negative	Reduced apoptosis following ischemia/reperfusion (I/R) injury (Yamamoto et al., 2003), general reduction in cardiomyocyte apoptosis, fibrosis, dilated cardiomyopathy and cardiac dysfunction, but no hypertrophy after MI (Odashima et al., 2007)
MST1/2	cKO	Cardiomegaly and myocardial expansion with preserved general architecture of the heart (Heallen et al., 2011)
LATS2	cTG	No effects on apoptosis at basal condition, reduced cardiomyocyte and ventricle size, increased apoptosis in response to pressure overload (Matsui et al., 2008)
	cTG of LATS2 dominant negative	Ventricular hypertrophy, less apoptosis in response to TAC (Matsui et al., 2008)
LATS1/2	Inducible cKO	Increased proliferation of adult cardiomyocytes, improved regeneration following apex resection (Heallen et al., 2013)
SAV1	cKO	Heart enlargement, myocardial expansion, increased cardiomyocyte proliferation (Heallen et al., 2011)
YAP	cKO	Embryonic lethality due to hypoplastic heart and thin myocardium, reduced cardiomyocyte proliferation (Xin et al., 2011)
	cKO	Early postnatal mortality, dilated cardiomyopathy, increased apoptosis and fibrosis, impaired neonatal regeneration (Del Re et al., 2013)
	cTG of constitutively active YAP	Thickened myocardium, increased trabeculation, enhanced cardiomyocyte proliferation (Xin et al., 2011)
	Inducible cTG of constitutively active YAP	Cardiomegaly due to increased proliferation but not hypertrophy, thickened myocardium (Von Gise et al., 2012)

1.2.3.2 Apoptosis in the heart

The effects of genetic modulation of the Hippo components on cardiomyocyte apoptosis is summarised in Table 1.2. Hippo core components MST and LATS kinases have been shown to regulate cell apoptosis. Transgenic mice overexpressing MST1 are reported to develop severe cardiomyopathy and ventricular wall thinning due to increased apoptosis (Yamamoto et al., 2003). In the event of I/R injury, the overexpression of dominant negative MST1 to supress the endogenous MST1 results in infarct size reduction due to decreased apoptosis. In other cell types, MST1 is shown to mediate apoptosis in primary mammalian neurons induced by hydrogen peroxide. These show that MST1 is required to mediate cardiomyocyte apoptosis in response to oxidative stress (Del Re et al., 2010; Yamamoto et al., 2003). Both autophosphorylation, induced by the tumor suppressor Ras associated domain containing protein 1 (RASSF1A), and caspase-dependent cleavage are thought to be involved in MST1 activation. Activated MST1 subsequently targets the pro-survival protein Bcl-xL which, when phosphorylated, inhibits proapoptotic protein Bax (Odashima et al., 2007; Yamamoto et al., 2003).

The overexpression of LATS2, but not LATS1, increases apoptosis in cultured cardiomyocytes (Matsui et al., 2008). In contrast, studies in other cell types have reported that both LATS1 and LATS2 increase apoptosis in cancer cells. This suggests that the effect of LATS1 and LATS2 may be dependent on the cell type. In mice, LATS2 overexpression does not affect the level of cardiomocyte apoptosis at baseline. In response to stresses such as pressure overload, however, LATS2 may play an important role in regulating cardiomyocyte apoptosis (Matsui et al., 2008). Yamamoto *et al*. showed that LATS2 expression is significantly elevated in mice subjected to transverse aortic constriction (TAC) (Yamamoto et al., 2003) . The suppression of endogenous LATS2, with the overexpression of dominant negative LATS2, significantly reduces cardiomyocyte apoptosis (Yamamoto et al., 2003). The precise mechanism of how LATS2 induces cardiomyocyte apoptosis is unclear.

Research in other cell types indicates that LATS2 directly targets other tumour suppressor genes to modulate apoptosis (Aylon et al., 2010).

Despite YAP being the major effector of the Hippo pathway, it is not clear whether activation of MST1 or LATS2 leads to YAP modulation to regulate apoptosis. Del Re *et al.* found that the RASSSF1A/MST1 axis does not lead to phosphorylation of either LATS or YAP, but directly targets mitochondrial protein Bcl-xL instead (Del Re et al., 2010). Contrarily, Matsui *et al.* reported that activated MST1 phosphorylated LATS2 and then YAP to regulate apoptosis in cultured cardiomyocytes (Matsui et al., 2008). Given that MST1 can induce apoptosis at basal condition whilst LATS2 cannot, it is likely that MST1 may regulate apoptosis via other pathways in addition to the downstream phosphorylation of LATS and YAP. YAP is a potent pro-survival protein. In the event of MI, cardiac-specific deletion of YAP causes an increase in cardiac apoptosis and fibrosis (Del Re et al., 2013). Although more research is still needed to elucidate the precise action of the Hippo pathway in regulating apoptosis, these findings suggest that Hippo pathway inhibition can promote cardiomyocyte survival and alleviate apoptosis.

1.2.3.3 Hippo pathway in cardiac hypertrophy

Several Hippo core components have been shown to modulate cardiac hypertrophy in response to pathological stimuli such as ischemia or pressure overload. The activation of the RASSF1A/MST1 axis has been shown to regulate cardiomyocyte apoptosis (Yamamoto et al., 2003). In mice subjected to pressure overload, cardiomyocte-specific knockout (cKO) of RASSF1A inhibits MST1 activation and prevents the development of cardiac hypertrophy with a marked reduction in cardiomocyte apoptosis and fibrosis (Del Re et al., 2010). It appears that MST1 inhibition seems to reduce heart damage and thus mitigate the hypertrophic response caused by pressure overload (Del Re et al., 2010). Likewise, Oceandy's Lab has reported that MST2 knockout mice display significantly less hypertrophy and fibrosis when subjected to TAC (Zi et al., 2014). Further examinations revealed that MST2 ablation has no effect on YAP activation, although it inhibits the activation of

the prohypertrophic Raf1-ERK1/2 pathway (Zi et al., 2014). Raf1 kinase and ERK1/2 are major components of the MAPK signalling cascade, which regulates many cellular processes in the heart including hypertrophy (Harris et al., 2004). While several studies show that Hippo inhibition leads to an attenuated hypertrophic response, contradicting results are described in studies investigating the effects of LATS and YAP. LATS2 expression is reported to be significantly upregulated after TAC. When endogenous LATS2 activity is suppressed by the α-MHC promoter–driven transgenic expression of dominant-negative LATS2, the heart displays significantly enhanced cardiac hypertrophy with reduced cardiomyocyte apoptosis (Matsui et al., 2008). These findings suggest that LATS2, in contrast to MST kinases, is required to negatively regulate hypertrophy in response to TAC.

The Hippo effector YAP was initially thought to only modulate cardiomyocyte proliferation without having any effect on hypertrophy. Forced expression of constitutively active YAPS112A in the embryonic heart results in increased cardiomyocyte number and a smaller cardiomyocyte size (Xin et al., 2011). Similarly, the conditional deletion of upstream Hippo components SAV or LATS1/2 in the developing heart leads to increased YAP activity, which, in turn, increase cardiomyocyte proliferation with no change in cardiomyocyte size (Heallen et al., 2013; Heallen et al., 2011). YAP also has no effect on physiological hypertrophy during postnatal cardiac growth. When cardiomyocytes start to transition from a proliferative to a hypertrophic mode of growth during the first week after birth, YAP activity is decreased. Furthermore, genetic gain of function or deletion of YAP after birth does not significantly alter cardiomyocyte size (Von Gise et al., 2012).

Interpreting the effects of YAP on cardiac hypertrophy is more difficult in experimental models of heart diseases. Several studies have reported that increased YAP activation improved cardiac regeneration and function post-MI via increased cardiomyocyte proliferation, not hypertrophy (Xin et al., 2013). On the other hand, Yang *et al.* showed that YAP induces cardiac hypertrophy via miR-206 following TAC (Yang et al., 2015b). Moreover, cardiomyocyte-specific miR-206 gain of function promotes hypertrophy after TAC and enhances cardiac function post I/R injury, while

the suppression of miR-206 prevents pressure-overload-induced hypertrophy and worsens cardiac function post I/R injury (Yang et al., 2015b). Collectively, these findings highlight the need for more research in investigating the role of the Hippo pathway in modulating physiological and pathological hypertrophy.

1.2.3.4 Hippo pathway in heart regeneration and MI

Lessons from studies in cancer indicate that YAP is a powerful driver of cell proliferation and a potent oncogene. In the heart, YAP has similarly been shown to induce cardiomyocyte proliferation and regeneration. Heterozygous deletion of YAP in adult mice results in increased infarct size and worsened cardiac function post-MI (Del Re et al., 2013; Von Gise et al., 2012). In contrast, inducible overexpression of constitutively active YAP (YAPS127A) in adult mice is sufficient to improve heart regeneration and function and reduce scar size post-MI. YAP activation is also found to induce the expression of developmental genes in adult hearts, such as natriuretic peptide gene A (NPPA) and B (NPPB), myosin heavy chain 7 (MYH7), and oncostatin M (OSM), suggesting the dedifferentiation of cardiomyocytes (Del Re et al., 2013; Morikawa et al., 2015; Tian et al., 2015; Xin et al., 2011). Heallen *at al*. found that YAP phosphorylation is increased at the same time as neonatal mouse cardiomyocytes exit the cell cycle at postnatal day 8 (Heallen et al., 2013). To examine whether Hippo pathway modulation can extend the regenerative window beyond postnatal day 8 in mice, they conditionally deleted upstream Hippo regulators SAV1 and LATS1/2 in cardiomyocytes (Heallen et al., 2013). The deletion of SAV1 could significantly promote heart regeneration and reduced scar size following apex resection in postnatal mouse hearts (Heallen et al., 2013). In addition, the deletion of SAV1 or LATS1/2 in cultured adult cardiomyocytes can significantly increase cardiomyocyte cell cycle re-entry and proliferation (Heallen et al., 2013). Heallen *et al.* also tested the effect of Hippo modulation in an MI model and found that Hippo deficiency, induced by SAV1 conditional deletion, induced cardiac regeneration in 8-day-old and adult mice. Enhanced cardiomyocyte proliferation is believed to be responsible for the increased heart regeneration observed in SAV1 knockout mice (Heallen et al.,

2013). Collectively, these studies indicate that the inhibition of the Hippo pathway or YAP activation is required to induce cardiac regeneration.

Activated YAP translocates to the nucleus and binds to transcription factor TEAD to facilitate the transcription of the genes involved in cell proliferation and survival. Several studies have identified direct transcriptional targets of YAP. Lin *et al.* identified PIK3CB, an alpha catalytic subunit beta of phosphatidylinositol-3-kinase, as one of the YAP effectors that enhances cardiomyocyte proliferation and survival (Lin et al., 2015). Increased expression of PIK3CB activates AKT, a major component of the PI3K-AKT pathway, through which the Hippo pathway regulates cardiomyocyte proliferation (Lin et al., 2015). In addition to PIK3CB, YAP also drives the expression of other proliferative genes such as CTGF (connective tissue growth factor), CYR61 (cysteine-rich angiogenic inducer 61), and ANKRD1 (ankyrin repeat domain 1) (Haskins et al., 2014). Stress response genes, such as PARK2, have recently been shown as downstream targets of YAP to improve cardiomyocyte survival and recovery (Leach et al., 2017). PARK2 encodes a ubiquitin ligase associated with mitochondrial quality control and is capable of salvaging damaged mitochondria (Dorn Ii, 2016). The deletion of PARK2 in adult mice results in bigger scar size, dilated cardiomyopathy and reduced survival post-MI (Leach et al., 2017).

Recently, Leach *et al.* conditionally deleted SAV1 in the cardiomyocytes of mice with established ischemic HF and discovered signs of HF reversal in SAV1-deficient mice, but not in the control mice (Leach et al., 2017). SAV1-deficient hearts were found to have increased angiogenesis in the border zone, significantly reduced fibrosis, recovery of pumping ability compared to the controls. Adeno-associated virus serotype 9 (AAV9) mediated delivery of short hairpin RNA against SAV1 results in the restoration of cardiac function and cell cycle re-entry (Leach et al., 2017). This highlights the therapeutic potential of the Hippo pathway as a target for the treatment of heart diseases.

1.2.4 Hippo pathway regulation

Given its diverse biological effects in mammals, it is not surprising that the Hippo pathway responds to a myriad of upstream signals. For example, the Hippo pathway has been shown to respond to physical cues such as cell contact and mechanical signals to restrict tissue growth and modulate cell proliferation (Meng et al., 2016). Several studies have reported that increased cell-to-cell contact in confluent cultures results in the activation of LATS kinase, leading to YAP inactivation and decreased proliferation (B. Zhao et al., 2007). Additionally, increased adherens junctions (AJ) and tight junctions associated with higher cell density contribute to the phosphorylation of LATS kinase and the inactivation of YAP and TAZ (B. Zhao et al., 2007). Other cell density signals, such as α-catenin and E-cadherin, have been shown to regulate the Hippo pathway as well (Kim et al., 2011; Schlegelmilch et al., 2011). Ectopic expressions of α-catenin in murine epidermis reduced keratinocytes proliferation via interaction with 14-3-3 protein and promotion of YAP cytoplasmic sequestration (Schlegelmilch et al., 2011). E-cadherin, which promotes homophilic binding between two cells, interacts with the catenin complex and subsequently increases YAP cytoplasmic sequestration (Kim et al., 2011).

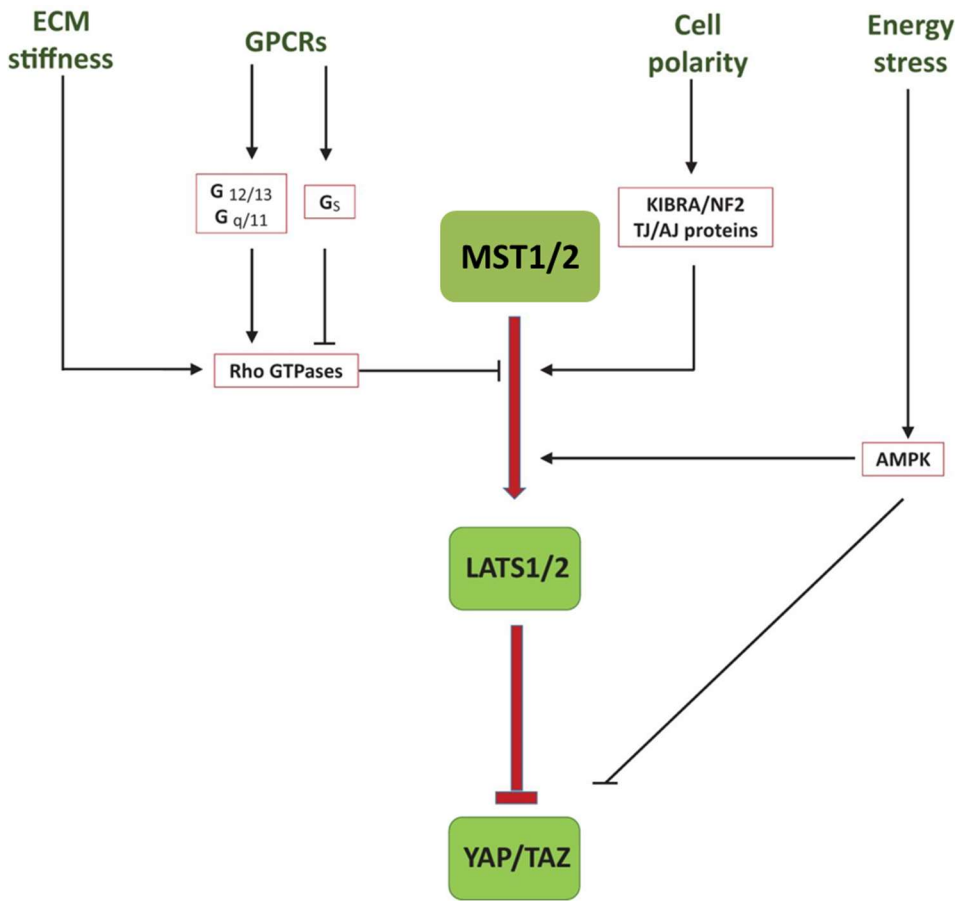

Figure 1.6 Summary of upstream regulators of the Hippo pathway. Regulation of the Hippo pathway by upstream signals. Cyclic stretch or high extracellular matrix stiffness inhibits LATS1/2 phosphorylation through Rho-GTPases. G-protein-coupled receptors (GPCRs) can either activate or suppress LATS1/2 depending on the types of the Gα proteins involved. The LATS1/2 activation is also controlled by cell polarity and architecture through KIBRA/NF2, adherens junctions (AJ), and tight junctions (TJ). Energy stress modulates YAP and TAZ activity via 5' adenosine monophosphate-activated protein kinase (AMPK).

In addition to cell density, mechanical signals, such as ECM stiffness, can be translated to biochemical stimuli which subsequently modulate YAP/TAZ (Meng et al., 2016). For example, Rho GTPases are the key modulators of the structure, function, and dynamics of cytoskeletal actomyosin, whereas actomyosin itself is a main cell component that responds to mechanical cues (Clark et al., 2007; Yu and Guan, 2013). In muscle cells, including cardiomyocytes, actomyosin, which comprises of F-actin and non-muscle myosin II, is critical for the modulation of contractility, cell shape, and tensile force (Murrell et al., 2015). Several studies have reported that the

inhibition of Rho and F-actin induces the cytoplasmic localisation of YAP and inhibits its transcriptional activity (Sorrentino et al., 2014; Zhao et al., 2012). On the contrary, increased actin polymerisation in Drosophila epithelial tissue promotes YAP activation and causes tissue overgrowth (Sansores-Garcia et al., 2011). Recently, Chakraborty *et al.* and Bassat *et al.* identified the role of Agrin, an ECM proteoglycan, in modulating the Hippo pathway (Bassat et al., 2017; Chakraborty et al., 2017). Physiologically, Agrin is required for the formation of neuromuscular junctions, and is also associated with the basal cell membranes of numerous other tissues, including the liver and the heart (Burgess et al., 2000; Chakraborty et al., 2015). In liver cancer, Agrin promotes oncogenesis and invasiveness of the cancer cells by antagonising LATS1/2 function and increasing YAP activity (Chakraborty et al., 2017). In the heart, Agrin is highly expressed in the ECM of neonatal hearts and is required for the robust regeneration that is observed in the early days after birth (Bassat et al., 2017). The administration of exogenous Agrin induces a substantial improvement in cardiac function post-MI with a modest, but significant, increase in cardiomyocyte proliferation (Bassat et al., 2017). This suggests that there are additional therapeutic mechanisms at play. Mechanistically, the data suggests that Agrin promotes YAP nuclear translocation through the disassembly of the dystrophin-glycoprotein complex (Bassat et al., 2017). Whether Agrin also acts by modulating the core components of the Hippo pathway in the heart is yet to be investigated.

Cell polarisation is the asymmetric organisation within cells that leads to distinct arrangements of cellular components along different axes and allows the development of specialised functions in complex organisms (Butler and Wallingford, 2017). Classical examples include epithelial cells, which display two key forms of cell polarity, apical-basal and planar cell polarity. The cellular components of epithelial cells are arranged specifically along the apical-basal (perpendicular) axis, leading to a defined apical membrane (facing the outer surface of the body or lumen of a cavity) and basal membrane (attached to basement membrane) (Butler and Wallingford, 2017; Meng et al., 2016). Some epithelial cells also have specialised structures that are distributed in a certain way within a plane of epithelial sheets, similar to the

orientation of fish scales or bird feathers (Butler and Wallingford, 2017). In Drosophila, major players in cell polarity, including Crumbs (Crb) homologs, the Scribble complex, αPKC, Merlin, Kibra, Expanded, Fat, and Dachsous have been implicated in Hippo pathway modulation (Schroeder and Halder, 2012). Crb modulates Hippo signalling by affecting YAP/TAZ localisation. It forms a complex with AMOT family proteins and other regulators which then interact with YAP/TAZ, thus, preventing its nuclear translocation (Chan et al., 2011). Crb can also work indirectly by increasing the kinase activity of Lats1/2 and subsequently promoting YAP/TAZ retention in the cytoplasm (Paramasivam et al., 2011). The hyperactivity of a Drosophila analogue of Yap, Yki has been reported in a Scribble complex mutant, which exhibits increased proliferation and cell survival (Doggett et al., 2011; Grzeschik et al., 2010). Kibra (Kbr) overexpression in Drosophila during eye development results in ectopic cell death and reduced eye size (Grzeschik et al., 2007). This indicates the function of Kbr as a tumour supressor gene. Further study suggests that Kbr modulates the Hippo pathway by forming a complex with Mer and Ex and activating the Hpo-Sav complex (Yu et al., 2010). The final result is Wts phosphorylation, which in turn promotes the cytoplasmic retention of Yki.

One of the major roles of the Hippo pathway is to modulate cell survival. Therefore, unsurprisingly, various stress signals, such as metabolic, oxidative, and endoplasmic reticulum stress, can modulate YAP and TAZ activities (Meng et al., 2016). Oxidative stressor hydrogen peroxide is capable of activating MST1, which in turn induces cell death in neurons (Lehtinen et al., 2006). On the other hand, YAP can physically interact with forkhead box O1 (FOXO1) to facilitate the transcription of catalase and manganese superoxide dismutase (MnSOD) genes, and thereby reduces the oxidative stress induced by ischemia-reperfusion injury (Shao et al., 2014). This suggests that the Hippo pathway may play an important role in reactive oxygen species (ROS) scavenging. Apart from oxidative stress, metabolic stress, induced by glucose deprivation, has been shown to induce the phosphorylation of YAP/TAZ via a crucial metabolic sensor AMPK (Deran et al., 2014). AMPK can directly phosphorylate YAP in several sites, interfere with YAP-TEAD binding, and subsequently inhibit TEAD-

mediated gene transcriptions (W. Wang et al., 2015). In addition, AMPK can act via angiomotin-like protein 1 (AMOTL1) phosphorylation, which in turn enhances LATS kinase phosphorylation and reduces YAP activity (Deran et al., 2014).

Finally, soluble factors, such as hormones and growth stimulating signals, can also modulate Hippo pathway activity. Two lipid molecules, lysophosphatidic acid (LPA) and sphingosine-1-phosphate (S1P), both of which can be found in serum, have been reported to increase nuclear YAP localisation via specific GPCR signalling (Miller et al., 2012; Yu et al., 2012). GPCRs are the largest family of transmembrane receptors in many species including worms, rodents, and mammals. They bind to a very diverse set of extracellular ligands, including drugs, hormones, neurotransmitters, and other proteins (Yu and Guan, 2013). GPCR activation can either inhibit or promote YAP activity depending on the coupled G-protein (Yu and Guan, 2013; Yu et al., 2012). GPCRs coupled to $G\alpha_{12/13}$, such as LPA and S1P receptors, $G\alpha_{q/11}$, and $G\alpha_{i/o}$, inhibit LATS and YAP phosphorylation via Rho GTPases (Yu et al., 2013). On the contrary, GPCRs coupled to $G\alpha_{s}$, such as glucagon and epinephrine receptors, inhibit Rho GTPases and thus increase LATS1 and YAP phosphorylation in a manner dependent on protein kinase A (PKA) (Yu et al., 2013; Yu et al., 2012). The elevation of GPCR expression leads to an aberrant increase in YAP activity and has been implicated in several diseases (Yu et al., 2014). For example, G-protein coupled estrogen receptor (GPER) expression is reported to be highly upregulated in breast cancer (Zhou et al., 2015). Furthermore, GPER activation by oestrogen increases the activity of YAP and TAZ, thus indicating the possible role of the Hippo pathway in breast tumorigenesis. The regulation of YAP/TAZ by GPCRs implies that the Hippo pathway can be modulated by a diverse set of molecules and opens the possibility of targeting by GPCR agonists or antagonists for disease intervention.

1.3 MiRNA as a potential novel modulator of the Hippo pathway

MiRNAs have recently emerged as a potential regulator of cardiomyocyte regeneration due to their ability to modulate gene expression. This section will

explore whether miRNAs can be used to target the Hippo pathway and enhance cardiac regeneration.

1.3.1 The biology of miRNAs

MiRNA is defined as a class of small non-coding RNA (21-30 nucleotides) and is associated with the Argonaute family protein to modulate gene expressions. It was first discovered in *C. elegans* two decades ago and was found in mammals a decade later. miRNAs are evolutionarily conserved across species (Hydbring and Badalian-Very, 2013). Their roles in physiological and pathological conditions have been heavily investigated ever since. In addition to miRNA, short interfering RNA and PIWI-interacting RNA constitute two other classes of small non-coding RNAs (Hodgkinson et al., 2015). The sequences of most miRNAs in humans are located in the intergenic region, while a minority of them are annotated in intronic regions. The remaining miRNAs are encoded in the exonic region. The majority of miRNAs are transcribed by RNA polymerase II as long primary transcripts (primary miRNAs/pri-miRNAs). RNA polymerase III is responsible for the transcription of a small minority of miRNAs, especially those which are associated with Alu repeats (Borchert et al., 2006). Pri-miRNAs have relatively longer sequences (approximately 1 kb) and a stem-loop structure in which mature miRNA sequences are located. They are then cleaved by a complex called Microprocessor, which is formed by RNAse III Drosha and its cofactor DiGeorge syndrome critical region 8 (DGCR8, Figure 1.5) (Gregory et al., 2004). The results are ~65 nucleotide-long hairpin-shape RNAs called pre-miRNAs. From the nucleus, pre-miRNAs are exported to the cytoplasm by a member of the Ran-dependent nuclear transport receptor family, called Exportin-5 (Yi et al., 2003). Pre-miRNAs are subsequently cleaved by a second RNAse III enzyme, called Dicer, near the terminal loop, resulting in small RNA duplexes (Ketting et al., 2001). The next step is binding between a small RNA duplex and an argonaute (AGO) family protein to form a complex called a pre RNA-induced silencing complex (pre-RISC) (Chendrimada et al., 2005). In humans, the AGO protein family has four homologs, AGO1-4, and all of them can interact with miRNA or siRNA duplexes (Hammond et al., 2001). In flies,

miRNA duplex tends to form a complex with AGO1 and a siRNA duplex with AGO2 (Tomari et al., 2007). miRNA duplex in a pre-RISC then undergoes an unwinding process to remove the passenger strand to generate a mature RISC. There is no strict criteria for selecting which duplex is going to be the mature strand. However, the thermodynamic stability of the strand has been shown to be an important factor in strand selection. The stability of a miRNA duplex is determined by the degree of pairing, which means that the duplex with the most base pair mismatch, gaps, or bulges will be the most unstable one. The strand with a relatively unstable 5'end will likely be chosen as the mature strand and the remaining passenger strand is normally degraded. However, it has been reported that in minority cases, a passenger strand can still be loaded into RISC and therefore remains active (Khvorova et al., 2003).

As mentioned above, the biological effect of miRNA is carried out through gene expression modulation. This happens at the post-transcriptional level in which miRNA can repress translation or promote mRNA degradation (Guo et al., 2010). miRNA in RISC functions as a guide to the 3' untranslated region (UTR) of a target mRNA. A single miRNA can target multiple genes and a single gene can be targeted by several miRNAs (Liu et al., 2012). Furthermore, to target a certain gene, a complete pairing between miRNA and its target is not required. These are the reasons why it is very difficult to predict miRNA targets comprehensively. One factor that is considered essential in predicting an miRNA target is seed matching. Seed matching is a perfect complementarity between the seed sequence of miRNA (nucleotide 2 – 8 from the 5' end of a miRNA) and the target transcript (Wang, 2014).This variable has been used widely in bioinformatics tools which predict miRNA target sites. In addition to seed sequence, other variables such as the degree of miRNA conservation across species and miRNA GC content are also considered in the database (Brennecke et al., 2005). However, despite the addition of other variables, the results of bioinformatics predictions have a high rate of false positives (Liu et al., 2012). This suggests that when conducting an miRNA study, any conclusion should not be based solely on bioinformatics data, but must be confirmed by a laboratory experiment.

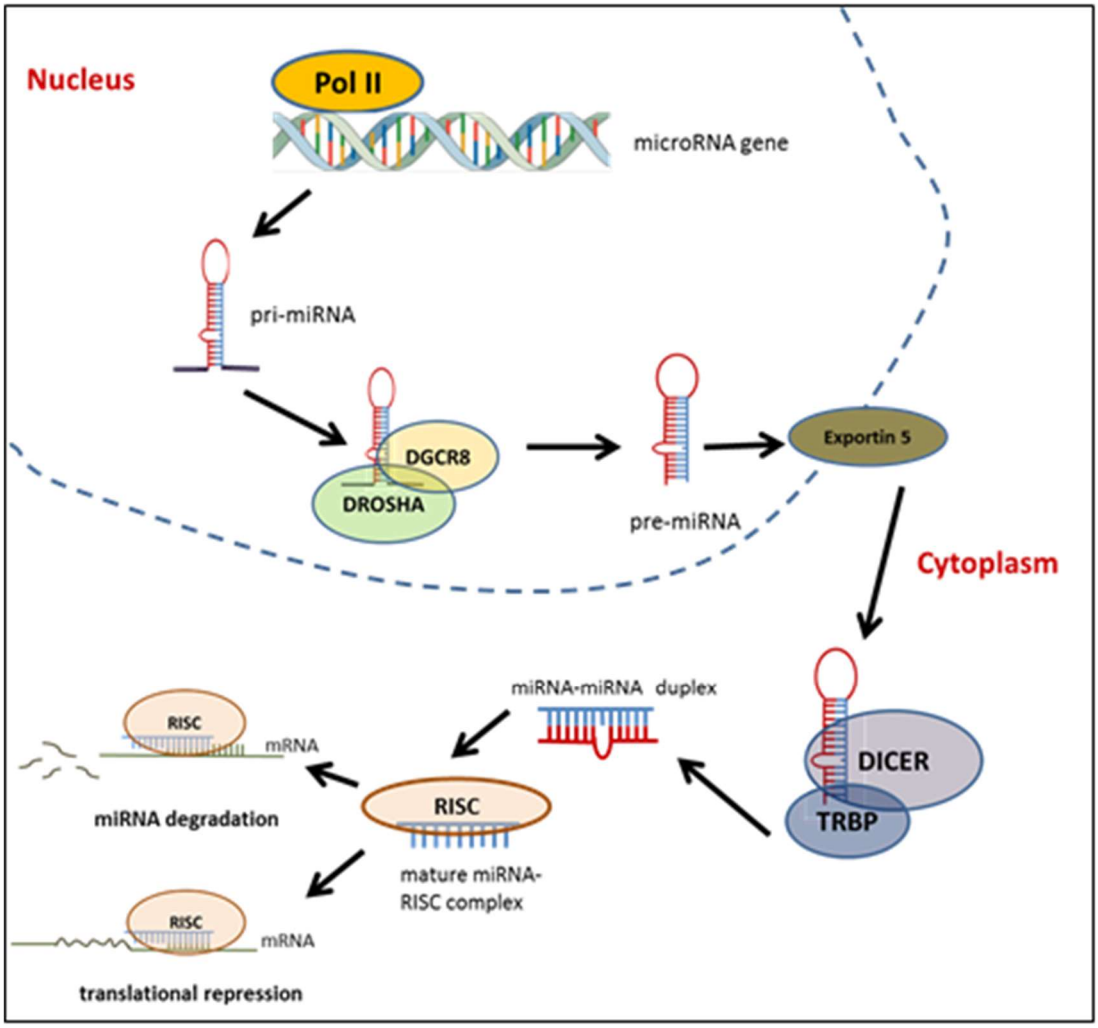

Figure 1.7 mirRNA synthesis in animals. MiRNAs are transcribed by RNA polymerase II (Pol II) as long primary miRNA (pri-miRNA). Pri-miRNAs are then cleaved by the RNAse III Drosha and DGCR8, resulting in hairpin-shaped precursor miRNAs (pre-miRNA). Pre-miRNAs are exported by the Exportin 5 protein to the cytoplasm where they are further cleaved by the RNAse III enzymes DICER and the RNA-binding protein (TRBP), yielding miRNA duplexes with imperfect matching. One of the strands from a miRNA duplex becomes a mature miRNA, which is then incorporated into the RNA-induced silencing complex (RISC). miRNAs in the RISC complexes recognise their targets based on nucleotides 2-8 from the 5' end of a miRNA (seed sequence). The association between a miRNA-RISC complex and its target results in mRNA degradation or translational inhibition. Adapted from van Rooij and Olson. (Van Rooij and Olson, 2012).

1.3.2 The role of miRNA in the heart

Embryonic cardiogenesis involves the transformation of a linear cardiac crescent to a fully developed heart with defined septation. These processes require the coordinated orchestration of cell proliferation and apoptosis, migration, and

differentiation. The importance of miRNAs in cardiac development and function was first reported by loss of function studies of miRNA processing enzymes, Dicer and DGCR8 (Table 1.3). Dicer and DGCR8 are required for miRNA synthesis in general; therefore, studies on either protein provide significant insight into the broad functions of miRNAs in cardiac development. It was initially difficult to investigate the role of miRNA in embryonic development as global deletion of Dicer in mice resulted in lethality at a very early stage of development (Bernstein et al., 2003; Yang et al., 2005). However, the creation of conditional knockout, which allows spatiotemporal flexibility in gene deletion, has made it possible to investigate the role of certain genes at specific organs or periods. Conditional knockout of Dicer using a Cre recombinase gene inserted into the 3' untranslated region (3' UTR) of the cardiac homeobox gene Nkx2-5 provides evidence that miRNAs are very important in cardiac outflow tract morphogenesis and chamber septation (Stanley et al., 2002). Dicer mutant mice die prematurely at postnatal day 4 and display severe left ventricular dilation, abnormal sarcomere architecture and severe HF. The deletion of DGCR8, an important protein for miRNA transcription, in mice results in similar structural and functional abnormalities which also lead to premature death at 2 months of age (Rao et al., 2009).

Recent research has successfully shown that specific miRNAs are also crucial for cardiac development (Table 1.3). For example, the deletion of muscle-specific miRNA, miR-1 family, in Drosophila disrupts the normal cardiac and somatic muscle patterning. In mice, the targeted deletion of miR-1-2, a member of the miR-1 family results in embryonic lethality due to structural anomalies (ventricular septal defects), arrhythmia, and cardiac dilation (Y. Zhao et al., 2007). Chiavacci *et al.* found that miR-218 mediated the effect of the TBX5 gene, a member of the T-box gene family, to regulate cardiomyocyte proliferation and development. The overexpression of miR-218 leads to incomplete cardiac looping and impaired atrial and ventricular formation (Chiavacci et al., 2012).

Table 1.3 Summary of miRNA roles in the development of the heart

miRNA	Mouse model	Phenotypes
miRNA processing enzymes (Dicer)	Global KO	Embryonic lethality (Bernstein et al., 2003; Yang et al., 2005)
	cKO	Premature death (P4), severe left ventricular dilation, abnormal sarcomere architecture, severe HF (Stanley et al., 2002)
DGCR8	cKO	Premature death at 2 months old, left ventricular malfunction, dilated cardiomyopathy (Rao et al., 2009)
miR-1-2	cKO	Embryonic lethality, ventricular septal defect, cardiac dilation (Chiavacci et al., 2012)
miR-128	Global TG	Incomplete cardiac looping, impaired atrial and ventricular formation in zebrafish (Chiavacci et al., 2012)

In adult mice, a variety of miRNAs (Table 1.4) have been shown to modulate several pathological processes in the heart, including pathological hypertrophy, cardiac fibrosis (miR-21 & miR-29), and cardiac conduction abnormalities (miR-328) (Bang et al., 2014; Dangwal and Thum, 2014). An alteration in cardiac miRNA expression profile is observed in response to pathological stimuli such as chronic hypertension, maladaptive hypertrophy, and cardiac pump failure. For example, the expression of the miR-212/132 family is relatively low in the normal heart, but increased substantially in human HF and animal models. It is hypothesised that the miR-212/132 family can promote the activity of the pro-hypertrophic calcineurin/NFAT pathway by targeting antihypertrophic transcription factor forkhead box O3 (Ucar et al., 2012). Two miRNAs that are crucial in heart

development, miR-1 and miR-133, have been shown to be associated with cardiac hypertrophy. Both miR-1 & miR-133 are downregulated in HF (Care et al., 2007). The overexpression of miR-133 is reported to inhibit hypertrophy, whereas its suppression promotes hypertrophy. An *in vivo* study using a miR-133 antagonist led to the development of marked hypertrophy and therefore further confirms the initial finding (Care et al., 2007). It is hypothesised that miR-1 modulates the hypertrophy pathway by reducing the level of calcium-calmodulin signalling and thus attenuating the calcineurin/NFAT pathway (Ikeda et al., 2009), whereas miR-133 induces hypertrophy via the β1-adrenergic pathway (Castaldi et al., 2014).

Table 1.4 Modulation of specific miRNAs in cardiovascular diseases

miRNA	Mouse model	Phenotypes
miR-21	antimiR	Reduced interstitial fibrosis, reduced hypertrophy in response to TAC (Thum et al., 2008)
miR-21-3p (derived from cardiac fibroblasts' exosomes)	antimiR	Reduced heart weight/body weight ratio, reduced cardiomyocyte size in angiotensin II induced hypertrophy (Bang et al., 2014)
miR-328	overexpression with adenoviral vector	Alleviate atrial fibrillation (AF), improved cardiac function in dog and mouse models of AF (Lu et al., 2010)
miR-212/132 family	cTG	Reduced life expectancy, cardiac hypertrophy, HF (Ucar et al., 2012)
	antimiR-132	Reduced hypertrophy, improved cardiac function in TAC-induced hypertrophy (Ucar et al., 2012)
miR-1	overexpression with adenoviral vector	Reduced cardiomyocyte hypertrophy in phenylephrine-induced hypertrophy model (*in vitro*) (Care et al., 2007)
miR-133	overexpression with adenoviral vector	Reduced cardiomyocyte size in phenylephrine or endothelin-1- induced hypertrophy (*in vitro*) (Care et al., 2007)
	antimiR	Increased LV/body weight ratio, Increased LV mass index
	overexpression with adenoviral vector	Reduced cardiomyocyte size and fetal gene expression in cardiac hypertrophy model induced by AKT overexpression (Care et al., 2007)

1.3.3 The role of miRNA in cardiomyocyte proliferation and regeneration

As discussed in the previous section, miRNAs are critical for cardiomyocyte proliferation and development. Furthermore, various studies have identified several miRNAs that may be involved in cardiomyocyte cell cycle exit and have shown that the modulation of these miRNAs may be used to induce cardiomyocyte proliferation in the adult heart (Table 1.5). Porrello *et al.* compared miRNA expression profiles in mouse ventricles at P1 and P10 and found that the expression of the miR-15 family, which consists of 6 members: miR-15a, miR-15b, miR-16-1, miR-16-2, miR-195, and miR-497, was upregulated at P10. The upregulation of one of the miR-15 family members, miR-195, *in vivo* causes a reduction in cardiomyocyte proliferation and the repression of mitotic genes. On the other hand, the administration of antimiRs against other members of the miR-15 family (miR-15b and miR-16) can significantly induce cell cycle re-entry in postnatal hearts. Moreover, the inhibition of the miR-15 family in adult mice can significantly enhance cardiac regeneration post-MI. These findings suggest that the miR-15 family is critical in post-natal cardiac mitotic arrest (Porrello et al., 2011a; Porrello et al., 2013).

Huang *et al.* performed a similar screening of miRNA expression profiles in mouse cardiac ventricles at P1, P7, and P28 and identified miR-128 as a novel modulator of cardiomyocyte cell cycle exit (Huang et al., 2018). Loss and gain of function studies revealed that miR-128 overexpression in mice results in premature cell cycle exit, compensatory pathological hypertrophy, and impaired cardiac function soon after birth. On the other hand, cardiomyocyte-specific knockout of miR-128 induces cardiomyocyte cell cycle re-entry in postnatal hearts (P14) and protects adult hearts against MI (Huang et al., 2018). In addition to the miR-15 family and miR-128, miR-34a expression is also upregulated at P7 and after induction of MI in adult mice. Treatment with antimiR-34a increases cardiomyocyte proliferation, reduces cardiomyocyte death and infarct size, and improves cardiac function post-MI (Yang et al., 2015a).

Table 1.5 Several miRNAs that can be used to enhance cardiac regeneration

miRNA	Mouse model	Route of delivery	Phenotypes post-MI	Side effects
miR-302/367 cluster	miRNA mimics	Systemic injection via tail vein, daily for 7 days after MI	Reduced infarct size, improved function, increased cardiomyocyte proliferation, reduced apoptosis post at 50 days after MI	No abnormalities in the lung, liver, and intestines (Tian et al., 2015)
	Conditional cKO	-	Reduced fibrotic scar, increased cardiomyocyte proliferation	Ventricular dilation, reduced cardiac function 3 weeks after MI (Tian et al., 2015)
miR-199a	AAV9	Intramyocardial injection	Increased cardiomyocyte proliferation, improved cardiac function	Not reported (Eulalio et al., 2012)
	miRNA mimics	Intramyocardial injection	Reduced infarct size, improved cardiac function, increased proliferation	Not reported (Lesizza et al., 2017)
	AAV6 (pig model)	Intramyocardial injection	Reduced scar size, marked improvement in global and regional contractility, increased muscle mass	Poor differentiation of new cardiomyocytes, sudden arrhythmic death (Gabisonia et al., 2019)
miR-590	AAV9	Intramyocardial injection	Increased proliferation, enhanced cardiac function	Not reported (Eulalio et al., 2012)
	miRNA mimics	Intramyocardial injection	Reduced infarct size, improved cardiac function, increased proliferation	Not reported (Lesizza et al., 2017)
miR-19a/19b	miRNA mimics	Intramyocardial injection	Improved ejection fraction and fractional shortening, increased cardiomyocyte proliferation	Not reported (Gao et al., 2019)

	miRNA mimics	Systemic injection via tail vein	Reduced scar size, improved cardiac function	Not reported (Gao et al., 2019)
	AAV9	Intramyocardial injection	Reduced infarct size, preserved cardiac function	Not reported (Gao et al., 2019)
miR-15 family	antimiR	Systemic via subcutaneous injection	Increased adult cardiomyocyte proliferation, improved cardiac function post-MI	Not reported (Porrello et al., 2013)
miR-128	inducible, cardiomyocyte-specific deletion	-	Increased cardiomyocyte dedifferentiation and proliferation, reduced infarct size, enhanced ejection fraction and fractional shortening, attenuated cardiac remodelling	Not reported (Huang et al., 2018)
miR-34a	antimiR	Intravenous injection	Reduced fibrotic area, improved cardiac function, increased proliferation	Not reported (Yang et al., 2015a)

Eulalio *et al*. used a high-content, high-throughput screening to screen the whole miRNAs in the library for their proliferative properties. They successfully identified 40 potential candidates and from these 40 miRNAs, miR-199a and miR-590 were reported to induce cell cycle re-entry and cytokinesis in cultured adult cardiomyocytes. AAV9-mediated delivery of miR-199a or miR-590 in an MI model resulted in reduced infarct size and fibrosis, and a substantial enhancement in cardiac regeneration and function (Eulalio et al., 2012). Gao *et al.* tested the ability of miR19a/19b, members of the miR-17-92 cluster, to stimulate cardiac regeneration (Gao et al., 2019). MiRNAs that regulate cardiomyocyte proliferation in the developing heart, such as miR-17-92 clusters, can potentially be used to enhance regeneration in the adult heart. The overexpression of miR19a/19b in adult mice lessens MI-induced cardiac damage and preserves cardiac function. Together, these

studies highlight the potential of miRNA modulation to induce cardiac regeneration following MI.

To enhance cardiac regeneration, miRNAs target multiple genes involved in the regulation of cardiomyocyte proliferation and survival. Several miRNAs have been shown to target genes involved in cell cycle regulation. For example, miR-195 directly targets Check1, a protein that promotes chromosome segregation and cytokinesis, to induce cardiomyocyte cell cycle re-entry in postnatal hearts (Porrello et al., 2011a). On the other hand, Eulalio *et al.* found that miR-199a and miR-590 do not target cell cycle regulators, but instead target the proteins HOMER1 and HOP homeobox, which are associated with cardiomyocyte calcium signalling and embryonic cardiomyocyte proliferation, respectively. MiRNAs are capable of targeting multiple genes and are thus very likely to target multiple cellular functions. For example, miR-34a has been reported to target genes that mediate cell cycle progression (Cyclin D1) and apoptosis (BCL2 and SIRT1). Similarly, Gao *et al.* found that miR-19a/19b enhanced cardiomyocyte survival by targeting the proapoptotic gene BIM1 (Gao et al., 2016) and the prosurvival gene PTEN (Mavrakis et al., 2010), and alleviated inflammation by targeting cytokine suppressor SOCS1 (Gao et al., 2019). These studies suggest that although many studies only highlight one or two miRNA target genes, miRNAs are capable of modulating multiple cellular functions to achieve cardiac regeneration.

1.3.4 Therapeutic potential of miRNAs in cardiovascular diseases

Based on the discussion in the previous section, it is clear that specific miRNAs are differentially expressed under certain pathological stress. These miRNAs are often associated with the pathological process itself, which makes them a promising therapeutic target. Based on this reasoning, the overexpression or inhibition of miRNA expression can be used to modify the pathological processes and thus halt or restrict the progression of diseases. Several studies have used viral vectors to deliver miRNA overexpression or deletion constructs due to its relatively high delivery efficiency (Zacchigna et al., 2014). AAV9 is commonly used in preclinical studies in cardiac diseases because, in addition to efficient delivery, it has the propensity to

infect cardiomyocytes (cardiac tropism) and the capability to drive the transgene expression for long periods of time without invoking an inflammatory response. AAV9 use in animal studies has allowed the phenotypic assessment of miRNA modulation *in vivo*. Recently, however, the prolonged overexpression of pro-regenerative miRNAs driven by AAV9 has been associated with severe adverse effects such as dilated cardiomyopathy and HF (Gabisonia et al., 2019; Tian et al., 2015). This finding poses a significant barrier for the application of viral-mediated delivery of miRNAs in humans.

The administration of synthetic miRNA analogues (mimics) or inhibitors (antimiR) using non-viral vectors can be an alternative to viral-mediated delivery of miRNA transgenes to reverse the ongoing pathological process in cardiac diseases. Non-viral vectors that are commonly used to deliver mimics or antimiRs are nanoparticles such as polyethilenimine (PEI) and lipid-based compounds (liposomes). Mimics and antimiRs are soluble in water or saline solution and are therefore suitable for systemic injection via an intravenous, subcutaneous, or intraperitoneal route. Site-specific delivery, such as intramyocardial or intracoronary injection, has also been simulated before with no apparent adverse effects (Zhang et al., 2013). After injection, circulating mimics, or antagomirs, can be taken up directly by the cells and subsequently bind to their target mRNAs.

Naked RNAs are unstable and have a very short half-life in the blood, primarily due to the degradation by nucleases. Therefore, the administration of miRNA mimics, with their structure being required to be as similar as possible to the endogenous miRNA, is initially thought to have little therapeutic value. Several studies have shown that the delivery of miRNA mimics by non-viral vectors can induce transient miRNA overexpression. Tian *et al*. reported that daily systemic administration of miR-302-367 mimics was sufficient to induce a proliferative response post-MI in mice (Tian et al., 2015). Similarly, Lesizza *et al.* recently showed that intramyocardial injection of miR-199a and miR-590 mimics can successfully induce miRNA overexpression that lasts for 12 days and that this duration is sufficient to induce cardiac regeneration post-MI (Lesizza et al., 2017). In contrast to miRNA mimics, antimiR structures have

been subjected to various modifications to increase stability and cellular uptake. An example of this modification is the addition of a cholesterol construct or unconjugated phosphorothioate via an 2'-O-methyl (2'-OMe) group to increase antimiR stability and efficiency (Broderick and Zamore, 2011; Krutzfeldt et al., 2005; Thum et al., 2008).

In addition to studies by Tian *et al.* and Lesizza *et al.*, several preclinical studies using either mimics or antimiRs have shown potential in treating cardiovascular diseases. In an MI model, the transient delivery of miR19a/19b mimics or antimiR-34a is capable of inducing significant enhancement in cardiac regeneration and function post-MI (Gao et al., 2019; Yang et al., 2015a). Systemic administration of antimiR-21 in a mouse model of hypertension reduces cardiac interstitial fibrosis and cardiac dysfunction (Thum et al., 2008). Sepramaniam *et al*. reported that the administration of antimiR-320a in a mouse model of stroke succesfully reduced infarct volume and cerebral oedema (Sepramaniam et al., 2010). Furthermore, two miRNA-based therapeutics, antimiR-122 and miR-34 mimics, have progressed to the early stages of clinical trials (Hydbring and Badalian-Very, 2013). AntimiR-122 is currently in a phase II clinical trial for the hepatitis C infection, and miR-34 mimics are curently in a phase I clinical trial for hepatocellular carcinoma. Collectively, these studies highlight the potential of the administration of mimics or antimiRs as a novel therapeutic approach for CVDs.

Despite the promising results, the development of miRNA-based therapeutics still faces several challenges. Due to its ability to target multiple genes, miRNA treatments can produce off-target effects. Furthermore, non-viral vectors lack organ specificity and the injected miRNAs can thereby end up in other organs. Given that many pro-regenerative miRNAs have been associated with cancers (Lee and Dutta, 2009), their effects in non-target organs need to be investigated. In conclusion, the reversal of the pathological process by the administration of mimics or antagomirs may offer a promising approach to treat CVDs. However, more research is required to ensure the safety and efficacy of this therapeutic approach in humans.

1.4 Targeting the Hippo signalling pathway with miRNAs to enhance cardiac regeneration

The inhibition of the Hippo pathway has been shown to enhance endogenous cardiomyocyte proliferation and stimulate cardiac regeneration and repair post-MI. However, targeting the pathway is difficult due to the lack of understanding of its upstream regulators. Recent studies have uncovered a connection between miRNAs and the Hippo pathway. The overexpression of the miR-302/367 cluster in adult mice leads to increased cardiac regeneration, improved cardiac proliferation and survival, and reduced apoptosis. Mechanistically, miR-302/367 suppresses the expression of Hippo core components MST1, LATS2, and MOB1B, which subsequently promotes nuclear YAP translocation and thus induces cell proliferation (Tian et al., 2015). Conversely, miRNAs have also been identified as downstream targets of the Hippo pathway. In Drosophila, Hippo-deficient cells are reported to show elevated *bantam* miRNA (a miRNA encoded by *bantam* gene) activities, which mediate cell growth and survival (Nolo et al., 2006). In mice, YAP can increase the expression of miR-206, which subsequently mediates cardiac hypertrophy and survival (Yang et al., 2015b). Collectively, these studies highlight the interactions between miRNA and the Hippo pathway in mediating cardiomyocyte proliferation and survival.

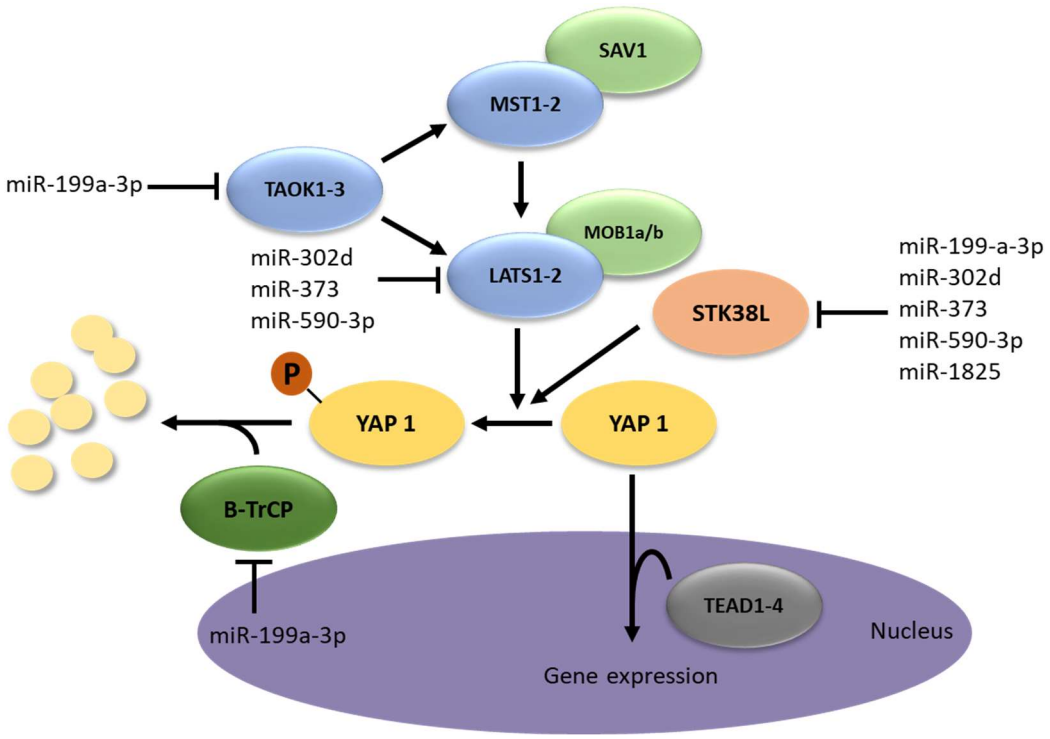

Figure 1.8 Pro-regenerative miRNAs target different pathways to converge on the Hippo pathway.miR-199a-3p targets YAP inhibitors TAOK1-3, STK38L, and ubiquitin ligase B-TrCP to increase YAP activation. The miR-590-3p and miR-302/367 cluster (miR-302d & miR-373) targets LATS and STK38L to enhance YAP activation. miR-1825 targets STK38L to inhibit YAP phosphorylation. Adapted from Torrini *et al.* (Torrini et al., 2019)

Several miRNAs that have previously been shown to induce cardiomyocyte proliferation have been described as targeting different genes. However, whether they act through multiple or specific pathways has not been thoroughly investigated. Torrini *et al.* recently found that previously identified pro-regenerative miRNAs act via different pathways before finally converging on YAP activation (Torrini et al., 2019). For example, miR-199a and miR-590, which were previously reported to target HOMER1 and the HOP homeobox protein, also targets the upstream YAP inhibitor, TAOK1-3 and STK38L (Figure 1.8), respectively (Eulalio et al., 2012; Torrini et al., 2019). Diez-Cunado *et al.* screened 875 human miRNAs for their ability to enhance the proliferation of human iPSC-derived cardiomyocytes (hIPSC-CM) and identified 96 pro-regenerative miRNAs (Diez-Cunado et al., 2018). Further analysis indicates that the majority of these miRNAs (67 out of 96) target the Hippo pathway and that their activity depends on increased YAP nuclear translocation. Other than the Hippo pathway, pro-regenerative miRNAs also target the Wnt/β-catenin and Notch

pathways. Both the Wnt/β-catenin and Notch pathways act downstream of the Hippo signalling pathway (Heallen et al., 2011). Together, these findings further highlight the importance of the Hippo pathway in mediating cardiomyocyte proliferation and demonstrate that targeting the Hippo pathway with miRNAs can serve as a novel therapeutic approach to enhance cardiac regeneration.

1.5. Summary of literature review

As the improvement of acute MI management leads to increased survival rates, a growing number of patients are at risk of developing heart failure at some point after an acute MI episode. This is due to the adverse cardiac remodelling, which is triggered by the failure of the adult human heart to replace the cardiomyocyte loss during MI. Current HF treatments alleviate symptoms and prolong survival, but are unable to reverse the remodelling process and address the primary cause of HF - the loss of cardiomyocytes. Stem cell transplantation has been developed to replace the lost cardiomyocytes post-MI. However, evidence shows that the administered cells fail to differentiate into cardiomyocytes. Moreover, several challenges, such as the selection of appropriate cell types and delivery routes, increased risk of arrhythmia and teratoma formation, and the hostile conditions in the infarcted tissue still need to be addressed in order to enhance the benefits of stem cell therapies. Recent studies have established that the endogenous renewal capacity of the adult human heart is measurable yet inadequate to respond in the event of extensive damage, such as MI. This finding suggests that enhancing the endogenous cardiac regenerative capacity can be a novel therapeutic approach for cardiac repair.

Recent discoveries have indicated that the inhibition of the Hippo pathway, a kinase cascade crucial for tissue growth control, can induce a robust self-reparative capacity post-MI. The activation of Hippo effector YAP significantly reduces infarct size and improves cardiac function post-MI. Furthermore, the inhibition of SAV1, one of the core kinases of the Hippo pathway, in mice with established ischemic heart failure can reverse the HF progression by reducing fibrosis, increasing scar border vascularity, and inducing the recovery of cardiac function. However, despite these

potentials, efforts to translate research on the Hippo pathway for treating patients are hampered by the lack of targetable regulators in the core Hippo pathway and the lack of knowledge on upstream Hippo regulators.

MiRNAs, small non-coding RNAs that can be used to modulate gene expressions, have recently garnered a lot of interest due to their potential for treating diseases, such as hepatitis C and cancers. Previous investigations have identified several miRNAs that can be used to target the Hippo pathway and improve cardiac structure and function post-MI. However, the number of these miRNAs is relatively small compared to the size of the miRNA library. Moreover, some miRNAs have subsequently been shown to cause severe adverse effects in animal models. For example, short-term overexpression of the miR-302/367 family and miR-199a in mice and pigs, respectively, enhances regeneration and recovery post-MI, but induces dilated cardiomyopathy and sudden arrhythmic death in the long-term (Gabisonia et al., 2019; Tian et al., 2015). Thus, it is important to find novel miRNAs that modulate the Hippo pathway and potentially can be targeted to induce cardiomyocyte regeneration. This project, therefore, will address this need.

1.5 Hypothesis

The Hippo pathway is strongly involved in the regulation of cardiomyocyte regeneration and survival and appears to be a promising target to enhance cardiac regeneration post-MI. Given that miRNAs are capable of modulating gene expression, including those related to the Hippo pathway, it is hypothesised that the identification of novel miRNA(s) that can to modulate the Hippo pathway will lead to the finding of novel factor(s) which are important in mediating cardiac regeneration.

1.6 Aims

1. To screen and identify candidate miRNA(s) that can modulate the Hippo pathway and increase YAP activity
2. To examine whether the candidate miRNA(s) can induce cardiomyocyte proliferation *in vitro* and *in vivo*
3. To investigate the effects of treatment with the candidate miRNA(s) in myocardial infarction models in mice
4. To investigate the mechanisms by which the candidate miRNAs mediate cardiac regeneration

CHAPTER 2

General materials and methods

Chapter 2 - General Materials and Methods

2.1 Materials

2.1.1 Primers used for quantitative polymerase chain reaction (PCR)

Primers used in this project were purchased either from Applied Biosystems or Qiagen (Table 2.1), or ordered from Sigma (Table 2.2).

Table 2.1 List of Taqman (Applied Biosystems) and Quantitect (Qiagen) primers used in this project.

Target miRNA or gene	Species	Assay ID
miR-186-5p	human, mouse, rat	002285 (Taqman)
miR-204-5p	human, mouse, rat	000508 (Taqman)
miR-25-5p	human, mouse, rat	000403 (Taqman)
miR-181a-5p	human, mouse, rat	000480 (Taqman)
miR-411-5p	human, mouse, rat	001610 (Taqman)
GAPDH	mouse	Mm_Gapdh_3_SG (Qiagen)
GAPDH	rat	Rn_Gapd_1_SG (Qiagen)

Table 2.2 List of primers and primer sequences ordered from Sigma. Rn = rat, Mm= mouse

Target gene	Species	Forward sequence	Reverse
LATS1	Rn	AAAGCCAGAAGGGTACAGACA	CCTAAGGGATTCTCGGATCTC
	Mm	AAAGCCAGAAGGGTACAGACA	CCTCAGGGATTCTCGGATCTC
LATS2	Rn	GGACCCCAGGAATGAGCAA	CCCTCATAGTTTGCACCGCC
	Mm	GGACCCCAGGAATGAGCAG	CCCTCGTAGTTTGCACCACC
MST1	Rn	TTATTCGGCTCCGAAACAAGA	GGCCTGCGACTCCAAAGTCTG
	Mm	TCATTCGGCTACGGAACAAGA	GACCTGCGACTCCAAAGTCTG
MST2	Rn	CCGGGTCCGTTTCAGACATAA	GCGTTTTGCCATCGTGTCTGTT
	Mm	CGGGGTCCGTTTCAGACATAA	GCGTTTTGCCATTGTATCTGTT
SAV1	Rn	CTGTCCCGCAAGAAAACCAAA	AATGAAGGCATGAGATTCCGC
	Mm	CTGTCCCGCAAGAAAACCAAA	AATGAAGGCATGAGATTCCGC
MOB1A	Rn	AGCAGGTCCCAGGTATGAATA	TCAAGCTGATCCTGAACCCAA
	Mm	GGCAGGTCCCAGGTATGAATA	TCAAGCTGATCCTGAACCCAA
MOB1B	Rn	ATGAGCTTCTTGTTTGGTAGTCG	ATAACGGCCATCCGCAGGTTG
	Mm	ATGAGCTTCTTGTTTGGTAGTCG	ATGACAGCCATCCGTAGGTTG
YAP1	Rn	ACCCTCGTTTTGCCATGAAC	TGTGCTGGGATTGATATTCCGTA
	Mm	ACCCTCGTTTTGCCATGAAC	TGTGCTGGGATTGATATTCCGTA
TAZ	Rn	CGTGGCGGAAAAAGATCCTCC	GTCGGTCACGTCATAGGACTG
	Mm	CATGGCGGAAAAAGATCCTCC	GTCGGTCACGTCATAGGACTG
BNIP3	Rn	TCCTGGGTAGAACTGCACTTC	GCTGCGCATCCAGCAGTATTT
	Mm	TCCTGGGTAGAACTGCACTTC	GCTGGGCATCCAACAGTATTT
SPRY4	Rn	GCGGCGTCCCTTTGAATCC	GCGGCGTCCCTTTGAATCC
	Mm	GCAGCGTCCCTGTGAATCC	TCTGGTCAATGGGTAAGATGGT

CDH2	Rn	AGCGCGGTCTTACCGAAGG	TCACTGCTTTCATACTGAACTTT
	Mm	AGCGCAGTCTTACCGAAGG	TCGCTGCTTTCATACTGAACTTT
MAP3K1	Rn	CGCCCTGCCCATCTACTTC	CTCCATCTCTCGACCGGAGG
	Mm	CGCCCTGCCCATCTACTTC	CTCCATCTCTCGACCGGAGG
DAAM2	Rn	GTGACCTTCCTGAGATTGAC	CTCTGCGAAGCAGACGTTGAG
	Mm	GTGACCTTCCCGAGATCGAC	CTCTGCAAAGCGGACATTGAG
WNT7A	Rn	GACTTCTCTTCGGTTGTGGC	TGAAACTGACACTCGTCCAGG
	Mm	GGCTTCTCTTCGGTGGTAGC	TGAAACTGACACTCGTCCAGG
WNT10B	Rn	GAAGGGCAGCGGTGAGCAGGA	GATTACAGCCACCCCATTCC
	Mm	GAAGGGTAGTGGTGAGCAAGA	GGTTACAGCCACCCCATTCC
MAP2K1	Rn	AAGGTGGGAGAGTTGAAGGAT	CGGATTGCGGGTTTGATCTC
	Mm	AAGGTGGGGGAACTGAAGGAT	CGGATTGCGGGTTTGATCTC
FOXO1	Rn	CCCAGGCCGGAGTTTAACC	GTTGCTCATAAAGTCGGTGCT
	Mm	CCCAGGCCGGAGTTTAACC	GTTGCTCATAAAGTCGGTGCT
CYLD	Rn	GGACAGTACATCCAAGACCGT	TCCTCACAGTTGGTAATTGCC
	Mm	GGACAGTACATCCAAGACCGT	TCCTCACAGTTGGTAATTGCC
ERBB4	Rn	TCCCCCAGGCTTTCAATATCC	GCACCCTGGGCGACTGGAG
	Mm	TCCCCCAGGCTTTCAACATAC	GCACCCTGAGCTACTGGAG
RYBP	Rn	GAAGGTTGAAAAGCCTGACAA	AGCTTCACTAGGAGGATCTTTCA
	Mm	GAAGGTCGAAAAGCCTGACAA	AGCTTCACTAGGAGGATCTTTCA
TLL1	Rn	GGTTGGTGGTCTCGGGTATTG	GGCGATGTCACCCCAAAACA
	Mm	GGTTGGTGGTCTCGGGTATTG	GGCGATGTCACCCCAAAACA
CCNT1	Rn	AACAAACGGTGGTATTTTACTCG	CCTGCTGGCGATAAGATAG
	Mm	AACAAGCGGTGGTATTTTACTCG	CCTGCTGGCGGTAAGAGAG
SLC6A4	Rn	TATCCAATGGGTACTCTGCAG	CCGCTCCCCTTGGCGAATCT
	Mm	TATCCAATGGGTACTCCGCAG	CCGTTCCCCTTGGTGAATCT
SP2	Rn	CCAACCTACCCCAAGGAAAC	GGGAGCCCTGAATCTGAAGTAT
	Mm	CCAGCCTACCCCAAGGAAAC	GGGAGCCCTGAATCTGAAGTAT
DBF4	Rn	AATAAGATACAGTGTTGGATCCC	ATCTTTCTGGAAACTGGGCTC
	Mm	AATAAGATACAGTGTCGGGTCCC	GTCCTTCTGGAAATTGGGCTC
PARDB6	Rn	GGAGCTGAGTTTCGGCGGTTT	CGTAGCCCACTAGCACGTC
	Mm	GGAGCTGAGTTTCGTCGGTTT	CGTAGCCCACCAACACGTC
DUSP1	Rn	GCTTCTGGATTGTCGCTCCTT	TTGGGCACGATATGCTCCAG
	Mm	GTTGTTGGATTGTCGCTCCTT	TTGGGCACGATATGCTCCAG
POU4F1	Rn	CGCGCAGCGTGAGAAAATG	CGGGGTTGTACGGCAAAATAG
	Mm	CGCGCAGCGTGAGAAAATG	CGGGGTTGTACGGCAAAATAG

2.1.2 Solutions and antibodies used for Western Blot

Solution recipes

Agarose gels

Agarose dissolved in 1x Tris-Acetate-EDTA (TAE) buffer
50x TAE buffer (2 M Tris-acetate, 50 mM EDTA in distilled H_2O)

Polyacrylamide gels

Resolving gel:
10% acrylamide
0.375 M Tris-base (pH 8.8)
0.1% SDS
0.1% ammonium persulphate
0.04% TEMED
Stacking gel:
5% acrylamide
0.375 M Tris-base (pH 8.8)
0.1% SDS
0.1% ammonium persulphate
0.04% TEMED

Solutions for western blots

TBS 10X
100 ml – 1 M Tris pH 8.0
300 ml – 5 M NaCl
600 ml – distilled H_2O 600 ml

TBS-T (TBS 1X -0.05% Tween20)
100ml - TBS 10X
900ml - dH_2O 900ml
0.5ml - Tween20

Tris-glycine (running buffer) 10X
30g of Tris base and 144g of glycine in 1000ml dH_2O

Running buffer 1X
100ml - Tris-glycine running buffer 10x
890ml – distilled H2O
10ml - 10% SDS

Transfer buffer (to transfer gel to the nitrocellulose membrane)
Tris-glycine running buffer 10x
200 ml - Methanol 200ml
700 ml - dH_2O 700ml

Stripping buffer
7.5 g glycine
500 ml dH_2O; adjusted with concentrated HCl final pH 2.5
RIPA lysis buffer
5 ml 10X PBS
5 ml 10% IGEPAL
2.5 ml 10% Na Deoxycholate
500 µl 10% SDS
250 µl 100 mM PMSF
25 µl 1 mg/ml Leupeptin
25 µl 1 mg/ml Aprotinin

125 µl 1 mg/ml Pepstatin A
36.575 ml distilled H_2O

Table 2.3 List of antibodies used for western blot

Antibodies (primary and secondary)	Blocking solution	Dilution	Supplier
GAPDH (HRP linked)	-	1:5000 in TBST	Cell Signalling Technology
B-actin (HRP linked)	-	1:5000 in TBST	Cell Signalling Technology
α-tubulin (HRP linked)	-	1:5000 in TBST	Abcam
PhosphoLATS1	5% milk	1:1000 in 5% BSA	Cell Signalling Technology
LATS1	5% milk	1:1000 in 5% milk	Protein Tech
LATS2	5% milk	1:1000 in 5% milk	Cell Signalling Technology
MST1	5% milk	1:1000 in 5% BSA	Cell Signalling Technology
MST2	5% milk	1:1000 in 5% BSA	Cell Signalling Technology
MOB1	5% milk	1:1000 in 5% BSA	Cell Signalling Technology
PhosphoYAP	5% milk	1:1000 in 5% BSA	Cell Signalling Technology
Active YAP	5% milk	1:1000 in 5% BSA	Cell Signalling Technology
Total YAP	5% milk	1:1000 in 5% milk	Santa Cruz
FOXO1	5% milk	1:1000 in 5% milk	Cell Signalling Technology

2.2 Methods

2.2.1 Real-time qPCR

2.2.1.1 Total small RNA (miRNA) isolation from cells

Total small RNA from cardiomyocytes, cardiac fibroblasts, neonatal, and adult rat hearts were extracted using TRIzol® (Invitrogen) followed by purification using PureLink™ miRNA isolation kit (Life Technologies) to enrich small RNA in the final isolation product. The extraction began by adding 1 mL of TRIzol® per well (6-well plate) into the cells or small chunks of hearts (50-100 mg). The cells were then scraped using cell scrapers, and the hearts were homogenised to assist the RNA isolation mechanically. All samples were then left for 5 minutes at room temperature to ensure complete dissociation of nucleoprotein complexes. Subsequently, 200 µL of chloroform was added to each tube followed by 15 seconds of rigorous shaking and

3 minutes incubation at room temperature. The mixtures were then centrifuged at 12,000 × *g* for 15 minutes at 4°C. After spinning, the mixtures were separated into a lower red phenol-chloroform, an interphase, and an upper aqueous phase. 400 µl of the upper aqueous phase was transferred to a fresh tube, and 215 µl of absolute ethanol was added to each tube followed by vortexing. The samples were then transferred to a spin cartridge supplied with the kit and spun for 1 minute at 12,000 x g. The spin cartridge was discarded and 700 µl absolute ethanol was added into the flow-through followed by thorough mixing. To bind the RNA to the membrane, 700 µl of the mixture was transferred to a new spin cartridge followed by centrifugation at 12,000 x *g* for 1 minute. This step was repeated for the remaining sample volume. The RNA was then washed by adding 500 µl washing buffer into the spin cartridge followed by centrifugation at 12,000 x *g* for 1 minute. The flow-through was discarded and the washing process was repeated one more time. Finally, the RNA was eluted by adding 50 – 100 µl of sterile, RNase-free water into the spin cartridge, followed by 1-minute incubation and 1-minute centrifugation at maximum speed. The final concentration of total small RNA was determined using a Nanodrop.

2.2.1.2 Total RNA isolation from cells

NRCMs grown in a 6-well plate were homogenised in 1 ml TRIzol® (Invitrogen) per well with a cell scraper (Ibidi). The cell homogenates were then transferred to clean, nuclease-free 1.5 ml Eppendorf tubes and incubated for 3 minutes at room temperature (RT). After adding 200 µl chloroform to each sample, samples were then shaken vigorously for 15 seconds and centrifuged (13,000 rpm, 15 minutes, 4°C). Subsequently, 400 µl of the upper aqueous layer was transferred into a clean tube and an equal volume of 70% ethanol in RNAse free water was then added. The tubes were vortexed briefly and inverted to disperse any precipitates that might form. Following this, the PureLink® RNA Mini Kit (Life Technologies) was used as per manufacturer's guidance to bind, wash, and elute RNA. Briefly, samples were transferred into a spin cartridge containing a collection tube (supplied with the kit) and centrifuged for 15 seconds at 13,000 rpm, RT. The flow-through were discarded

and samples were washed with 700 µl wash buffer I and spun for 15 seconds at 13,000 rpm, RT. The spin cartridge was then transferred into a clean collection tube and samples were washed with 500 µl wash buffer II and centrifuged for 15 seconds at 13,000 rpm, RT. Following this, the flow-through was discarded and the spin cartridge was inserted back into the collection tube. The spin cartridge was centrifuged again for 15 seconds at 13,000 rpm, RT to remove the remaining wash buffer and transferred into a recovery tube. After this, the RNA was eluted by adding 40µl of RNAse free water into the centre of the spin cartridge. The spin cartridge was then incubated for 1 minute at RT and centrifuged for 2 minutes at 13,000 rpm, RT. The resulting RNA was stored at -80°C.

2.2.1.3 Simultaneous total miRNA and total RNA extraction from tissue

This step was done primarily to investigate the expression of miR-411 target genes in tissue samples obtained following *in vivo* injection of miR-411 mimics (see section 2.11.1). Total small RNA and total RNA were both isolated from each tissue sample at the same time using TRIzol® extraction, followed by purification with PureLink™ miRNA isolation kit (for total miRNA) and PureLink® RNA Mini Kit (Life Technologies) for total RNA. First, the tissue samples were treated with 1 ml TRIzol®, homogenised using a Dounce homogeniser, and incubated for 3 minutes at RT. Subsequently, 200 µl chloroform was added into each sample followed by 15 seconds of vigorous shaking. Then, samples were incubated for 2-3 minutes at RT and centrifuged for 15 minutes at 13,000 rpm, 4°C. 400 µl of the upper aqueous layer was transferred to a nuclease free 1.5 mL Eppendorf tube and 215 µl of absolute ethanol was added to each sample to obtain a final concentration of 35%. All 615 µl of the lysate was then transferred to a spin cartridge with a collection tube. The samples were centrifuged for 1 minute at 13,000 rpm, RT. The flow through was kept and used for further steps (binding, washing, and elution) as described in section 2.2.1 to obtain total miRNA. The spin cartridge was inserted into a fresh collection tube and used to isolate total RNA by following procedures described in section 2.2.2. The final RNA samples were stored at -80°C.

2.2.1.4 RNA quantification

All isolated RNA was quantified using a nanodrop (ND-8000). First, a blank recording was made using RNAse-free water and then 1 µl of re-suspended RNA was placed on top of the pedestal. RNA concentration (ng/µl) and 260/280 absorbance values were recorded to assess RNA quality. Samples with 260/280 absorbance value of ~2.0 are considered pure RNA.

2.2.1.5 Reverse transcription

2.2.1.5.1 miRNA to cDNA reverse transcription

Total miRNA was reverse transcribed using TaqMan™ MicroRNA Reverse Transcription Kit (Thermo Fisher Scientific). 10 ng RNA in a volume of 5µl was mixed with the following: 0.15 µl 100 mM dNTPs with dTTP, 1 µl MultiScribe™ Reverse Transcriptase, 1.5 µl 10× Reverse Transcription Buffer, 0.19 µl RNase inhibitor, 4.16 µl of nuclease-free water, and 3 µl stem-loop primers specific for small nuclear RNA U6 (U6 snRNA), hsa-miR-411-5p, hsa-miR-186-5p, hsa-miR-204-5p, hsa-miR-25-5p, or hsa-miR-181a-5p (TaqMan™ MicroRNA Assays, Thermo Fisher Scientific). After thorough mixing, the samples were run on a thermal cycler (MJ Research PTC-200, BioRad) under the pre-set conditions listed in Table 2.4 below.

Table 2.4 Cycling conditions for miRNA reverse transcription

Step Type	Time (min)	Temperature (°C)
HOLD	30	16
HOLD	30	42
HOLD	5	85
HOLD	∞	4

2.2.1.5.2 RNA to cDNA reverse transcription

DNase treatment

RNA samples were treated with DNAse before converting them into cDNA. DNase (Sigma) treatment was performed according to manufacturer's instructions. RNA (1 µg) was mixed with Amplification grade DNase 1 (1 µl), DNase 1 reaction buffer (1 µl, Sigma), and nuclease-free water to a final volume of 10 µl. The mixtures were then incubated for 15 minutes at RT. To inactivate the DNase I enzymes, 1µl of 25 mM EDTA

stop solution (Sigma) was added and samples were incubated for 10 minutes at 70°C.

cDNA conversion

The High-Capacity cDNA Reverse Transcription Kit (Applied Biosystems) was used to convert RNA samples to cDNA according to the manufacturer's instructions. Mastermix was made by mixing components from the kit as shown in Table 2.5. The mastermix was then added to the DNase treated samples (10 µl) in PCR tubes and briefly centrifuged before being placed in a MJ Research PTC-200 Thermal Cycler (Bio-Rad), and run according to the conditions shown in Table 2.6.

Table 2.5 Mastermix components for RNA to cDNA conversion

Component	Volume per reaction (µL)
Nuclease-free water	4.2
10X RT Buffer	2
10X RT Random Primers	2
Multiscribe Reverse Transcriptase	1
25X dNTP Mix	0.8
Total per reaction	**10**

Table 2.6 Cycling conditions for mRNA to cDNA conversion

Steps	Temperature	Time
Step 1	25°C	10 min
Step 2	37°C	120 min
Step 3	85°C	5 min
Step 4	4°C	∞

Resulting cDNA samples were stored at -20°C. Samples without MultiScribe Reverse Transcriptase™ or RNA were generated and used as controls during quantitative PCR to account for the possibility of DNA contamination.

2.2.1.6 Real time qPCR

2.2.1.6.1 qPCR using Taqman™ probes to investigate miRNA expression

qPCR was used to determine the relative expression of miRNA candidates. 0.67 µl reverse transcription product was mixed with the following: 5 µl TaqMan™ Universal PCR Master Mix II (2×), 3.83 µl nuclease-free water, and 0.5 µl qPCR primer (TaqMan™ Small RNA Assay) for U6 snRNA, hsa-miR-411-5p, hsa-miR-186-5p, hsa-

miR-204-5p, hsa-miR-25-5p, or hsa-miR-181a-5p. The mixtures were loaded in a 96-well plate in triplicate and run on an Applied Biosystems® 7500 Fast Real-Time PCR System using the program listed below.

Table 2.7 qPCR reaction conditions

Step		Enzyme activation	PCR	
		HOLD	CYCLE (40 cycles)	
			Denature	Anneal/Extend
Temperature	50°C	95°C	95°C	60°C
Time	2 minutes	10 minutes	15 seconds	60 seconds

2.2.1.6.2 qPCR using SYBR Green to investigate gene expression

Quantitative real-time PCR was used to assess gene expression. The qPCR reaction was performed using Brilliant III Ultra-Fast SYBR® Green QPCR Master Mix (Agilent Technologies). All qPCR reactions were loaded in triplicate in a 96-well qPCR plate (Starlab), with each well containing the components shown in Table 2.8. Primers (Sigma) were reconstituted in nuclease-free water according to the manufacturer's instruction to make 100 µM solution. From this stock, they were further diluted to make 10 µM stock. Primers used are listed in Section 2.1.1.

Table 2.8 Components for SYBR Green mastermix *When using pre-mixed primers (Quantitect Primer Assay, Qiagen), 1 µl of primer was added

Reagent	Volume (µl)
cDNA	1.0
SYBR Green	5.0
Forward primer (10 µM)	0.5
Reverse primer (10 µM)	0.5
Reference Dye	0.15
Nuclease free H_2O	2.85
Total	10

qPCR was run using an Applied Biosystems® 7500 Fast Real-Time PCR System with the program listed in Table 2.9. Expression of target genes was quantified using the comparative CT method (ΔCT). To standardise all values, the CT value generated for the gene of interest was normalised against the CT value for the endogenous

(GAPDH) and experimental controls, all values were then analysed using the formula $2^{-\Delta\Delta CT}$.

Table 2.9 Cycling conditions for SYBR Green RT-qPCR

Stage	Temperature	Time	No of cycles
Initiation	95°C	15 min	1
Cycling	95°C	5 sec	40
	60°C	25 sec	
Melt curve	95°C	15 sec	1
	60°C	1 min	
	95°C	15 sec	
	60°C	15 sec	
Holding	4°C		∞

2.2.2 Western Blot

2.2.2.1.1 Protein extraction

NRCMS were seeded on a 6-well plate at a density of $2.5x10^6$ cells/well and left overnight in a humidified incubator at 37°C, 5% CO_2. The next day, the cells were washed with DPBS and transfected with cel-mir-239b, hsa-miR-411-5p, hsa-miR-181a-5p or control miRNA for 48 hours. The cells were then washed several times with DPBS and protein samples were collected by lysing the cells in radioimmunoprecipitation (RIPA) buffer. RIPA buffer contained 1% IGEPAL CA-630, 0.5% sodium deoxycholate, 0.1% SDS, 0.5 mM phenylmethylsulfonyl fluoride, 500 ng/mL leupeptin, 2.5 mg/mL pepstatin A, and 1 mg/mL aprotinin in PBS. 150 µL of RIPA buffer was added to each well, and the cells were incubated on a shaker at 4°C for 30 minutes. The cells were scraped using cell scrapers, and the lysates were transferred into 1.5 mL Eppendorf tubes. To remove cell debris, the tubes were centrifuged at 10,000 rpm, 4°C for 10 minutes and the supernatant was transferred to new tubes and stored at -80°C.

2.2.2.1.2 Protein concentration

The protein concentration was measured using Pierce BCA Protein assay kit (Thermo Scientific) according to the manufacturer's manual and calculated based on

the absorbance reading at 562nm (Multiskan Ascent Plate Reader, Thermo).

2.2.2.1.3 Gel Electrophoresis

Samples for immunoblotting were prepared by mixing 15µL samples containing 20 – 30 µg protein with 15 µL 2x Laemmli buffer, followed by heating at 95°C for 5 minutes to denature the protein. 30 µL protein was loaded onto 10% acrylamide gel and separated by SDS-PAGE at 130V for 1.5 hours. During separation, the gel was put in an electrophoresis tank and immersed in running buffer. The proteins were then transferred onto polyvinylidene difluoride (PVDF) membrane (Millipore) by semi-dry transfer (400mA, 21V) for 2 hours. The membrane was blocked in 5% (w/v) BSA (Sigma-Aldrich) in Tris-buffered saline with 0.05% Tween-20 (TBST) for 1 hour and incubated overnight with primary antibodies diluted (1:1000) in the blocking buffer at 4°C on a shaker. The membrane was washed three times with TBST and incubated with the horseradish-peroxidase-conjugated anti-rabbit or anti mouse secondary antibody (1:5000 in TBST, Cell Signalling Technology) for 2 hours on a shaker at room temperature. Finally, the membrane was washed three times with TBST, visualised by ECL Western Blotting Detection Reagent (Amersham), and imaged using ChemiDoc XRS+ System (BioRad). The primary antibodies used are listed in Table 2.3. Solutions used for protein extraction and western blot are described in Section 2.1.2.

2.2.3 Statistical analysis

All data are expressed as mean ± standard error of means (SEM). Unpaired two-tailed Student's t-test, Mann-Whitney test, or one-way ANOVA followed by post-hoc Tukey or Bonferroni test was used where appropriate to compare means between sample groups. GraphPad Prism 7 was used to analyse all data. The data was considered significant if p value < 0.05.

CHAPTER 3

Identification of novel miRNAs to induce cardiomyocyte regeneration

Chapter 3 - Identification of novel miRNAs to induce cardiomyocyte regeneration

3.1 Introduction

MiRNAs are endogenous small non-coding RNAs, typically between 21-30 nucleotides long, which are critically important for post-transcriptional gene regulation. MiRNAs function via base-pairing between their seed sequences, mostly situated at positions 2-7 from the miRNA 5'end, and their complementary sequences within mRNAs, leading to the degradation of target mRNAs. MiRNAs are abundant in a wide range of species, many of which are evolutionarily conserved between species. The latest update from the primary public repository for miRNAs, miRBase, published 38,589 miRNA hairpin sequences from 271 species which produce 48,860 mature miRNA sequences. In humans, there are 1917 annotated miRNA hairpin precursors and 2654 mature miRNA sequences (v22.1) (Kozomara et al., 2019). This number increased sharply from the 988 mature miRNA sequences, which were previously annotated in 2009 (v13.0). This increase is largely driven by the rapid development in RNA deep sequencing tools (Kozomara and Griffiths-Jones, 2011).

The ever-increasing size of miRNA libraries, from one point of view, highlights the regulatory potentials of miRNAs. However, it also reflects the difficulty of finding biologically relevant miRNAs (Eulalio and Mano, 2015). Several investigators have focused on the altered miRNA expression profiles in pathological conditions based on the notion that the expression dysregulation correlates strongly with diseases (Small et al., 2010). For example, by using hypertrophied or failing heart tissue as sample sources, several investigators have found several miRNAs that can potentially be used as disease modulators (Lin et al., 2009; Thum et al., 2007; Thum et al., 2008; Van Rooij et al., 2006). Further studies have characterised a few of these miRNAs by experimentally changing their cellular concentration and have thus shown whether they can elicit or prevent pathological responses (Small et al., 2010). These studies not only confirmed the importance of miRNAs in cardiac pathophysiology, but they

also highlighted the potentials of miRNAs for diagnosis, prevention, or treatment of cardiac diseases.

Although these studies could successfully identify several disease-modifying miRNAs, by focusing only on a few significantly changed miRNAs, they are at risk of neglecting mid to low abundance miRNAs that may have marked effects on diseases. This may be one reasons why only a few functionally relevant miRNAs, relative to the size of the miRNA library, have been identified in cardiac diseases. In addition, finding dysregulated miRNAs is not sufficient because more intensive investigation is required to elucidate their functions. Taking these arguments into account, assay-based screening that allows for the direct correlation of miRNAs with cellular function can potentially be a promising alternative (Jentzsch et al., 2012). This method is developed based on the principles that despite their relatively small number, miRNAs have been shown to regulate approximately 60% of the human transcriptome (Friedman et al., 2009) and thus virtually modulate all physiological and pathological processes in cells, such as proliferation, apoptosis, and survival (Eulalio and Mano, 2015).

In the context of cardiovascular diseases, functional high-throughput miRNA screening has been conducted to find miRNAs that are capable of modulating different aspects of cardiovascular physiology. In order to identify miRNAs that are capable of regulating cardiomyocyte hypertrophy, Jentzsch *et al.* developed a high-throughput assay where they induced hypertrophy in NRCMs seeded in a 96 well-plate with phenylephrine (PE), then transfected a library of 230 conserved miRNA mimics afterwards, and evaluated the cell size post transfection through fully automated image acquisition and analysis (Jentzsch et al., 2012). They successfully identified a number of miRNAs, which were previously not linked to hypertrophy.

In addition to hypertrophy, weakened heart contractility is one of the hallmarks of heart failure. Wahlquist *et al.* developed a high-throughput functional assay to screen miRNAs that target one of the main modulators of the calcium cycle - the calcium-transporting ATPase SERCA2a (Wahlquist et al., 2014). They created a

reporter construct by fusing the SERCA2a 3'UTR downstream of the enhanced green fluorescent protein (eGFP) coding sequence, thereby allowing the detection of active miRNAs by observing changes in the eGFP fluorescence signal. They successfully characterised miR-25 as a strong modulator of SERCA2a and found that the inhibition of miR-25 in mice with established heart failure could significantly improve cardiac function and survival (Wahlquist et al., 2014).

The next aspect of cardiovascular physiology that has garnered a lot of attention recently is cardiomyocyte proliferation. Contrary to popular belief that adult cardiomyocytes are terminally differentiated and hence unable to regenerate, recent evidence suggests that they can proliferate albeit at a very low rate (Bergmann et al., 2009). This encourages several investigators to find a way to improve cardiomyocyte regeneration to compensate for the massive myocyte loss during MI. Eulalio *et al.* performed a high content microscopy, high throughput functional assay to find miRNAs that can stimulate endogenous cardiomyocyte proliferation. They screened 988 miRNAs annotated in miRBase v13.0 and used 5-ethynil-2'-deoxyuridine (EdU) incorporation as a surrogate marker for proliferation (Eulalio et al., 2012). They successfully identified two miRNAs, miR-590-3p and miR-199a-3p, that are capable of increasing cardiomyocyte proliferative capacity and improving outcomes post MI. The effects of these miRNAs are mediated primarily by the downregulation of Homer1, a protein involved in calcium handling and HOPX, a modulator of embryonic cardiomyocyte proliferation (Eulalio et al., 2012).

Recently, the modulation of the Hippo signalling pathway, a kinase cascade that inhibits adult cardiomyocyte proliferation, has emerged as a potential means to increase cardiac regenerative capacity (Liu and Martin, 2019). Activation of its terminal effector YAP or conditional deletion of one of its core component SAV in adult mouse hearts can significantly induce regeneration and improve cardiac function post MI (Heallen et al., 2013; Lin et al., 2014). However, translating this knowledge into the development of therapeutic tools for clinical practice remains a considerable challenge because most of the Hippo pathway core components are not conventional drug targets. Due to its ability to silence the expression of genes, miRNA

can potentially be used as an alternative to target traditionally 'undruggable' proteins (Johnson and Halder, 2014). For example, the administration of modified antimiR-122 has been shown to be effective and safe for treating patients with hepatitis C infection (Janssen et al., 2013).

As discussed in Chapter 1 Section 1.4, the ability of miRNAs to inhibit the Hippo pathway in the heart has been investigated by Tian *et al.* who found that inducible overexpression of miR-302/367 post MI promotes adult cardiac regeneration through downregulation of the Hippo core components MST1, LATS2, and MOB1b (Tian et al., 2015). In addition, recent studies have reported that many pro-proliferative miRNAs that have been previously investigated converge on the Hippo pathway, further highlighting the importance of the Hippo pathway in cardiac regeneration (Diez-Cunado et al., 2018; Torrini et al., 2019). This chapter describes a functional screening method aimed at finding a novel miRNA that can be used to target the Hippo pathway and increase cardiomyocyte proliferation.

3.2 Aims

1. To find a novel miRNA capable of improving cardiomyocyte regeneration by modulating the Hippo pathway.
2. To test the effects of overexpressing candidate miRNAs on NRCM proliferation.

3.3 Methods

All methods specific to this chapter will be listed below. For general qPCR and western blot protocols see Chapter 2 Section 2.2.

3.3.1 Identification of novel miRNAs that regulate the Hippo/YAP pathway

Candidate miRNAs were screened using a combination of literature, bioinformatics, a YAP luciferase assay screening followed by examination of candidate miRNA expression profiles. The screening process will be described further in Section 3.4.1.

3.3.2 Neonatal rat cardiomyocytes (NRCM) isolation

Cardiomyocytes were isolated from the hearts of 2-3 days old Sprague-Dawley rats (Charles River Laboratories). In brief, the pups were sacrificed by cervical dislocation, and the hearts were taken out via anterior chest incision. They were subsequently transferred to ice-cold, sterile artificial digestion solution (ADS) buffer (116 mM NaCl, 20 mM HEPES, 1mM NaH_2PO_4, 6 mM glucose, 5 mM KCl, 0.8 mM $MgSO_4$, adjusted to pH 7.4 with 1N NaOH and stored at 4°C after being filter sterilised with a vacuum filtration unit). Inside a class II tissue culture hood, the hearts were cut longitudinally into two pieces and dissociated in a serial enzymatic digestion in 7 ml ADS supplemented with collagenase A (0.33 U/mL, Roche) and pancreatin (100 mg/mL, Sigma). The dissociation process was performed at 37°C for 10 – 15 cycles of 5 minutes digestion under constant agitation. Between each cycle, the dissociating hearts were triturated around 30 times using a 25 ml strippete to assist the digestion mechanically. The resulting suspension was then passed through a cell strainer and 3 ml Fetal Bovine Serum (FBS, Gibco) was added to stop the digestion process. The collected cells were spun at 1,200 rpm for 5 minutes, and the resulting pellets were resuspended in 40 ml of pre-plating media (67% Dulbecco's modified Eagle media (DMEM), 17% Medium 199, 10% Horse Serum, 5% FBS, 1% Penicillin-Streptomycin, 1% Fungizone). All components of the media were manufactured by Gibco. The cell

suspension was seeded onto an uncoated 10 cm tissue culture dish in a 37°C, 5% CO_2 humidified incubator for 1 hour. This step allowed the attachment of cardiac fibroblasts and thus separated them from cardiomyocytes. The supernatant which was comprised of mostly cardiomyocytes was collected, and the cells were counted. Cardiomyocytes were plated in plating media (67% DMEM, 17% Medium 199, 10% Horse Serum, 5% FBS, 1% Penicillin-Streptomycin, 1% Amphotericin B (Fungizone), and 1µM Bromodeoxyuridine (BrdU)) and further incubated at 37°C, 5% CO_2. After 24 hours, the cells were washed several times with PBS, and the medium was replaced with maintenance medium (80% DMEM, 20% Medium 199, 1% Fetal Bovine Serum, 1% Penicillin-Streptomycin, 1% Fungizone (Amphotericin B), and 0.1% (1 µM) BrdU).

3.3.3 miRNA mimics and siRNA transfection

Isolated NRCMs were transfected with human miR-411 (hsa-miR-411-5p) or miR-181a (hsa-miR-181a-5p) or cel-miR-239b as a negative control at a final miRNA concentration of 25 nM. All miRNA mimics were purchased from Dharmacon, Horizon Discovery and resuspended in 1x siRNA buffer (Thermo Scientific) at a final concentration of 5 µM and kept in a -20°C freezer.

Isolated NRCMs were seeded overnight in an incubator at 37°C, 5% CO_2. The following day, the cells were washed several times with DPBS and fresh maintenance media were added to each well. Two sets of 1.5 ml Eppendorf tubes were prepared to make the transfection solution. In the first set of tubes, miRNA mimics were diluted in OPTI-MEM (5% dilution, Life Technologies) and in the second set of tubes, the transfection reagent (1% dilution, DharmaFECT, Thermo Scientific) were diluted in OPTI-MEM as well. Both solutions were incubated at room temperature for 5 minutes and subsequently mixed. The resulting solution was further incubated for 30 minutes at room temperature and finally added into each well. The plates were shaken carefully to ensure thorough mixing. The cells were then kept in an incubator at 37°C, 5% CO_2 for 48 hours.

3.3.4 Immunofluorescence staining for cell proliferation assay

3.3.4.1 EdU incorporation assay

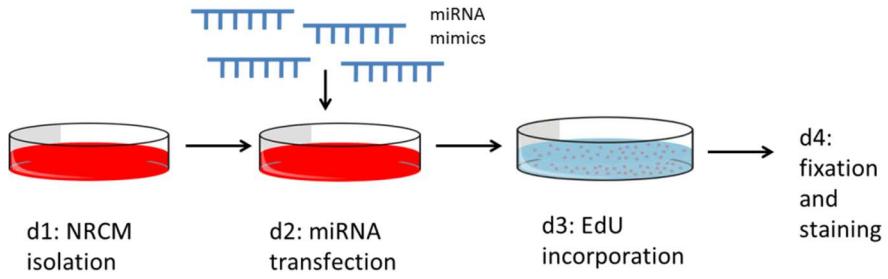

Figure 3.1 Illustration of EdU incorporation assay procedures

This assay was performed to monitor cell proliferation rate by assessing EdU incorporation during DNA synthesis. Steps involved in the EdU incorporation assay are briefly illustrated in Figure 3.1. NRCMS were seeded on laminin-coated, UV-sterilised coverslips in a 24-well plate at a density of 250,000 – 300,000 cells/well. After transfection with miRNA mimics or control, the cells were starved in low serum media (80% DMEM, 20% Medium 199, 1% PenStrep, 1% FBS) for 4 hours. The media were then replaced with fresh low serum media and EdU was added to each well at a concentration of 5 µM. The plate was incubated in a humidified incubator at 37°C, 5% CO_2 for 24 hours. On the following day, the cells were washed with DPBS and fixed in 4% paraformaldehyde (PFA) solution on a shaker at room temperature for 15 minutes. PFA solution was removed, and the coverslips were washed with DPBS three times for 5 minutes each. After that, the cells were permeabilized in 0.5% Triton-X for 20 minutes and washed again with DPBS three times. The coverslips were then incubated in Click-IT EdU reaction cocktail containing Alexa Fluor Azide 488 (Invitrogen) for 30 minutes to stain the EdU+ nuclei. To differentiate cardiomyocytes from cardiac fibroblasts, the cells were incubated in second staining solution containing sarcomeric α-actinin antibody (1: 250 dilution in 0.5% bovine serum albumin (BSA), Sigma-Aldrich) for 2 hours, followed by 1 hour secondary antibody incubation containing Alexa Fluor 647-conjugated anti-mouse IgG antibody (1: 200 dilution in 0.5% BSA). The coverslips were washed three times with DPBS between these steps. Finally, the cells were counterstained with 4',6'-diamidino-2-phenylindole/DAPI (1:5000 dilution

in DPBS, Invitrogen) for 1 minute, washed three times, and mounted on slides using Vectashield mounting media.

The coverslips were then imaged with fluorescence microscopes at 20x magnification and analysed with ImageJ. For one technical replicate, EdU positive nuclei were counted from between 5-10 images per coverslip or until the total number of NRCMs reached between 800 – 1000 cells. The percentage of EdU positive cells was calculated by dividing the total number of EdU positive cardiomyocytes by the total number of cardiomyocytes.

3.3.4.2 Analysis of proliferation markers (Ki-67 and phosphoHistone H3)

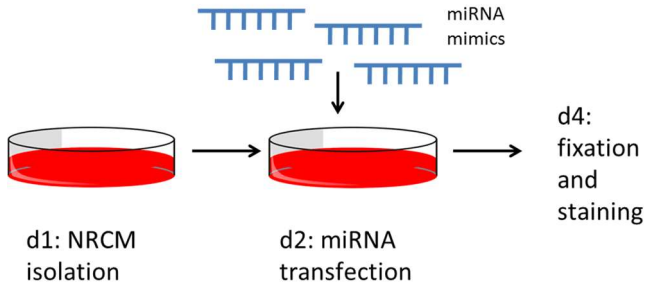

Figure 3.2 Illustration of Ki-67 and pHH3 proliferation assay

Ki-67 and phopho-Histone H3 (pHH3) expressions were used as markers for cell proliferation. Steps for Ki-67 and pHH3 immunofluorescence staining are briefly illustrated in Figure 3.2. NRCMs were plated on laminin-coated, UV-sterilised coverslips in 24-well plates at a density of 250,000 – 300,000 cells/well. The following day, the cells were transfected with miR-411-5p, miR-181a-5p, or control mimics. Forty-eight hours post-transfection, the cells were washed with DPBS and fixed in a 3.7% PFA solution for 15 minutes. The cells were washed with DPBS 3 times 5 mins each, permeabilized by 0.1% Triton-X in DPBS for 10 minutes, and blocked in 0.5% BSA in PBS for 1 hour. The cells were subsequently incubated overnight with either anti Ki-67 (1: 100, Abcam) or anti-phosphorylated (Ser 10) Histone 3 antibody (1:200, CST) followed by washing and 2 hours incubation with Fluorescein (FITC)-conjugated anti-rabbit antibodies (Jackson ImmunoResearch Laboratories). For pH3 staining, the secondary antibody incubation was unnecessary as the primary antibody used was already conjugated with FITC. The cells were washed three times and incubated for 2

hours with anti-sarcomeric α-actinin antibody (1:200 dilution in 0.5% BSA in DPBS, Sigma-Aldrich) to stain cardiomyocyte-specific cytoskeleton. After that, the cells were washed and incubated for 2 hours with secondary Alexa Fluor 647-conjugated anti-mouse IgG (1:200 in 0.5% BSA in DPBS). Finally, the cells were counterstained with DAPI for 1 minute (1:5000 dilution in DPBS, Invitrogen) and the coverslips were mounted using Vectashield mounting media (Vector Laboratories).

The coverslips were then imaged with fluorescence microscope at 20x magnification and analysed with ImageJ. For one technical replicate, Ki-67 or pHH3 positive nuclei were counted from between 5-10 images per coverslip or until the total number of NRCMs reached between 800 – 1000 cells. The percentage of Ki-67 or pHH3 positive cells was calculated by dividing the total number of Ki-67 or pHH3 positive cardiomyocytes by the total number of cardiomyocytes.

3.3.4.3 Fluorescence imaging

All images were collected on a Zeiss AxioImager upright fluorescence microscope using a 10x / 0.5 EC Plan-neofluar objective and captured using a Coolsnap HQ2 camera (Photometrics) through Micromanager software v1.4.23. Specific band pass filter sets for DAPI, FITC and Texas Red were used to prevent bleed through from one channel to the next. Images were then processed and analysed using Fiji ImageJ ((http://imagej.net/Fiji/Downloads). The researcher was blinded during data acquisition and analysis.

3.3.5 Adenovirus amplification and purification from secondary stock

Adenoviruses bearing GAL4-TEAD or UAS-luciferase constructs, previously generated in Oceandy's Lab, were amplified by transducing the virus seed into HEK293 cells. The viruses were then left to replicate inside an incubator at 37°C, 5% CO_2 for 72 hours. After 95% of the cells had detached, the media were collected and spun at 1,000 rpm for 5 minutes to harvest the crude form of adenovirus. Purification of the crude adenovirus was conducted using chloroform (Fisher).

3.3.6 YAP luciferase reporter assay

A luciferase reporter assay was used to measure YAP activity by utilising two types of adenoviruses: Ad-GAL4-TEAD and Ad-UAS-luciferase. The principle of the YAP-luciferase reporter system has been described in a previous publication (Tian et al., 2010). In brief, NRCMs were seeded in 24 well plates at a density of 3×10^5 cells/well and incubated for 24 hours at 37°C, 5% CO_2. The next day, the media were replaced with fresh maintenance media and NRCMs were transfected with control, hsa-miR-411 or hsa-miR-181a mimics. 24 hours later, NRCMs were transduced with both Ad-GAL4-TEAD and Ad-UAS-luciferase. After 48 hours, cell media were aspirated; cells were washed two times with PBS and lysed with 1x cell lysis buffer (Promega) on a shaker for 20 minutes at room temperature. To measure luciferase signal, 5 µl cell lysate was mixed with 50 µl Dual Luciferase Assay reagent (Promega) and read using a Lumat LB9507 Tube Luminometer (Berthold).

3.3.7 Western blot

The changes in the expression of core Hippo components post miR-411 transfection were investigated using western blot (described in Section 2.2.2) using antibodies listed in Section 2.1.2.

3.4 Results

3.4.1 Initial screening of miRNAs for their effects on cardiomyocyte proliferation and the Hippo signalling

Identification of miRNAs that modulate the Hippo pathway was conducted in four different steps: a literature search, comparison with pilot data generated in Oceandy's laboratory, *in silico* analyses, and quantitative real-time polymerase chain reaction (qPCR). The steps are illustrated in Figure 3.3. The first step was developing a miRNA library from two published papers: (1) Eulalio *et al.* (Eulalio et al., 2012) and (2) Bang *et al.* (Bang et al., 2014). Eulalio *et al.* screened the whole miRNA library for their ability to stimulate cardiomyocyte proliferation, whilst Bang *et al.* profiled miRNAs expressed in cardiac fibroblast derived exosomes (Bang et al., 2014; Eulalio et al., 2012). MiRNAs were then selected based on these following criteria: (i) commonly found in all two papers (ii) capable of inducing a high cardiomyocyte proliferation rate, or (iii) predicted to target at least one Hippo pathway core component according to online prediction databases TargetScan and miRdb (Agarwal et al., 2015; Nam et al., 2014; Shin et al., 2010; Wong and Wang, 2015). The resulting library is listed in Table 3.1.

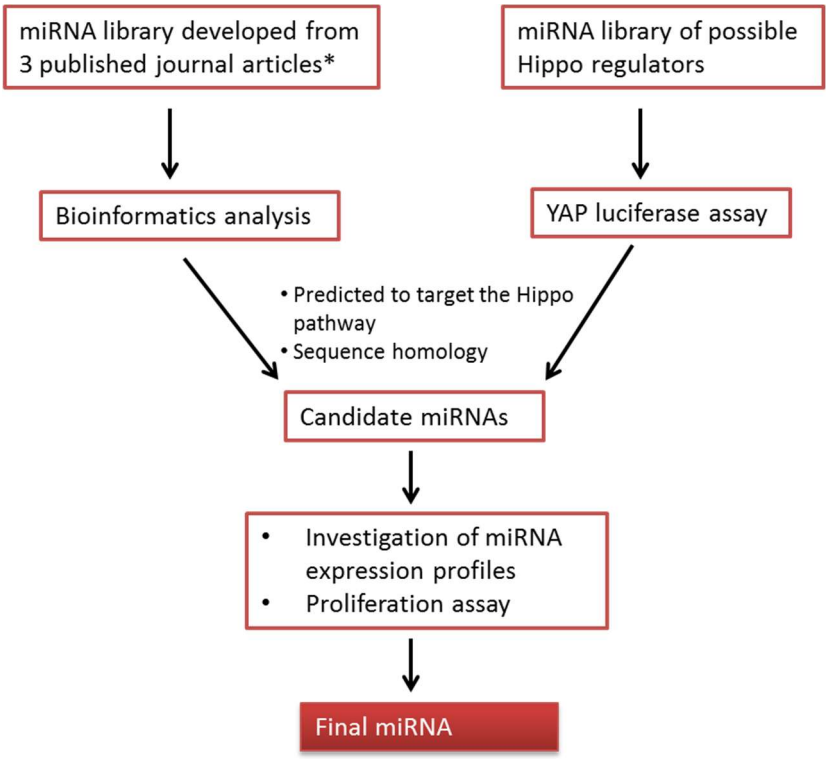

Figure 3.3 Schematic workflow describing steps of miRNA screening

The candidate miRNAs (Table 3.1) were then compared to a panel of miRNAs that were screened for their induction of YAP activity in H9c2 rat myoblast cells during a pilot study conducted in Oceandy's lab prior to the start of this project (data not shown). In this screening, a library of miRNA mimics previously shown to have a large influence on cardiomyocyte proliferation rate, whether increasing or decreasing, was tested for their effects on YAP activity using a YAP luciferase reporter assay. In addition, each miRNA sequence was double-checked using the online database miRBase to ensure sequence homology between mouse, rat, and human (Griffiths-Jones, 2004; Griffiths-Jones et al., 2006). At the end, 7 miRNAs were selected but two of them, miR-191a and miR-214, were dropped from the list leaving only five because their sequences are not conserved (Table 3.2).

Table 3.1 miRNA library developed from bioinformatics and YAP screening. S = SAV, L1 = LATS1, L2 = LATS2, Ma = MOB1A, Mb = MOB1B, Y = YAP

miRNA ID	Accession number	Sequence	% proliferating cardiomyocytes according to Eulalio *et al.*		Predicted Hippo targets	
			Rat	Mouse	TargetScan	MiRdB
hsa-let-7b-3p	MIMAT0004482	CUAUACAACCUACUGCCUUCCC	22.56		Mb	L1,Mb
hsa-let-7d-3p	MIMAT0004484	CUAUACGACCUGCUGCCUUUCU	7.75			
hsa-miR-125a-5p	MIMAT0000443	UCCCUGAGACCCUUUAACCUGUGA	6.3			
hsa-miR-132-3p	MIMAT0000426	UAACAGUCUACAGCCAUGGUCG	30.73	2.63	Y,M2	
hsa-miR-139-5p	MIMAT0000250	UCUACAGUGCACGUGUCUCCAG	21.13			Mb
hsa-miR-181a-5p	MIMAT0000256	AACAUUCAACGCUGUCGGUGAGU	32.64	11.18		L1
hsa-miR-181b-5p	MIMAT0000257	AACAUUCAUUGCUGUCGGUGGGU	22.53			L1
hsa-miR-186-5p	MIMAT0000456	CAAAGAAUUCUCCUUUUGGGCU	24.26		Ma	L1,L2,Ma, Mb,Y
hsa-miR-191-3p	MIMAT0001618	GCUGCGCUUGGAUUUCGUCCCC	30.61	3.66		L1
hsa-miR-204-5p	MIMAT0000265	UUCCCUUUGUCAUCCUAUGCCU	32.8	7.08	S,L1,L2,Ma	L1,L2
hsa-miR-21-5p	MIMAT0000076	UAGCUUAUCAGACUGAUGUUGA	11.08		Y	L1, Y
hsa-miR-211-5p	MIMAT0000268	UUCCCUUUGUCAUCCUUCGCCU	31.87	7.68	S,L1,L2,Ma	L1,L2
hsa-miR-214-3p	MIMAT0000271	ACAGCAGGCACAGACAGGCAGU	7.91			L2
hsa-miR-23a-3p	MIMAT0000078	AUCACAUUGCCAGGGAUUUCC	34.25	5.57		
hsa-miR-23b-3p	MIMAT0000418	AUCACAUUGCCAGGGAUUACC	35.98	18.04		
hsa-miR-25-3p	MIMAT0000081	CAUUGCACUUGUCUCGGUCUGA	12.75		L2	L1,L2
hsa-miR-30a-3p	MIMAT0000088	CUUUCAGUCGGAUGUUUGCAGC	30.99	12.29	L2,Ma,Mb,Y	Ma,Mb
hsa-miR-30a-5p	MIMAT0000087	UGUAAACAUCCUCGACUGGAAG	15.93		L2	L2
hsa-miR-30c-5p	MIMAT0000244	UGUAAACAUCCUACACUCUCAGC	15.94		L2	L2
hsa-miR-320a-3p	MIMAT0000510	AAAAGCUGGGUUGAGAGGGCGA	4.39			S,L1
hsa-miR-410-3p	MIMAT0002171	AAUAUAACACAGAUGGCCUGU	36.08	5.25	Y,S,L1,L2, Ma	S,Mb
hsa-miR-411-5p	MIMAT0003329	UAGUAGACCGUAUAGCGUACG	31.3	4.34	Y,Mb	
hsa-miR-455-3p	MIMAT0004784	GCAGUCCAUGGGCAUAUACAC	39.09	5.73		
hsa-miR-455-5p	MIMAT0003150	UAUGUGCCUUUGGACUACAUCG	28.74	11.32	Y	Ma
hsa-miR-495-3p	MIMAT0002817	AAACAAACAUGGUGCACUUCUU	43.61	7.31	S	S,Mb,Y
hsa-miR-497-3p	MIMAT0004768	CAAACCACACUGUGGUGUUAGA	30.85	7.5	S,L2,Ma,Y	L2
hsa-miR-548b-3p	MIMAT0003254	CAAGAACCUCAGUUGCUUUUGU	30.31	5.55	L2,Mb,Y	L2
hsa-miR-548c-3p	MIMAT0003285	CAAAAAUCUCAAUUACUUUUGC	41	9.63	L2,Ma,Mb,Y	Ma,Mb,Y
hsa-miR-548d-3p	MIMAT0003323	CAAAAACCACAGUUUCUUUUGC	26.55	4.47	Y,S,L1,L2	L2,Ma, Mb
hsa-miR-548d-5p	MIMAT0004812	AAAAGUAAUUGUGGUUUUUGCC	27.7	3.8	S,L1,Ma,Mb ,Y	L1,Mb
hsa-miR-548f-3p	MIMAT0005895	AAAAACUGUAAUUACUUUU	30.88	5.08	S,Ma,Mb,Y	L1,Mb
hsa-miR-548o-3p	MIMAT0005919	CCAAAACUGCAGUUACUUUUGC	29.09	5.55	S,Ma,Mb,Y	Mb
hsa-miR-548p	MIMAT0005934	UAGCAAAAACUGCAGUUACUUU	31.64	4.64	L2,Ma,Y	L2,Ma,Y
hsa-miR-9-3p	MIMAT0000442	AUAAAGCUAGAUAACCGAAAGU	2.8		S,Ma,Y	S,L1,Ma

Table 3.2 Candidate miRNAs selected from initial screening. Seven candidate miRNAs were initially picked up. However, two candidates, miR-191a and miR-214, were dropped from the list due to the lack of sequence homology. Nucleotides highlighted in red indicate sequence difference between rats and humans.

	miRNA	Sequence	
		Rat	Human
1	miR-411	UAGUAGACCGUAUAGCGUACG	UAGUAGACCGUAUAGCGUACG
2	miR-186	CAAAGAAUUCUCCUUUUGGGCU	CAAAGAAUUCUCCUUUUGGGCU
3	miR-204	UUCCCUUUGUCAUCCUAUGCCU	UUCCCUUUGUCAUCCUAUGCCU
4	miR-25	CAUUGCACUUGUCUCGGUCUGA	CAUUGCACUUGUCUCGGUCUGA
5	miR-181a	AACAUUCAACGCUGUCGGUGAGU	AACAUUCAACGCUGUCGGUGAGU
6	miR-191a	GCUGCACUUGGAUUUCGUUCCC	GCUGCGCUUGGAUUUCGUCCCC
7	miR-214	ACAGCAGGCACAGACAGGCAG	ACAGCAGGCACAGACAGGCAGU

The final step, which will described further below, was quantitative polymerase chain reaction (qPCR) to investigate the expression level of each miRNA selected in the previous step. The RNA samples were isolated from 4 types of samples: neonatal rat cardiomyocytes (NRCM), neonatal rat cardiac fibroblasts, and whole hearts extracted from neonatal and adult rats. miRNA expression level was compared between specific cell types (NRCMs vs cardiac fibroblasts) and between neonatal vs adult hearts. Final miRNA candidates were chosen for further experiments based on the following criteria: (1) predicted to target core components of the Hippo pathway, (2) highly expressed in NRCMs and/or in neonatal hearts, and (3) capable of inducing cardiomyocyte proliferation in NRCMs.

3.4.2 The expression profile of candidate miRNAs in NRCMs, cardiac fibroblasts, and whole hearts

Dysregulation of miRNA expression is tightly linked to diseases, such as cancer and HF. This is the reason why it is important to investigate miRNA expression profiles, which can provide significant clues on the physiological importance of certain miRNAs. One of the important aspects of miRNA expression profiles is cell

type specificity. The abundance of miRNAs in specific cell types may indicate their distinctive roles and therefore their importance in those cell types (Guo et al., 2014). The expression level of five candidates in NRCMs was examined using qPCR and was compared to that in cardiac fibroblasts as they are the predominant non-myocyte cells in the heart (Camelliti et al., 2005). Similar to NRCM the cardiac fibroblasts were also isolated from rat neonates. Figure 3.4A shows the relative expression of five candidate miRNAs in NRCMs compared to cardiac fibroblasts. The expression of miR-25, miR-181a, and miR-411 is significantly higher in NRCMS compared to the cardiac fibroblasts while the expression of miR-204 and miR-186 is similar in both cell types.

In addition to cell type specificity, the temporal difference of miRNA expression was also assessed by comparing expression levels in neonatal rat whole hearts (post-natal day 2 or 3) and adult rat whole hearts. Figure 3.4B&C shows that among 5 candidates, only miR-411 has a significantly higher expression in neonatal hearts compared to adult hearts - by approximately 200 fold on average. This suggests that miR-411 may have an important role in cardiac growth and development. Based on miRNA expression profiles, three miRNAs were selected: miR-25, miR-411, and miR-181a. However, miR-25 was finally dropped from the list, leaving only miR-411 and miR-181a, as its role in cardiac pathophysiology, specifically HF, has already been published (Wahlquist et al., 2014).

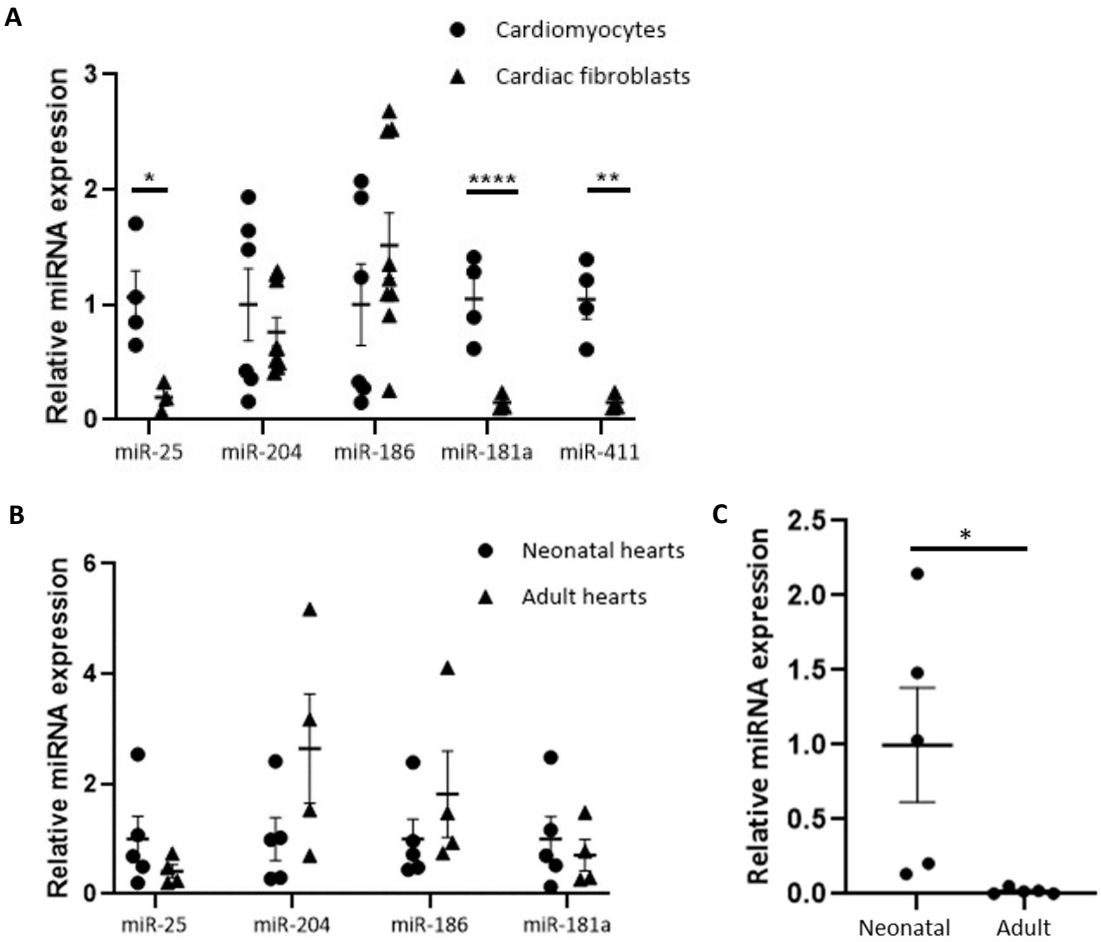

Figure 3.4 Analysis of miRNA expression profiles in neonatal cardiomyocytes *vs.* Neonatal cardiac fibroblast and in neonatal whole hearts *vs.* adult hearts. MiR-25, miR-181a, and miR-411 have significantly higher expressions in cardiomyocytes than cardiac fibroblasts. n=4-6 for cardiomyocytes, 3-9 for fibroblasts (A). Only miR-411 has a significantly higher expression in neonatal hearts compared to adult hearts. n=4-5 (B, C). *p<0.05, **p<0.01, ****p<0.0001, unpaired Student's t-test.

3.4.3 The effects of candidate miRNA overexpression on NRCM proliferation and survival

Cardiomyocyte proliferation and survival were tested after overexpressing candidate miRNAs in NRCMs. To validate the overexpression model, transfection efficiency and miRNA expression post transfection were investigated. Figure 3.5A shows representative immunofluorescence images of NRCMs transfected with Dy547-labelled miRNA mimics for 24h, 48h, and 72h post transfection. These images show that the transfection of miRNA mimics with lipid-based transfection vector

Dharmacon® under the protocol described in Section 3.3.3 resulted in a high transfection efficiency without apparent toxicity. The delivery of miRNA mimics is further ascertained using qPCR. Figure 3.5B shows that the expression of both miR-411 and miR-181a post transfection is significantly higher compared to the vehicle only.

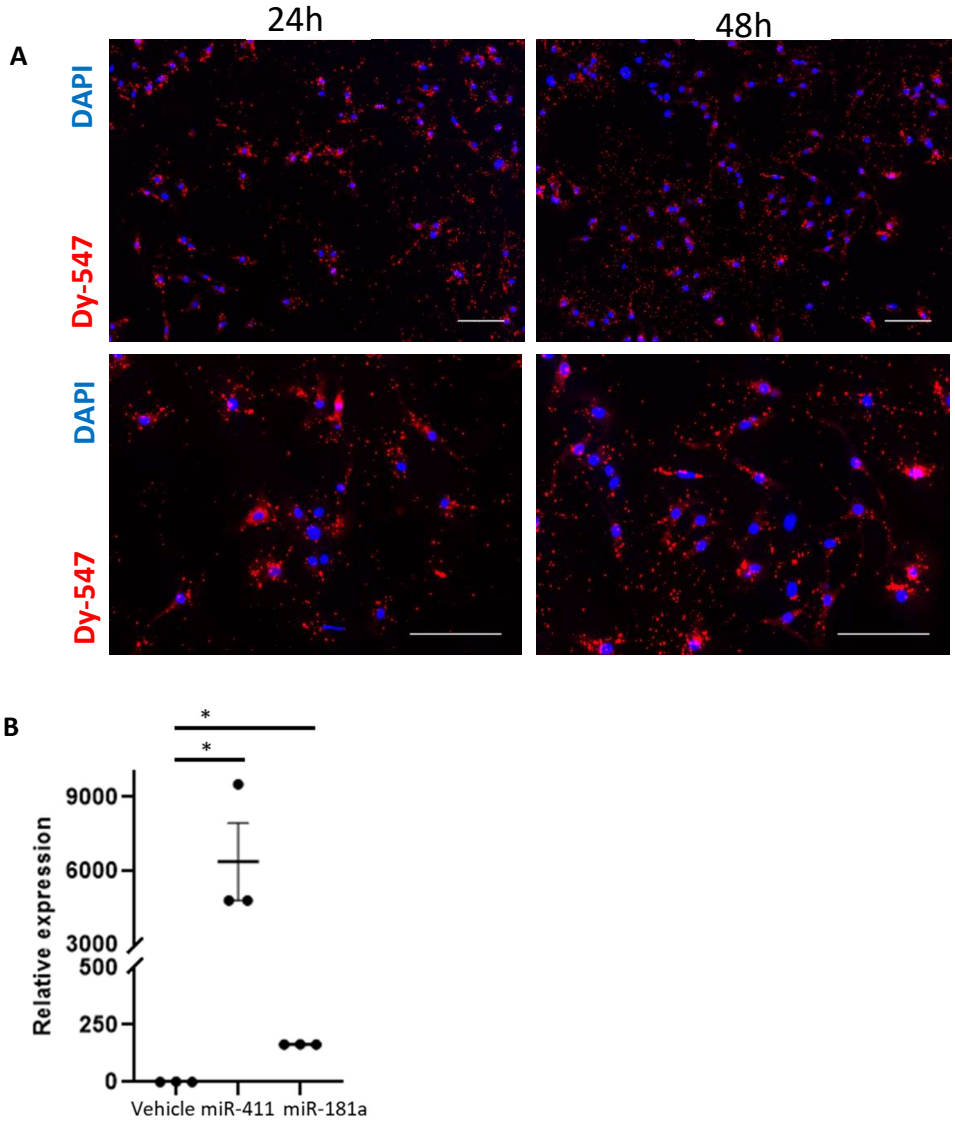

Figure 3.5 Evaluation of miRNA transfection in NRCMs. (A) Representative images of NRCMs transfected with fluorescent-labelled miRNA (Dy547-cel-miR-67) at 24 & 48 h after transfection. (B) Relative miR-411 and miR-181a expression in NRCMs at 48 h post transfection. Scale bar = 100 µm, n=3, *p<0.05, unpaired Student's t-test.

The effects of miRNA overexpression on NRCM proliferation was examined by analysing 2 markers of cell proliferation: Ki-67, and phospho-Histone H3 (pHH3), as well as by performing an EdU incorporation assay. The Ki-67 protein is strictly associated with proliferation and expressed during all active phases of the cell cycle except the resting phase (G0). EdU is a nucleoside analogue of thymidine and a specific marker for the S phase (synthesis) once incorporated in cell nuclei. The third marker, pHH3, is a phosphorylated form of the Histone H3 chromatin protein. Histone H3 is phosphorylated only during mitosis and therefore can be used as a specific marker for the M phase (mitosis). The EdU-incorporated nuclei and previously labelled Ki-67 and pHH3 proteins were tagged with a fluorescent-labelled secondary antibody and imaged with a fluorescent microscope (Fig 3.6). The overexpression of miR-411 caused a significant increase in all three markers compared to the control (50% increase in Ki-67, 50% increase in EdU, and 60% increase in pHH3 positive nuclei). On the other hand, the overexpression of miR-181a did not increase proliferation as indicated by similar rates of Ki-67, EdU, and pHH3 positive nuclei between miR-181a and the control group (Fig 3.6A,B,C).

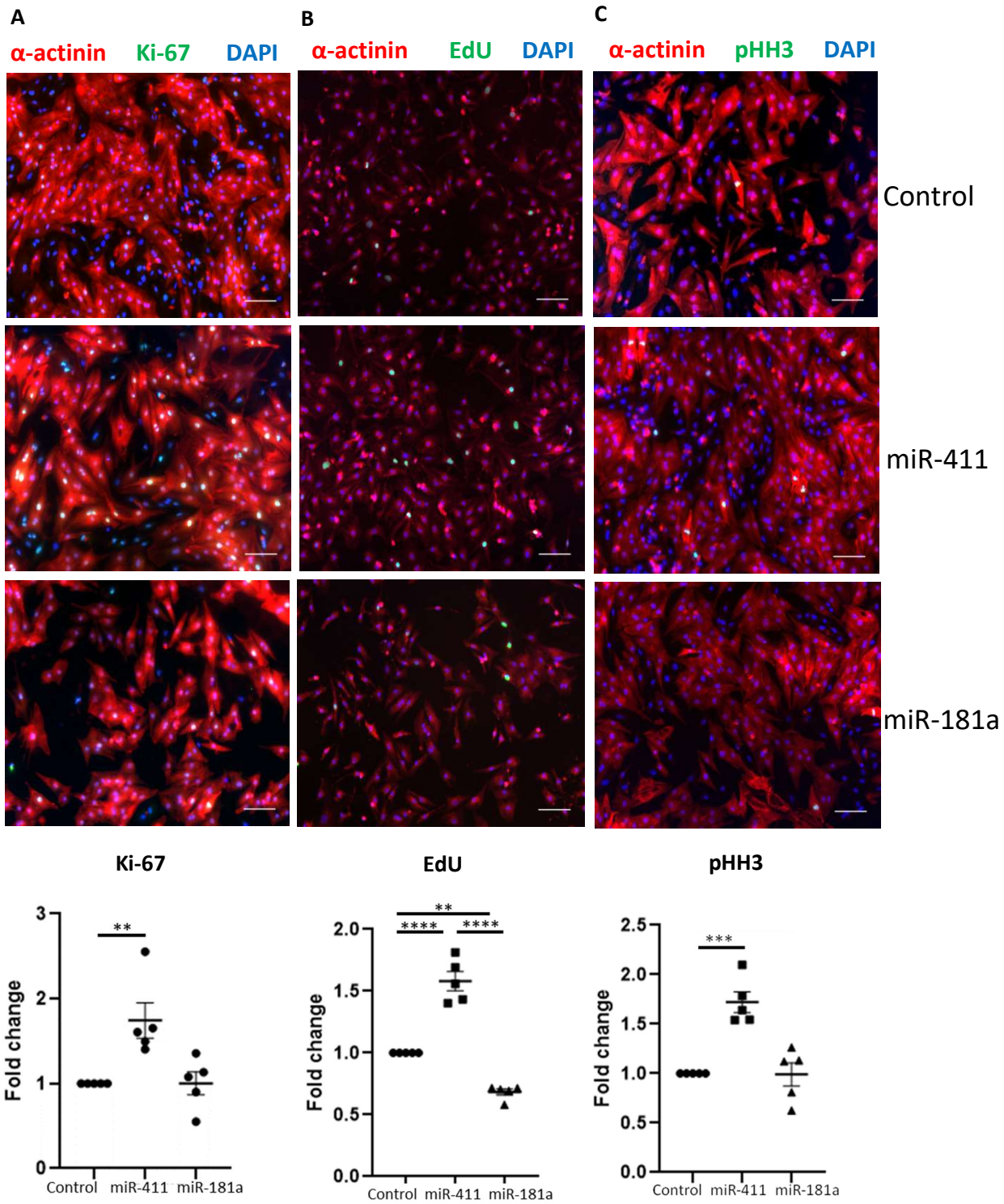

Figure 3.6 The effect of miR-411 and miR-181a overexpression on NRCM proliferation. (A,B,C) Representative images of Ki-67, EdU, and pHH3 immunofluorescent staining with the corresponding quantification at the bottom. Scale bar=100 µm. n=5 from 3 independent batches of NRCM isolations, total cardiomyocytes counted = 2500 – 3000 cells per batch, **p<0.01, ***p<0.001, ****p<0.0001, One-way ANOVA with Tukey's post-hoc test for multiple comparisons.

3.4.4 Investigation of miRNA overexpression effects on the Hippo pathway

The negative regulation of any Hippo components upstream of YAP can lead to a decline in YAP degradation, thus increasing the chance of YAP translocating to the nucleus. A YAP luciferase reporter assay, in which YAP-TEAD binding drives the expression of the luciferase reporter, was used to measure any changes in YAP activity post miRNA transfection. This assay revealed a two-fold increase in YAP activity in NRCMs overexpressing miR-411 compared to the control. On the other hand, NRCMs overexpressing miR-181a exhibited a two-thirds decrease in YAP activity compared to the control (Fig 3.7). Next, western blot was performed to investigate any changes in YAP phosphorylation level. Figure 3.8A revealed that miR-411 overexpression reduced the pYAP/tYAP ratio while miR-181a overexpression did not.

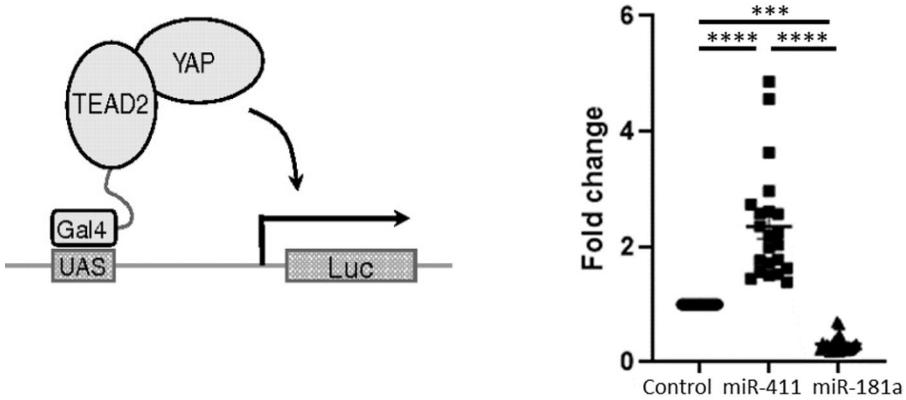

Figure 3.7 YAP activity in NRCMs transfected with miR-411 and miR-181a mimics. (A) Schematic illustration of YAP luciferase assay. Active YAP will bind to the Gal4-TEAD fusion protein and together they will bind to the UAS elements at the promoter of the luciferase reporter and drive its expression (taken from Tian et al. 2010) (B) Relative YAP activity of NRCMs post miR-411 or miR-181a transfection. n=22 from 4 independent experiments, ***p<0.001, ****p<0.0001, one-way ANOVA with Tukey's post-hoc test for multiple comparisons.

To investigate whether or not the changes observed in YAP phosphorylation are caused by the miRNA dependent-downregulation of the Hippo core components, the level of core Hippo members was investigated using western blot. Figure 3.8B illustrates that compared to control no changes were observed in the levels of

LATS1/2, MST1/2, and MOB1 in either the miR-411- or miR181a-treated groups. This result indicates that none of the candidate miRNAs target the core components of the Hippo pathway.

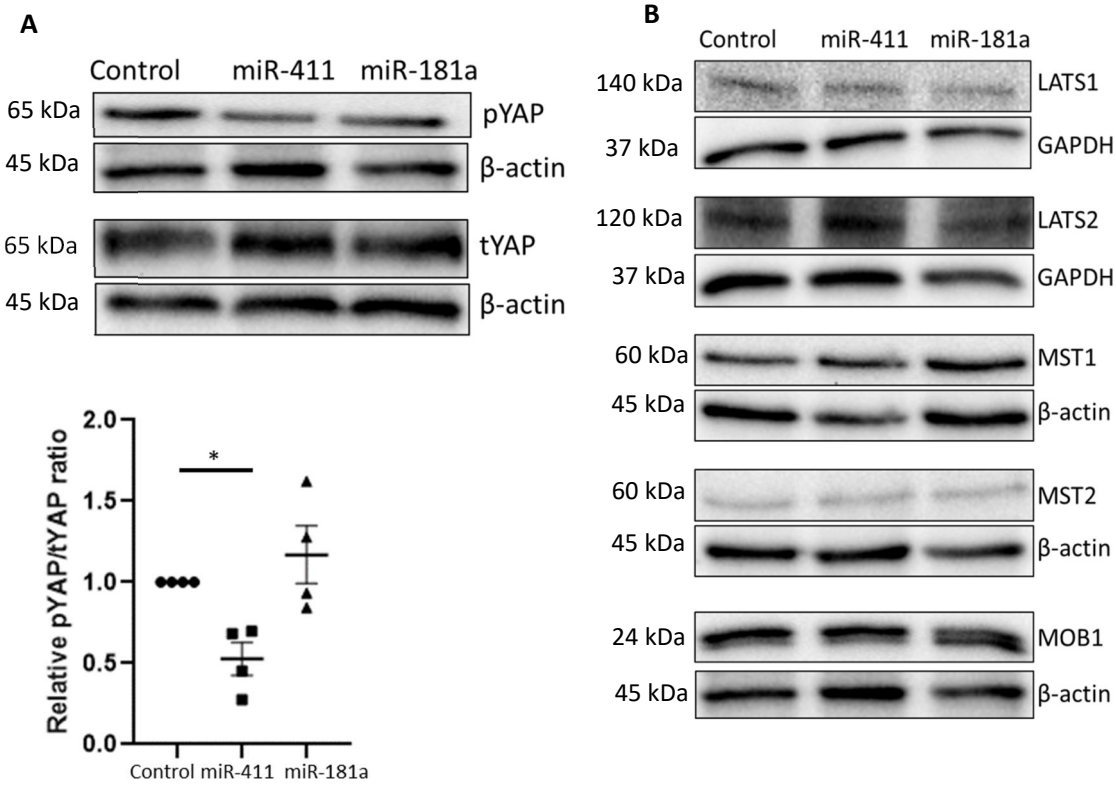

Figure 3.8 The effect of miR-411 and miR-181a overexpression on the Hippo pathway. (A) Western blots showing the levels phosphorylated YAP and total YAP in NRCMs treated with miR-411 or miR-181a mimics. Corresponding quantification is shown at the bottom. n=4, *p<0.05, one-way ANOVA with Tukey's post-hoc test. (B) Western blots showing the levels of core Hippo components 48 h post transfection

3.5 Discussion

The inhibition of the Hippo pathway in the heart has been reported to increase cardiomyocyte proliferation and improve functional recovery after MI (Liu and Martin, 2019). This finding shows that the Hippo pathway is an attractive target for inducing adult cardiomyocyte proliferation. A series of screenings, described in this chapter, were applied to identify novel miRNAs that can modulate the Hippo pathway and induce cardiomyocyte proliferation. First, a combination of literature studies, bioinformatics screening, and YAP luciferase assay results in the identification of 5 candidate miRNAs: miR-25, miR-204, miR-186, miR-181a, and miR-411. A Subsequent examination of miRNA expression profiles revealed that miR-181a and miR-411 are highly expressed in cardiomyocytes and/or neonatal hearts, thus eliminating the other candidates. Both miR-181a and miR-411 were then tested to identify whether or not they can induce proliferation in NRCMs. The results showed that only miR-411 is capable of inducing cardiomyocyte proliferation by reducing YAP phosphorylation and increasing YAP activity. This discussion will therefore focus on miR-411 as the potential candidate to improve cardiac regenerative capacity.

3.5.1 miRNA 411 is differentially transcribed in cardiomyocytes and neonatal hearts

Albeit short-lived, the mammalian heart still retains a robust cardiac regenerative response during the early days after birth (Porrello et al., 2011b). Studies in rodents have reported complete heart regeneration due to cardiomyocyte proliferation after apical resection and LAD ligation surgery in postnatal day 1 and, to a lesser extent, postnatal day 2 (Porrello et al., 2011b). A similar finding is also reported in humans where a case of perinatal MI due to cryptogenic thrombotic LAD occlusion results in a complete functional and structural recovery after 1 year (Haubner et al., 2016). In mice, this regenerative response gradually diminishes until it ceases to exist at P7 when cardiomyocytes exit the cell cycle (Porrello et al., 2011b). These data suggest that differentially expressed genes or proteins during this two

day-proliferative window may have important roles in modulating cardiac regeneration (Wang et al., 2019).

The differential expression of miR-411 at P2-3 found in this study is in line with the findings of a previous study which reported increased miR-411 expression in human foetal hearts at a 23 week gestation age (Thum et al., 2007). While the exact role of miR-411 during early heart development has not yet been fully elucidated, other miRNAs, which have been found to be upregulated in embryonic and neonatal hearts such as the miR-302/367 cluster and miR-708, have been shown to increase cardiomyocyte proliferation and improve functional recovery post MI (Deng et al., 2017; Tian et al., 2015). These provide an indication that miR-411 can potentially be used for the same purpose. Moreover, miR-411 expression was reported to be significantly upregulated at 5d and 28d post MI (Muthusamy et al., 2014). Given that endogenous cardiomyocyte proliferation is increased post MI (Senyo et al., 2013), this further highlights the possible role of miR-411 in cardiac regeneration.

3.5.2 miR-411 can significantly increase proliferation in NRCMs

Both miR-411 and miR-181a were previously reported to increase EdU-positive nuclei in NRCMs compared to the control. However, in this study, only miR-411 was found to significantly induce cardiomyocyte proliferation as indicated by significantly higher rates of Ki-67-, EdU-, and pHH3-positive nuclei. MiR-181a, on the other hand, does not seem to affect – and even possibly reduces – cardiomyocyte proliferation as indicated by a significantly lower rate of EdU-positive nuclei compared to the control. These results suggest that miR-411 is more likely to improve cardiac regeneration compared to miR-181a.

3.5.3 miR-411 can significantly reduce YAP phosphorylation and thereby increase YAP activity

YAP is the main effector of the Hippo pathway; therefore, any changes in its activity may result from Hippo pathway modulation. Many studies have shown that YAP-induced gene expression is dependent on its binding to TEAD, thus proving a YAP

luciferase reporter assay to be a reliable measurement of YAP activity (Lamar et al., 2012; Tian et al., 2010). The assay revealed that miR-411 can significantly increase YAP activity, while miR-181a does the opposite. This indicates that in NRCMs overexpressing miR-411, there is an increase in non-phosphorylated YAP that can translocate to the nucleus and facilitate the expression of proliferative genes (Dong et al., 2007). These findings can potentially explain the results of the proliferation assays from both miRNAs.

Western blot results showed a reduced pYAP/tYAP ratio in the miR-411-transfected group, suggesting that increased YAP activity is caused by reduced YAP phosphorylation without changes in total YAP. Direct targeting of the Hippo core components by miRNAs, as reported previously, can lead to reduced YAP phosphorylation (Tian et al., 2015). However, the level of LATS1/2, MST1/2, and MOB1 remains unchanged after miR-411 transfection. This suggests that miR-411 induced- YAP activation is likely due to the modulation of protein(s) beyond the core Hippo signalling.

One of the distinct characteristics of miRNAs is their ability to target multiple genes (Bartel, 2004). Therefore, it is possible that miR-411 could target other genes involved in other pathways that subsequently act in a synergistic manner to increase proliferation (Lin et al., 2013). Table 3.3 displays several genes that have thus far been identified as miR-411 direct targets. Aside from FOXO1 and ITCH (itchy E3 ubiquitin protein ligase), none of these genes are directly linked with the Hippo pathway. FOXO1 is but one of four members of the Forkhead Box O transcription factors family, the other three being FOXO3, FOXO4, and FOXO6. Among the four members, FOXO1 is the most important factor in governing cardiac cellular functions, including proliferation, apoptosis, cell survival, cardiac metabolism, and oxidative stress (Puthanveetil et al., 2013). FOXO1 has recently been shown to regulate the oxidative stress response in the heart, together with the Hippo pathway. Active YAP physically interacts with FOXO1 and activates the FOXO1-mediated transcription of catalase and manganese-dependent superoxide dismutase genes and subsequently reduces oxidative stress (Shao et al., 2014). FOXO1 also plays an important role in

proliferation by facilitating the transcription of cell cycle inhibitors, p21 and p27, and thus acts as a tumour suppressor (Zhao et al., 2016). It will be interesting to discover whether miR-411 also targets FOXO1 in the heart and whether the miR-411-mediated downregulation of FOXO1 works via the Hippo pathway or independently via cell cycle modulation, as suggested above, to regulate cardiomyocyte proliferation.

Target gene	Tissue origin
Tumour suppressor FOXO1	Human lung cancer cell lines (Zhao et al., 2016)
Tumour suppressor ITCH	Human hepatocellular carcinoma cell lines (Xia et al., 2015)
Oncogene KPNA2 (Karyopherin alpha 2)	Human oesophageal squamous cell carcinoma tissue and cell lines (Song et al., 2019)
HIF-1α (Hypoxia inducible Factor 1α)	Deep vein thrombosis model in rat (Ai et al., 2018)
Oncogene CDH2 (Cadherin 2)	Human renal cell carcinoma tissue and cell lines (D. Zhang et al., 2019)
Oncogene SETD6 (SET domain containing 6)	Gastric cancer cell lines (Bai et al., 2019)
Oncogene ZnT1 (Zinc Transporter 1)	Human bladder cancer tissue and cell lines (Liu et al., 2018)
Tumour suppressor SPRY4 (Sprouty RTK Signaling Antagonist 4) and TXNIP (Thioredoxin Interacting Protein)	Human non-small cell lung carcinoma tissue and cell lines (C. Zhang et al., 2019)
Oncogene MLLT11 (MLLT11 Transcription Factor 7 Cofactor)	Human bladder cancer tissue and cell lines (Jin et al., 2018)
Proapoptotic Fas ligand	Rat model of acute spinal cord injury (Gong et al., 2018)
Oncogene STAT3 (signal transducer and activator of transcription 3)	Human cervical cancer tissue and cell lines (Shan et al., 2019)
Tumour suppressor MTSS1 (metastasis suppressor protein 1)	Human osteosarcoma tissue and cell lines (Xu et al., 2018)
Oncogene SP1 (Specificity protein 1)	Human breast cancer tissue and cell lines (Guo et al., 2016)
Oncogene PIK3R3 (Phosphoinositide-3-kinase regulatory subunit 3)	Human colorectar cancer tissue and cell lines (Zhao et al., 2018)
Oncogene GRB2 (Growth Factor Receptor Bound Protein 2)	Human breast cancer tissue and cell lines (Zhang et al., 2016)
MMP3 (Matrix Metalloproteinase 3)	Human osteoarthritic tissue and human chondrocytes cell lines (G. Wang et al., 2015)
SPRY4 (Sprouty RTK Signaling Antagonist 4)	Human rhabdomyosarcoma cell lines (Sun et al., 2015)
Prometastatic IL8 (Interleukin 8)	Human malignant pleural mesothelioma cell lines (Yamamoto et al., 2014)

Table 3.3 Validated miR-411 target genes

ITCH is a member of the NEDD4-like family of E3 ubiquitin ligases and is characterised by distinct domain architectures, consisting of a N-terminal Ca^{2+}-dependent phospholipid-binding C2 domain involved in membrane targeting, a multiple protein-protein interaction WW domain, and a HECT (homologous to the E6-AP carboxyl terminus)-type ligase domain providing the catalytic E3 activity. Physiologically, ITCH plays an important role in ubiquitination, a post-translational modification that is required in many cellular processes including protein degradation by proteasome, endocytosis, DNA repair, cell cycle regulation, and gene expression (Salah et al., 2011). ITCH can physically interact with and regulate the stability of LATS1 by binding between the WW domains of ITCH and the PPxY motifs of LATS1. ITCH overexpression stimulates the proteasomal degradation of LATS1 and thus reduces YAP phosphorylation and enhances proliferation. On the other hand, reduced ITCH expression significantly increases LATS1 and YAP phosphorylation, leading to increased cell death and reduced proliferation (Ho et al., 2011). The phenotypes that we found here, constant LATS1 level and increased cardiomyocyte proliferation, are not consistent with those caused by ITCH downregulation. Therefore, it is unlikely that miR-411 directly targets ITCH in this scenario.

The results so far have clearly shown that compared to miR-181a, miR-411 has the potential to increase cardiomyocyte proliferation through the Hippo pathway. However, further research needs to be done to investigate what genes are targeted by miR-411 in the heart and how these genes modulate the Hippo pathway.

3.5.4 Limitations and future work

One of technical challenges within this *in vitro* project is the relatively marked variation within miRNA expression data sets (Section 3.4.2, Fig 3.4). MicroRNA profiling can be a challenging process due to inherent characteristics of miRNA such as the lack of poly(A) tail, the short sequence of mature miRNAs, and length variation between pri-, pre-, and mature miRNAs (Pritchard et al., 2012). In general, qPCR is a popular method to measure the miRNA expression and great for confirmatory assay due to its reliability, reproducibility, and large dynamic range (Chugh and Dittmer,

2012). However, variations between experiments are relatively common as can be seen in Figure 3.4. qPCR data variations can happen in every step of qPCR from sample isolation and handling, pipetting skills, RNA to cDNA conversion, qPCR itself, and data normalisation (Chugh and Dittmer, 2012; Chugh et al., 2010). The principles of small RNA extraction are generally similar to total RNA extraction, except that the protocols for small RNA isolation are often modified to enrich the small RNA fraction (Pritchard et al., 2012). The quality and quantity of isolated small RNAs may vary due to different isolation methods and sample types. Small RNAs isolated from cell line usually have a higher yield and better quality than small RNAs isolated from tissue (Chugh and Dittmer, 2012; Pritchard et al., 2012). In this project, we used a combination of Trizol® and a kit from Invitrogen designed specifically for small RNA extraction. Despite some problems with the quality of small RNA at the beginning of the project, subsequent isolations yielded small RNAs with optimal quantity and quality for further analyses. Previous studies showed that cDNA synthesis reaction can cause considerable variations up to 100-fold in the qPCR final product (Kitchen et al., 2010; Lee et al., 2010). Effects of RNA secondary structures, variations in priming efficiency, and properties of reverse transcription enzymes can contribute to these variations (Ståhlberg et al., 2004). Currently, there are two different techniques of cDNA synthesis available: using sequence specific RT primers or universal tailing primers to enzymatically generate poly(A) tail (Chugh and Dittmer, 2012). In this project, we used sequence-specific stem-loop RT primers from TaqMan™ to reverse transcribe miRNA candidates. The advantage of using this approach is increased specificity and reduction of non-specific priming. This approach works significantly better for highly and moderately abundant miRNAs; however, it may not be sensitive enough to detect low abundance miRNAs (Chugh and Dittmer, 2012). Universal tailing system, on the other hand, increases the possibility of non-specific amplifications which contributes to a large number of false positive results (Chugh and Dittmer, 2012). Data normalisation is another critical factor which may cause variations in qPCR results (Masè et al., 2017). In this experiment, small nuclear RNA U6 was used as a reference to normalise the expression of candidate miRNAs. U6

snRNA together with RNU44 and RNU48 are classified as small nuclear RNA and commonly used as references to measure relative expression of miRNA using qPCR (Lamba et al., 2014; Schwarzenbach et al., 2015). Previous papers have argued that snRNAs are not suitable for endogenous reference because they are different from miRNAs in terms of transcription, processing, and tissue-specific expression patterns (Gee et al., 2011; Schwarzenbach et al., 2015). Moreover, several studies have suggested that the stability of U6 snRNA expression may be tissue specific as it was found to display a high variability in the hepatic tissue, serum, and renal cells but stable in pleural effusion and lung adenocarcinoma (Lamba et al., 2014). To overcome this problem, Torres *et al*. suggested that multiple references (at least three) are necessary to provide more reliable and robust normalisation (Torres et al., 2013). The qPCR results in Fig 3.1 display relatively high variability; however, the trend is always consistent in every experiment. This suggests that although improvements must be made in the future to minimise variability between experiments, the findings from the current project can reflect the expression level of candidate miRNAs in various sample types.

As described in Section 3.4.3, this study uses Ki-67, EdU, and pHH3 markers to evaluate cell cycle progression of cardiomyocytes. However, the presence of cytokinesis, the last stage of cell cycle, have not been investigated yet. In the future, aurora kinase B or investigation of midbody positioning can be used to analyse cytokinesis in cardiomyocytes.

Finally, although the expression of genes upstream of YAP has been investigated in this chapter, the changes in genes expression downstream of YAP remains elusive. As discussed in Section 1.1.4, YAP targets several proproliferative pathways or genes, such as PI3K/AKT, Wnt/β-catenin, ANKRD1, CTGF, PARK2, and CYR61. In the future, the expression of these genes need to be investigated to elucidate how YAP stimulate proliferation after miR-411 transfection.

3.6 Conclusion

In conclusion, the screening results show that miR-411 is expressed higher in NRCMs compared to other cell populations in the heart and in the neonatal heart compared to the adult heart. Further experiments show that overexpression of miR-411 can increase YAP activity and cardiomyocyte proliferation *in vitro*. Overall these suggest that miR-411 is a potential regulator of the Hippo pathway and thus can likely be used to promote regeneration in the heart.

CHAPTER 4

The effects of miR-411 mimic injection into the myocardium

Chapter 4 - The effects of miR-411 mimic injection into the myocardium

4.1 Introduction

Although cardiomyocyte proliferation is responsible for embryonic heart growth, the vast majority of mammalian cardiomyocytes will withdraw from the cell cycle soon after birth (Porrello et al., 2011b), which results in adult hearts having a very limited renewal capacity (Bergmann et al., 2009; Senyo et al., 2013). The cardiomyocyte cell cycle exit is accompanied by the downregulation of pro-mitotic factors, such as cyclins and cyclin dependent kinases (CDKs), as well as an upregulation of cell cycle inhibitors such as CDK inhibitors, p21, p27, and p57 (Poolman and Brooks, 1998; Tane et al., 2014). These changes in the cell cycle regulatory molecules are intricately orchestrated by several signalling pathways including but not limited to the Notch (Zhao et al., 2014), AKT , Hippo, Wnt (Heallen et al., 2011; Lin et al., 2015), and JAK/STAT pathway (Miyawaki et al., 2017). In addition, transcription factors such as Meis1 (Mahmoud et al., 2013) and E2F (Ebelt et al., 2008), paracrine factors like Neuregulin-1 and IGF-1 (Hertig et al., 1999), microRNAs such as miR-15 family (Porrello et al., 2013), and extracellular matrix protein like Agrin (Bassat et al., 2017) also contribute to the shift in the balance of the cell cycle modulators during cardiomyocyte cell cycle exit.

As cardiomyocytes exit the cell cycle, they begin to undergo extensive remodelling and acquire more mature phenotypes. This remodelling process is extensive and virtually affects all aspects of cardiomyocyte morphology and functions. Structurally there are three prominent hallmarks of cardiomyocyte maturation: a transition of cardiomyocyte growth from proliferative state/hyperplasia to hypertrophy accompanied by multinucleation and polyploidisation, increased myofibrillar densities with increased sarcomere alignment, and improved intercellular Ca^{2+} propagation via t-tubule formation (Li et al., 1996). The reason behind these changes is still poorly understood but it is likely

to allow for stronger and more coordinated contractions to meet the increasing metabolic demands.

Although cardiomyocyte maturation is crucial for contraction and Ca^{2+} handling efficiency, previous studies indicate that the structural changes during the maturation process limit the ability of adult cardiomyocytes to proliferate (Gonzalez-Rosa et al., 2018; Y. Zhang et al., 2010). This in turn necessitates dedifferentiation where cardiomyocytes must revert back to less mature phenotypes in order to proliferate (D'uva et al., 2015; Jopling et al., 2010). In the event of injury such as MI, the proportion of adult cardiomyocytes that undergo dedifferentiation and proliferation is increased, especially in the border zone (Senyo et al., 2013; Wang et al., 2017). However, this increase is far from sufficient to replace the lost cardiomyocytes following MI (Senyo et al., 2013; Y. Zhang et al., 2019). The damaged myocardium will instead be replaced by scar tissue, leading to reduced contractility and eventually HF. Targeting the signalling pathways or the molecules involved in modulating cardiomyocyte proliferation may provide new therapeutic opportunities to enhance regeneration and reduce the severity of MI.

Based on evidence accumulated in recent years, the modulation of the Hippo pathway may represent a promising therapeutic target for MI (Leach et al., 2017; Lin et al., 2014). As it is difficult to target most of the core components of the Hippo pathway, the identification of novel Hippo pathway regulators which can be targeted for therapeutic purposes is very important. In the previous chapter, this project has identified miR-411 as a novel Hippo modulator that can significantly increase YAP activity and cardiomyocyte proliferation in cultured primary NRCMs. However, the modulation of proliferation in NRCMs is arguably easier because they are still in the proliferative state. The next step, therefore, is to investigate the effect of miR-411 on adult cardiomyocyte cell cycle re-entry. To achieve this aim, *in vivo* experiments will be performed by overexpressing miR-411 in the heart. This approach was preferred over the use of transfection of miR-411 mimics in cultured primary cardiomyocytes. This decision was made due to the presence of evidence that the character and morphology of isolated cardiomyocytes may change when grown in a culture plate.

Zhang *et al.* reported that cultured adult cardiomyocytes spontaneously flattened, lost their striation, and expressed cardiac progenitor cell markers, thus rendering them more malleable to proliferative stimuli (Y. Zhang et al., 2010). Adopting an *in vivo* approach will eliminate this variable and allow for the investigation of cardiomyocyte proliferation in the cardiomyocytes' normal physiological environment.

The effect of miR-411 on injured hearts will also be investigated using a mouse model of MI. MI will be induced by ligating the main branch of the left coronary artery - the left anterior descending (LAD) coronary artery (Salto-Tellez et al., 2004). LAD ligation is considered as a standard procedure to induce MI in mice (Klocke et al., 2007). *In vivo* miR-411 overexpression in both normal and injured hearts was achieved by direct intramyocardial injection of miR-411 mimics (Lesizza et al., 2017).

4.2 Aims

- To investigate the effect of miR-411 overexpression on adult cardiomyocyte cell cycle re-entry *in vivo*
- To investigate the effect of miR-411 overexpression on cardiac structure and function post MI

4.3 Methods

4.3.1 Animal experiments

Animal experiments were performed under project license (PPL) No. P3A97F3D1 under Dr Elizabeth J. Cartwright as the project license holder. All regulated procedures were performed in accordance with the United Kingdom Animals (Scientific Procedures) Act 1986 and also approved by the University of Manchester Ethics Committee. All animals used in this study were housed in the University of Manchester biological service facility (BSF) in standard housing conditions for laboratory animals. All experiments were performed in male C57Bl/6 mice (purchased from Envigo, UK) which were provided with food and water ad libitum. *In vivo* procedures involving anaesthesia, surgery and injection were performed by Dr Min Zi with the assistance of Mr Sukhpal Prehar and the author whilst tail vein blood sampling and echocardiograpy were performed by the author after receiving appropriate training.

4.3.1.1 Intramyocardial injection of miRNA mimics in normal mice

Each animal received 5 µg of miR-411 mimics mixed with PEI (nucleic acid to PEI ratio 1:2.5) and resuspended in 5% dextrose solution, in a total volume of 25 µl. Control animals received an injection of 25 µl 5% dextrose solution.

Before the procedure, the hair from the ventral neck area and left half of the thorax of the mice was removed. Buprenorphine 0.1 mg/kg was administered intraperitoneally to manage pain. Eight week old mice were anaesthetized with isoflurane 3% supplemented with O_2 1L/minute, intubated, and subsequently ventilated using a Minivent 845 (Harvard Apparatus), set at 200 breaths per minute and tidal volume of 0.1 ml. They were laid down in a supine position on a warmer pad set at 37°C. A 5-mm incision was made near the left sternal border to expose the underlying muscles. Forceps were used to lift the pectoralis major muscle to expose the ribs. The 4th intercostal space was pierced and enlarged with a retractor to visualise the heart. The 5% dextrose or mimic solution was injected directly into the

myocardium below the left atrial appendage using a 0.3 ml insulin syringe with a 30-gauge needle. The needle was held in place for a few seconds to reduce the risk of miR-411 mimic solution being ejected from the site of injection. After injection, the chest cavity was closed with 6-0 Prolene suture and mice were administered 0.1ml sterile saline/30g body weight intraperitoneally to prevent dehydration during recovery. Mice were then laid in a prone position in an oxygenated chamber until recovered from anaesthetics. They were transferred to a new cage and put in a warm cabinet at 30°C before being transferred back to normal housing. Additional dose of buprenorphine was given 24 hours post surgery to manage pain. Three days post injection, 50 mg/kg EdU was injected intraperitoneally to assess cardiomyocyte proliferation after miR-411 mimic injection. Two days after EdU injection (5 days after miR-411 mimic injection), the mice were sacrificed by cervical dislocation. Hearts were divided according to the Figure 4.1. The parts reserved for immunofluorescence staining were fixed in 4% PFA in PBS whilst the parts reserved for molecular analysis were stored in -80°C.

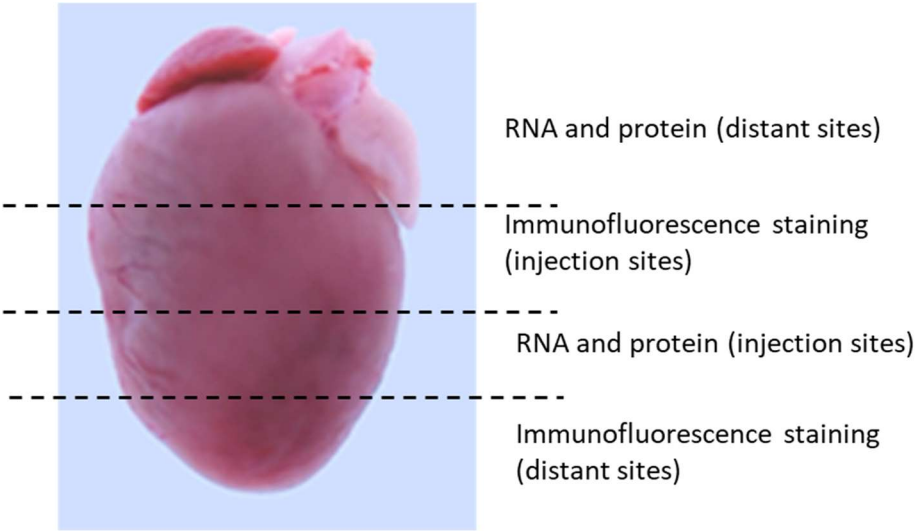

Figure 4.1 Methods used to divide the hearts for immunofluorescence and molecular analysis.

4.3.1.2 Myocardial infarction model

Myocardial infarction was induced by ligating the LAD in 10-12 weeks old C57Bl/6 mice. Before the procedure, the hair from the ventral neck area and left half of the thorax of the mice was removed. Mice were anaesthetised with 3% isoflurane (by inhalation) supplemented with oxygen at a flow rate of 1L/min. Buprenorphine (0.1mg/kg) was administered via intraperitoneal injection to provide analgesia. The mice were then intubated, placed on a heating pad (37°C) and ventilated using a Minivent 845 (Harvard Apparatus), set at 200 breaths per minute and tidal volume of 0.1 ml. Throughout the procedure, mice were maintained under general anaesthesia with 1.5-3% isoflurane in 100% oxygen. The procedure began by making a 5 mm skin incision at the left sternal border using a binocular stereomicroscope (Olympus) to aid vision, 2 mm below the armpit level, thus exposing the underlying muscle. The pectoralis major muscle was lifted up and fixed with retractors, followed by dissection of the pectoralis minor to expose the ribs. The fourth intercostal space was pierced and retracted to expose the heart. The pericardium was stripped to locate the LAD coronary artery. Following this, the LAD artery was permanently ligated with 8-0 nylon suture (ETHILON) at the level of the left atrial appendage. Ligation was deemed successful once the anterior wall of the left ventricle turned pale. 25 µl of control mimics – PEI solution, or hsa-miR-411 – PEI solution, or no mimic controls (PEI solution only) was then injected into the anterior wall of the left ventricle. After injection, the rib retractors were released and the intercostal space, muscles, and skin were then sutured and the animals were extubated to establish normal breathing. The mice were then transferred to a recovery chamber supplemented with 1L/minute oxygen. Sterile saline (0.1ml/30g body weight) was administered intraperitoneally to compensate for blood loss during the procedure. Once the mice recovered, they were transferred to a new cage and subsequently placed in an incubator at 30°C where they were closely monitored and kept for several hours before they were transferred to normal housing. Sham operated controls underwent the same surgical procedures without the ligation of the LAD coronary artery. Mashed food was provided to all mice for three to five days post-surgery.

4.3.1.3 Cardiac Troponin I analysis

Blood sampling and plasma preparation

Blood samples were collected from the lateral tail vein 24 hours post MI and sham surgery. The mouse tail was locally anaesthetised with anaesthetic cream (Lidocaine 2.5% and Prilocaine 2.5%, EMLA™ cream) approximately 20 minutes before the start of the procedure. The mouse was then placed on a heating pad to vasodilate the vein and transferred into a restraint tube in order to minimise movement during blood collection. Povidone-iodine solution was applied to the tail to disinfect the puncture site. After the tail vein was located, a small transverse incision was made over the vein with a sterile blade. 40 µl blood was collected with a 200 µl pipette and then transferred to a sterile tube containing 40 µl 3.2% sodium citrate to prevent coagulation. The samples were put on ice between collection. Once all the blood samples were collected, they were spun at 8000 rpm for 6 minutes at 4°C. Finally, the plasma-containing supernatant was transferred to new Eppendorf tubes and stored at -80 °C until the assay was performed.

Cardiac troponin I (cTnI) assay

Cardiac troponin I is expressed specifically in cardiomyocytes and released to the bloodstream following injury such as MI. The cTnI level is a reliable biomarker for MI and routinely used clinically. In this study, the level of cTnI was examined using plasma samples collected 24 hours post-surgery to confirm the occurrence of MI. A high sensitivity mouse cTnI ELISA kit (Life Diagnostics) was used to measure cTnI levels according to the manufacturer's guidelines. First, the plasma samples were diluted five times with plasma diluents supplied with the kit. Standards were prepared by serially diluting cTnI stock to known cTnI concentrations. 100 µl of HRP-conjugates were added into a 96-well ELISA plates coated with anti mouse cTnI antibodies (supplied with the kit). The standards and diluted plasma samples were then dispensed into each well. After this, the plate was incubated for 1 hour at RT

under agitation to allow the cTnI in the samples to react with both anti mouse cTnI antibodies and HRP-conjugates. The plate was then washed 5 times to remove unbound HRP conjugates. Tetramethylbenzidine (TMB), which is an HRP substrate, was then added to the wells and the plate was incubated for 20 minutes at RT under agitation. A resultant blue colour was formed, which changed to yellow upon addition of the stop solution to stop the reaction. Absorbance at 450nm was measured using a plate reader and plotted on the standard curve to measure the cTnI concentration.

4.3.1.4 Echocardiography

To evaluate the left ventricular dimensions and function at 4 weeks post-MI, transthoracic two dimensional echocardiography was performed with a VisualSonics Vevo 770 ultrasound machine equipped with a 30 MHz transducer. Before the procedure, the hair of the left hemithorax of the mice was removed using hair removal cream. Following this, the mice were anaesthetised with 3% isoflurane inhalation, and placed on a heat pad. The mice were maintained under general anaesthesia with 1% isoflurane with additional 1 L/minute oxygen during the whole echocardiography procedure. Pre-warmed ultrasound transmission gel was applied to the chest, and an M-mode image of the heart was generated using VisualSonics software.

Evaluation of left ventricular chamber dimensions was performed by assessing two-dimensional M-mode images of the heart at different levels in both the parasternal short axis and long axis. Using the parasternal short axis, several M mode images were recorded at the level with the largest left ventricular diameter lying between the papillary muscles and the bicuspid valve. The M mode images (Figure 4.2) were then used to measure left ventricular anterior and posterior wall thickness, septum thickness and left ventricular internal diameter at end-systole and end-diastole, which were used to calculate the left ventricular ejection fraction and fractional shortening with the formulas shown in Table 4.1. The researcher who performed the echocardiography and conducted the analysis were blinded to treatment group.

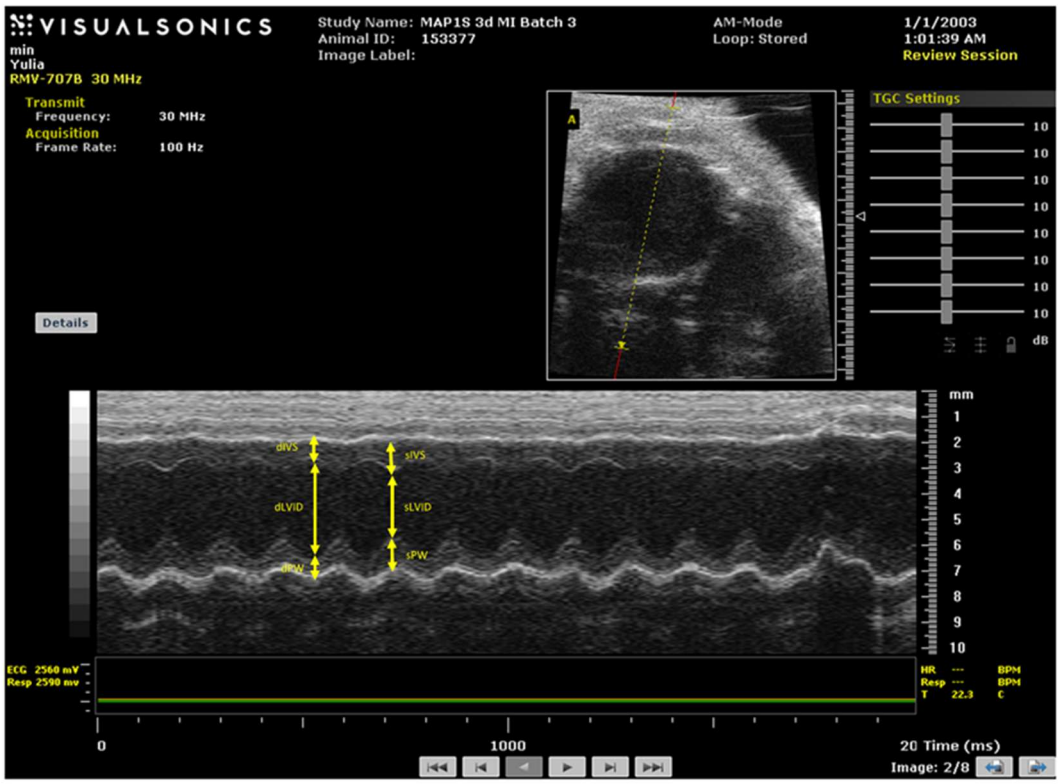

Figure 4.2 M-mode echocardiography image of the heart. Echocardiography image from parasternal short axis view. Posterior wall (PW), left ventricular internal diameter (LVID) and intra-ventricular septum thickness (IVS) at diastole (d) and systole (s) were used to calculate ejection fraction and fractional shortening.

Parameters	Formula
Fractional Shortening (FS %)	[(dLVD- sLVD/ dLVD)] x 100
Ejection Fraction (EF %)	[(EDV-ESV)/EDV] x 100
Left Ventricular Mass (LVM)	1.055 x[(dLVD + dPW + dIVS)3 – dLVD3]
Relative Wall Thickness (RWT)	(dIVS + dPW) / dLVD

Table 4.1 Parameters used to analyse cardiac function in MI experiments. Note: 1.055 is the specific gravity of the myocardium (g/mL), dLVD: Left Ventricle end-diastolic Diameter, sLVD: Left Ventricle end-systolic Diameter, EDV: end-diastolic volume, ESV: end systolic volume.

4.3.2 Histology analysis

4.3.2.1 Tissue fixation, processing, and sectioning

Formalin fixation and paraffin embedding

At the end of MI experiments (4 weeks), mice were sacrificed by cervical dislocation and the whole hearts were extracted from the chest cavity and cleaned of blood clots by washing with sterile PBS briefly. The hearts were then dried and weighed. In addition to the hearts, the lungs were also weighed to examine the signs of heart failure. Body weight and tibia length were recorded to normalised the heart and lung weight. Following this, the hearts were fixed with 4% paraformaldehyde (Sigma) for 24 hours at 4°C under agitation to evenly distribute the fixative. The hearts were then placed in histology cassettes and immersed in 70% ethanol before being transferred to a Leica ASP300 for tissue processing. The tissue processor uses different concentrations of industrial methylated spirits (IMS) for tissue dehydration, as well as xylene and molten-wax. The protocol is shown in Table 4.2.

Table 4.2. Tissue processing protocols used in this study.

Reagent	Time (min)	Reagent	Time (min)
1. 70% alcohol	20	8. Xylene	20
2. 70% alcohol	30	9. Xylene	30
3. 90% alcohol	45	10. Xylene	40
4. 90% alcohol	60	11. Wax	70
5. 100% alcohol	30	12. Wax	70
6. 100% alcohol	45	13. Wax	70
7. 100% alcohol	60	Proceeded for tissue embedding	

After tissue processing, the hearts were embedded in paraffin wax. The hearts were then sectioned at 5µm thickness from 6-8 different levels of the heart starting from the apex, using an automated rotary microtome (Leica 2255) with 500µm intervals

between each level (Figure 4.3). The sections were then mounted onto poly-l-lysine-coated slides (VWR), left to dry overnight in a 37°C oven and then stored at room temperature.

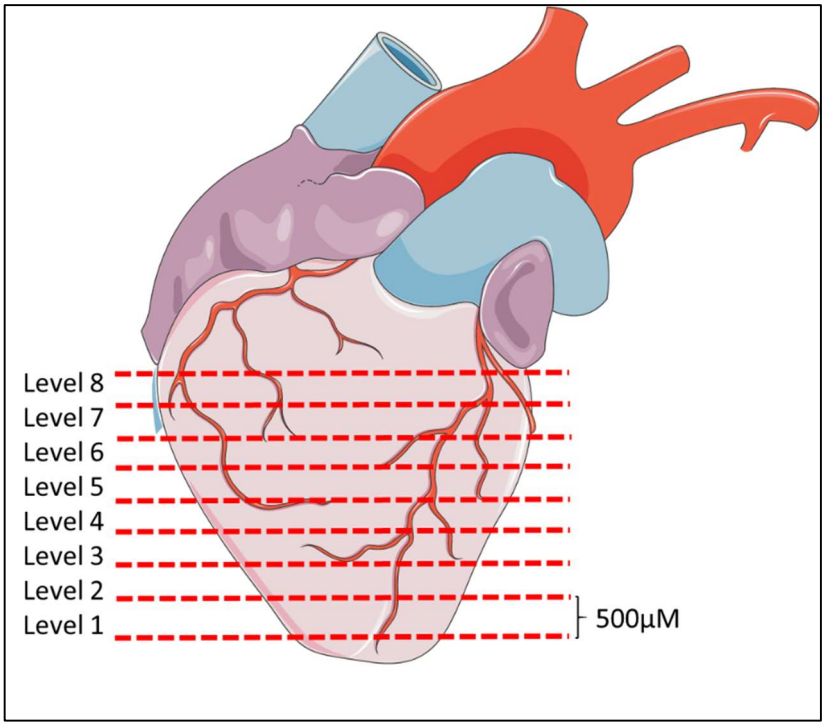

Figure 4.3. **The method used to section the heart tissue in this study.**

Frozen section

In addition to using the FFPE (formalin fixed parafin embedded) technique, some of the hearts were preserved using a cryofixation technique. After harvesting, the hearts were placed in tissue molds, embedded in optimum cutting temperature (OCT) media (Thermofisher Scientific), and frozen in isopentane pre-chilled with dry ice. The hearts were sectioned at 6 µm thickness as per Figure 4.3 using a Leica cryostat and stored in -80°C freezer.

4.3.2.2 Masson's trichrome

Masson's trichrome staining was performed to evaluate infarct/ fibrotic scar size at 4 weeks post-MI. Briefly, sections of mouse hearts were deparaffinised by placing them on the 60°C heat block and then in xylene for 5 minutes. Following this,

the sections were rehydrated by serial rehydration in decreasing concentrations (100%, 90%, and 75%) of IMS for 2 minutes each and then washed in distilled water before staining. To improve staining quality, sections were treated in Bouin's fixative (Sigma) for 2 hours at room temperature, then washed until clear in tap water. Harris' Haematoxylin (Sigma) was added to sections for 3 minutes to stain nuclei. After being washed with water, sections were briefly differentiated in 1% HCl in 70% Ethanol solution and washed again in warm running tap water for 5 minutes. Sections were then immersed in Red solution (each 100 ml contains 90 ml of 1% w/v Biebrich Scarlet (Sigma) in ddH_2O and 10 ml of 1% of Fuchsin (Sigma) in ddH_2O) to stain muscle for 5 minutes, and then treated with 2.5% (w/v) phosphomolybdic acid (Sigma) for 15 minutes to differentiate red stain from connective tissue. Next, sections were stained with Aniline blue (Sigma, 2.5% w/v solution in 2% acetic acid) solution for 3 minutes or longer if necessary to stain the collagen and then treated with 1% acetic acid for 2 minutes. All sections were then sequentially dehydrated in IMS solution with increasing concentration (50%, 75% and 100% for 2 minutes each). Finally, all slides were cleared in xylene for 20 minutes and mounted with DPX mounting media (Sigma) and coverslips. Slides were left to dry for several hours and then imaged with a 3D Histech Panoramic 250 Flash II slide scanner and analysed with Pannoramic Viewer software. Scar size was quantified using a midline length measurement approach as described by Takagawa *et al.* (Takagawa et al., 2007).

4.3.2.3 TUNEL staining

FFPE sections

Terminal deoxynucleotidyl transferase mediated nick end labelling (TUNEL) staining, which labels DNA strand breaks, has been routinely used to assess cardiomyocyte apoptosis in histological sections (Scarabelli et al., 1999). In this study, TUNEL staining was performed using a commercial in situ Cell Death Detection Kit, Fluorescein (Roche) according to the manufacturer's protocol. First, deparaffinised and rehydrated sections were incubated with 3% H_2O_2 for 15 minutes then washed 3 times in PBS for 10 minutes each. Sections were first treated with proteinase K (20

µg/ml in PBS, Invitrogen) for 15 minutes at 37°C and then subjected to a second round of permeabilisation by incubating in a solution containing 0.1% Triton X and 0.1% sodium citrate for 8 minutes at RT. Sections were placed in a humidifying chamber and incubated with TUNEL mixture containing enzyme solution diluted in labelling agent (1:10 dilution, supplied with the kit) for 1 hour at 37°C. Sections were then blocked in 1% BSA for 1 hour at room temperature followed by overnight incubation with primary antibodies (mouse anti α-actinin, Sigma, 1:100 in blocking solution). The following day, sections were washed with PBS and incubated with Secondary Alexa Fluor 647-conjugated anti-mouse IgG antibody (1:100 in PBS) for 1 hour at RT followed by nuclei counterstaining with 50 nM 4',6'-diamidino-2-phenylindole (DAPI, Invitrogen). Slides were then mounted with Vectashield mounting medium.

Frozen sections

First, sections were thawed at RT for 30 minutes, fixed in 4% paraformaldehyde in PBS pH 7.4 for 15 minutes, and washed in PBS. Sections were then permeabilised with 0.2% Triton X-100 in 0.1% sodium citrate at 4°C for 2 minutes and washed again with PBS 2 times for 15 minutes each. From this point, the following steps are identical to the protocol used for FFPE tissue described above.

The sections were imaged using a Zeiss™ fluorescence microscope (Carl Zeiss, Jena, Germany) at 10X magnification and analysed with ImageJ. All areas that contained TUNEL positive cells were imaged and the same number of images were taken from each sample. The number of positive cells was quantified through the FITC channel in each image and presented as the number of TUNEL positive cardiomyocytes per visual field.

4.3.2.4 Immunofluorecence staining on tissue sections

FFPE tissue

Sections of mouse hearts were deparaffinised by placing them on the 60°C heat block and then in xylene for 5 minutes. Following this, the sections were rehydrated by serial rehydration in decreasing concentrations (100%, 90%, and 75%) of IMS for

2 minutes each and then washed in distilled water before staining. The sections were subjected to an antigen retrieval process by boiling in a sodium citrate buffer (10 mM sodium citrate, 0.05% Tween 20, adjusted to pH 6.0 with 1N HCl) for 20 minutes. After the sections cooled down to room temperature, they were rinsed several times in distilled water, permeabilised in 0.3% Triton-X in PBS for 30 minutes, and blocked for 1 hour in 10% goat serum diluted with permeabilisation buffer. Following this, sections were incubated with primary antibodies (Rabbit Ki-67 antibody, Abcam, and mouse anti sarcomeric α-actinin, Sigma, 1:100 dilution in blocking buffer) in a humidifying chamber at 4°C overnight. The sections were then washed three times with PBS, and incubated with secondary antibodies (FITC conjugated anti-rabbit secondary antibody and Alexa 647 conjugated anti-mouse secondary antibody, Jackson Immunoresearch, 1:100 dilution in blocking buffer) in a dark humidifying chamber for 1 hour at room temperature. The sections were then washed with PBS three times, counterstained with DAPI (Invitrogen, 1:5000 dilution in PBS), and mounted with Vectashield mounting medium.

For EdU staining, after the blocking step sections were incubated with primary antibody mouse anti sarcomeric α-actinin (Sigma, 1:100 dilution in blocking buffer) in a humidifying chamber at 4°C overnight. After being washed three times with PBS, sections were subsequently incubated with Alexa 647 conjugated anti-mouse secondary antibody (Jackson Immunoresearch, 1:100 dilution in blocking buffer) in a dark humidifying chamber for 1 hour at room temperature and washed again three times with PBS. Then EdU immunofluorescence staining was performed on the sections by using the Click-iT® EdU Imaging Kits (Alexa Fluor® 488, ThermoScientific) according to the manufacturer's instructions. Sections were washed, counterstained with DAPI (Invitrogen, 1:5000), and mounted with Vectashield mounting medium.

Frozen section

First, sections were thawed at RT for 30 minutes, fixed in 4% paraformaldehyde in PBS pH 7.4 for 15 minutes, and washed in PBS. For permeabilisation, sections were immersed in 0.25% Triton X-100 in PBS for 10 minutes and washed again in PBS 3

times 5 minutes each. Next, sections were blocked with 1% BSA in PBS containing 0.25% Triton X-100 and incubated with primary antibodies (Rabbit Ki-67 antibody, Abcam, and mouse anti sarcomeric α-actinin, Sigma, 1:100 dilution in blocking buffer) in a humidifying chamber at 4°C overnight. After being washed 3 times with PBS, sections were incubated with secondary antibodies (FITC conjugated anti-rabbit secondary antibody and Alexa 647 conjugated anti-mouse secondary antibody, Jackson Immunoresearch, 1:100 dilution in blocking buffer) in a humidifying chamber for 1 hour at RT, and washed again with PBS. Incubation with DAPI (1:5000 in PBS) for 1 minute was then used to counterstain the nuclei. Finally, sections were washed with PBS, rinsed with distilled water, air dried, and mounted with Vectashield mounting medium.

The sections were imaged by Zeiss™ fluorescence microscope (Carl Zeiss, Jena, Germany) at 10X magnification and analysed with ImageJ. All areas that contained Ki-67 or EdU positive cells were imaged and the same number of images were taken from each sample. The number of positive cells was quantified through the FITC channel in each image and presented as the number of Ki-67 or EdU positive cardiomyocytes per visual field.

4.4 Results

4.4.1 Delivery of miR-411 mimics by direct intramyocardial injection

Intramyocardial injection combined with the use of non-viral vector PEI was used in this project because previous evidence had demonstrated that it could effectively deliver miRNAs to the heart and was relatively safe without causing obvious toxicity to the animals (Lesizza et al., 2017; Wahlquist et al., 2014). Intramyocardial injection was also expected to only deliver miRNA mimics locally and thus could avoid off target effects in distant organs and enhance the specificity of miRNA delivery. Furthermore, non-viral vectors including PEI only drive short-term miRNA overexpression (Lesizza et al., 2017) instead of long-term overexpression, which has been shown to cause severe cardiac adverse effects (Gabisonia et al., 2019; Tian et al., 2015). Collectively, these suggest that combination of local delivery and non-viral vectors might be a potential approach for future miRNA-based therapeutics in MI.

Before examining the effect of miR-411, it was necessary to confirm successful delivery of the miR-411 mimics into the myocardium. The expression of miR-411 was measured 5 days post injection using qPCR and was compared between the injection and distant sites. Figure 4.4A & B show that the qPCR strongly suggests an increase in miR-411 expression in the injection site (34.5 ± 11.11 fold) but not in the distant sites. MiR-411 expression was also measured in other organs, including the lung (Fig. 4.4C), liver (Fig 4.4D), and kidney (Fig 4.4E), to investigate whether or not the miR-411 mimics entered systemic circulation and ended up in those organs. Although it is not statistically significant, the results consistently show that miR-411 expression is increased in the miR-411 group compared to the control in the three organs that were examined, with the biggest increase being observed in the liver, followed by the kidney and the lung, respectively.

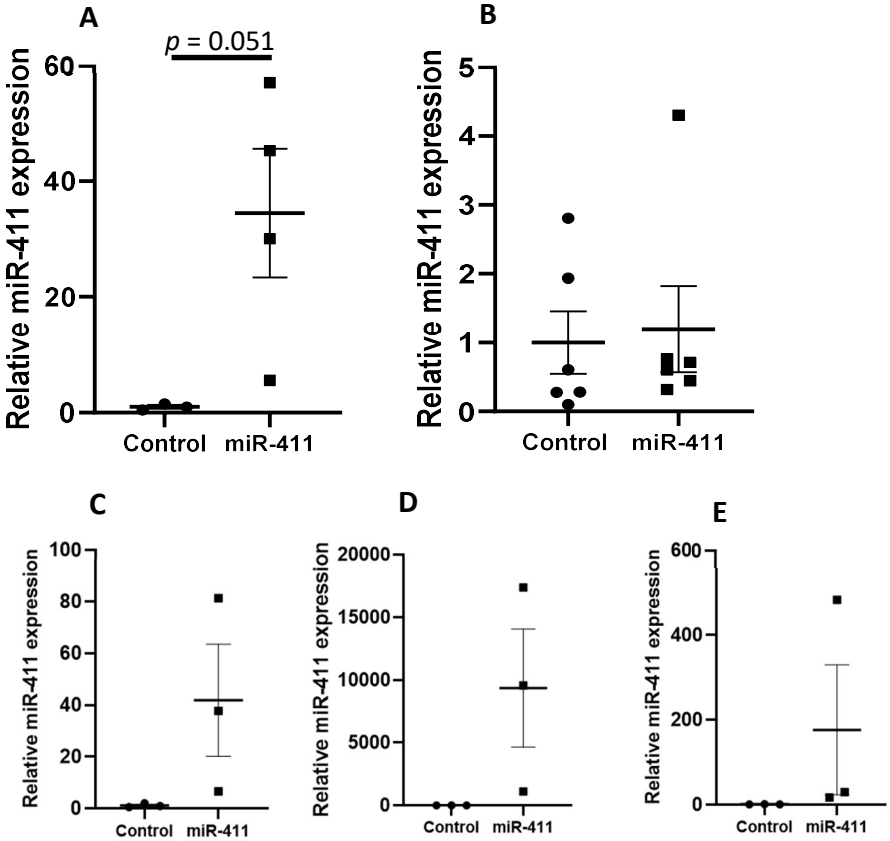

Figure 4.4 miR-411 expression level at 5 days post injection. (A) The expression of miR-411 in the mIR-411 group is markedly increased in the injection site (*p*=0.051, n=3 for controls, n=4 for miR-411 group, unpaired Student's t-test) but not in the distant site (B, n=6). There is a trend that miR-411 expression is higher in the lung (C), liver (D), and kidneys (E) that were harvested from miR-411 injected mice (n=3)

4.4.2 The effect of miR-411 on cardiomyocyte cell cycle re-entry

To examine whether miR-411 overexpression would increase the number of proliferating cardiomyocytes, the expression of the cell cycle marker Ki-67 was analysed 5 days post injection. Figure 4.5 shows representative Ki-67 immunofluorescence images from heart sections near the injection sites. The results show a significant increase in the rate of Ki-67 positive cardiomyocytes in the miR-411 group compared to controls. In the distant sites, however, the rate of Ki-67 positive cardiomyocytes does not differ significantly between the control and miR-411 groups (Fig 4.6).

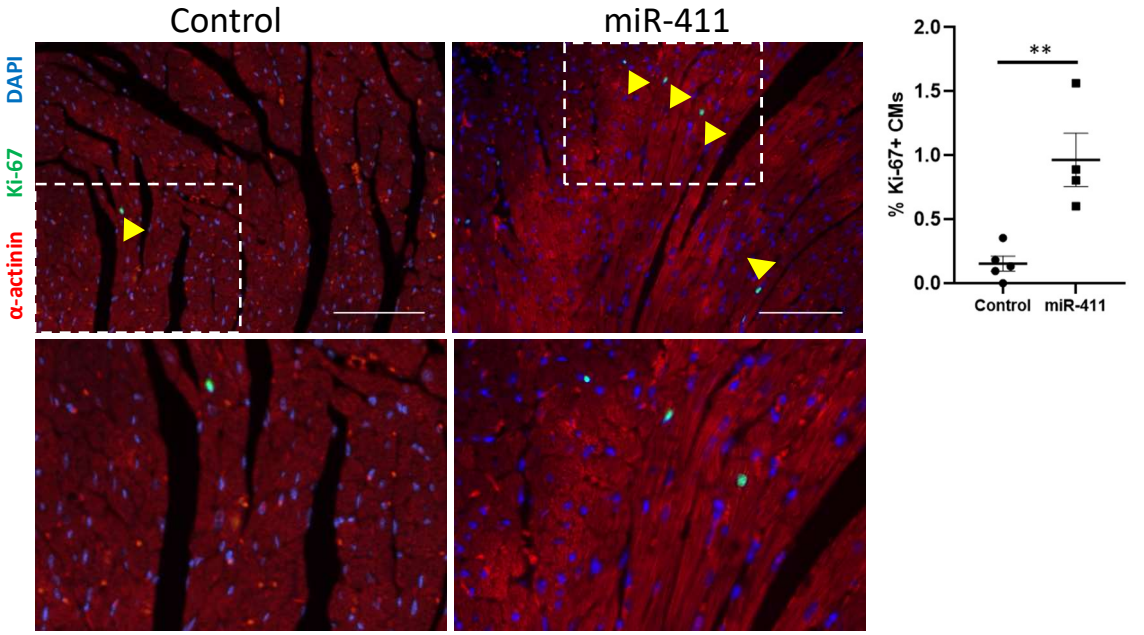

Figure 4.5 Representative Ki-67 immunofluorescence images from heart sections near the injection site. The number of Ki-67 positive cardiomyocytes is significantly increased in the miR-411 groups compared to controls (**p≤0.01,n=5 for control, n=4 for miR-411 group, unpaired Student's t-test).

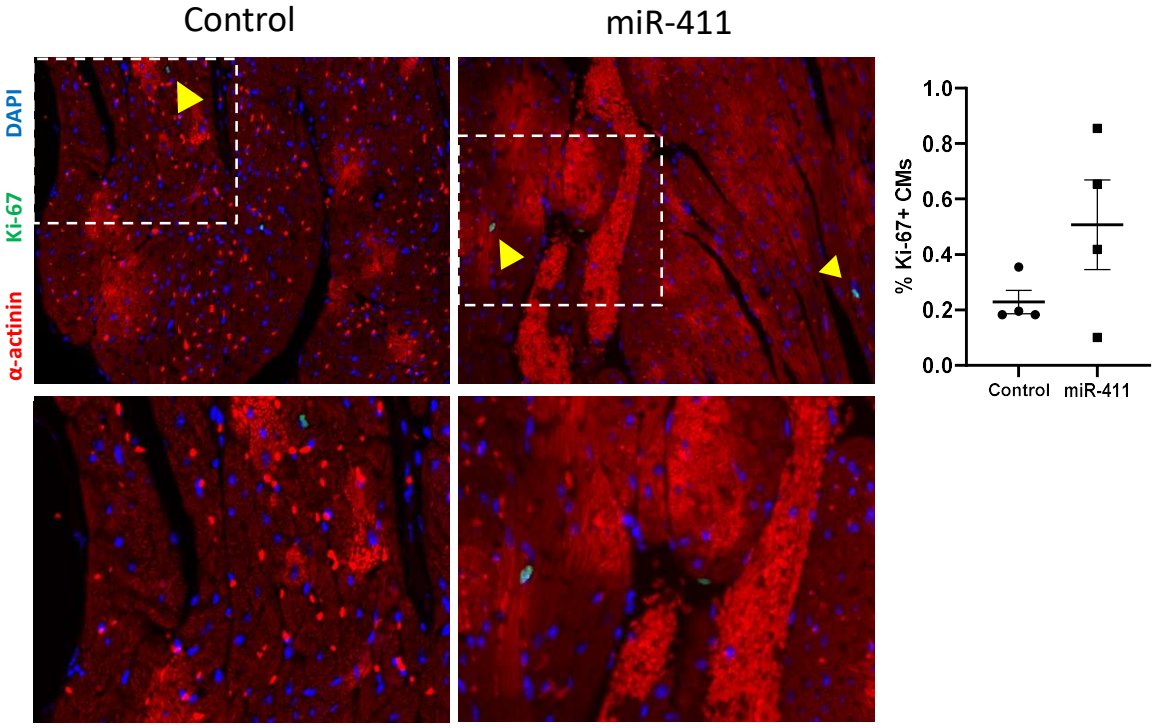

Figure 4.6 Representative Ki-67 immunofluorescence images from heart sections near the distant site. There is no significant difference in the rate of Ki-67 positive cardiomyocytes between the control and miR-411 groups (n=4).

In addition, cardiomyocyte proliferation was also assessed by analysing the EdU incorporation rate as a surrogate marker of cell proliferation. EdU incorporation is associated with DNA synthesis and an indication that the cells have entered the S phase of the cell cycle. EdU (50 mg/kg) was injected intraperitoneally two days following miRNA injection. The mice were kept for three days after EdU injection before they were sacrificed. EdU incorporation was first examined in the spleen, which is one of the organs with a high cellular turnover rate in the body. Figure 4.7 illustrates that the EdU is successfully delivered and incorporated into the splenic cells. In the heart, the rate of EdU positive cardiomyocytes follows a similar pattern to the one observed in Ki-67 detection. Near the injection site, EdU is significantly higher in the miR-411-treated group compared to the control (Fig 4.8). However, in locations that are further from the injection site, this difference in EdU positive nuclei between the miR-411 treated group and the control is no longer observed (Fig 4.9).

Together, the data indicates that *in vivo* miR-411 overexpression can significantly induce cell cycle re-entry in adult cardiomyocytes and that the effects of the intramyocardial injection of miRNA mimics seem to be limited to the area near the injection site.

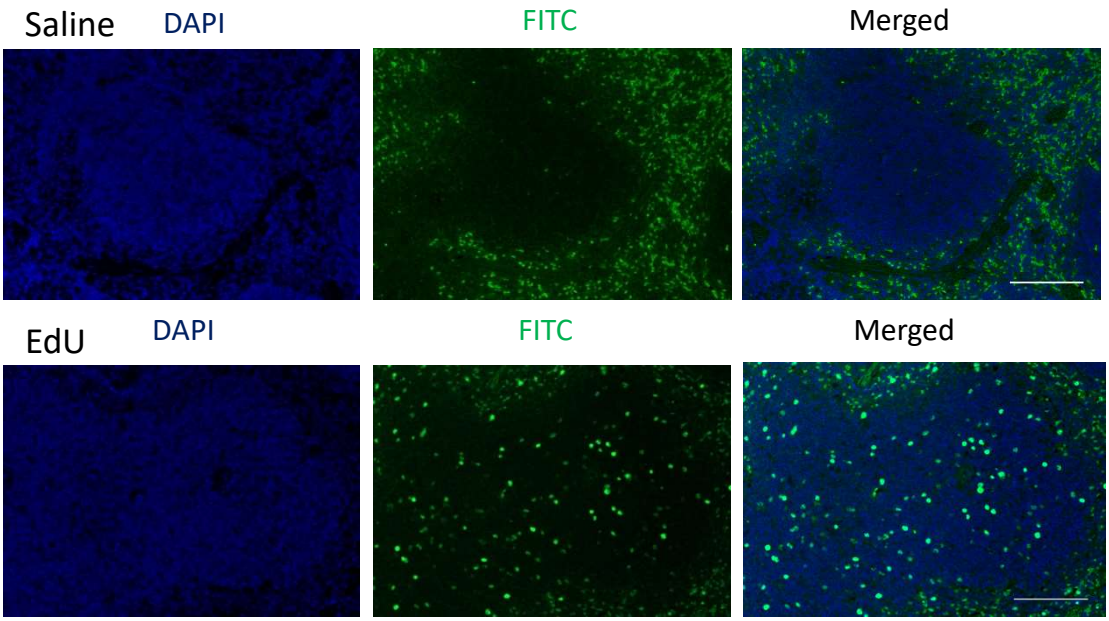

Figure 4.7 Validation of EdU injection *in vivo*. The delivery of EdU in EdU-treated mice is confirmed through the detection of EdU positive nuclei in the spleen.

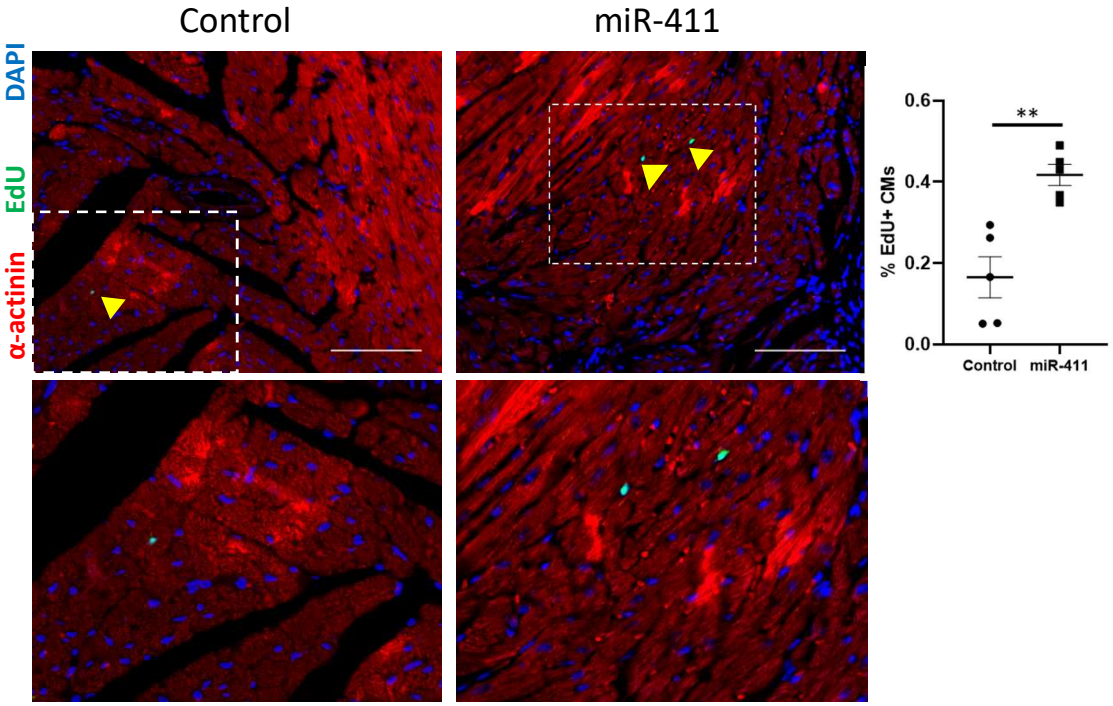

Figure 4.8 Representative EdU immunofluorescence images from heart sections near the injection site. The number of EdU positive cardiomyocytes is significantly increased in the miR-411 groups compared to controls (**$p \leq 0.01$,n=5, unpaired Student's t-test).

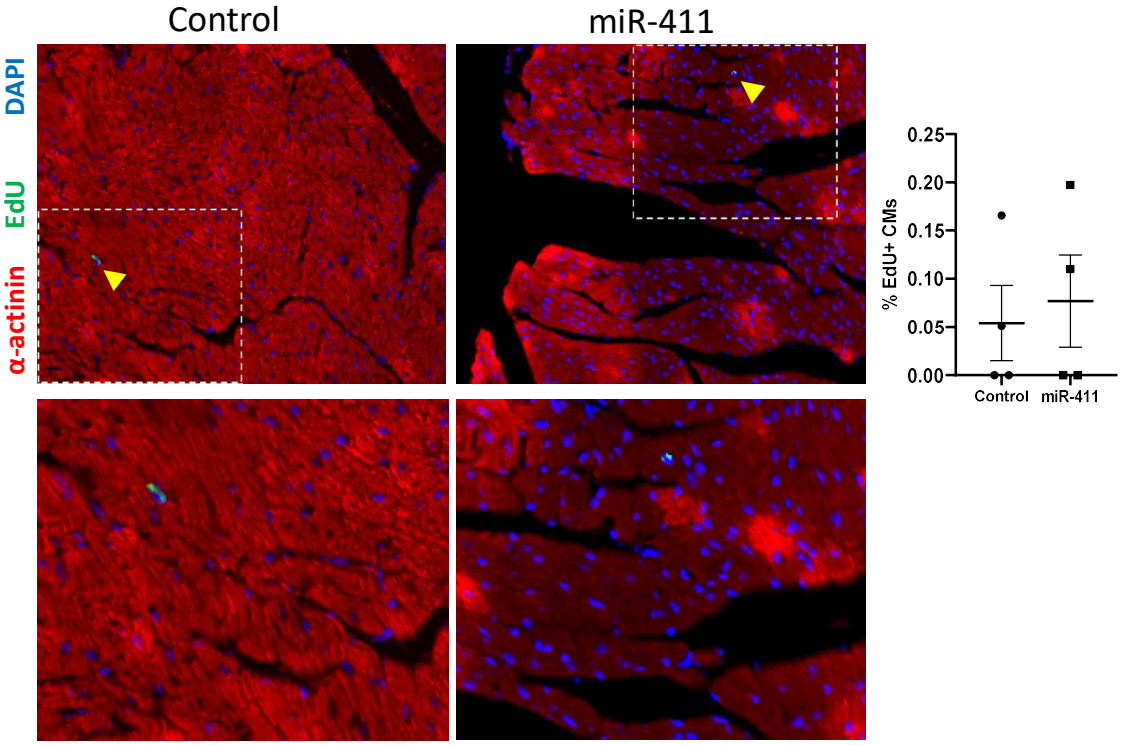

Figure 4.9 Representative EdU immunofluorescence images from heart sections near the distant site. There is no significant difference in the rate of EdU positive cardiomyocytes between the control and the miR-411 groups (n=4)

4.4.3 The effect of *in vivo* miR-411 overexpression on Hippo pathway activation

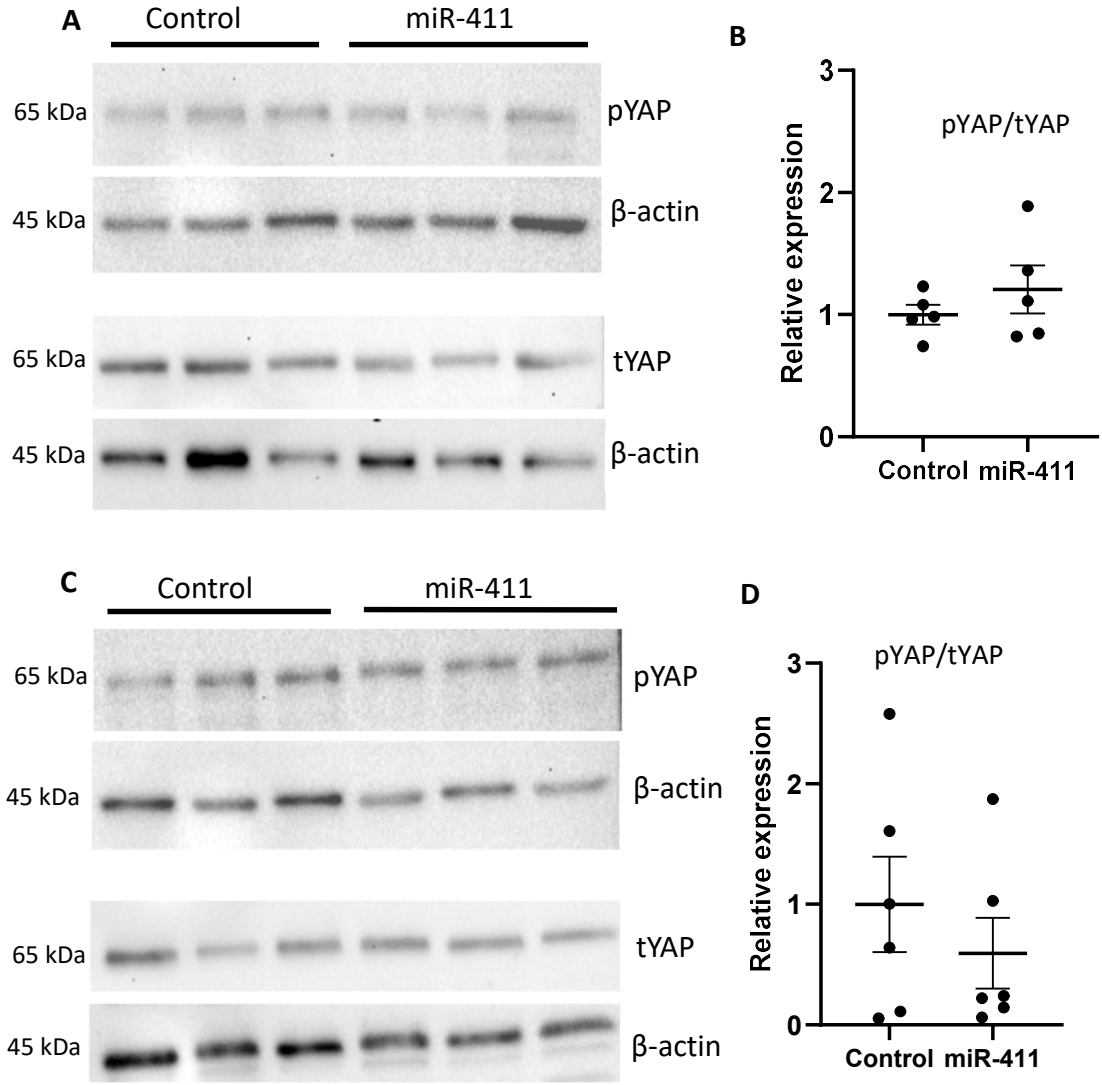

Figure 4.10 YAP phosphorylation post miR-411 overexpression *in vivo*. (A) & (B) Near the injection sites, the YAP phosphorylation level in the miR-411 group is similar to that of the controls. n=5. (C) & (D) In the distant sites, the YAP phosphorylation level does not change between the controls and the miR-411 group. n=6.

To investigate the effect of miR-411 overexpression on Hippo pathway activation *in vivo*, the levels of phosphorylated (pYAP) and total YAP (tYAP) were investigated using western blot. Figure 4.10A-D shows that in the injection site, as well as in the distant sites, the pYAP to tYAP ratio in both the control and the miR-411 groups remains constant. This indicates that YAP phosphorylation does not change following miR-411 overexpression *in vivo*.

4.4.4 The effect of miR-411 overexpression on cardiac structures and functions post MI

4.4.4.1 The plasma troponin I level post myocardial infarction

After assessing the effect of miR-411 on adult cardiomyocytes, the next step is to assess the effects of miR-411 overexpression following MI. This is an initial step to address whether miR-411 can be used as a therapeutic option for MI. To achieve this aim, a single intramyocardial injection of miR-411 mimics was administered to the heart after LAD ligation. To confirm the occurrence of MI and to evaluate the degree of myocardial damage, the level of cardiac specific troponin I (cTnI) was assessed from plasma samples collected 24 hours post MI surgery. As expected, the cTnI levels were significantly increased in all MI groups (vehicle, control, and miR-411 groups) compared to sham (Fig 4.11A). No significant differences in cTnI levels were identified between the MI groups, suggesting that the treatment given after LAD ligation (vehicle, control, or miR-411 mimics) does not affect the cTnI levels. This data also suggested that, in average, there was no difference in the level of myocardial damage at the start of MI experiments (up to 24 hrs after ligation). In addition to cTnI levels, the survival rate of the mice post-surgery was monitored over the 4-weeks experimental period (Fig 4.11B). Regardless of the treatment, most deaths occurred within the first week post MI surgery, with a couple of exceptions, i.e., one each in both the vehicle and miR-411 groups. The survival rates in this experiment ranged from 73% in the miR-411 group to 86% in the control group. However, these differences were not statistically significant.

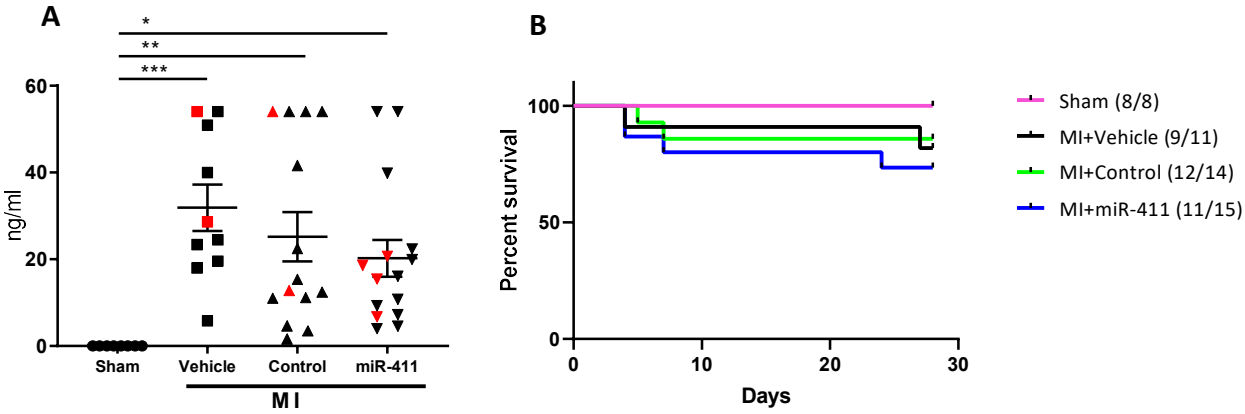

Figure 4.11 The troponin level and survival rate post-MI. (A) The cTnI level is significantly increased in all MI groups compared to sham (***p≤0.001, **p≤0.01, *p≤0.05, n=8 for sham, n=11 for vehicle, n=12 for control, and n=15 for miR-411, one-way ANOVA with Bonferroni's post-hoc test). The red marks represent mice that died before the end of the experiment. (B) Kaplan-Meier survival curve of the four experimental groups during the 4 week experimental period. The survival rates do not differ significantly between the groups.

4.4.4.2 Evaluation of cardiac structures post-MI

One of the normal adaptive responses to MI is cardiac hypertrophy and remodelling to compensate for diminished contractility. Several variables including heart weight, lung weight, and cardiac dimension indices obtained from transthoracic echocardiography were used to evaluate the extent of the remodelling in the heart 4 weeks post-MI. First, as expected, the normalised heart weight was significantly increased as a result of MI in both the vehicle and control groups compared to sham, with the biggest increase being observed in the control group followed by the vehicle group (Fig 4.12A). The miR-411 group, as can be seen in Figure 4.12A, had a substantially lower normalised heart weight than both the vehicles (8.46 ± 0.24 mg/mm vs 9.66 ± 0.64 mg/mm, ns) and the controls (8.46 ± 0.24 mg/mm vs 10.91 ± 0.86 mg/mm, $p<0.05$). This reduction in HW/TL ratio was statistically significant when compared to the controls but was not significant when compared to the vehicle group. This was probably due to a smaller increase in HW/TL ratio in the vehicle group compared to the control group. However, due to the possible side effects of miRNA injection, such as inflammation, the appropriate control to evaluate the effects of

miR-411 should be the control group (mice injected with control miRNAs), not the vehicle injected group.

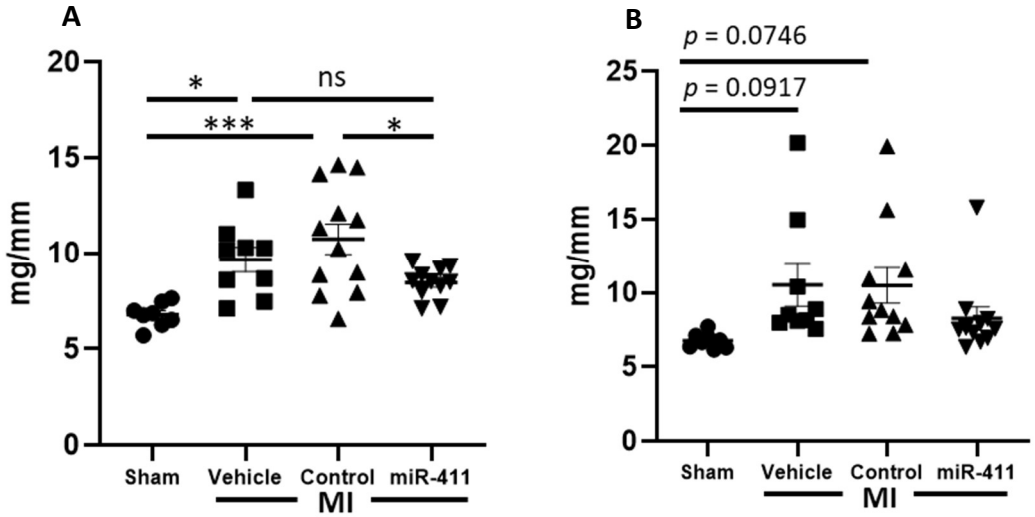

Figure 4.12 Normalised heart weight and lung weight at 4 weeks post-MI. (A) The HW/TL ratio is significantly increased in both the vehicles and the controls compared to sham whilst the miR-411 group have reduced HW/TL compared to both the vehicles and controls (***p≤0.001, *p≤0.05, n=8 for sham, n=9 for vehicle, n=12 for control, n=11 for miR-411, one way ANOVA with Bonferroni's post-hoc test). (B) There is a trend that the LW/TL ratio in the miR-411 group to be reduced compared to both the vehicles and controls (n=8 for sham, n=9 for vehicle, n=12 for control, n=11 for miR-411, one way ANOVA with Bonferroni's post-hoc test).

One of the hallmarks of severe heart failure is the accumulation of fluid in the lung, and therefore, the lung weight was measured and normalised to the tibia length to further compare the degree of heart failure between groups (Fig 4.12B). The mice in both the vehicle and the control groups exhibited substantially increased LW/TL ratio compared to sham - a phenotype consistent with heart failure. The increase in the LW/TL ratio in the miR-411 group was markedly smaller than both the vehicles and controls, indicating the ability of miR-411 to slow the heart failure progression. However, none of these differences were statistically significant. This probably indicates that the time frame used in this experiment is not sufficient to induce severe heart failure phenotypes.

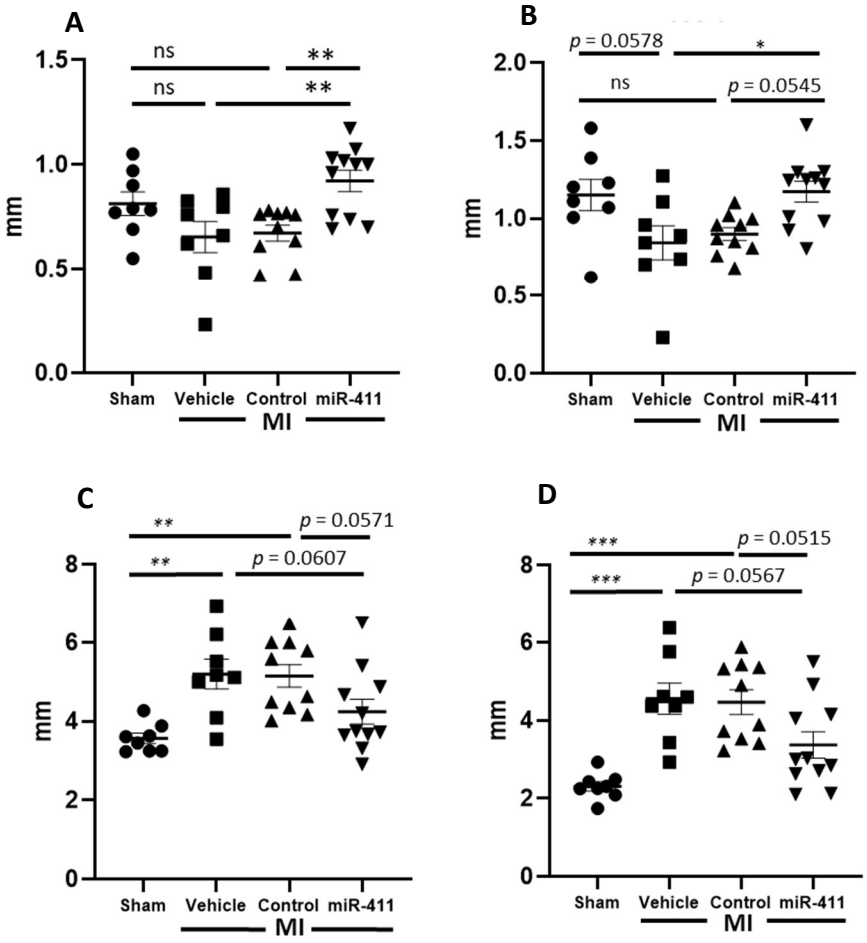

Figure 4.13 Left ventricular septum thickness and internal diameter at 4 weeks post MI. Increased left ventricular septum thickness at diastole (A) and systole (B) in the miR-411 group compared to both the vehicles and controls. Reduced internal diameter of the left ventricles at both diastole (C) and systole (D) in the miR-411 group compared to both the vehicles and controls (***p≤0.001, **p≤0.01, *p≤0.05, n=8 for sham, n= 8 for vehicles, n=10 for control, n=11 for miR-411, one way ANOVA with Bonferroni's post-hoc test).

To gain further insight into the extent of cardiac remodelling post MI, the internal left ventricular diameter and the ventricular septum thickness obtained from echocardiography were analysed. Interestingly, the increase in HW/TL ratio post MI in the vehicle and control groups was not accompanied by significant increases in the ventricular septum thickness both at diastole and systole (Fig 4.13A&B). In fact, both parameters were slightly decreased in both groups. At the same time, the internal diameter of the left ventricles, both at diastole and systole, was significantly increased in both the vehicle and control groups compared to sham (Fig 4.13C&D).

By taking into account the increase in LW/TL ratio, these findings suggest that at 4 weeks post MI, the mice in the vehicle and control groups already exhibited signs of left ventricular dilation and heart failure.

In the miR-411 group, the thickness of the interventricular septum at diastole and systole was significantly higher than in both the vehicle and control groups whilst still being comparable to those in the sham group. The internal diameter of the left ventricles at both systole and diastole in the miR-411 group slightly increased but did not differ significantly to those in the sham group. When compared to both the vehicle and control groups, both parameters are markedly lower in the miR-411 group. These findings indicate that, in contrast to the vehicle and control groups, the miR-411 group exhibited only minimal signs of hypertrophy, as indicated by the significantly lower HW/TL ratio and relatively constant interventricular septum thickness, in addition to early signs of remodelling as indicated by a substantially lower left ventricular internal diameter and a lower LW/TL ratio.

4.4.4.3 Evaluation of cardiac functions post-MI

To investigate the cardiac functions at 4 weeks post-MI, echocardiography was performed at the end of the experiment. The relative wall thickness (RWT), defined as 2 times posterior wall thickness divided by the left ventricular diastolic diameter, is a measure of left ventricular morphology, particularly the relationship between the wall thickness and cavity size. Previous evidence shows that it can be used as an independent predictor of cardiac function. Figure 4.14A shows that the vehicle and control groups had significantly lower RWT than the sham operated and miR-411 groups. The miR-411-treated mice displayed the opposite result as they had a similar RWT value as sham. These results support the findings from the previous section where the vehicle and control groups exhibited signs of dilated LV and thus were predicted to have reduced cardiac contractility. Likewise, the higher RWT in the miR-411 group confirmed that it displayed only early/minimal signs of remodelling and thus is assumed to have better cardiac contractility.

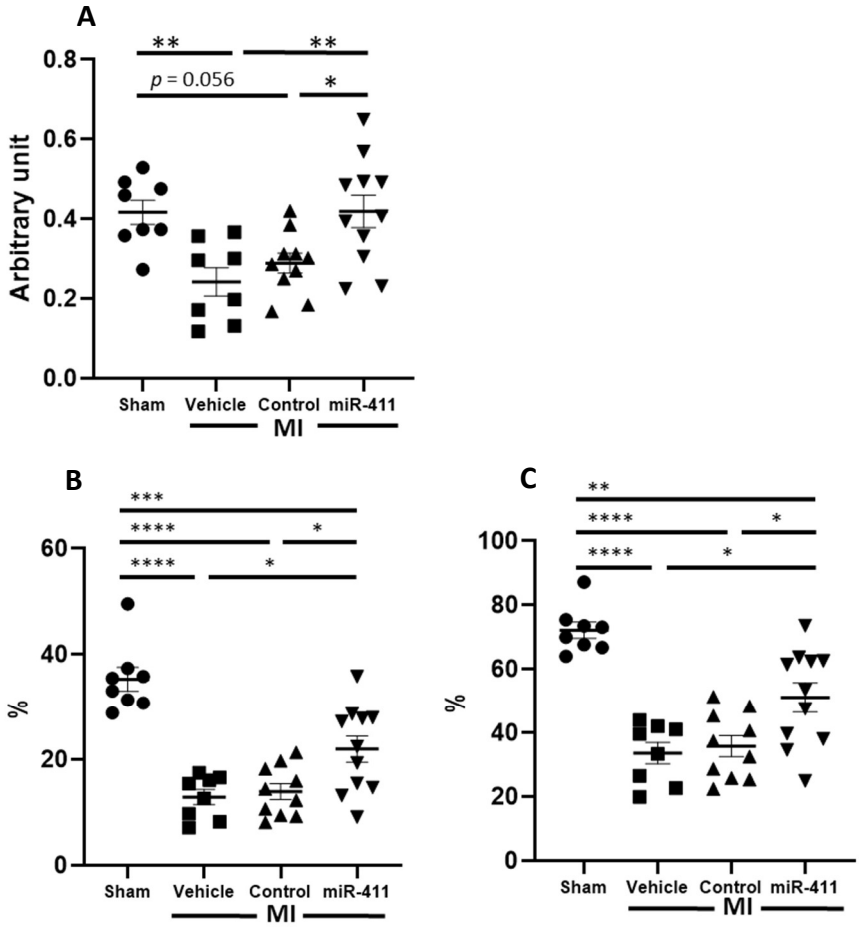

Figure 4.14 Cardiac functions at 4 weeks post-MI. Increased RWT (A), fractional shortening (B), and ejection fraction (C) in the miR-411 group compared to both vehicles and controls. (****p≤ 0.0001, ***p≤0.001, **p≤0.01, *p≤0.05, n=8 for sham, n= 8 for vehicles, n=10 for control, n=11 for miR-411, One way ANOVA with Bonferroni's post-hoc test)

To investigate the cardiac contractility of each group, the fractional shortening and ejection fraction were calculated and analysed using echocardiographic measurements described in Section 4.3.1.4. The findings displayed in Figure 4.14B&C show that both parameters in the miR-411 group were significantly reduced compared to sham, but were still significantly higher than in the vehicle and control groups. These results validated the LV function predicted by RWT and showed that miR-411 overexpression preserved cardiac functions at 4 weeks post-MI.

4.4.4.4 The effects of miR-411 on cardiomyocyte proliferation and death post-MI

To investigate the effect of miR-411 on cardiomyocyte proliferation, immunofluorescence staining was used to detect the presence of cell cycle marker Ki-67 (Fig 4.15). An increased number of Ki-67 positive cardiomyocytes per visual field was observed in the miR-411 group compared to the vehicle group (4.09 ± 0.86 vs 1.68 ± 0.84 %, p=0.053) and control group (4.09 ± 0.86 % vs 1.32 ± 0.58 %, p<0.05). Increased cardiomyocyte death is one of the hallmarks of cardiac remodelling post-MI. Therefore, the rate of cell death in this experiment was investigated with TUNEL staining (Fig 4.16). As expected, the number of apoptotic cells overall was higher in the MI groups (vehicle, control, and miR-411) than in sham. The control groups had the most significant increase in the number of TUNEL positive cardiomyocytes per visual field compared to sham (2.67 ± 0.90 vs 0.21 ± 0.04, p<0.05), followed by the vehicle group (1.8 ± 0.33 vs 0.21 ± 0.04, p=0.095). The number of TUNEL positive cardiomyocytes in the miR-411 group was lower than those in both the vehicle (0.66 ± 0.18 vs 1.8 ± 0.33, ns) and control groups. However, the difference was only statistically significant when compared to the controls (0.66 ± 0.18 vs 2.67 ± 0.90, p<0.05).

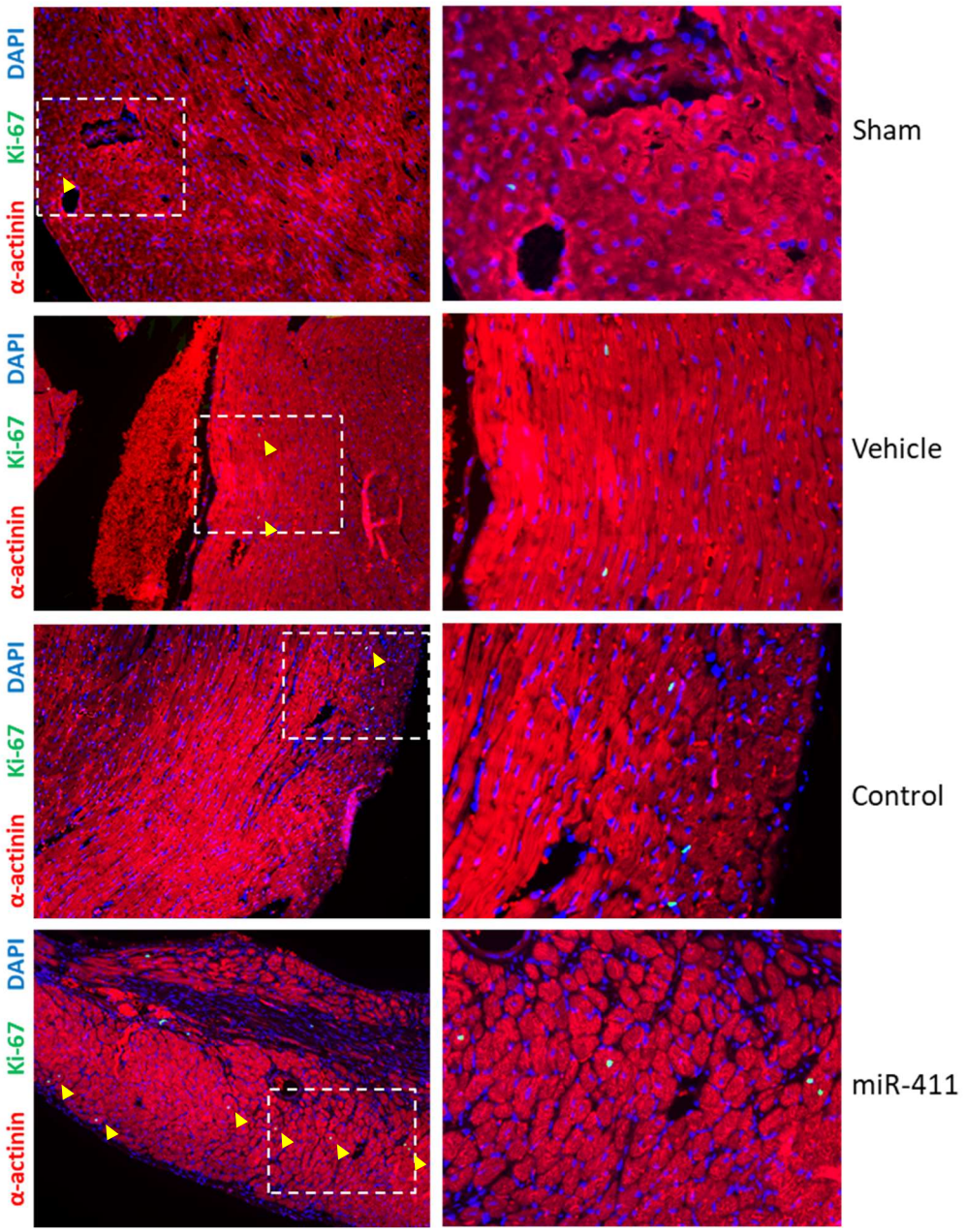

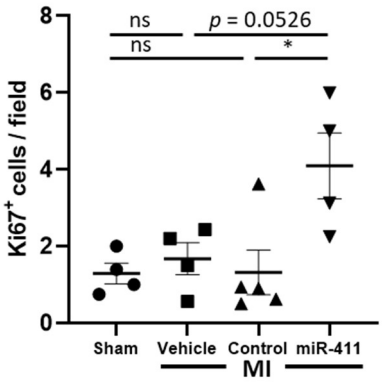

Figure 4.15 Cardiomyocyte proliferation (Ki-67) at 4 weeks post-MI.

The number of Ki-67 positive cardiomyocytes is increased in the miR-411 group compared to both vehicles and controls (*$p \leq 0.05$, n=4 for sham, vehicle, and miR-411, n= 5 for control, one way ANOVA with Bonferroni's post-hoc test)

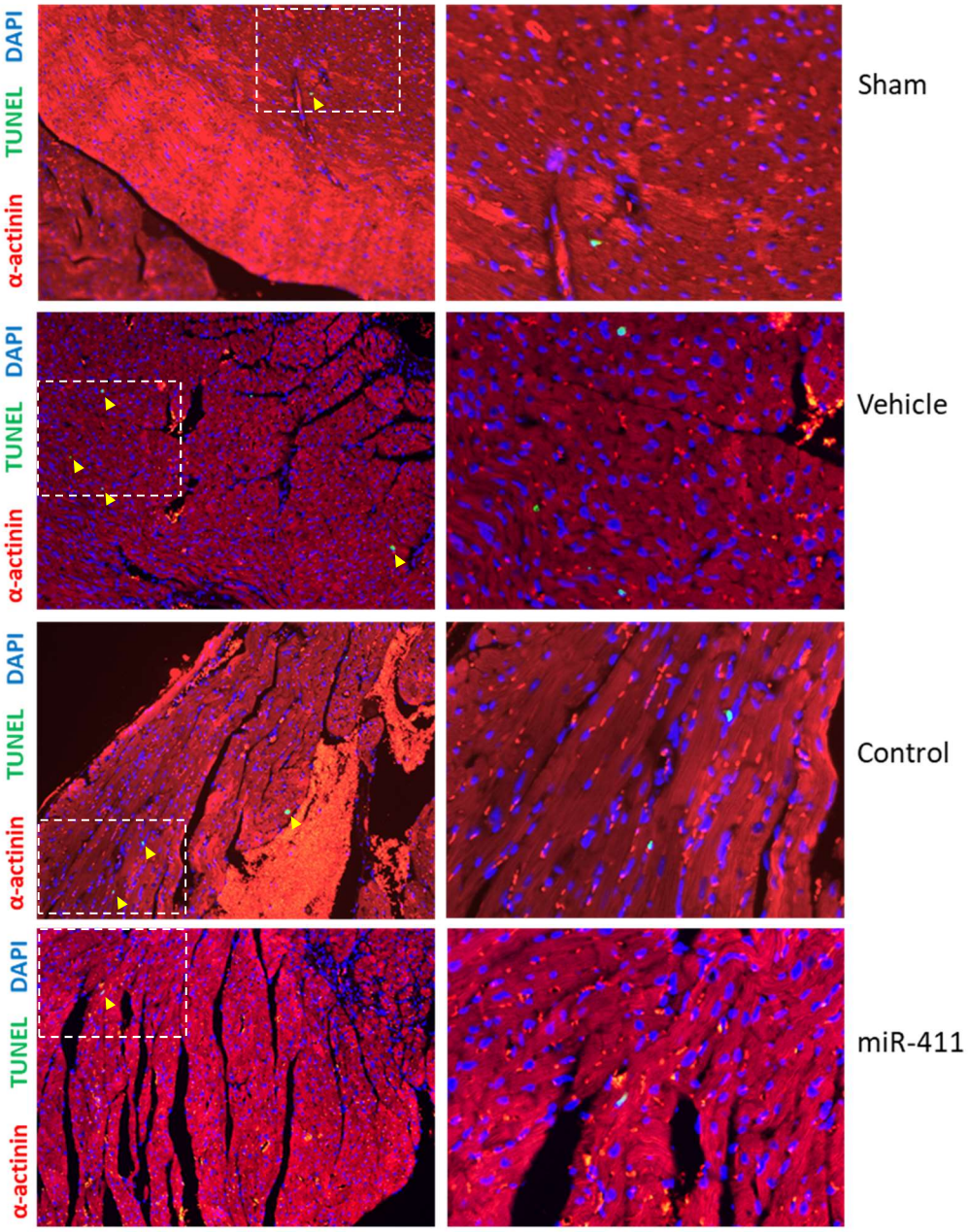

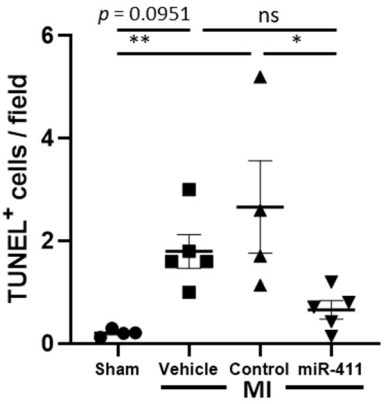

Figure 4.16 Cardiomyocyte death at 4 weeks post-MI

Decreased TUNEL positive cardiomyocytes in the miR-411 group compared to both vehicles and control (**p≤0.01, *p≤0.05, n=4 for sham, control, and miR-411, n=5 for vehicle, one way ANOVA with Bonferroni's post-hoc test)

4.4.4.5 The effect of miR-411 on infarct size at 4 weeks post-MI

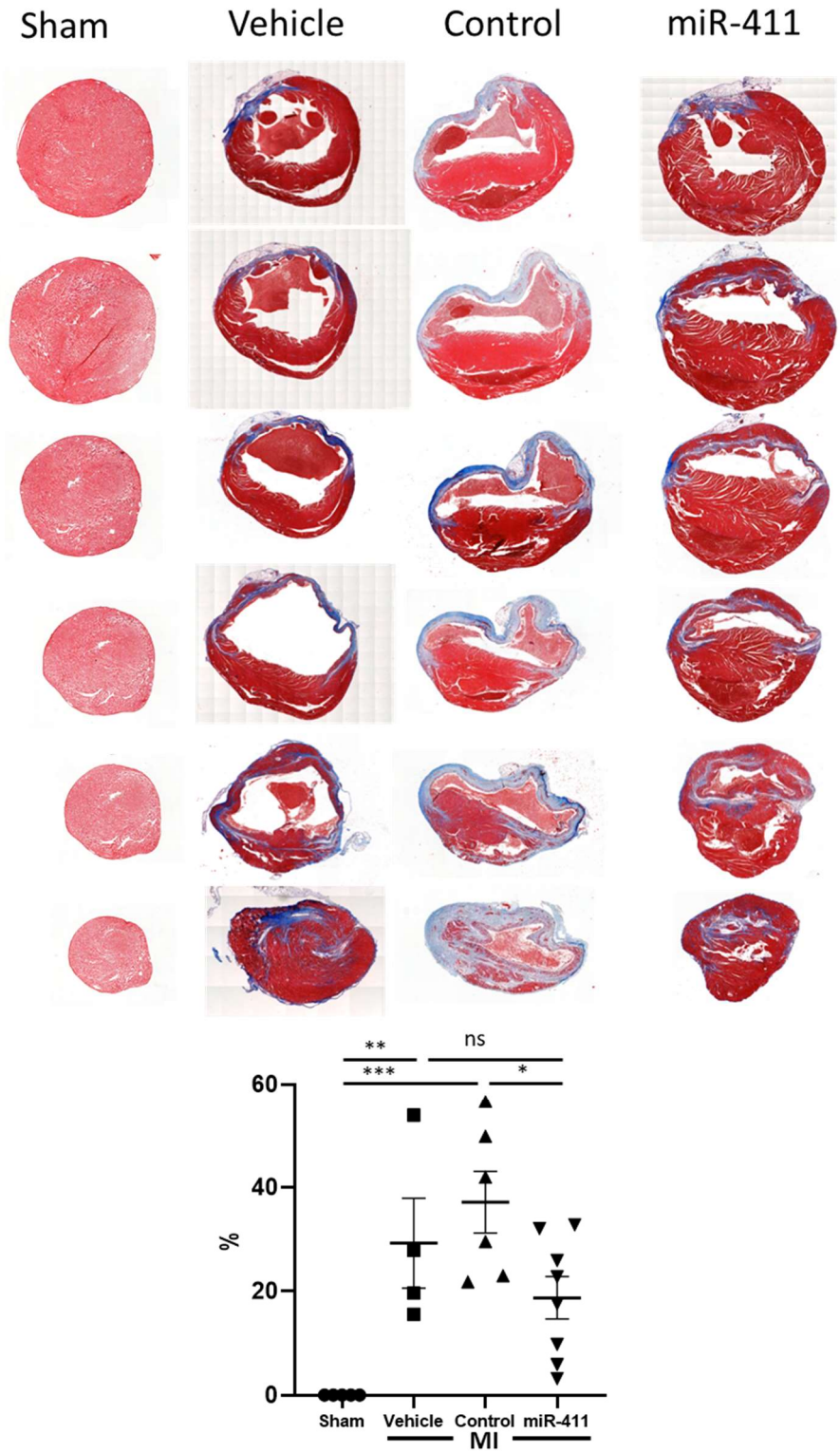

Figure 4.17 Infarct size at 4 weeks post-MI. Reduced infarct size in the miR-411 group compared to both the vehicles and controls (***p≤0.001, **p≤0.01, *p≤0.05, n=5 for sham, n=4 for vehicle, n= 6 for control, n= 8 for miR-411, one way ANOVA with Bonferroni's post-hoc test).

To assess the effect of miR-411 overexpression on the infarct size, Masson's trichrome staining was performed on transverse sections of the heart samples. Representative images of each group are illustrated in Figure 4.17. The miR-411 group had a markedly lower infarct size compared to vehicles (18.74 ± 4.08 % vs 29.25 ± 8.61 %, ns) and a significantly reduced infarct size compared to controls (18.74 % ± 4.08 vs 37.15 ± 5.94 %, $p<0.05$). These results indicate that miR-411 overexpression can significantly reduce the infarct size at 4 weeks post-MI.

4.5 Discussion

Recent reports have revealed that although cardiomyocyte renewal beyond the perinatal period is measurable, it is very small in magnitude and is inadequate to respond in the event of extensive cardiac damage such as MI (Bergmann et al., 2015; Porrello et al., 2011b). However, recent studies on rodents and zebrafish have yielded mechanistic insights into the regulation of cardiomyocyte proliferation and have thus uncovered the possibilities of feasible therapeutic approaches to stimulate endogenous cardiac regeneration (Eulalio et al., 2012; Jopling et al., 2010). In the previous chapter, a novel miRNA, miR-411, was found to have the capacity to induce proliferation *in vitro*. This chapter therefore will explore the effects of miR-411 on the adult heart under both normal condition and pathological stress (MI). The key finding from this chapter is that miR-411 can be delivered into the heart successfully *in vivo* and can be used to induce cell cycle re-entry in adult cardiomyocytes as well as to improve cardiac function post-MI. This discussion will delve into how miR-411 overexpression changes the expression of several cell proliferation markers in the normal adult heart and how it affects cardiac remodelling post MI.

4.5.1 Successful delivery of miR-411 mimic-PEI complexes into the myocardium by intramyocardial injection

Due to its ability to target multiple genes, miRNA expression modulation can potentially produce unpredictable off-target effects (Bartel, 2004). Therefore, it is of great importance to devise a delivery method which can deliver miRNA-based

therapeutics safely and efficiently into the intended organs/cells. A viral delivery system, especially adeno-associated virus serotype 9 (AAV9), is the most common strategy to deliver gene-based therapies in the cardiac disease models due to its high efficiency, relatively weak immunogenicity, and peculiar tropism for heart and muscle cells (Bish et al., 2008; Lovric et al., 2012; Wang et al., 2011; Zaiss et al., 2002). Moreover, cardiomyocyte-specific promoters can be engineered into the AAV9 to enhance its tissue-specificity (Pacak et al., 2008). However, AAV9 can drive a prolonged transgene expression which may raise important safety concerns. Recent evidence shows that prolonged overexpression of pro-regenerative miRNAs in mouse and pig models of MI could cause deleterious effects such as dilated cardiomyopathy and sudden cardiac death (Gabisonia et al., 2019; Tian et al., 2015). To avoid this limitation, non-viral gene vectors, such as polymer and liposome-based delivery systems, can be used as alternatives (Yin et al., 2014). Unlike AAVs, non-viral gene vectors do not cause a stable integration of nucleic acid materials into the host genome and therefore any effect caused by nucleic acid materials they carry is temporary. A previous investigation using lipid-based vectors reported that miRNA delivered via intramyocardial route can cause significant downregulation of target genes, starting from 12-24 h post injection until 12 days post injection (Borden et al., 2019; Gao et al., 2019; Lesizza et al., 2017).

Here, nanopolymer PEI was shown to have the ability to deliver miRNA mimics into the heart as indicated by a significant increase in miR-411 expression at 5 days post intramyocardial injection. Interestingly, this increase is limited to the area near the injection site as the area further from it has a similar miR-411 expression as the controls. This suggests that intramyocardial injection of miR-411 mimics results in local overexpression only. Alternatively, it is possible that the 5 days period used in this experiment is insufficient to allow the even distribution of the injected miRNA mimics throughout the whole of the heart. Whilst the detection of miRNA expression post injection is useful for indicating whether or not miRNA delivery is successful, it cannot tell whether the miRNAs injected can successfully enter the cytoplasm or only accumulate in the extracellular space. Investigations of miRNA direct targets can be

done in the future to assess the results of exogenously administered miRNAs (Lesizza et al., 2017).

In addition to delivery vectors, the delivery route is also an important factor to be considered in miRNA-based therapeutics. Following systemic injection of PEI-miRNA complexes, a significant increase in miRNA expression is observed in many organs in the body, including the lung, liver, pancreas, spleen, and kidney (Schlosser et al., 2018). In the context of miRNA-based therapeutics development in cardiac diseases, cell and organ type specificity is important because many miRNAs associated with cardiovascular pathology are shown to be related to cancer development somewhere else in the body. MiR-411 itself has been reported to contribute to the development of non-small-cell lung cancer (Zhao et al., 2016). To minimise the risk of non-specific organ targeting and enhance the delivery efficiency to the heart, an intramyocardial route was used in this project. Nevertheless, there is an indication that some of the injected miR-411 mimics entered the systemic circulation and ended up in the lung, liver, and kidney. It seems that completely avoiding the risk of miRNA mimics ending up in the non-targeted organs is very difficult or even impossible, especially if non-viral gene vectors are used, and there will always be a chance of this occuring when miRNA mimics enter the systemic circulation via capillary vessels in the myocardium or via the LV chamber due to inaccurate injection. Therefore, it is important to investigate the effects of increased miRNA expression in those organs in the future. Several parameters, such as local cellular proliferation, fibrosis, and changes in the level of tumour markers can be examined to detect adverse effects caused by miRNA off-target effects.

In summary, the efficacy of PEI shown in this project ais in agreement with the result of several previously published studies (Cheng et al., 2019; Wahlquist et al., 2014). Moreover, non-viral gene vectors, polymer and lipid based alike, have significant advantages over their viral counterparts due to their relative ease of production and greater biosafety (Yin et al., 2014; Zhang et al., 2013). These further highlight the potential for non-viral gene vectors to be translated clinically. However, compared to viral-based vectors, they also have significant drawbacks, such as

relatively lesser efficiency, potential toxicity, and lack of specificity (Yin et al., 2014). Whilst there is no doubt that these challenges need to be addressed before they can be widely adopted for clinical uses, the results of this experiment demonstrate the feasibility of non-viral vectors for clinical application.

4.5.2 MiR-411 overexpression can induce cardiomyocyte cell cycle re-entry in the adult heart

Cell cycle withdrawal is believed to be the primary reason for the dramatic reduction in the proliferative capacity of the adult cardiomyocytes. Therefore, the ability to modulate postnatal cell cycle re-entry would represent a powerful tool to increase cardiac regeneration (Huang et al., 2018; Quaife-Ryan et al., 2017). This experiment demonstrates that miR-411 overexpression can significantly increase the number of Ki67- and EdU- positive cardiomyocytes, indicating the ability of miR-411 to induce cell cycle re-entry. However, consistent with the localised miR-411 overexpression, the increased expression of proliferation markers is also limited to the area near the injection site only.

Chapter 3 Section 3.4.3 and 3.4.4 describes that miR-411 is capable of inducing NRCM proliferation by increasing YAP activity. In the *in vivo* experiment, however, YAP phosphorylation remains constant despite increased cardiomyocyte proliferation following miR-411 overexpression. The reason behind this finding is not clear. It is possible that due to localised miR-411 overexpression, changes in YAP phosphorylation become more difficult to detect. A further investigation of miR-411 target genes using *in vivo* samples may reveal the mechanisms through which miR-411 increases cardiomyocyte cell cycle re-entry.

Whilst Ki-67 and EdU are important markers for cell-cycle re-entry, the dedifferentiation process has not been deeply explored in this experiment. As mentioned earlier in the introduction section, cardiomyocyte dedifferentiation is an important step before cell cycle re-entry and proliferation (Jopling et al., 2010). In addition to the structural changes described earlier in this chapter, dedifferentiating

cardiomyocytes usually display several changes in the transcription profiles, including higher progenitor cell marker expression, such as c-Kit (Ai et al., 2018), RUNX1 (Osorio et al., 2011), Nkx2.5 (Y. Zhang et al., 2010) and DAB2 (Osorio et al., 2011); a higher β-myosin heavy chain (MYH7) to α-myosin heavy chain (MYH6) ratio (Ikeda et al., 2019); higher cell cycle promoter expression, such as CCNE1 (cyclin E1), CCNA2 (cyclin A2), and CCNB1 (cyclin B1) (Eulalio et al., 2012); and higher Destrin (a marker for cytoskeletal filament disorganisation) expression (Kubin et al., 2011). These markers, therefore, can serve as surrogate markers for the structural changes observed during dedifferentiation and investigating these markers in the future would further support the evidence that miR-411 overexpression can induce cell-cycle re-entry in adult cardiomyocyctes.

4.5.3 Transient miR-411 overexpression protects the heart from MI

The findings from the MI experiment demonstrate that a single intramyocardial injection of miR-411 mimics leads to a significant enhancement of cardiac repair at 4 weeks post-MI. Moreover, miR-411 seems to target various aspects of cellular functions such as increasing cardiomyocyte cell cycle re-entry as suggested by the increased Ki-67 positive cardiomyocytes, reducing cardiomyocyte death as indicated by reduced the TUNEL positive cardiomyocytes, as well as limiting the infarct size. Collectively, these enhance cardiac structure and function post-MI.

Adverse cardiac remodelling caused by decreased contractility post MI is the main cause of heart failure post-MI (Struthers, 2005). At 4 weeks post MI, mice in the vehicle and control group display signs of pathological dilation and thinning of the left ventricular wall as indicated by a significant increase in HW/TL ratio, left ventricle internal diameter, and relative wall thickness, as well as a significantly lower of interventricular septum. As a consequence, the cardiac function in both the vehicle and control groups is severely deteriorated, as indicated by significantly lower fractional shortening and ejection fraction. Contrarily, mice that were given miR-411 mimics have a significantly lower heart weight/tibia length ratio, a significantly thicker interventricular septum, a markedly lower left ventricle internal diameter,

and a normal RWT, which collectively indicate minimal hypertrophy. Also, mice in the miR-411 group display enhanced cardiac function as indicated by significant improvements in fractional shortening and ejection fraction. Therefore, miR-411 seems to be able to halt or at least significantly slow down the cardiac remodelling process post-MI.

The significant improvement seen in the miR-411 group is likely as a result of infarct size reduction, which consequently attenuates the cardiac remodelling process. The reduction in infarct size can be attributed to the induction of cardiomyocyte proliferation, as suggested by increased rates of Ki-67 positive cardiomyocytes (discussed in Chapter 3 Section 3.4.3). However, as Ki-67 presents in all stage of cell cycle, its presence does not guarantee true proliferation.

Another important factor that may contribute to the reduced infarct size observed in this study is a significant reduction in apoptosis. In addition to proliferation, microRNA-411 has been reported to reduce cell apoptosis in several types of cancers (C. Zhang et al., 2019). In line with this evidence, miR-411 has also been shown to reduce cardiomyocyte apoptosis post-MI in this project. This suggests that miR-411 also protects cardiomyocytes against a hypoxic condition during MI and, in turn, restricts the infarct size and limits cardiac remodelling. Whilst the mechanisms behind the benefits of miR-411 are yet unclear, they can be attributed to the ability of miR-411 to increase YAP activity (Section 3.4.4). Increased YAP is associated with increased proliferation, reduced apoptosis, and improved survival (Johnson and Halder, 2014). Therefore, it is possible that, in addition to proliferation and cell death, miR-411 also targets cardiomyocyte survival which further limits infarct expansion. Molecular studies are needed in the future to investigate miR-411 target genes and further elucidate the mechanisms behind the benefits conferred by miR-411 overexpression.

4.5.4 Limitations and future work

There are limitations with regards to certain experimental design and techniques within this *in vivo* experiment. To show the proliferation level, Ki-67 was the only marker used to represent proliferation. As Ki-67 presents in all stage of cell cycle, it is difficult to establish whether or not true cardiomyocyte proliferation is really present. The presence of proliferation markers, such as Ki-67 and EdU, in cardiomyocytes suggests that these cells have re-entered the cell cycle, but not necessarily completed true division (complete karyokinesis and cytokinesis) (Salic and Mitchison, 2008; Scholzen and Gerdes, 2000). Instead, this may result in endoreplication after which cardiomyocytes become polyploid and/or multinucleated. Although proliferation markers indicating later stages of mitosis, such as pHH3 and Aurora B kinase, strongly indicate mitosis and cytokinesis, these are also present during binucleation and do not guarantee true proliferation (Engel et al., 2006). Polyploidy, with or without multinucleation, in mammalian cardiomyocytes marks the transition from hyperplasia to hypertrophy, which occurs during the early postnatal period (Li et al., 1996). In addition, increased cardiomyocyte ploidy has also been associated with hypertrophy and heart failure, which may suggest that increased cell cycle re-entry is an adaptive response to injury (Herget et al., 1997). However, there is no direct evidence thus far that links increased cell cycle re-entry with preservation of cardiac function post-MI.

Despite the lack of evidence for true cardiomyocyte proliferation in this project, its presence cannot necessarily be excluded. It is possible that the increased cell cycle re-entry observed in the miR-411 group was followed by complete proliferation to a certain degree. Moreover, the difficulty in finding signs of true proliferation can be attributed to several technical factors. As previously mentioned, the effect of miRNA overexpression after single intramyocardial injection only persists temporarily for around 12 days (Lesizza et al., 2017). Given that in this case the experiment was ended after 28 days (4 weeks), it is safe to say that the effect of miR-411 was no longer apparent when the mice were sacrificed. A previous

investigation using a similar approach found signs of true cardiomyocyte proliferation, such as pHH3 and aurora B kinase positive cardiomyocytes, at three days post LAD ligation and miRNA mimic injection, further suggesting that the effect of miRNAs is most apparent during the early days post-MI and injection (Gao et al., 2019). Other strategies such as clonal analysis and investigation of midbody positioning – a recently discovered cytokinesis marker – may be useful in determining true cardiomyocyte proliferation in the future (Hesse et al., 2018; Lin et al., 2014).

Another factor that complicates the assessment of cardiomyocyte proliferation *in vivo* is the difficulty identifying cardiomyocyte nuclei in histological preparations. Although cardiomyocytes occupy approximately 70% of the heart volume, they only contribute to 20 – 30% of the total nuclei. Additionally, the heart comprise of a very diverse cell population which makes it even harder to distinguish cardiomyocyte nuclei from those of other cell types. The method used in this study (Section 4.3.2.4) relies on the widely used double immunofluorescent labelling of cardiomyocyte specific markers such as α-actinin and DNA dye such as DAPI (Eulalio et al., 2012; Gao et al., 2019; Huang et al., 2018). However, for a rare event, such as proliferation or apoptosis, the use of a specialised mouse line with constitutive or conditional reporter system to track specific cell lineages can enhance interobserver agreement and minimise margin of errors (Ang et al., 2010). For example, Soonpaa *et al*., used a transgenic mouse line in which cardiomyocyte specific αMHC promoter drove the expression of a nuclear β-galactosidase reporter (Soonpaa et al., 2013). Cardiomyocyte nuclei of these mice can be detected by immunohistochemistry (reaction with chromogenic β-galactosidase substrate) or immunofluorescence (probed with fluorophore-conjugated anti β-galactosidase antibody).

Finally, due to time limitation, the duration of miRNA overexpression post intramyocardial injection *in vivo* has not been investigated. As discussed in Section 4.4.1, a previous study reported that injected miRNA mimics–liposome complex remains detectable 12 days post injection (Lesizza et al., 2017). In the future, because this project used nanopolymer PEI it will be interesting to see whether the duration of miRNA overexpression in this project is similar to that of aforementioned study.

4.6 Conclusion

In summary, this chapter explores a novel role for miR-411 in the cardiomyocyte cell cycle and cardiac repair *in vivo*. There are three findings that can be highlighted from this chapter: (1) Nanopolymer PEI can successfully deliver miR-411 mimics into the heart via intramyocardial route, (2) *in vivo* miR-411 overexpression can induce cell cycle re-entry of adult cardiomyocytes and enhance cardiac structure and function post-MI, and (3) MiR-411 can potentially be used as a therapeutic tool to promote cardiac regeneration and repair post-MI.

CHAPTER 5

Investigation of the mechanisms responsible for the miR-411 mediated increase in cardiomyocyte proliferation

Chapter 5 - Investigation of the mechanisms responsible for the miR-411 mediated increase in cardiomyocyte proliferation

5.1 Introduction

The findings presented in Chapter 3 and 4 have highlighted the role of miR-411 in inducing cardiomyocyte proliferation and improving the phenotype following myocardial infarction likely via modulation of the Hippo pathway. However, little is known about the mechanism of miR-411-mediated Hippo pathway regulation, and there is only limited evidence pertaining the role of miR-411 in the heart. MiR-411 expression in the heart is reported to be increased during embryonic heart growth and in the early weeks post-MI (Muthusamy et al., 2014; Zhou et al., 2014). MiR-411 is also reported to suppress vein wall fibrosis in the mouse model of deep vein thrombosis (Ai et al., 2018). Nonetheless, the exact role of miR-411 in the heart is not completely understood.

In Chapter 3, miR-411 was shown to target the Hippo pathway by reducing YAP phosphorylation and thereby increasing YAP activity. Further investigations revealed that the expression of Hippo main kinases remains unchanged following miR-411 transfection, which suggests that miR-411 targets genes beyond the core components of the Hippo pathway. From the several genes that have been identified as miR-411 direct targets (discussed in Chapter 3), only FOXO1 can potentially explain the effects of miR-411 overexpression in cardiomyocytes (Shao et al., 2014). This chapter, therefore, will further investigate miR-411 target genes and explore how the modulation of these gene(s) leads to a decrease in YAP phosphorylation.

5.2 Aims

1. To identify and characterise miR-411 target gene(s) in cardiomyocytes
2. To investigate the mechanisms linking miR-411 target genes and the Hippo pathway

5.3 Methods

This chapter will cover the techniques used to determine miR-411 target genes and investigate mechanisms involved in miR-411. Both qPCR and western blot was used to assess gene expressions (described in Chapter 2 section 2.2) post siRNA or miRNA transfection.

5.3.1 Investigation of miR-411 target genes

5.3.1.1 The screening process to identify possible miR-411 target genes

Possible miR-411 target genes were screened using online bioinformatics tools, such as TargetScan, miRdB, and Exiqon. The steps used are described in further detail in Section 5.4.1. Twenty one genes selected from this step, combined with 9 core components of the Hippo pathway (miR-411 is hypothesised to target the Hippo pathway) resulted in 30 possible miR-411 target genes.

5.3.1.2 qPCR screening

In vitro RNA samples were obtained from NRCMs that had been transfected with miR-411 for 48 hours (Chapter 3, Section 3.3.3) whilst samples from tissue were isolated from the same animals used for experiments in Chapter 4 Section 4.4.2, using protocols described in Chapter 2 Section 2.2.1.3. Pooled RNA samples were initially used to generally screen and narrow down possible miR-411 target genes. RNA samples from 4-5 independent experiments (200 - 250 ng from each sample mixed together to make 1 µg RNA in total) were reverse transcribed and probed using qPCR and primers described in Chapter 2 (Section 2.1.1 and 2.2.1.4 – 2.2.1.6). Confirmatory qPCR was then done using individual samples to ascertained the expression of most likely candidates.

5.3.1.3 siRNA transfection

Isolated NRCMs were transfected with siRNAs against rat SERT or FOXO1 or negative control according to the manufacturer's protocol. siRNAs were purchased from Dharmacon, Horizon Discovery and resuspended in 1x siRNA buffer (Thermo

Scientific) at a final concentration of 5 µM and kept in a -20°C freezer. Isolated NRCMs were seeded overnight in an incubator at 37°C, 5% CO_2. The following day, the cells were washed several times with DPBS and fresh maintenance media were added to each well. Two sets of 1.5 ml Eppendorf tubes were prepared to make the transfection solution. In the first set of tubes, siRNAs were diluted in OPTI-MEM (5% dilution, Life Technologies) and in the second set of tubes, the transfection reagent (1% dilution, DharmaFECT, Thermo Scientific) were diluted in OPTI-MEM as well. Both solutions were incubated at room temperature for 5 minutes and subsequently mixed. The resulting solution was further incubated for 30 minutes at room temperature and finally added into each well. The plates were shaken carefully to ensure thorough mixing. The cells were then kept in an incubator at 37°C, 5% CO_2 for 48 hours.

5.3.1.4 Immunofluorescence staining

NRCMs were plated on laminin-coated, UV-sterilised coverslips in 24-well plates at a density of 250,000 – 300,000 cells/well. The following day, the cells were transfected with siRNA control or SERT. Forty-eight hours post-transfection, the cells were washed with DPBS and fixed in a 3.7% PFA solution for 15 minutes. The cells were washed with DPBS 3 times 5 mins each, permeabilized by 0.1% Triton-X in DPBS for 10 minutes, and blocked in 0.5% BSA in PBS for 1 hour. The cells were subsequently incubated overnight with anti SERT antibody (1: 100, ImmunoStar) followed by washing and 2 hours incubation with Fluorescein (FITC)-conjugated anti-rabbit antibodies (Jackson ImmunoResearch Laboratories). The cells were washed three times and incubated for 2 hours with anti-sarcomeric α-actinin antibody (1:200 dilution in 0.5% BSA in DPBS, Sigma-Aldrich) to stain cardiomyocyte-specific actin binding proteins. After that, the cells were washed and incubated for 2 hours with secondary Alexa Fluor 647-conjugated anti-mouse IgG (1:200 in 0.5% BSA in DPBS). Finally, the cells were counterstained with DAPI for 1 minute (1:5000 dilution in DPBS, Invitrogen) and the coverslips were mounted using Vectashield mounting media (Vector Laboratories).

The coverslips were then imaged with fluorescence microscope at 20x magnification and analysed with ImageJ. For one technical replicate, Ki-67 or pHH3 positive nuclei were counted from between 5-10 images per coverslip or until the total number of NRCMs reached between 800 – 1000 cells. The percentage of Ki-67 or pHH3 positive cells was calculated by dividing the total number of Ki-67 or pHH3 positive cardiomyocytes by the total number of cardiomyocytes.

5.3.1.5 YAP luciferase reporter assay

The principles of YAP luciferase assay used in this chapter have been described in detail in Chapter 3 Section 3.3.6. The only difference is that the NRCMs were transfected with siRNA control, SERT, or FOXO1 instead of miRNA mimics before being transduced with Ad-GAL4-TEAD and Ad-UAS-luciferase.

5.3.2 Generation of luciferase constructs bearing wild type and mutant fragments of miRNA target sequence within the 3'UTR and Exon 4 of the SERT gene

5.3.2.1 Amplification of wild type SERT 3'UTR and Exon 4

Full length SERT 3'UTR region (1.66 kb) and SERT Exon 4 (1.22 kb) were amplified by PCR from mouse genomic DNA using (wild type C57Bl/6) primer pairs listed in Table 2.8. To facilitate cloning, restriction sites for restriction enzymes (NheI and SalI for 3'UTR, SacI and SalI for Exon 4, NEB) listed in Table 5.1 were added to the primers. 2 µl of cDNA was amplified using PfU Turbo Hotstart DNA polymerase (Agilent Technologies) in a 50 µl reaction with 5 µl 10x PfU reaction buffer, 1 µl dNTPs, 2.5 µl of each primer (forward and reverse, 10 µM stock), 2 µl PfU polymerase, and 35 µl nuclease-free H_2O. Cycling conditions (for 30 cycles) were 95°C for 15 minutes (initial denaturation), 94°C for 15 seconds (denaturation), 62°C for 30 seconds (annealing), 72°C for 45 seconds (extension) and 72°C for 7 minutes (final extension). PCR products (inserts) were run on a 1% agarose gel and purified by cutting bands of the appropriate size under UV-light, followed by extraction of the DNA from the gels with QIAquick gel extraction kit (Qiagen) according to the manufacturer's instruction.

For cloning, both inserts and plasmid backbones were digested with restriction enzymes and separated by electrophoresis on a 1% agarose gel. The DNA fragments of both inserts and backbones were then cut from the gel and purified with QIAquick gel extraction kit (Qiagen).

Table 5.1 Primers used to amplify SERT 3'UTR and Exon 4 regions

Primers	Sequence
SERT 3'UTR-NheI (Forward)	TCAATGCTAGCTTTCTTCCCAACAGCGCATTATTA
SERT 3'UTR-SalI (Reverse)	GGAGTGTCGACGGAAGAGACACCGGGAAAGGAGAT
SERT Exon 4-SacI (Forward)	CTCAATGAGCTCACGTTAACGGCTTGGGCTTGATG
SERT Exon 4-SalI (Reverse)	GGAGTGTCGACGACCTTAACAGACCACCCCACCTC

5.3.2.2 Cloning steps

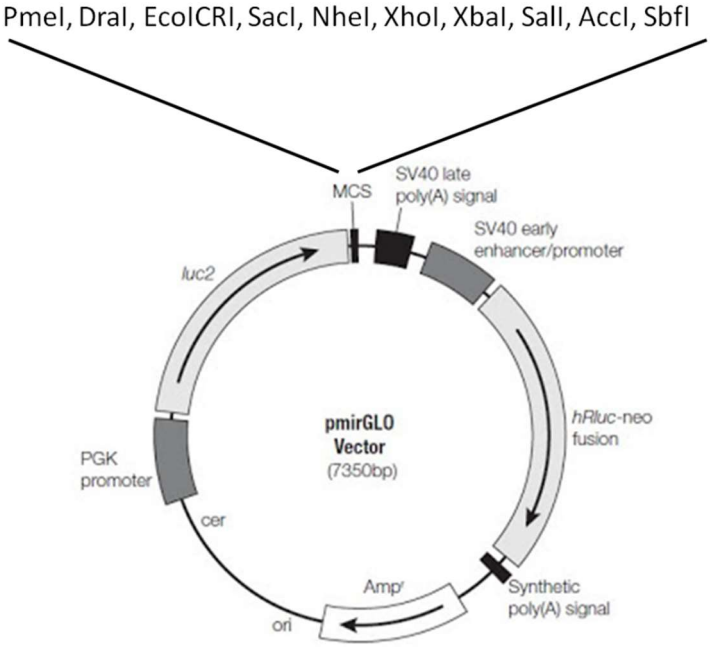

Figure 5.1 Illustration of pmiRGLO vector. The vector contains multiple cloning sites (MCS) 3' of the Firefly luciferase reporter gene (*luc2*). Humanised Renilla luciferase-neomycin resistance cassette (hRluc-neo) is used as a control reporter for normalisation of luciferase activity. Amp' (ampicillin resistance gene) allows bacterial selection for vector amplification. PGK promoter: human phosphoglycerate kinase promoter.

To evaluate miR-411 activity, predicted miR-411 target sites on SERT mRNA were cloned in the pmiRGLO Dual Luciferase miRNA target expression vector (Figure

5.1, Promega, E1330). SERT 3'UTR was inserted between NheI and SalI restriction sites whilst SERT Exon 4 was inserted between SacI and SalI restriction sites.

2 µg of plasmid backbone was digested with 1 µl SacI and 1 µl SalI for SERT 3'UTR cloning and 1 µl NheI and 1 µl SalI for SERT Exon 4 cloning. 8 µl of purified PCR product (amplified SERT 3'-UTR or SERT Exon 4) was also digested with 1 µl SacI and 1 µl SalI and 1 µl NheI and 1 µl SalI, respectively. For subsequent cloning, linearised vector DNA was dephosphorylated following which linearised plasmid DNA and inserts were purified on a 1.5% agarose gel. For ligation, 100 ng of digested vector DNA was incubated with inserts in three different molar ratios (vector to insert 1:1, 1:2, 1:3) along with 1 µl of 10x ligase buffer and 1 µl T4 DNA ligase overnight at 16°C. Competent E. coli cells (DH5α, SigmaAldrich) were transformed with ligated plasmids. 2 ml of LB medium supplemented with ampicillin (final concentration of 100 µg/ml) was inoculated with a single bacterial colony and incubated overnight at 37°C with shaking (200 rpm). Plasmid DNA was purified using the PureLink™ HiPure Plasmid Filter Maxiprep Kit (Life Technologies) according to manufacturer's guidance. For restriction analysis, plasmid DNA bearing SERT 3'UTR or Exon 4 was incubated with the restriction enzymes 1 µl SacI and 1 µl SalI or 1 µl NheI and 1 µl SalI, respectively, for 1.5 h at 37°C to confirm the presence of the correct ligation of SERT 3'UTR or Exon 4 inserts in the pmirGLO vector. Examples of restriction analysis are presented in Figure 5.2.

A

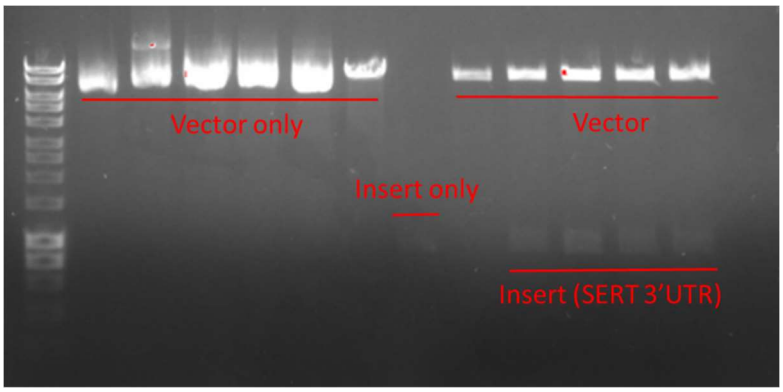

B

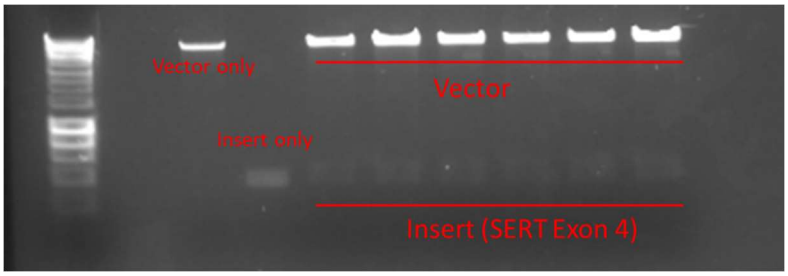

Figure 5.2 Restriction analysis of pmiRGLO-SERT 3'UTR and pmiRGLO-SERT Exon 4. (A) Restriction analysis of pmiRGLO-SERT 3'UTR. The four plasmids at the right end contain both vector (8kb) and insert (3'UTR, 1.66 kb). (B) Restriction analysis of pmiRGLO (8 kb)-SERT-Exon 4 (1.22 kb). All 6 plasmids that were screened contain both vector and insert.

5.3.2.3 Generation of mutant SERT 3'UTR and Exon 4

Mutant SERT 3'UTR and Exon 4 with nucleotide substitutions for two predicted miR-411-5p binding sites was generated by QuickChange II Site-Directed Mutagenesis Kit (Agilent Technologies). Primers used are listed in Table 5.2. Mastermix and DNA template were mixed according to Table 5.3 and run in a thermal cycler with cycling conditions listed in Table 5.4.

Table 5.2 Primers used to generate mutant pmiR-GLO-SERT 3'UTR and pmiR-GLO- SERT Exon 4

Primers	Sequence
SERT 3'UTR mutant (Forward)	CTCTGTAGCCGGAATAGGCTAGAACCCTGTAACC
SERT 3'UTR-mutant (Reverse)	GGTTACAGGGTTCTAGCCTATTCCGGCTACAGAG
SERT Exon 4-mutant (Forward)	CCATCATAGCCTGGGCGCAAGACTACCTCATCTCCTCC
SERT Exon 4-mutant (Reverse)	GGAGGAGATGAGGTAGTCTTGCGCCCAGGCTATGATGG

Table 5.3 Components for mutagenesis reaction

Components	Amount
10x Reaction buffer	5 µl
Forward primer (125 ng)	1.25 µl
Reverse primer (125 ng)	1.25 µl
dNTP mix	1 µl
Plasmid DNA template (50 ng)	1 µl
Nuclease-free H_2O	9.5 µl
PfUUltra HF DNA polymerase (2.5 U/µl)	1 µl

Table 5.4 Cycling conditions for mutagenesis reactions

Segment	Cycles	Temperature	Time
1	1	95°C	30 seconds
2	16	95°C	30 seconds
		55°C	60 seconds
		68°C	8 minutes

DpnI digestion was then used to eliminate parental DNA and select for plasmids that contained mutations. 1 µl DpnI restriction enzyme was added to the

amplification reaction and the mixture was then incubated at 37°C for 1 hour. DpnI-treated plasmids were then mixed with a 50 µl aliquot of XL1-Blue supercompetent cells in a pre-chilled 14-ml BD Falcon polypropylene round-bottom tube and incubated on ice for 30 minutes to transform the mutant plasmids. Following this, the mixtures were then heat shocked for 45 seconds at 42°C and then placed on ice for 2 minutes. 0.5 mL NZY^+ culture media were added into the mixtures to facilitate the growth of the competent cells. Finally, the transformation reaction was incubated with shaking at 200 rpm at 37°C for 1 hour and plated on LB-ampicillin agar at 37°C overnight.

To amplify the plasmid, 2 ml LB medium supplemented with ampicillin (final concentration of 100 µg/ml) was inoculated with a single bacterial colony and incubated overnight at 37°C with shaking (250 rpm). Plasmid DNA was purified using the Purelink Plasmid Kit (Thermo Fisher) according to manufacturer's instructions. The presence of the mutations was evaluated with sequencing.

5.3.2.4 Luciferase reporter assay

Cardiomyoblast H9C2 cell line was seeded at a density of 100,000 cells/well in a 24-well plate 24 hours prior to transfection, and transfected with either control or hsa-miR-411 mimics at a final concentration of 25 nM for 24 hours. The following day, the old media was removed and the cells were transfected with 1 µg control or SERT-3'UTR or SERT-Exon 4 plasmids mixed with Lipofectamine 2000 (Invitrogen) according to the manufacturer's protocol for 24 hours. The following day, the cells were washed with PBS, lysed with 100 µl 1x Passive Lysis Buffer (Promega), and incubated for 20 minutes at RT under agitation. Both luciferase (Firefly) activity and Renilla were measured with Luciferase Assay System (Promega) and Renilla Luciferase Assay systems (Promega), respectively. Measurement of Renilla luciferase activity was performed to take into account the transfection efficiency. 10 µl cell lysate was mixed with 50 µl luciferase reagent (Firefly or Renilla) in a luminometer tube which was then read using a luminometer (Berthold Technologies Lumat LB 9507). The final data was analysed based on ratio of Firefly/Renilla activity.

5.4 Results

5.4.1 Bioinformatics screening to select candidate miR-411 target genes

Candidate miR-411 target genes were screened using online miRNA target prediction databases: TargetScan (Agarwal et al., 2015), miRdb (Chen and Wang, 2019), and Exiqon (Qiagen). They used different algorithms to predict miRNA targeting using criteria such as seed complementarity, thermodynamics, Baynesian inference, and support vector machine. First, predicted miR-411 targets according to the three databases were listed based on the probability ranking (Table 5.5). The candidates were further selected based on these criteria: (i) present in at least two databases and (ii) have been associated with proliferation, the Hippo pathway components, or cardiovascular function. In the end, a list of 30 genes (Table 5.6) consisted of 9 core components of the Hippo pathway (because miR-411 is hypothesised to target the Hippo pathway) and 21 candidate genes (obtained from the screening, written in blue) were selected for further analysis.

Table 5.5 List of predicted miR-411 target genes according to TargetScan, mirdB, and Exiqon databases

PART 1			PART 2		
Target Scan	mirdB	Exiqon	Target Scan	mirdB	Exiqon
ELFN1	ELFN1	ACAN	ASB14	SP2	MMP13
BNIP3	BNIP3	ACOXL	MIB1	STON2	MRPS25
SSUH2	FBXL5	ACSBG2	POU4F1	NEMF	NFATC2IP
PXDC1	SET	ALDH3A2	FZD4	CENPC	NHSL1
FBXL5	EBF2	C11orf21	KLF7	FOXO1	NXPE4
CAMLG	EXOSC3	C12orf73	MAML2	MAN2A2	PAQR8
HNRNPH3	AUTS2	C14orf119	KDM6A	C11orf21	PIGH
RAB21	PXDC1	C15orf23	CAMSAP1	PCDHAC2	PM20D2
SP2	UBE2R2	C16orf52	KLHL3	CD200	PPM1F
C21orf91	EIF4G2	C21orf91	APOLD1	DBF4	PPP1R1C
LRIG2	PGAM5	CADM2	KIAA1549L	RAD23B	PRELID2
SPRY4	RAPGEF2	CALML4	SEMA3A	C21orf91	PRPF38B
NRF1	PRELID2	CCPG1	ZDHHC3	GUCD1	PXDC1
MMP19	MICB	CDH2	RAB10	PCDHA9	RAB30
EIF4G2	RAB21	CEACAM1	KPNA2	NRF1	RBM33
SCD5	MAL2	CRYZL1	ANTXR2	LRRFIP1	RBMX
GTF2I	DUSP1	CYBRD1	YAF2	MTMR9	RECQL
HNRNPUL1	SPRY4	EIF1AX	UBE2R2	HNRNPA3	REEP5
VAMP1	NR3C1	ELFN1	CYLD	GGA1	SCARA5
NUDT5	KIAA0430	ELMO2	LRP12	DNAJC19	SETD5

DUSP1	RHOQ	EML4	PSMD12	PARD6B	SKAP2
NUDT4	KCNIP4	ENSG00000125046	UBE2W	ZNF518A	SLC12A4
NFATC2IP	TNPO1	ENSG00000214106	ERBB4	NXPE4	SLC16A12
DUSP13	GDAP2	ENSG00000226733	MPHOSPH8	GLYAT	SLC22A2
HNRNPA1	PUM1	ENSG00000228277	SP1	ZNF81	SLC35A1
SF3B3	GTF2I	ENSG00000229246	TGFBR2	FBXO34	SLC38A9
PDS5A	EPC1	ENSG00000230516	USP49	DSCR4	SLC4A7
CDH2	MAP3K1	ENSG00000231304	CAMKK2	EIF1AX	SLCO2B1
ATP5F1	DAAM2	ENSG00000234503	SHANK2	NABP2	SNTG1
GRID2	ATAD2B	ENSG00000234899	MFRP	TBL2	SP2
CTDP1	SF3B3	ENSG00000237262	CALML4	LANCL2	SPRY4
AKAP5	BTBD7	ENSG00000237407	NAV3	KIAA0930	STK17A
WNT7A	PDCD2	ENSG00000238097	CCDC85C	LOC101927955	SULT4A1
RYBP	MEGF8	ENSG00000240355	VPS53	CDC42SE2	TARBP2
CACNB4	KIAA1614	ENSG00000248215	CSNK1G1	AUH	TCHHL1
SSR3	SMARCA2	ENSG00000248708	EPC1	SGK494	TRIM37
SLC30A6	TLL1	ENSG00000248835	RP11-315D16.2	STK17A	UBE2R2
CATSPERG	NRBP1	ENSG00000249099	FRMD4A	GRM3	UQCRQ
GNAZ	MAGEA5	ENSG00000249882	RAB3C	HSP90AA1	WASF1
FBXL3	MAGEA10-MAGEA5	ENSG00000253898	NFE2L3	RAB10	ZBTB46
PUM1	GTPBP8	ENSG00000254343	PREX1	ZNF280C	ZNF148
ZFAND5	KLRD1	ENSG00000258332	FNIP1	C18orf42	ZNF551
CPT1A	C9orf72	ENSG00000265091	LNX1	MLLT11	ZNF7
EBF2	CALML4	ENSG00000266667	MYPN	SKAP2	
CLIP2	ZNF680	EPPK1	IL17RB	SCD5	
RAPGEF2	LRRC6	FAM65B	CLCN5	RNF2	
HMGN3	SYT4	FAM92A1	RANBP2	CDH2	
C16orf52	GPA33	GDAP2	FAM204A	TMCO1	
CCNT1	NDC1	GGA1	RP11-210M15.2	ENKUR	
RUNX1T1	ZNF551	GJE1		CALB1	
CD200	MTMR4	GKAP1		NAB1	
PREX2	GPR65	GRM3		TMEM30A	
MAML3	HNRNPUL1	GTF3C3		ITGBL1	
NPFFR1	MITD1	GTPBP8		POLR1A	
AGO1	NUP214	HNRNPH1		RCC2	
WNT10B	MKL2	HNRNPH3		CLHC1	
RP11-644F5.10	RAB9B	HSDL2		SAMD5	
RORB	LETM2	HSP90AA1		SLCO1C1	
PPTC7	41883	ISY1		LZTFL1	
TLE2	HNRNPH3	JAGN1		ZFYVE20	
SRSF10	CD226	KCNQ5		ZNF721	
LRRC59	PREPL	KIAA1614		PAQR8	
ATP2B4	SLC30A6	LINC00638		HSDL2	
STIM2	ISY1	LNX1		ZNF609	
FAM175B	C16orf52	MEGF8		NOTCH2NL	
SLC6A4	ARHGAP28	METTL7A		CPT1A	
ZNRF3	PPAPDC1A	MICB		ZNHIT6	
MAP2K1	C11orf54	MITD1			

Table 5.6 Candidate miR-411 target genes.

No	Genes	Abbreviations	Roles
1	LATS1	Large tumor suppressor kinase 1	Hippo pathway component
2	LATS2	Large tumor suppressor kinase 2	Hippo pathway component
3	SAV	Salvador homologue	Hippo pathway component
4	MST1	Mammalian STE20-like kinase 1	Hippo pathway component
5	MST2	Mammalian STE20-like kinase 2	Hippo pathway component
6	MOB1A	MOB kinase activator 1A	Hippo pathway component
7	MOB1B	MOB kinase activator 1B	Hippo pathway component
8	YAP	Yes associated protein	Hippo pathway component
9	TAZ	Tafazzin transcriptional activator	Hippo pathway component
10	BNIP3	BCL-2 interacting protein 3	Pro-apoptotic protein
11	SPRY4	Sprouty RTK signalling antagonist 4	LATS transcriptional target, modulating cell proliferation in several types of cancers
12	CDH2	N-cadherin	An integral part of adherens junction residing in the intercalated discs of cardiac muscle
13	MAP3K1	Mitogen-activated protein kinase kinase kinase 1	Stimulate cell proliferation
14	DAAM2	Dishevelled associated activator of morphogenesis 2	A key regulator of Wnt signalling pathway, required in myocardial maturation and sarcomere assembly
15	WNT7A	Wingless-related integration site family member 7A	Member of Wnt pathway, increase cell proliferation
16	WNT10B	Wingless-related integration site family member 10B	Member of Wnt pathway, control pluripotency and cell fate, attenuation of fibrosis in the heart
17	MAP2K1	Mitogen-activated protein kinase kinase 1	Activation of ERK pathway, stimulate cell proliferation
18	FOXO1	Forkhead box O1	Tumour suppressor, reduce cell proliferation and increase cell death
19	CYLD	Ubiquitin-specific -processing protease	Negative regulator of the Hippo pathway by limiting Hpo phosphorylation in Drosophila
20	ERBB4	Erb-B2 receptor tyrosine kinase 4	Important component of neuregulin pathway, stimulate cardiomyocyte proliferation
21	RYBP	RING1 and YY1 binding protein	Play a role in cardiac progenitor cell development and differentiation
22	TLL1	Tolloid-like protein 1	Important in heart development, possible target for preventing scar formation following MI
23	CCNT1	Cyclin T1	Cell cycle regulation
24	SLC6A4	Solute carrier family 6 member 4	Serotonin receptor gene, affect cardiac development, heart rate variability, etc
25	SP2	Sp2 transcription factor	Modulating cell cycle pathway
26	DBF4	DBF4 protein serine/threonine kinase	Wnt signalling inhibitor, important for cardiac development
27	POU4F1	Brain-specific homeobox/POU domain class 4 transcription factor 1	Modulation of apoptosis, important for neural cells differentiation and survival
28	PARD6B	Par-6 family cell polarity regulator beta	Cell polarity regulator, modulate Hippo pathway
29	DUSP1	Dual Specificity Phosphatase 1	MAPK signalling regulator
30	RHOQ	Ras Homolog Family Member Q	Cell shape, attachment, and motility regulator

5.4.2 Identification of miR-411 target genes *in vitro*

After obtaining 30 possible miR-411 target genes, qPCR was used to investigate the expression of these genes following miR-411 transfection in NRCM. First, pooled RNA samples from 5 independent miR-411 transfection were used to narrow down the candidate miR-411 target genes (Fig 5.3). The results show that the expression of two genes, FOXO1 and serotonin transporter (SERT/SLC6A4) was substantially reduced. On the other hand, the expression of two genes, WNT7A and POU4F1, was markedly increased post miR-411 transfection. Both WNT7A (Eisenberg and Eisenberg, 2006) and POU4F1 (Maskell et al., 2017) are important during cardiac development. As miRNAs regulate gene expression mostly through mRNA downregulation, it is unlikely that the increased expression of both genes is a direct effect of miR-411.

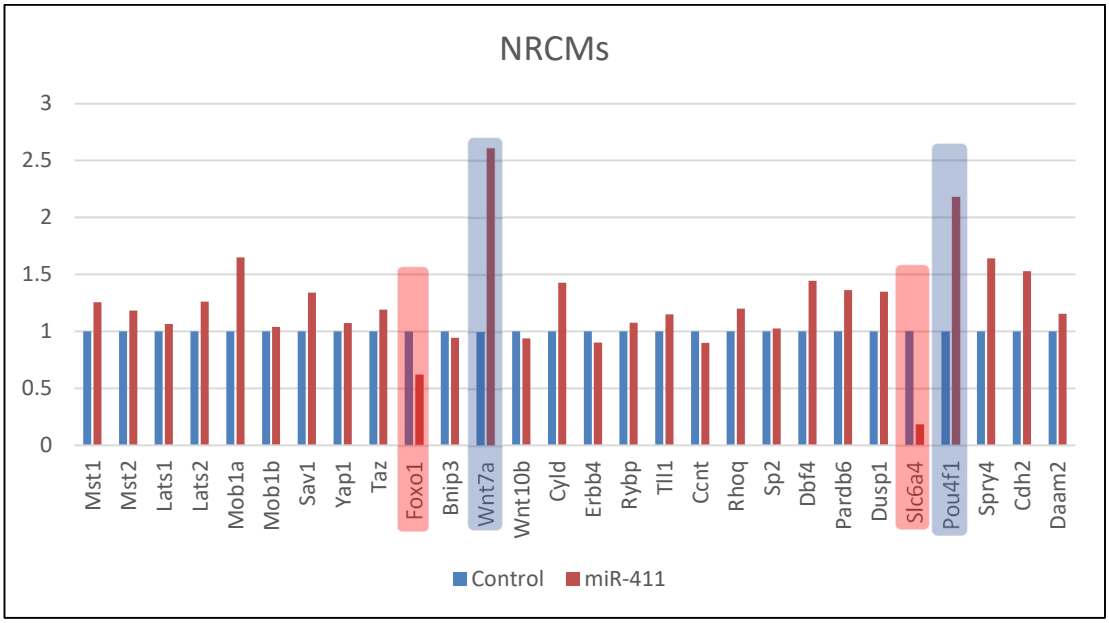

Figure 5.3 Screening analysis to identify miR-411 target genes in NRCM. FOXO1 and SERT are the two most reduced genes whilst WNT7A and POU4F1 are the two most upregulated genes in miR-411 transfected-NRCMs

To verify the expression of two strongest candidates of miR-411 target genes, FOXO1 and SERT, qPCR using individual samples were carried out. The expression of FOXO1 was found to be significantly reduced by approximately 38% (37.74 ± 7.55%)

through qPCR (Fig 5.4A) and 60% (60.06 ± 8.43%) through a western blot (Fig 5.4B-C). Similarly, miR-411 overexpression also significantly reduced the expression of SERT by approximately 80% (81.57 ± 4.29%, Fig 5.4D) which was further confirmed through immunofluorescence staining (Fig 5.4E).

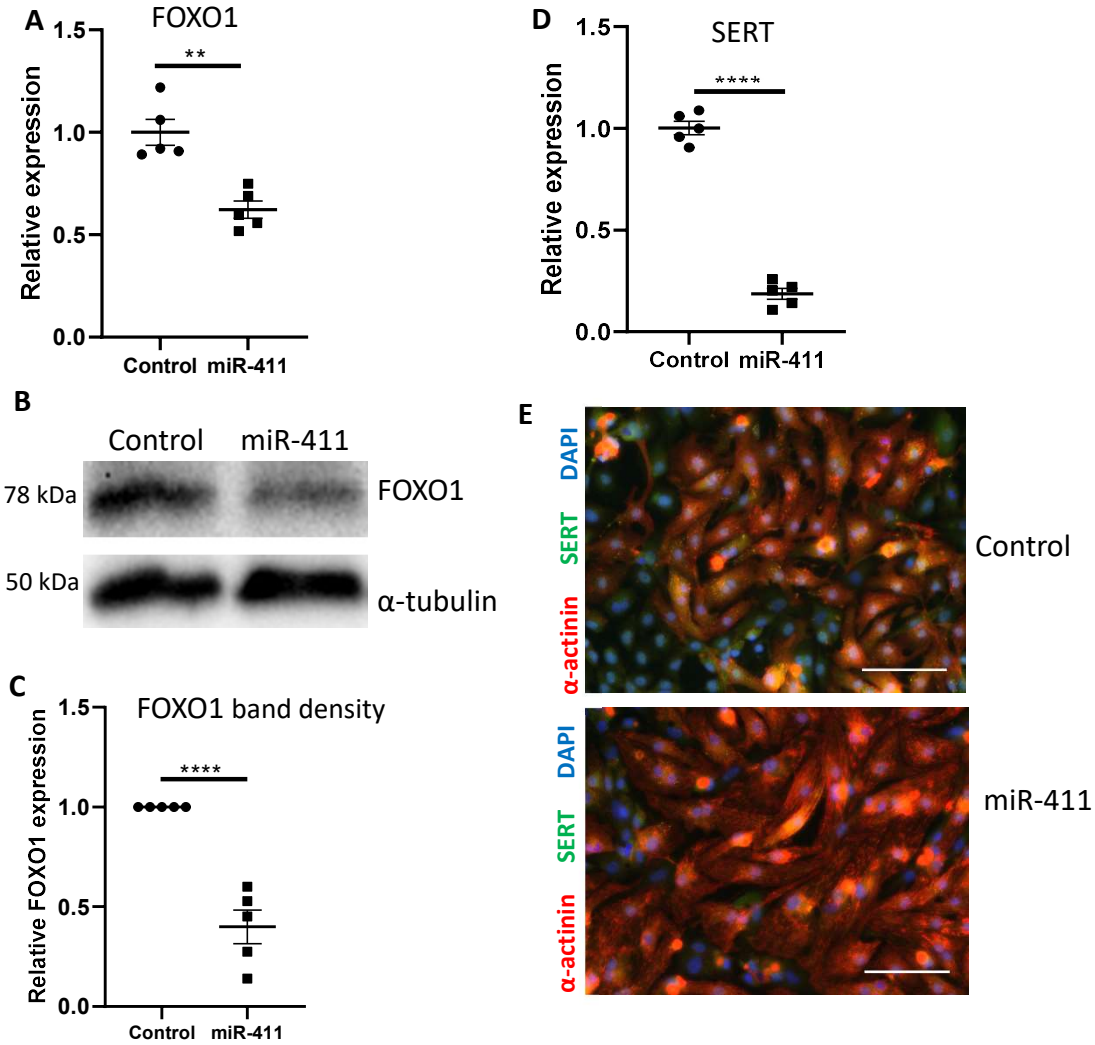

Figure 5.4 Confirmation of miR-411 target genes *in vitro*. (A) & (D) qPCR using individual samples shows that FOXO1 and SERT expression is significantly reduced in miR-411 transfected-NRCMs. n=5. ***p*<0.01, ****p*<0.0001. unpaired Student's t-test (B)&(C) Western blot showing significant reduction in the FOXO1 protein after miR-411 transfection. n=5 (E) Representative immunofluorescent images showing a qualitative comparison of SERT expression in the control and miR-411 groups. Scale bar=100 µm

Next, as the expression of Hippo core kinases did not change following miR-411 transfection (Section 3.4.4), the phosphorylation of Hippo kinases was investigated. Figure 5.5 shows that the level of LATS1 phosphorylation in miR-411

treated NRCMs was significantly reduced by approximately 40% (39.3 ± 8.4%) compared to the control.

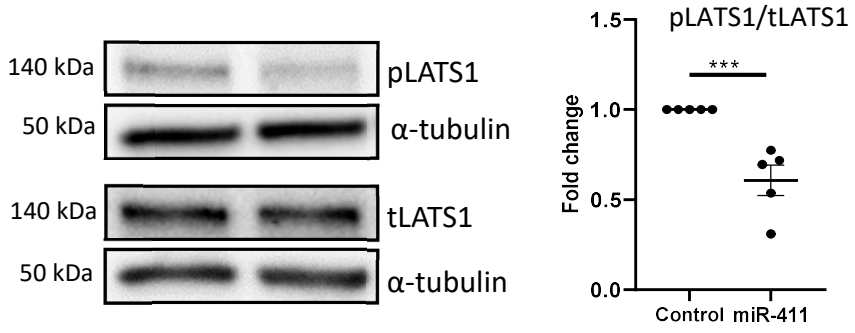

Figure 5.5 LATS1 phosphorylation post miR-411 transfection. Western blot showing a significant reduction in the pLATS1 to tLATS1 ratio in miR-411 transfected-NRCMs. n=5, ***$p < 0.001$, unpaired Student's t-test)

5.4.3 Investigation of miR-411 target genes *in vivo*

In addition to NRCMs, miR-411 target genes were also investigated in the whole heart following direct myocardial injection of miR-411 mimics (Chapter 4 Section 4.4.2). RNA samples were extracted from mouse hearts which had received injection of either control or miR-411 mimics five days prior. Similar to the analysis presented in Chapter 4 Section 4.4.2, the analysis in this section is also divided into the injection sites and the distant sites. First, the miR-411 target genes were screened using pooled RNA samples (equal amount of RNA from 4-6 independent experiment mixed into one) from both the injection sites (Fig 5.6A) and distant sites (Fig 5.7A). In the injection sites, contrary to the *in vitro* experiment, FOXO1 mRNA expression was unchanged (Fig 5.6B). On the other hand, and consistent with results using NRCM, SERT expression was found to be substantially reduced after miR-411 injection. The significant reduction of SERT expression post miR-411 expression was later confirmed with qPCR of individual samples (Fig 5.6C). In the distant sites, the expression of both FOXO1 and SERT remained unchanged post miR-411 expression (Fig 5.7B&C).

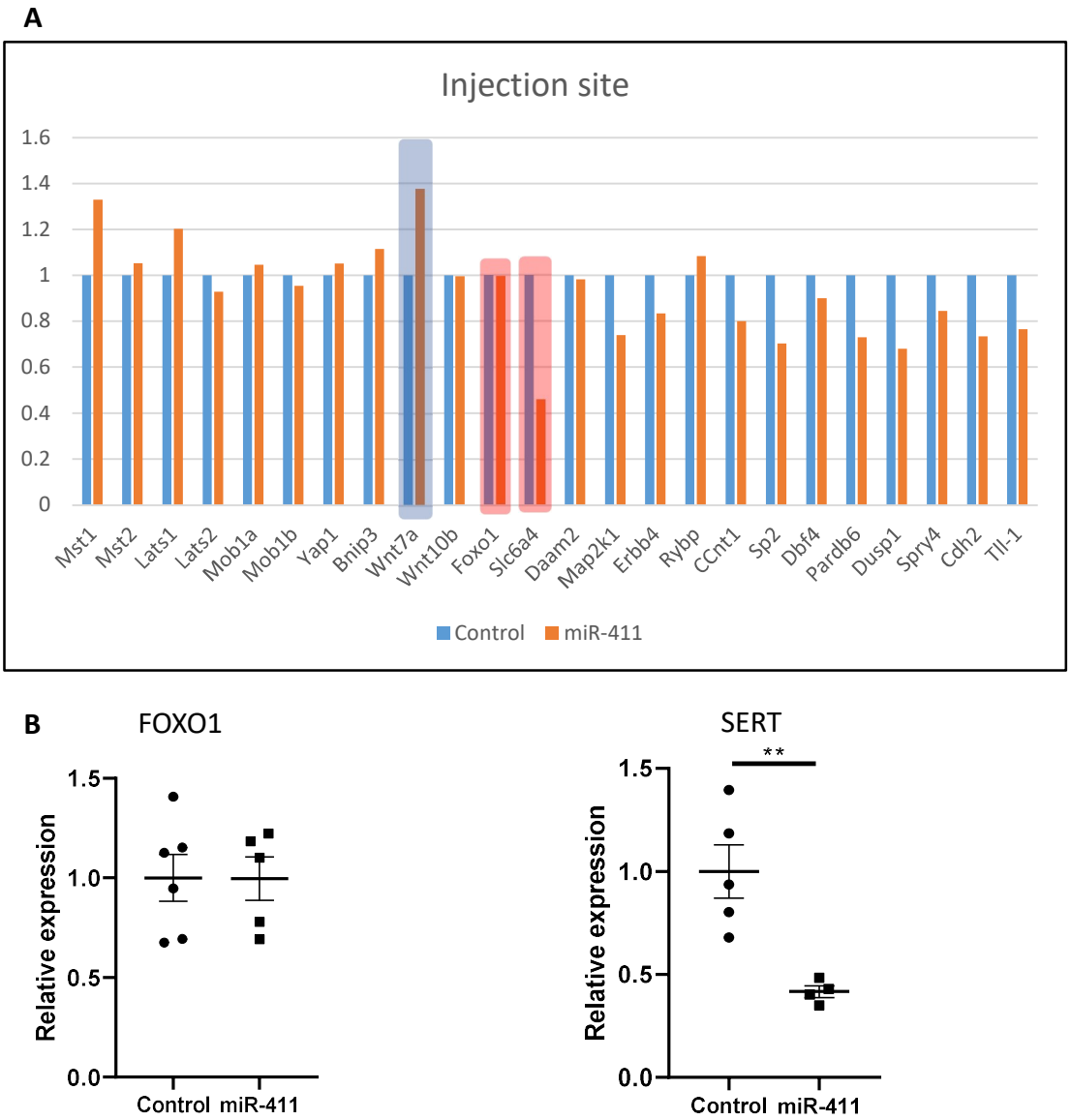

Figure 5.6 Investigation of miR-411 target genes from *in vivo* samples isolated near the injection site. (A) Screening of miR-411 target genes using pooled RNA samples. The biggest reduction is observed in SERT expression whilst FOXO1 expression remains unchanged following miR-411 transfection. (B) qPCR using individual samples confirms the screening results. SERT expression is significantly reduced after miR-411 transfection. (n= 5, $^{**}p < 0.01$, unpaired Student's t-test)

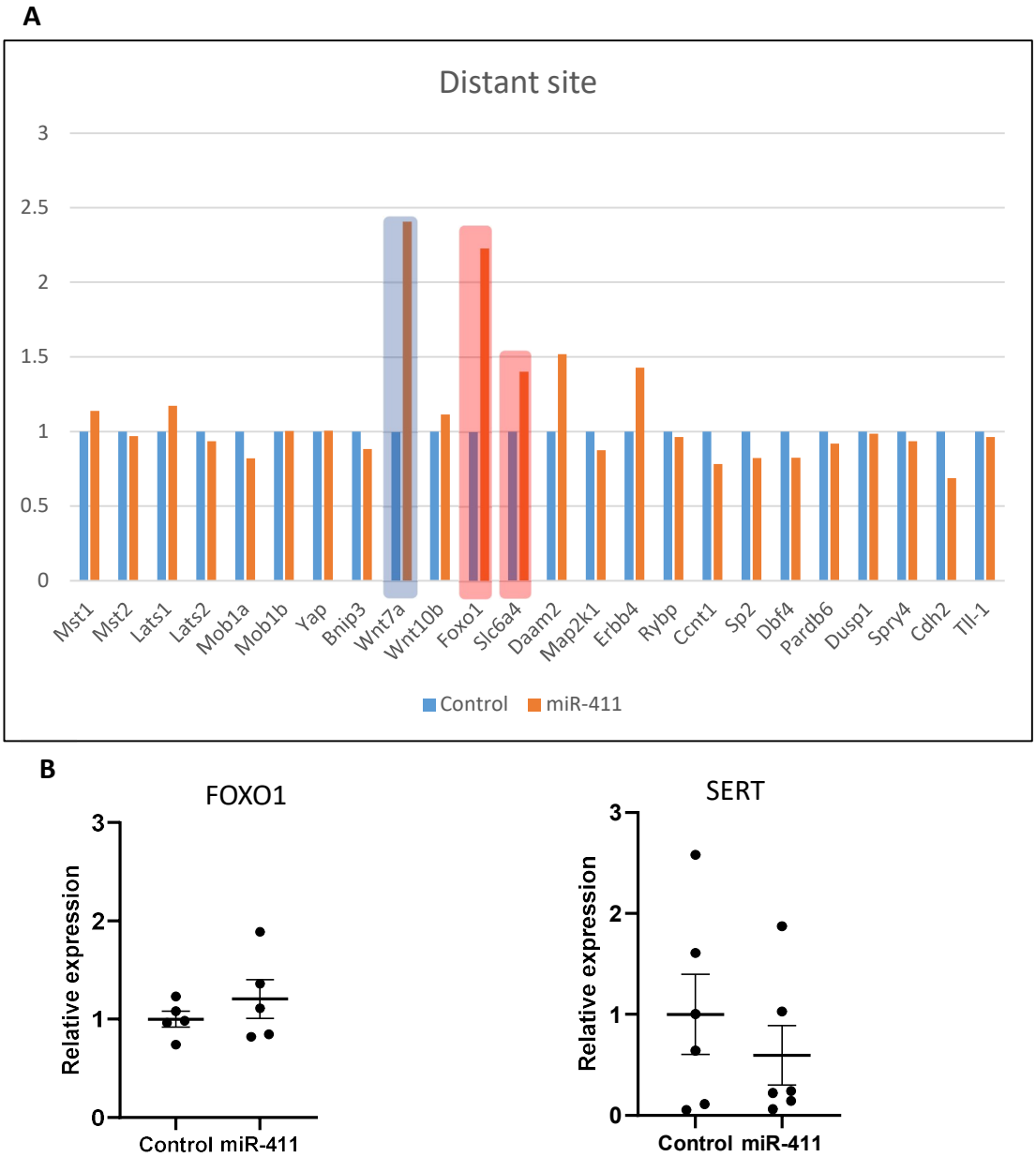

Figure 5.7 Investigation of miR-411 target genes from *in vivo* samples isolated from the distant site. (A) Screening of miR-411 target genes using pooled RNA samples. FOXO1 and SERT expression does not change following miR-411 transfection. (B) qPCR using individual samples confirms the screening results. In the distant site, the expression of both FOXO1 and SERT is similar between the control and miR-411 group. (n=5, unpaired Student's t-test)

Although SERT is the most downregulated gene in the injection sites, several other genes such as DUSP1, SP2, CDH2, MAP2K1, TLL-1, PARDB6, CCNT-1, and ERBB4 are markedly decreased as well. Some of these genes, including SP2 (Terrados et al., 2012), CDH2 (Tseng et al., 2019), MAP2K1 (Adamowicz et al., 2018), TLL1 (Sabirzhanova et al., 2009), CCNT1 (Bywater et al., 2020), and ERBB4 (Bersell et al., 2009) have been shown to stimulate proliferation in cardiomyocytes or other cell types. The remaining two genes, MAPK phosphatase DUSP1 (Toulouse and Nolan, 2015) and polarity regulator PARDB6 (Alarcon, 2010) have also been shown to reduce apoptosis and induce proliferation in breast cancer, respectively. The downregulation of these genes after miR-411 transfection therefore seems in contradiction with the pro-proliferative effect (Chapter 3 Section 3.3.4) and anti-apoptotic effect (Chapter 4 Section 4.4.4) of miR-411. Further experiments are needed to elucidate the significance of the observed reduction of these genes, especially considering that this reduction is not found in *in vitro* results presented above (Section 5.4.2), and whether it causes observable effects on cardiomyocyte functions. The results so far show that FOXO1 and SERT are still the strongest candidate of miR-411 target genes (Fig 5.2 and Fig 5.4) and thus the analysis from this point will focus on these two genes.

Similar to the findings from the *in vitro* experiment, the expression of WNT7A was increased in the injection sites and, unexpectedly, in the distant sites as well. WNT7A is a part of the WNT/β-catenin pathway, which has been shown to act downstream of the Hippo pathway (Varelas et al., 2010). Therefore, it is possible that the observed upregulation in WNT7A expression is secondary to the Hippo modulation by miR-411. Further investigations are required to elucidate the association between miR-411 overexpression and WNT7A upregulation in cardiomyocytes.

5.4.4 Verification of SERT as miR-411 target gene

To examine whether SERT is the direct target of miR-411, the predicted binding sites of miR-411 in SERT mRNA was analysed using several miRNA target prediction databases. Two predicted binding sites, in SERT 3'UTR (Fig 5.6A) and Exon 4 (Fig5.6B), were identified. These fragments were then isolated and cloned in luciferase reporter vectors, which are specifically designed and used to test the predicted miRNA binding (pmiR-Glo). Mutant reporter constructs were also generated by using site directed mutagenesis. These mutant constructs were used as negative controls.

MiR-411 mimics and the luciferase reporter vectors bearing wild type or mutant sequences of predicted miR-411 binding sites were co-transfected into H9C2 ventricular myoblastic cells. The luciferase assay showed that luciferase activity was significantly reduced in the 3'UTR group (Fig 5.7A). The suppressive effect of miR-411 was subsequently abrogated by mutations in the miR-411 binding region in the SERT 3'UTR. Similar to the 3'UTR group, luciferase activity in the Exon 4 group was also significantly reduced after miR-411 mimic transfection (Fig 5.7B), although it remains significantly reduced in the Exon 4 mutant group. This data indicates that miR-411 targets SERT mRNA via binding with the predicted binding site in the 3'UTR and Exon 4 region.

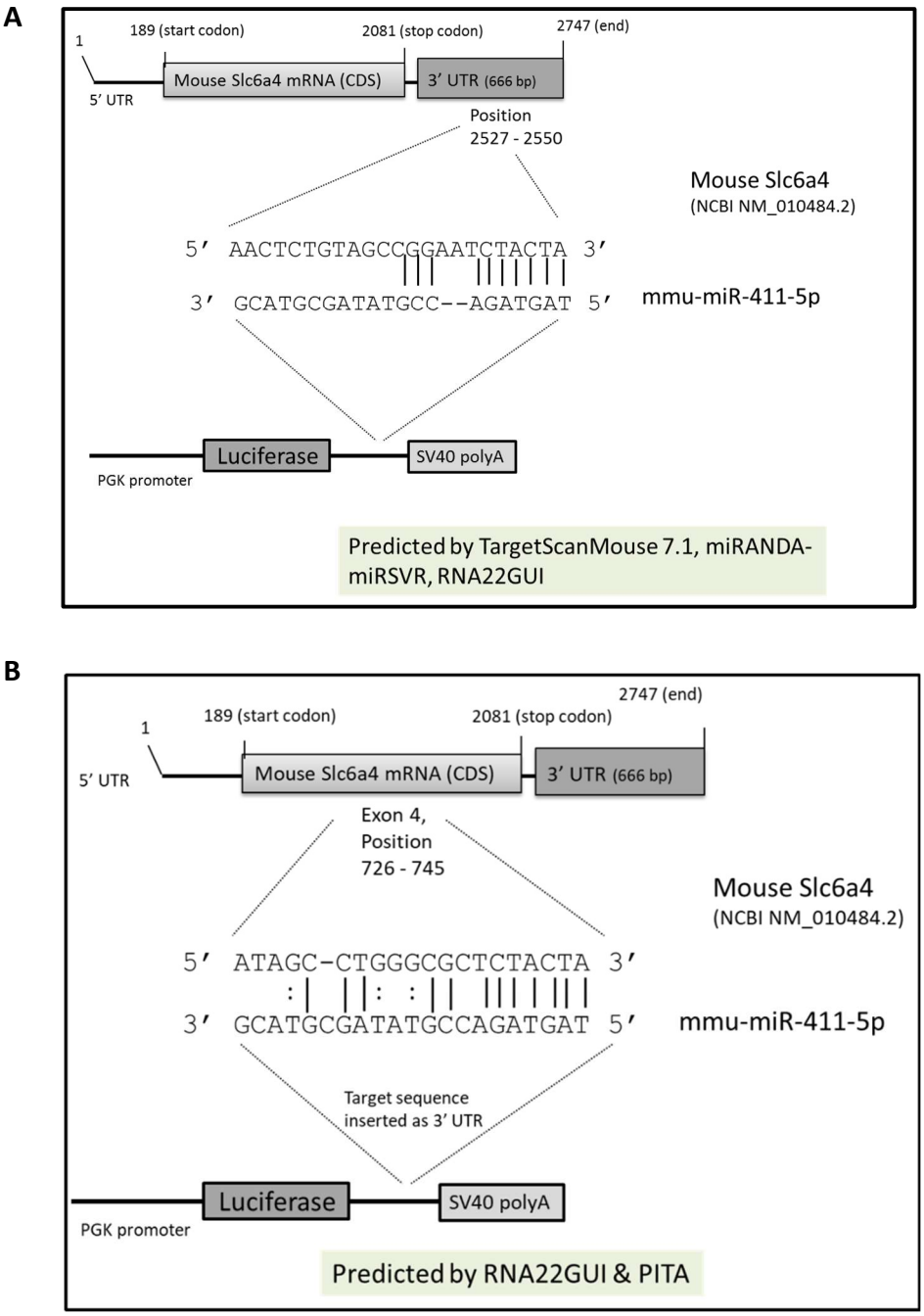

Figure 5.8 Predicted binding sites of miR-411 on SERT mRNA. MiR-411 is predicted to bind to SERT mRNA on two sites : (A) 3'UTR & (B) Exon 4

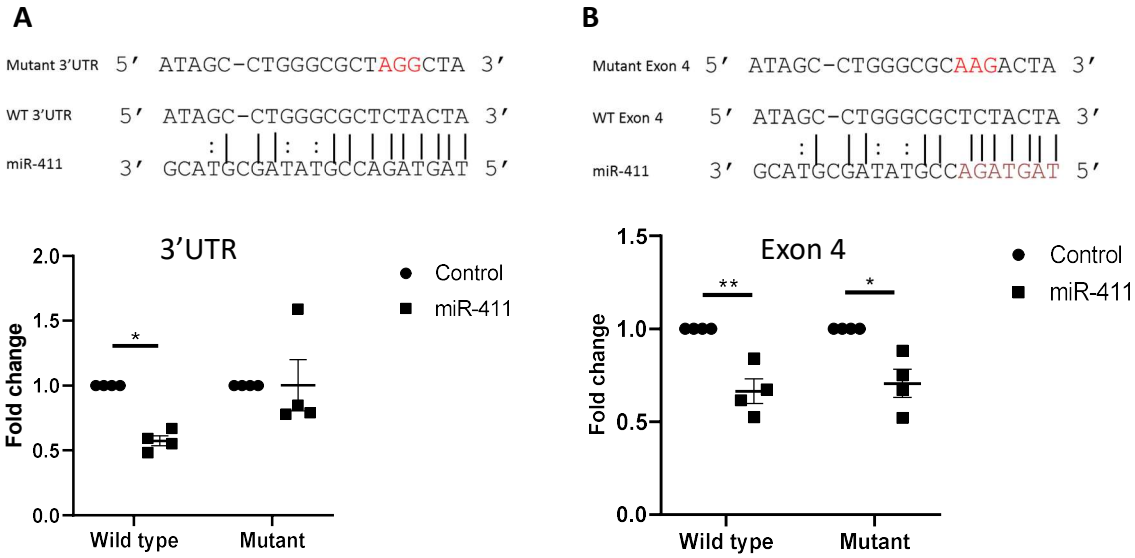

Figure 5.9 Predicted miR-411 binding sites in SERT 3'UTR and Exon 4 and corresponding sequence of mutant 3'UTR and Exon 4 tested. Luciferase reporter assay showing repression of SERT following cotransfection of miR-411 and either a (A) 3'UTR construct or (B) Exon 4 construct. Loss of repression is observed in the mutant 3'UTR group but not in the mutant Exon 4 group. n=4, *$p < 0.05$, **$p < 0.01$, unpaired Student's t-test

5.4.5 The connection between miR-411 target genes and the Hippo pathway

MiR-411 was shown to increase YAP activity by reducing LATS1 phosphorylation (Section 3.4.4) and directly targeting FOXO1 and SERT (Section 5.4.2 and 5.4.3). However, whether or not changes in YAP activity are mediated by these genes is yet to be investigated. To answer this question, the expression of FOXO1 or SERT in NRCMs were knocked down with siRNAs (Fig 5.10A-B) and whether this resulted in changes in YAP activity was subsequently investigated. Figure 5.11A shows that YAP activity is significantly increased in the SERT knockdown group compared to the control, but remains unchanged in the FOXO1 knockdown group. These results were further confirmed through a western blot (Fig 5.11B) which showed a significant increase in active YAP expression in the SERT knockdown group but not in the FOXO1 knockdown group. This suggests that miR-411 modulates the Hippo pathway through SERT downregulation.

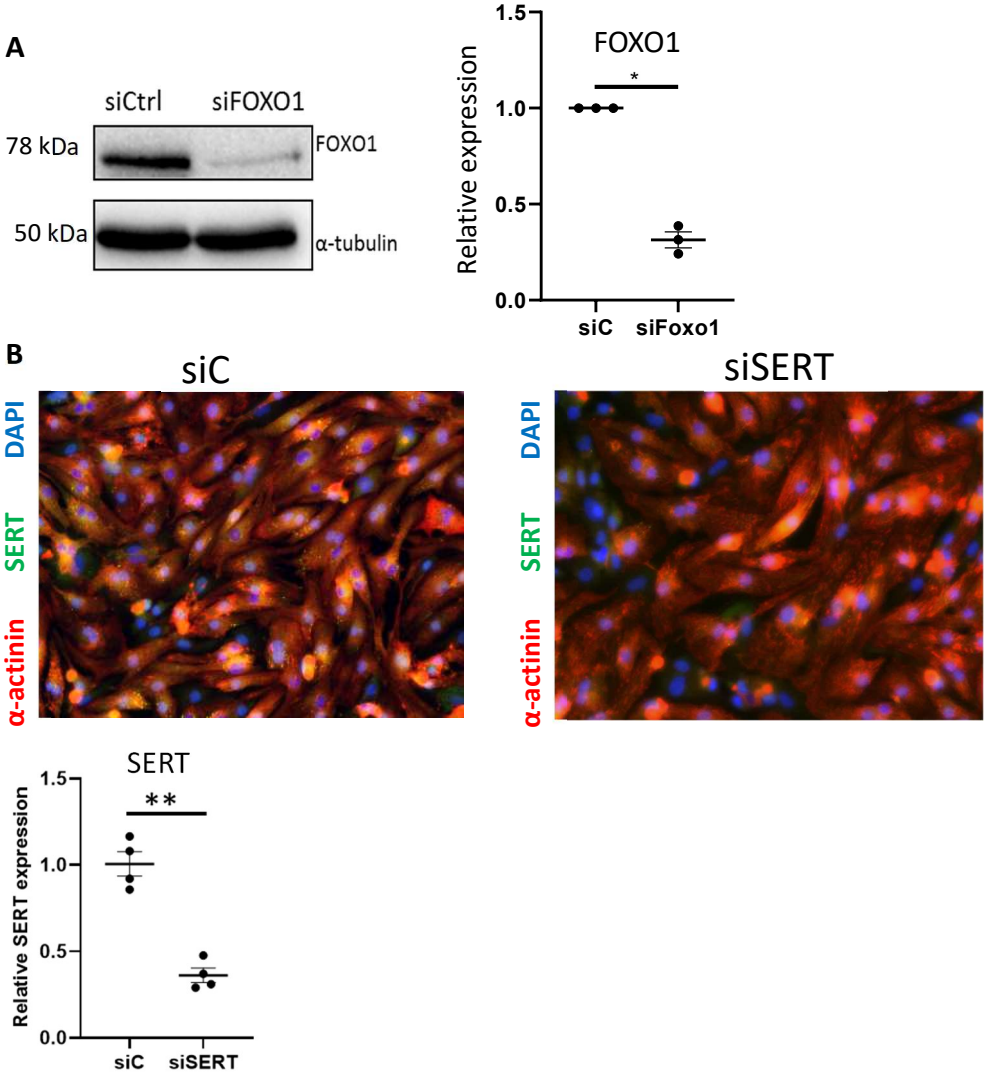

Figure 5.10 FOXO1 and SERT knockdown in NRCMs with siRNAs.

(A) Western blot showing significant reduction of FOXO1 following siRNA treatment. (B) Representative images showing qualitative distribution of SERT in both control and siSERT group. (C) qPCR showing significant reduction in SERT expression following siRNA treatment. n=3, *$p < 0.05$, unpaired Student's t-test

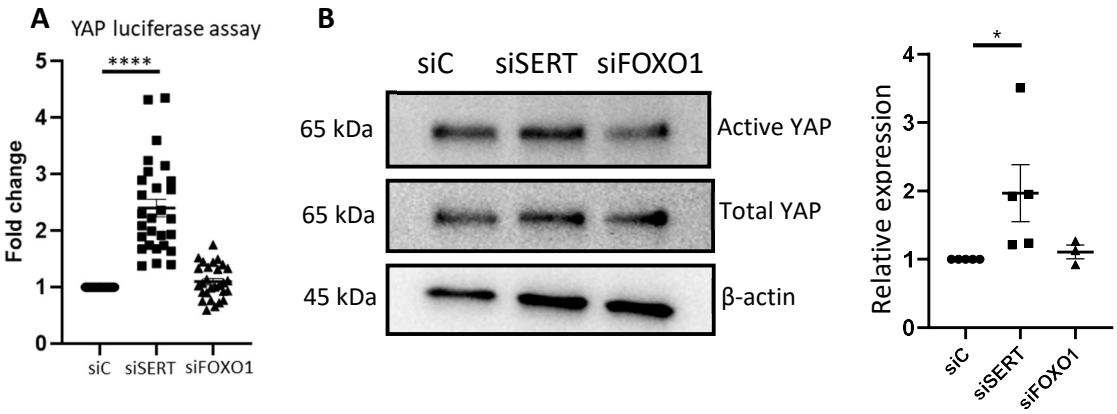

Figure 5.11 Changes in YAP activity following SERT and FOXO1 downregulation. (A) Luciferase assay showing a significant increase in YAP activity in the SERT knockdown group. Yap activity in the FOXO1 knockdown group does not differ from the controls. n=28 replicates from 4 independent experiments, ****$p < 0.0001$, one way ANOVA (B) Western blot showing the active YAP level following SERT and FOXO1 knockdown. SERT knockdown causes a significant increase in YAP activity whilst FOXO1 knockdown does not cause any changes in YAP activity. n=5 for siC and siSERT, 3 for siFOXO1, *$p < 0.05$, one way ANOVA with Tukey's post-hoc test.

5.4.6 A proposed model for Hippo pathway regulation through serotonin signalling

The results have so far shown that the ability of miR-411 to modulate the Hippo pathway is mediated by SERT. However, the exact mechanism of how SERT regulates the Hippo pathway has not been investigated. SERT is a crucial part of serotonin signalling which functions as the regulator of serotonin level in the extracellular space. The other important components of the serotonin signalling system are serotonin itself and serotonin receptors. Serotonin can bind to these receptors and elicits diverse effects in the cardiovascular system (illustrated in Fig 5.12A). Serotonin in the heart is initially thought to come from somewhere else in the body, such as the gastrointestinal tract or the serotonin reserve in platelets. However, previous studies have shown that cardiomyocytes are capable of producing endogenous serotonin even in culture (Ikeda et al., 2005; Pönicke et al., 2012).

Recently, G-protein coupled receptors have been shown to regulate LATS1 phosphorylation and increase YAP activity via the Rho kinase protein (ROCK1) (Yu et

al., 2013) (Fig 5.12B). As most serotonin receptors belong to the GPCR family (Millan et al., 2008), increased serotonin receptor activation is likely to have the same effects, i.e., activating ROCK1 and reducing LATS1 phosphorylation. Combining the serotonin signalling and this pathway (Fig 5.12C) can potentially explain how miR-411 mediated changes in serotonin signalling can modulate the Hippo pathway. The reduction of SERT expression by miR-411 will increase the concentration of serotonin in the extracellular space. Consequently, the activation of serotonin receptors will also be increased, leading to increased ROCK1 activity. ROCK1 will then inhibit LATS phosphorylation and eventually reduce YAP phosphorylation and increase YAP activity.

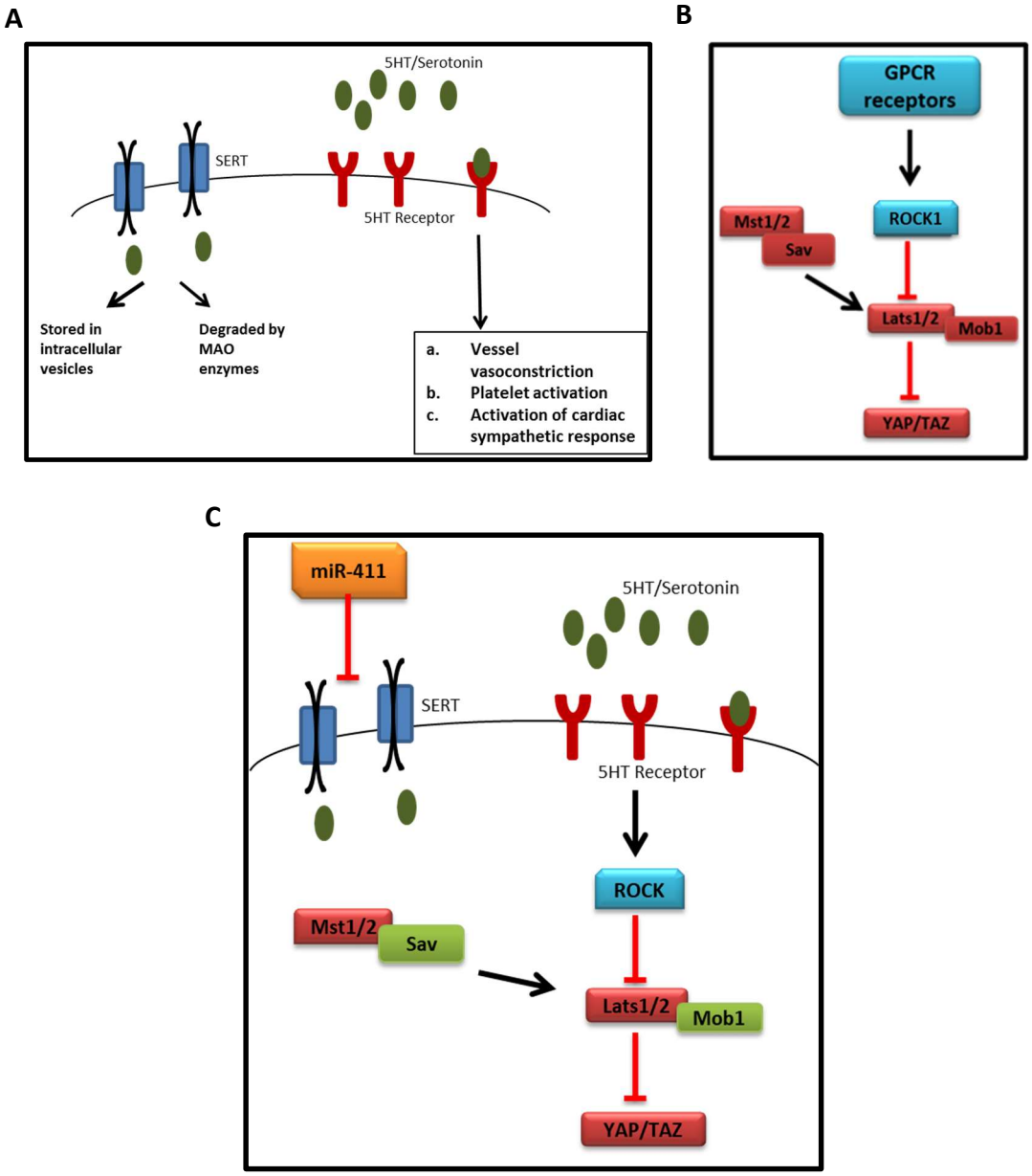

Figure 5.12 Schematic illustration of serotonin signalling and regulation of the Hippo pathway by GPCR family. (A) Serotonin signalling (B) Regulation of the Hippo pathway by GPCR family (C) The proposed model describing how miR-411 mediated SERT downregulation leads to increased YAP activity. MiR-411 reduces the SERT expression which causes increased extracellular serotonin concentration and increased serotonin receptor activation. Increased activation of serotonin receptors will then activate ROCK1 activity leading to decreased LATS1 phosphorylation and increased YAP activity.

To validate the proposed model, SERT expression in NRCMs was knocked down with siRNAs and the activity of ROCK1 or serotonin receptors were subsequently inhibited with pharmacological compounds in separate experiments (Fig 5.13A). SiRNAs against SERT was used instead of miR-411 because it seems that increased YAP activity caused by miR-411 is almost exclusively mediated by SERT downregulation (Section 5.4.5, Figure 5.11A & B). ROCK1 inhibitor (Y-27632, Sigma) was used to block ROCK1 activity in SERT deficient NRCMs whilst a global serotonin inhibitor metergoline was used to block the serotonin receptors (Fig 5.13A). If the proposed model is true, the administration of ROCK1 inhibitor or metergoline will abolish increased YAP activity observed in SERT deficient NRCMs. Figure 5.13B shows that after the administration of ROCK1 inhibitor (Liao et al., 2007), there was a dose dependent reduction in YAP activity in the SERT knockdown group with significant reductions observed at 4 µM and 6 µM concentrations. Similar results were also found after administration of metergoline (De Ponti, 2004) in the SERT knockdown group. Metergoline could significantly reduce YAP activity in a dose dependent manner with significant reductions observed at all concentrations tested (1, 3, and 5 µM concentrations) (Fig 5.13C). These results appear to confirm the proposed model above.

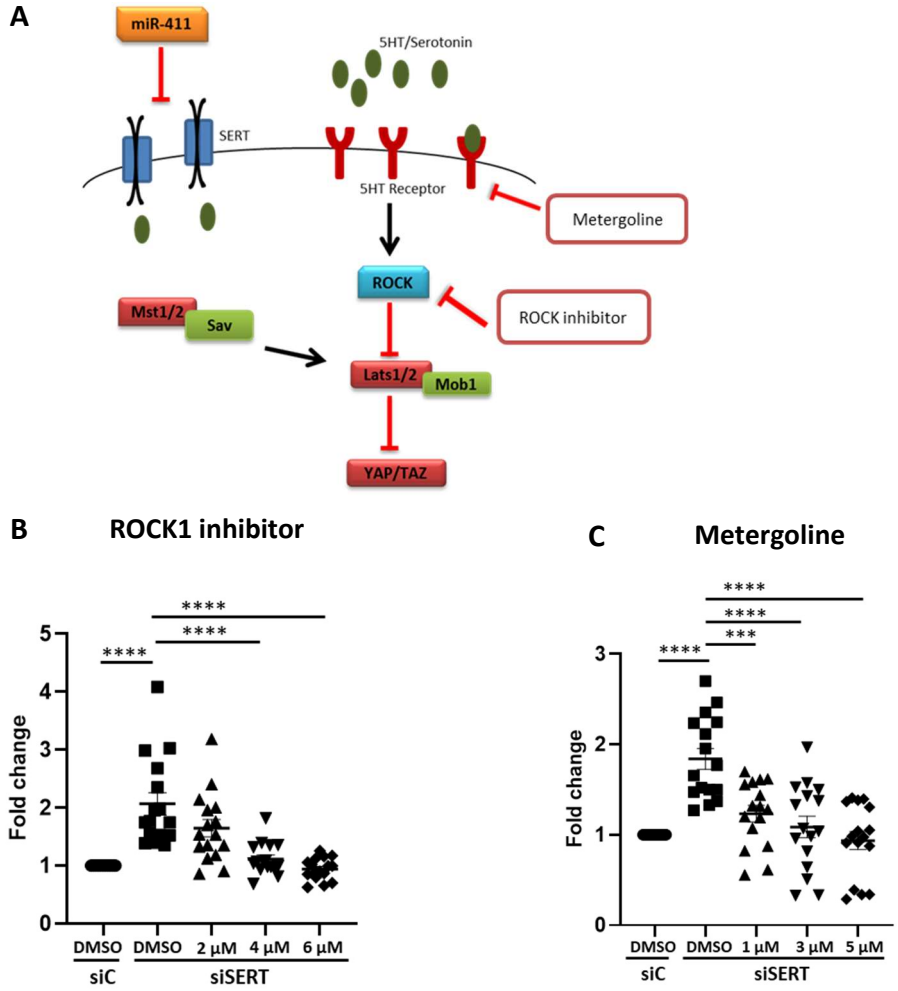

Figure 5.13 Validation of the proposed mechanism describing how miR-411 modulates the Hippo pathway via SERT downregulation. (A) To validate whether miR-411 mediated reduction of SERT increases YAP activity via ROCK1 and serotonin receptor activation, ROCK inhibitor or serotonin receptor blocker metergoline was administered in SERT deficient NRCMs. (B) The effects of ROCK inhibitor on YAP activity in SERT deficient NRCMs was assessed using a YAP luciferase reporter assay. ROCK inhibitor can abolish increased YAP activity caused by SERT knockdown at 4 and 6 µM concentrations (C) The effects of metergoline on YAP activity in SERT deficient NRCMs a YAP luciferase reporter assay. Metergoline can return YAP activity to a level similar to controls at 1, 3, and 5 µM concentrations. n=16 replicates from 4 independent experiments, ***$p < 0.001$, ****$p < 0.0001$, One-way ANOVA with Bonferroni's post-hoc test.

Next, to further validate the proposed model above, the changes in YAP activity in SERT deficient NRCMs following treatments with ROCK inhibitor or metergoline was examined using western blot. In addition, the level of LATS1 phosphorylation was also investigated. As shown in Figure 5.5, 5.11, and 5.12C , miR-

411 mediated reduction in SERT expression leads to both reduced LATS1 phosphorylation and increased YAP activity. As expected, SERT knockdown could significantly reduce LATS1 phosphorylation and thus increase YAP activity. These effects, however, were subsequently abolished by administration of 4 µM ROCK inhibitor and 3 µM metergoline, i.e., both LATS1 phosphorylation and YAP activity returned to levels similar to those of controls after treatment with both agents (Fig 5.14A-D). These results seem to confirm the hypothesis (Figure 5.12C) that SERT downregulation modulates the Hippo pathway via serotonin receptor and ROCK1 activation.

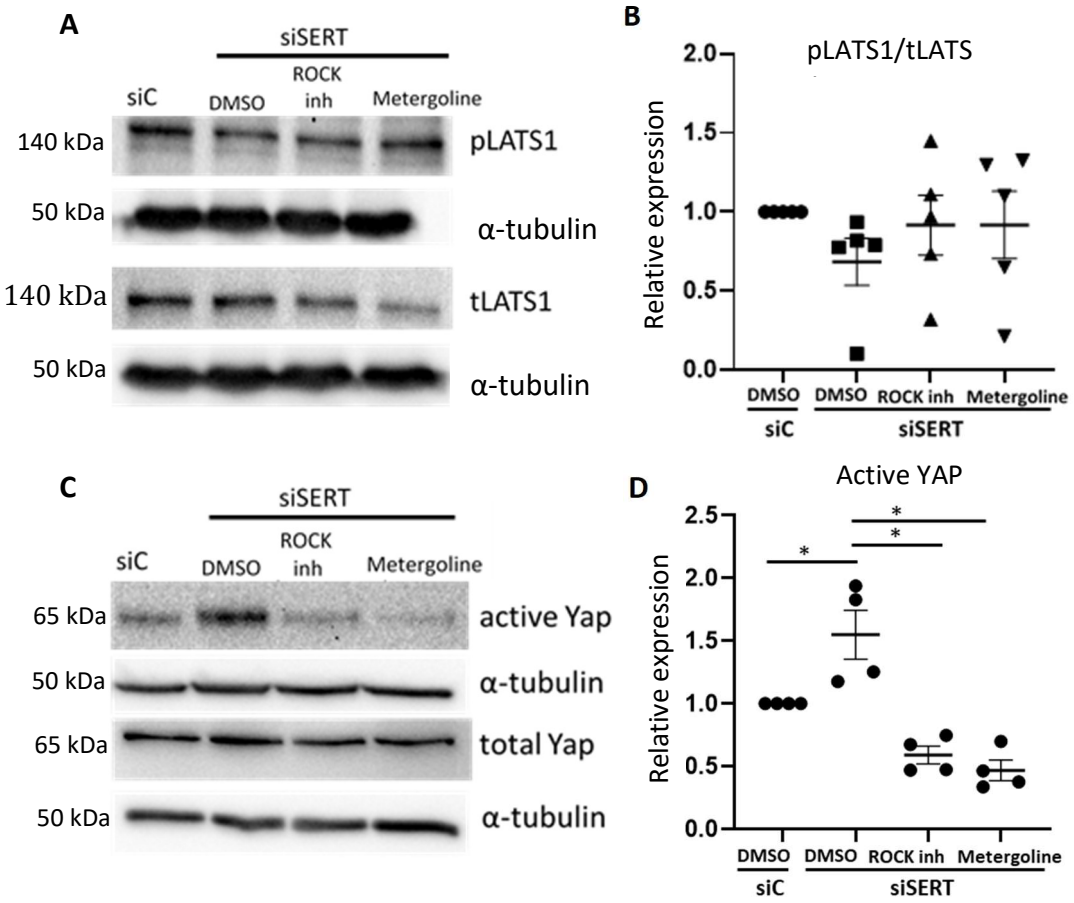

Figure 5.14 Western blot showing the effects of ROCK inhibitor and metergoline on active YAP and LATS1 phosphorylation level. (A)&(B) The level of pLATS1/tLATS1 ratio is reduced following SERT knockdown but back to a level similar to the control after the administration of ROCK inhibitor or metergoline. n=5. (C)&(D) The level of active YAP/tYAP ratio is increased following SERT knockdown but significantly reduced after the administration of ROCK inhibitor or metergoline. n=4. *p<0.05. One-way ANOVA with Bonferroni's post-hoc test.

5.5 Discussion

In the previous chapters, the functional role of miR-411 in protecting the heart in response to MI was observed. However, the mechanistic models behind this effect are not yet understood. This chapter will, therefore, discuss the mechanisms responsible for the protective role of miR-411, starting from establishing miR-411 direct targets to a more complete model that can explain how changes in miR-411 target genes leads to the Hippo pathway modulation.

5.5.1 MiR-411 directly targets FOXO1 and SERT in the heart

Investigations with qPCR and a western blot demonstrate that FOXO1 is significantly reduced post miR-411 overexpression in NRCMs, suggesting that FOXO1 is a direct target of miR-411. This finding is in line with the findings of a previous study, which validated FOXO1 as one of the miR-411 target genes in human lung cancer cell lines (Zhao et al., 2016). However, the reduction in FOXO1 expression cannot be seen following *in vivo* miR-411 overexpression in mice. The reason behind this difference is unclear. One of the possible causes is the degree of conservation of miR-411 binding sites on the FOXO1 mRNA. However, this is unlikely as, according to several miRNA target prediction databases, the target site of miR-411 on FOXO1 3'UTR is conserved not only in mice and rats but also in humans, pigs, and several other mammals (Agarwal et al., 2015; Chen and Wang, 2019; Miranda et al., 2006).

Another possible explanation for the phenotypic differences between *in vitro* and *in vivo* is due to the complexity of the miRNA regulatory functions *in vivo* (Tarang and Weston, 2014). A single miRNA has been shown to target multiple genes and a single gene can be targeted by multiple miRNAs (Bartel, 2004; Bartel, 2009). Therefore, the effects of miRNA targeting may not be apparent due to the compensatory mechanisms by other miRNAs or genes. Moreover, the phenotypes of miRNA targeting *in vivo* are often subtle (Bartel, 2009). The subtle effects of miRNA

targeting combined with a highly heterogeneous environment *in vivo* make the detection of miRNA targets even more challenging. Nevertheless, the evidence of FOXO1 reduction post miR-411 overexpression from the *in vitro* experiment is adequate to warrant further investigations.

The second candidate for miR-411 target genes obtained from the experiment is SERT. Contrary to FOXO1, SERT expression levels are significantly and consistently reduced after miR-411 overexpression both *in vitro* and *in vivo*. This strongly suggests that SERT is a direct target of miR-411 in the heart. Furthermore, two miR-411 binding sites (miRNA recognition elements / MREs) on the SERT mRNA, one in the 3'UTR and the other in the coding region (Exon 4) have been validated. Although MREs are primarily located in the 3'UTR of mRNAs, non-traditional locations of MRE, such as the mRNA coding sequences are also important. Chi *et al.* demonstrated that miRNAs can possibly target as much as 25% of the sites in the coding region of a gene (Chi et al., 2009). A luciferase reporter assay demonstrated a significant decrease in the luciferase activity after co-transfection of miR-411 mimics and wild type 3'UTR constructs. This decrease was abolished when mutant 3'UTR constructs were introduced. A significant decrease in the luciferase activity is also observed following co-transfection of miR-411 mimics and Exon 4 constructs. However, a significant decrease is still observed in the mutant Exon 4 group. This suggests that a presence of multiple miR-411 binding sites in the SERT Exon 4, or partial binding between miR-411 and its binding site on the SERT Exon 4, is adequate to reduce luciferase activities. Overall, these results have verified that SERT is a direct target of miR-411.

5.5.2 The role of miR-411 in regulation of the Hippo signalling pathway is mediated by SERT downregulation

Initially, FOXO1 was thought to mediate the regulatory effect of miR-411 on the Hippo pathway as it has been shown to interact with YAP to facilitate the expression of genes that are necessary for oxidative stress responses (Shao et al., 2014). The SERT protein, on the other hand, has never been associated with the Hippo pathway in the heart previously. The results, however, show that the level of

active YAP remains unchanged following FOXO1 knockdown whereas in the SERT knockdown group it is significantly increased. These results suggest that miR-411 mediated-regulation of the Hippo pathway is dependent on the SERT protein.

The SERT (serotonin transporter or 5-HTT) protein is encoded by the solute carrier 6 member 4 (SLC6A4) gene. It is a member of a wider solute carrier 6 family, which comprises 20 transporters that are responsible for transporting neurotransmitters, amino acids, osmolytes, and energy metabolites (Broer and Gether, 2012; Rudnick, 2006). As has been discussed before, SERT is part of the serotonin signalling pathway and is capable of diminishing serotonin function by removing serotonin from outside the cell and transporting it back to the intracellular space (Broer and Gether, 2012). Therefore, SERT is crucial in the regulation of the serotonin level in the extracellular space and the peripheral circulation (Eddahibi et al., 2000).

Several studies have demonstrated that serotonin and serotonin receptors play important roles in embryonic heart growth and cardiomyocyte proliferation (Choi et al., 1997; Lauder et al., 2000; Nebigil et al., 2000; Yavarone et al., 1993). The data on SERT, on the other hand, are very limited. During embryonic growth, SERT gene expression is first detected within the aortic wall and the heart tube at between embryonic day 10 and 11 (Lauder et al., 2000; Pavone et al., 2008). From this point, the SERT expression becomes more intense until it peaks at E18 and remains unchanged until E21. At this time, SERT distribution is localised to the endocardium (Lauder et al., 2000; Pavone et al., 2008). Two published studies reported slightly different phenotypes found in SERT deficient mice. Pavone *et al.* found that genetic ablation of SERT in mice produced no obvious developmental abnormalities at birth (Pavone et al., 2009). However, the mice were later reported to develop cardiac fibrosis and valvulopathy at 8 to 10 weeks of age. Another study which used SERT Cre knock-in mice ($SERT^{Cre/+}$) to generate SERT knockout (SERT-KO) mice reported more severe phenotypes with premature death of 75% mutant mice within the first week after birth. Histological analysis revealed that the mutant mice developed severe cardiac fibrosis with increased collagen accumulation in the myocardium and the

valvular region, consistent with the first paper (Mekontso-Dessap et al., 2006). In addition to genetic ablation, the use of pharmacological agents to modulate SERT activity during embryonic heart growth appears to further support these findings. For example, the administration of fluoxetine in pregnant mice results in post-natal mortality due to severe heart failure caused by dilated cardiomyopathy (Noorlander et al., 2008). Moreover, the treatment of cultured foetal heart cells with paroxetine reduces cell proliferation (Sari and Zhou, 2003). Overall, these studies highlight the significance of SERT in heart morphogenesis.

The mechanisms by which SERT exerts its effects have not been fully investigated. In a SERT-KO mouse heart, increased expression of serotonin receptor $5HT_{2A}$, phospho-SMAD2/3 and phospho-ERK1/2 are detected and thus can potentially explain the increased cardiac fibrosis observed in SERT-KO mice. The absence of SERT leads to an excess of serotonin in the extracellular space and in turn causes increased activation of $5HT_{2A}$. Increased $5HT_{2A}$ activation is postulated to subsequently increase SMAD2/3 and ERK1/2 phosphorylation via TGF-β1 signalling and induce the expression of cardiac fibroblast marker α-smooth muscle actinin (α-SMA) and collagen deposition (Pavone et al., 2009). In addition, phospho-SMAD2/3 and phospho-ERK1/2 also have some roles in cell proliferation and apoptosis. However, it is unclear whether SERT also modulates these cellular processes.

Here, this project has found a novel evidence that SERT can modulate the Hippo pathway activities and in turn increase cardiomyocyte proliferation. This finding seems to contradict the available evidence on the roles of SERT in the developing heart. Several studies indicate that the activities of serotonin signalling are finely tuned both spatially and temporally (Sari and Zhou, 2003). Therefore, the fact that this experiment is conducted specifically in the heart of adult mice might explain why the finding from this experiment is different from what is reported in the existing literature. Additionally, the duration of SERT knockdown is likely to contribute to this discrepancy as well. For example, long term (permanent) SERT deficiency in mice induces an anxiety-like behavioural phenotype (Adamec et al., 2006; Carroll et al., 2007), whilst administration of serotonin selective reuptake

inhibitors causes the opposite, i.e., alleviates anxiety-like symptoms (Murphy et al., 2008). It is postulated that long-term or permanent SERT deficiency alters serotonin homeostasis which results in chronic serotonin deficiency.

Until now, there has been no available evidence in the existing literature that demonstrates the association between the SERT protein and the Hippo pathway. However, there exists some evidence which suggests that serotonin signalling, as a whole, can modulate the Hippo pathway in cancer cases. Exogenous serotonin administration in hepatocellular carcinoma cell lines has been shown to increase YAP activity by activating $5HT_{2B}$ receptors (Liu et al., 2017). This, in turn, leads to increased cancer growth and invasiveness. Further investigation is required to elucidate the exact mechanism of Hippo pathway modulation by serotonin signalling in the heart and investigate how the SERT protein fits in this model.

5.5.3 The crossover between serotonin signalling and the Hippo pathway

The main nexus that links serotonin signalling and the Hippo pathway is the fact that serotonin receptors are almost exclusively members of the GPCR family (Millan et al., 2008). The regulation of the Hippo pathway by the GPCR family has been established by several studies. Yu *et al.* showed that GPCRs could either increase or reduce YAP activity by inhibiting or stimulating LATS respectively, depending on the receptor subfamily (Yu et al., 2012). GPCRs with $G\alpha_{12/13}$ subunits are the most potent enhancers of YAP activity, followed by $G\alpha_{q/11}$, and $G\alpha_{i/o}$ subunits. On the other hand, GPCRs with $G\alpha_s$ subunits increase LATS phosphorylation, thereby reducing YAP activity.

A more recent study found that Rho GTPases act downstream to GPCRs to inhibit LATS phosphorylation and increase YAP activity (Yu et al., 2013). Rho GTPases regulate the actin cytoskeleton and dynamics by activating its major effector, Rho-associated protein kinase 1 (ROCK1) (Amano et al., 2010). ROCK 1 has been shown to associate with both SERT (Mair et al., 2008) and LATS1 (Zhou et al., 2015) to modulate

cell proliferation. Therefore, it is likely that ROCK1 mediates the observed reduction in LATS1 phosphorylation by acting downstream to serotonin receptors (Fig 5.13A).

To validate the proposed model that links serotonin signalling and the Hippo pathway (Fig 5.13A), ROCK inhibitor or metergoline were used to block the effects of the SERT mediated-increase in serotonin receptor activation and subsequent induction in YAP activity. Both agents have successfully abolished the changes in LATS and YAP phosphorylation caused by the SERT knockdown. These results, therefore, have validated the proposed model.

5.5.4 Limitations and future work

Several challenges were met during the execution of experiments involved in this chapter. First, the ability to detect SERT protein using western blot or immunofluorescence was hampered because the lack of reliable SERT antibody. Attempts had been made to test several anti SERT antibodies from different manufacturers but there was not a single antibody that worked particularly well against heart tissue lysates or histological sections. In the future, more optimisations need to be done to find a more reliable anti SERT antibody. This will further allow the investigation of SERT expression post MI *in vivo* in addition to improving SERT detection post treatments with miR-411 or siRNA *in vitro*.

In an attempt to validate the hypothesis that describes the novel connection between the serotonin signalling and the Hippo pathway, a global serotonin receptor blocker (metergoline) was used to blocked the activation of serotonin receptors (Fig 5.13C). Considering that serotonin receptors have several subtypes (discussed in Section 6.3), the future experiment should identify the specific type of the receptors that is activated post miR-411 transfection.

5.6 Conclusion

In conclusion, the results suggest that miR-411 modulates the Hippo pathway by directly targeting SERT and thus suggests a novel interaction between the Hippo pathway and serotonin signalling. The miR-411 mediated-downregulation of SERT increases the extracellular concentration of serotonin which triggers the activation of the serotonin receptors-ROCK1-LATS1 axis and subsequently reduces YAP phosphorylation and increases YAP activity.

CHAPTER 6

General Discussion

Chapter 6 - General Discussion

Cardiac remodelling post MI and subsequent HF remains one of the leading causes of cardiovascular disease related death globally (Mensah et al., 2019). The advances in the treatments of acute MI have dramatically reduced the mortality rate associated with the condition (Briffa et al., 2009). However, the infarcted myocardium will be permanently replaced with fibrosis which subsequently triggers long-term remodelling and leads to a growing number of patients developing heart failure (Cahill and Kharbanda, 2017). Current treatments for HF are limited and do not lead to the regeneration and repair of the lost tissue (Gheorghiade and Goldstein, 2002; Sweitzer, 2003). Therefore, novel strategies are urgently needed to address this problem. A considerable number of basic and translational studies have been carried out to develop cell transplantation aimed at replacing the infarcted tissue and restoring cardiac function (Lin and Pu, 2014). However, this field still faces several challenges, such as cell survival after injection and the integration of the transplanted cells into the host myocardium, which need to be addressed to maximise the therapeutic effects (Dodson and Levine, 2015).

Several studies have established that mammalian hearts possess the age-dependent ability to regenerate (Porrello et al., 2011b). Neonatal mammalian hearts have the most potent regenerative capacity which lasts for a short period after birth (Porrello et al., 2011b). After this period, the vast majority of cardiomyocytes will exit the cell cycle, thus leading to a dramatic decrease in regenerative capacity (Porrello et al., 2013). However, recent evidence shows that adult human hearts are capable of renewal, with a decreasing rate from 1% annually at the age of 25 to 0.45% at the age of 75 (Bergmann et al., 2009; Bergmann et al., 2015). Although these rates seem low, it is estimated that up to 39% of all cardiomyocytes in a 75-year old person are generated postnatally (Bergmann et al., 2015). This evidence challenges the long held paradigm that the adult heart is incapable of regeneration and highlights the possibilities to induce cardiac regeneration after injury.

However, there remain lingering questions pertaining to the source and the extent of cardiomyocyte renewal in the adult heart (Bergmann et al., 2009; Eschenhagen et al., 2017; Mensah et al., 2019). Recent studies by Senyo *et al.* and Zhang *et al.* in mice using genetic lineage tracing seem to confirm that new cardiomyocytes generated postnatally predominantly come from pre-existing cardiomyocytes (Senyo et al., 2013; Y. Zhang et al., 2019), not from cardiac progenitors or other stem cells of noncardiac lineage as previously suggested (Ellison et al., 2013; Hsieh et al., 2007; Van Berlo et al., 2014). Also, the number of proliferating cardiomocytes is increased after myocardial injury in the border region (Senyo et al., 2013; Y. Zhang et al., 2019). These findings suggest that understanding the mechanisms underpinning age-dependent cardiac regeneration is crucial for developing new treatments that are aimed at improving cardiac regeneration. Moreover, these studies also further support the idea of stimulating the proliferation of resident cardiomyocytes rather than relying on the transplantation of exogenous cells into the heart.

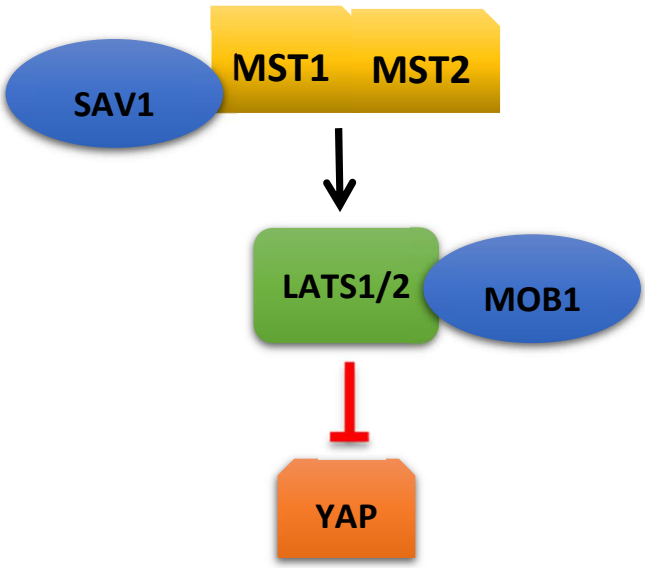

Figure 6.1 Core kinases of the Hippo pathway.

A comparison of transcriptomic profiles between proliferating (embryonic and neonatal) and adult cardiomyocytes has led to the identification of several

pathways that can regulate cardiomyocyte proliferation. Hippo signalling (Fig 6.1), a kinase cascade crucial for organ size control, has recently garnered a great deal of interest as it can be modulated to induce cardiomyocyte proliferation (Heallen et al., 2013; Heallen et al., 2011; Lin et al., 2014). For example, the cardiomyocyte-specific inactivation of SAV1, one of the Hippo adaptor molecules, has been reported to increase the activity of the main Hippo effector YAP and enhance cardiomyocyte proliferation with functional restoration after MI (Leach et al., 2017). Contrarily, stimulating the Hippo pathway through the overexpression of MST1 and LATS2, two of the main Hippo kinases, causes increased cardiomyocyte apoptosis, reduced heart size, and heart dysfunction (Matsui et al., 2008; Yamamoto et al., 2003). These findings suggest that Hippo pathway inhibition can be used to stimulate cardiomyocyte proliferation. In the recent decades, many studies have uncovered novel Hippo modulators, thus dramatically improving our understanding of how the Hippo pathway is regulated. However, only a few studies have the potential to be translated into development of novel therapies that can be used for clinical practice. One of the examples is the recent discovery of small molecule TT-10, the enhancer of YAP-TEAD1 interactions. The administration of TT-10 post-MI has been shown to promote cardiomocyte proliferation, reduce infarct size, and improve cardiac function (Hara et al., 2018). Additionally, the MST1/2 inhibitor, XMU-MP1, reduces cardiomyocyte hypertrophy and preserves cardiac function following pressure overload (Triastuti et al., 2019).

Several studies have demonstrated that microRNAs, small non-coding RNAs that can modulate the expression of their target genes, have a translational potential in the treatment of cardiovascular diseases. Several miRNAs have been shown to target the Hippo pathway and have been evidenced to be capable of inducing heart regeneration and improving cardiac functions in an MI model (Borden et al., 2019; Eulalio et al., 2012; Gao et al., 2019; Huang et al., 2018; Tian et al., 2015). Moreover, in other fields such as infectious disease and oncology, miRNA-based treatments have entered the early phases of clinical trials with very promising results (Bonneau et al., 2019; Hanna et al., 2019). Overall, this evidence supports the strategy of developing

miRNA-based therapeutics in the treatment of cardiovascular diseases. Several limitations, however, have prevented the immediate clinical translation of miRNA-based therapeutics. An uncontrolled overexpression of pro-regenerative miRNAs such as the miR-302/367 cluster and miR-199a, in an MI model has been shown to cause serious adverse effects, including dilated cardiomyopathy, arrythmia, and heart failure. This highlights the need for more research in order to identify better targets and delivery systems. The key aim of this PhD project is to find a novel miRNA that can target the Hippo pathway and subsequently stimulate heart regeneration and functions post-MI. The results of this project led to the identification of a novel miRNA, miR-411, which can target the Hippo signalling pathway and enhance cardiac regeneration post-MI.

6.1 MiR-411 is a novel Hippo modulator that can stimulate cardiomyocyte proliferation and protect the heart post-MI

Based on the screening process involving bioinformatics studies, a YAP luciferase assay as well as subsequent examinations of candidate miRNA expression profiles, this project has identified miR-411 as a potential Hippo modulator and a pro-regenerative miRNA in the heart. A previous investigation has reported that miR-411 is dynamically expressed during embryonic heart growth, indicating the role of miR-411 in the development of the heart (Zhou et al., 2014). In concordance with this study, the results of this project (Chapter 3 Section 3.4.2) have revealed that miR-411 expression was higher in the neonatal heart compared to the adult heart, thus supporting the possible role of miR-411 in heart development. Until now, however, there has been no investigation that has elucidated the functional role of miR-411 in the heart. This study is the first to show that miR-411 can modulate cardiomyocyte proliferation in NRCMs and cardiomyocyte cell cycle re-entry in the adult heart.

Another significant finding of this study is that a single intramyocardial injection of miR-411 mimics was shown to be capable of inducing heart regeneration and conferring some benefits against the deterioration of cardiac functions post-MI. This finding supports previous evidence that shows that a single intramyocardial injection

of miRNA mimics is sufficient to drive short-term overexpression (up to 12 days post-injection) and the subsequent functional recovery post-MI (Lesizza et al., 2017). Nevertheless, the benefits elicited by this approach are often modest albeit significant. For example, although miR-411 overexpression in this study causes significant improvements in cardiac functions compared to the control, the overall cardiac functions in the miR-411 group are significantly lower than sham. Several studies which used the same approach to deliver miRNA mimics also reported similar trends. They found that the benefits of transient miRNA overexpression are less in magnitude compared to a more robust delivery vector such as AAV9 (Gao et al., 2019; Lesizza et al., 2017). However, prolonged overexpression of pro-regenerative miRNAs driven by AAV9 can induce massive cardiomyocyte dedifferentiation and eventually dilated cardiomyopathy (Gabisonia et al., 2019; Tian et al., 2015). In conclusion, direct intramyocardial injection may become the method of choice for miRNA delivery in the future, but more research is required to investigate the long-term consequences of pro-regenerative signal expression in the adult heart and refine the miRNA delivery system to get the maximum benefit with minimum adverse effects.

6.2 miR-411 can modulate the Hippo pathway via SERT-dependent mechanisms

Data from this study showed that miR-411 could target the Hippo pathway as indicated by a reduction in LATS1 phosphorylation and an increase in YAP activity. Further investigations, however, revealed that the expression of core Hippo kinases remained constant after miR-411 transfection. This finding then led to a quest to find the direct targets of miR-411 that mediated the elevation of YAP activity. Two genes, FOXO1 and SERT, were highlighted as possible miR-411 targets but based on the YAP luciferase assay and western blot, only SERT was found to be capable of modulating the Hippo pathway. Although Hippo modulation by miR-411 is dependent on SERT, it remains possible that FOXO1 contributes to the phenotypes elicited by miR-411. miRNAs are known to have the ability to target multiple genes and thus modulate multiple pathways that are often synergistic. FOXO1 is a known tumour suppressor and is crucial in embryonic heart development, cell cycle modulation, and

angiogenesis (Ronnebaum and Patterson, 2010). Mice overexpressing a cardiomyocyte-specific FOXO1 transgene die before birth due to abnormal expression of cyclin-dependent kinase inhibitors $p21^{cip1}$ and $p27^{Kip1}$. On the other hand, the overexpression of the dominant negative FOXO1 transgene increases cardiomyocyte proliferation (Evans-Anderson et al., 2008). These suggest that FOXO1 plays a significant role in cardiomyocyte proliferation and it is very plausible that FOXO1 may contribute to the benefits seen after miR-411 overexpression. In fact, given that miRNA can target multiple genes, it is very likely that there are other miR-411 target genes contributing to the beneficial effects conferred by miR-411 overexpression.

Another novel aspect of this study is the discovery and validation of SERT as one of the miR-411 direct targets in the heart. This study is also the first to show the link between serotonin signalling and the Hippo pathway. Increased concentration of extracellular serotonin, mediated by miR-411-dependent downregulation of SERT, can cause increased activation of serotonin receptors which subsequently decreases the phosphorylation of LATS1 and YAP via ROCK1 activation (Fig 5.11A). Serotonin signalling has been shown to play a central role in several psychiatric disorders such as anxiety and depression (Marazziti, 2017). These findings can therefore potentially implicate the Hippo pathway in psychiatric disorders (Stepan et al., 2018) and provide additional explanations regarding the effects of psychiatric disorders on the risks of cardiac diseases, which cannot be explained with the available knowledge on the heart-brain axis. For example, the link between depression and heart disease has long been characterised as a two-way relationship where one can affect the other (De Hert et al., 2018). Previous studies have attributed inflammation as a factor that links these two conditions, but the exact mechanisms are not yet understood (Khandaker et al., 2019). The novel link between serotonin signalling and the Hippo pathway proposed in this study can provide an alternative explanation for this phenomenon.

6.3 The role of serotonin signalling in the cardiovascular system

Serotonin (5-hydroxytryptamine, 5-HT) is a monoamine neurotransmitter which regulates many processes in the body (Cote et al., 2004). The roles of 5-HT are widely studied in the central nervous system where it plays significant roles in the regulation of mood, behaviour, memory, learning, sleep, and appetite. Despite its importance in neuronal functions, the amount of serotonin in the CNS is only a minor proportion of the total serotonin in the body (Peroutka, 1991). Over 95% of the total serotonin in the body is produced by enterochromaffin cells in the gastrointestinal tract where it regulates intestinal motility and mesenteric circulation (Choi and Maroteaux, 1996). The other significant reservoir of serotonin in the body is the cardiovascular system where it can be found circulating in the blood or stored in platelets. Serotonin appears to have diverse effects on the cardiovascular system, such as in the regulation of blood pressure, cardiovascular function, and blood coagulation. It also mediates several cellular functions, such as cardiomyocyte proliferation and death (Ramage and Villalon, 2008).

Several studies have confirmed that serotonin signalling also plays a crucial role during embryonic development. Serotonin is actively transported to the embryo via the placenta in the early days of embryonic development and is later produced in the enterochromaffin cells and craniofacial tissue of the embryo (Shearman et al., 1998; Yavarone et al., 1993). Although the evidence regarding the specific role of serotonin in the developing heart remains limited, serotonin is believed to be a crucial mitogenic factor. At a physiological concentration of 4 µM, serotonin stimulates an optimal proliferation of isolated foetal heart cells, whereas changing the concentration to either side reduces the proliferation (Sari and Zhou, 2003). Additionally, when serotonin or serotonin-selective reuptake inhibitors (SSRIs) are administered in embryo cultures, a dose-dependent reduction in the proliferation of myocardium, cardiac mesenchyme, and endothelium has been reported (Yavarone et al., 1993). These findings suggest that serotonin level is finely tuned during embryonic development to modulate cardiomyocyte proliferation.

The action of serotonin is mediated by its binding to serotonin receptors, which are widely distributed in the body. To date, there are at least 15 sub-types that belong to four classes: 5-$HT_{1/5}$, 5-HT_2, 5-HT_3, and 5-$HT_{4/6/7}$ (Hoyer et al., 1994). All of these receptors are members of the GPCR receptors family, except for the 5-HT_3 receptor which is a ligand gated ion channel. Several studies have demonstrated that the 5-HT_{2B} receptor is the one responsible for mediating serotonin effects on cardiomyocyte proliferation and embryonic heart growth (Choi et al., 1997; Lauder et al., 2000; Nebigil et al., 2000; Nebigil et al., 2001). In mice, 5-HT_{2B} receptor mRNAs reach peak expression at 8 – 9 days post-fertilisation and are mainly localised in neural crest cells, the heart myocardium, and somites (Choi et al., 1997). The significance of 5-HT_{2B} receptors in the developing heart was initially discovered from experiments with serotonin receptor antagonists (Choi et al., 1997; Lauder et al., 2000). Treatments of embryo cultures with high affinity $5HT_{2B}$ antagonist ritanserin result in severe cardiac defects due to decreased proliferation and increased cell death. These include the absence of the trabecular layer in the ventricular myocardium, abnormal sarcomeric arrangement, and growth retardation (Choi et al., 1997; Lauder et al., 2000). On the other hand, treatments with antagonists targeting other receptor sub-types (5-$HT_{2A/C}$ or 5-HT_{2A} alone) result in either significantly less severe phenotypes or no phenotypes at all (Lauder et al., 2000). These findings suggest that 5-HT_{2B} plays a more dominant role in the embryonic development of the heart than serotonin receptors.

Furthermore, more recent studies in mice have demonstrated that 5-HT_{2B} loss of function results in trabeculation defects in embryonic hearts, similar to the phenotypes caused by antagonist administration, and a 30% lethality in the middle of gestation (Nebigil et al., 2000; Nebigil et al., 2001). The surviving mice are born with cardiomyopathy and severe cardiac hypoplasia, characterised by significantly fewer cardiomyocytes and smaller cell size. These mice subsequently exhibit signs of HF and die prematurely. Contrarily, cardiac-specific overexpression of 5-HT_{2B} receptors in mice results in cardiac hypertrophy without signs of pressure overload, diminished cardiac function, or increased fibrosis. Further investigations revealed

that these phenotypes are caused by increased cardiomyocyte proliferation and size and reduced apoptosis (Nebigil et al., 2003b). Serotonin signalling via 5-HT_{2B} has previously been shown to protect cardiomyocytes against apoptosis caused by serum deprivation (Nebigil et al., 2003a). These findings further confirm that serotonin signalling is crucial in regulating cardiomyocyte proliferation and survival.

As has been discussed in Chapter 5, the remaining component of serotonin signalling, SERT, is crucial in the modulation of serotonin receptor activation by regulating the extracellular serotonin concentration (Hahn and Blakely, 2007; Ramamoorthy et al., 2011). The roles of SERT are well-known in the central nervous system, including in the regulation of physiological mental functions such as mood, memory, and sleep and pathological conditions such as depressive disorders. SERT is also the target of serotonin-selective reuptake inhibitors (SSRIs), the drugs commonly used to treat depression (Hahn and Blakely, 2007; Ramamoorthy et al., 2011). In the cardiovascular system, several studies indicate that SERT plays an important role in heart development (Chapter 5). In addition, SERT has been implicated in several heart diseases in humans, including hypertension and MI (Eddahibi et al., 2003; Fumeron et al., 2002). The transcription of SERT in humans is modulated by repeat length polymorphisms in the promoter region of the SERT gene. The long variant (L) is associated with approximately a three-fold increase in SERT transcriptional activity compared to the short variant (S) (Melke, 2003). Fumeron *et al*. reported that patients with the LL genotype are found to have a significantly higher risk for MI (Fumeron et al., 2002). On the contrary, other studies found that depressed patients who took SSRIs, and thus had a lower SERT activity, had a reduced risk of MI (Coupland et al., 2016; Sauer et al., 2003). Furthermore, the administration of SSRIs in MI patients who suffer from depression is associated with a reduce risk of MI recurrence and other cardiovascular adverse events such as HF and death (O'connor et al., 2010). These findings suggest that lower SERT activity is associated with a lower risk of MI and overall benefits for the heart.

Previous studies have proposed several mechanisms to explain the cardiovascular benefits of SSRI administration. One of the possible explanations is

the antiplatelet effect of serotonin (Halperin and Reber, 2007; Serebruany et al., 2005). After vascular injury, serotonin is released from platelets and triggers vasoconstriction and platelet aggregation. SSRI treatments reduce the level of intraplatelet serotonin and subsequently impair the formation of platelet thrombus. This, however, cannot explain why post-MI patients taking SSRI sertraline have a reduced risk of cardiovascular adverse events, such as death and heart failure (O'connor et al., 2010). The novel association between serotonin signalling and the Hippo pathway reported in this study can potentially explain this phenomenon. A SERT-mediated increase in YAP activity can act directly in the cardiac parenchyma and confer protective effects against adverse cardiac remodelling post-MI.

In the cardiovascular system, the roles of serotonin as a vasoactive, vasopressor, and prothrombotic substance are relatively well established. However, its roles in cellular functions, such as cardiomyocyte proliferation and survival, have not been completely elucidated. This is further confounded by often inconsistent or contradicting findings from different studies. One of the challenges in investigating serotonin signalling is the many receptors mediating the effects of serotonin in tissue. Moreover, a coupling of a receptor does not only trigger one linear pathway, but a complex network of signal transduction with alternative bifurcations and feedback mechanisms (Masson et al., 2012). Future investigations should consider the effects of each serotonin receptor sub-type on the modulation of the Hippo pathway.

Although this project has proposed that miR-411 modulates the Hippo pathway via activation of 5HT receptors followed by induction of ROCK1 (Section 5.5.3), the specific type of receptors responsible for mediating ROCK1 activation remains elusive. Preliminary work in Oceandy's Lab has revealed that the overexpression of 5-HT_{2B} receptors in NRCMs significantly increases YAP activity and cardiomyocyte proliferation. This, in combination with the available evidence on the importance of the 5-HT_{2B} receptor in the heart (discussed above), leads to a hypothesis that this receptor is the most likely candidate for mediating the interaction between the Hippo pathway and serotonin signalling (Fig 6.2). More studies, however, are required in order to validate this model.

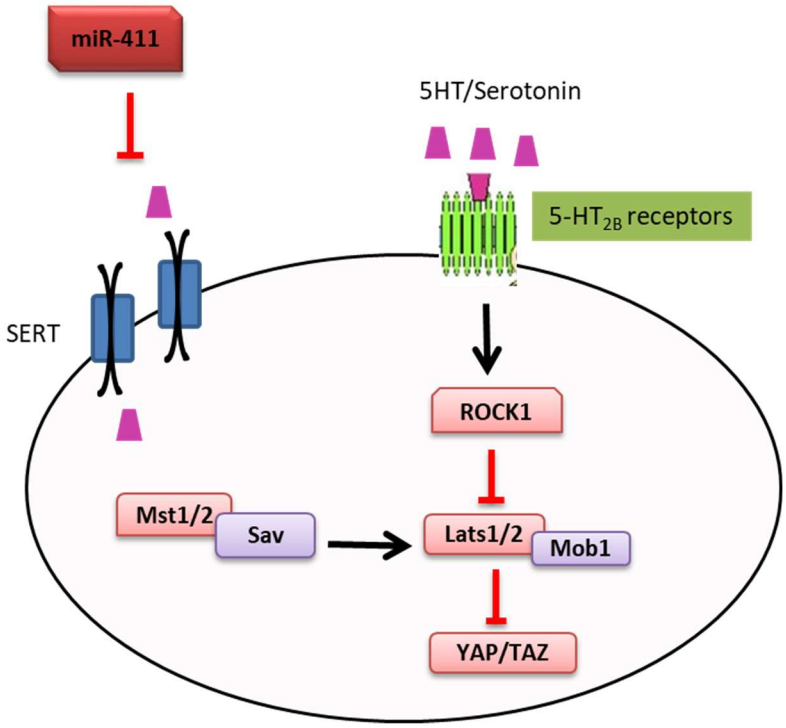

Figure 6.2 The interaction between the Hippo pathway and serotonin signalling.
MiR-411 downregulates SERT expression and subsequently increases the extracellular concentration of serotonin. As a result, the 5-HT_{2B} receptors are activated and mediate the reduction in LATS1 and YAP phosphorylation via ROCK1.

6.4 Potential impact and possible translational relevance of this project

In summary, this project has found two novel modulators of the Hippo pathway: miR-411 and the serotonin signalling and thus contributed to the knowledge of the Hippo pathway regulation. The Hippo pathway is an evolutionarily conserved regulator of organ size and growth with critical roles in cell proliferation, cell fate, and survival (Halder and Johnson, 2011). Modulation of the Hippo pathway has been shown to induce cardiomyocyte proliferation in postnatal hearts and promote regeneration after MI in animal models (Leach et al., 2017; Porrello et al., 2013; Tian et al., 2015; Xin et al., 2013). These suggest that this pathway has a great potential for therapeutic manipulation in CVDs, especially MI. However, the promise of the Hippo pathway is hampered, at least partially, by difficulty in targeting its core components and lack of knowledge of its upstream regulators. This project has shown

that miR-411 and the serotonin signalling are capable to modulate the Hippo-YAP pathway and also provided a proof of concept that overexpression of miR-411 can potentially be used as a therapeutic tool to enhance cardiac regeneration post-MI.

Recently, the development of miRNA-based therapeutics has gained a lot of interests due to promising preclinical studies. Although none have been approved for clinical use yet, several miRNA-based therapeutics has progressed into early stages of clinical trials. Some of these miRNAs such as antimiR-122 for hepatitis and miR-34 mimics for hepatocellular carcinoma have been discussed in Section 1.3.4. In the cardiovascular field antimiR-92a and antimiR-132 are currently in phase I clinical trial (Huang et al., 2020). AntimiR-92a, which has been shown to have proangiogenic properties (Hinkel et al., 2013), is being tested for its ability to accelerate wound healing (Gallant-Behm et al., 2018) whilst antimir-132 is capable to reduce pathological cardiac fibrosis in preclinical studies (Foinquinos et al., 2020) and currently being tested in patients with stable HF (Huang et al., 2020). Overall, these suggest that miRNA-based therapeutics is a promising and feasible approach to be translated into clinical practice.

In addition to miR-411, the results of this project also provides a preliminary evidence of the connection between the serotonin signalling and the Hippo pathway in the heart. The serotonin signalling has been extensively studied in the nervous and gastrointestinal system and to a lesser extent in the cardiovascular system as well (Choi and Maroteaux, 1996). It is relatively easier to target because its inhibitors and agonists are already available on the market with many of them already being widely used in the clinics (Bleakley, 2013). This opens the possibility of repurposing some of these drugs to treat cardiovascular disorders. More research, however, needs to be done to elucidate the safety and efficacy of these drugs in the cardiovascular system.

Despite encouraging results of miR-411 and the serotonin signalling effects on MI model, there are several challenges that need to be addressed. This will be discussed in further detail below.

6.5 Limitations and future work

This study has shown that miR-411 can promote regeneration post-MI and thus may have the potential to be translated clinically. However, there are several questions and challenges that need to be addressed before reaching clinical stages. The effects of transient miR-411 overexpression, described in Chapter 4 Section 4.4.4, are relatively modest and signs of true cardiomyocyte proliferation are not found in cardiac tissue sections 4 weeks post-MI. These are likely caused by the delivery approach used in this project. The delivery of miRNA mimics using non-viral vectors is reported to be short-lived and less effective compared to viral vectors such as AAV9. In the future, the delivery of miRNA mimics *in vivo* needs to be enhanced, possibly by using AAV9 or repeated injections. Additionally, the mouse model used in this study successfully provided a proof of concept that miR-411 has the practical potential to be developed as a novel therapeutic tool for MI. For translational research, however, miR-411 needs to be tested in large animal models that more closely resemble the clinical and pathological characteristics of human diseases.

Another barrier for the application of miRNA-based therapeutics is the possibility of off-target effects due to the ability of miRNAs to target multiple genes. There are several other methods that we can explore to address this problem. Several studies have used AAV9 with tissue-specific promoters to enhance the specificity of miRNA delivery. However, AAV9 tends to cause prolonged miRNA overexpression, which is proven to be deleterious in post-MI hearts (Gabisonia et al., 2019; Tian et al., 2015). New generations of nanoparticle-based delivery systems have been developed to overcome this problem. For example, Yang *et al.* developed an *in vivo* delivery system using nanoparticles resuspended in a shear-thinning injectable hydrogel (Yang et al., 2019). They showed that they can achieve more localised and efficient delivery of miRNA mimics.

After intramyocardial injection of miR-411 mimics, increased level of miR-411 was found in the lung, kidney, and liver. In the future, whether this will cause any observable effects needs to be examined to identify the potential adverse effects of

miR-411 mimics injection. Investigating the whole targets of miR-411 with high-throughput experiments, such as chromatin immunoprecipitation (ChIP) sequencing, is also crucial for better predicting the potential off-target effects in addition to obtaining a more complete picture of the genes targeted by miR-411.

Last but not least, this project shows that serotonin signalling modulation may confer certain cardiovascular benefits and thus open the possibility of repurposing several drugs such as SSRIs or serotonin agonists to treat cardiovascular diseases. However several challenges need to be addressed before they can be used for cardiovascular indications. First, further experiments are need to elucidate the specific type of serotonin receptors responsible for mediating the activation of ROCK1-LATS1-YAP axis (discussed in Section 6.3). Secondly, as there are various SSRIs and serotonin agonists in the market, a proper screening and efficacy studies should be done to find the most effective drugs for CVDs. Finally, given that many of these drugs are widely used to treat neurological and psychiatric disorders, concerns about side effects may arise. Further investigations are needed to determine the safety of these drugs when used to treat non psychiatric disorders.

6.6 Overall conclusion

The results presented in this PhD study have identified miR-411 as a novel modulator of the Hippo pathway and cardiomyocyte proliferation. In addition, transient administration of miR-411 in an MI model is shown to enhance cardiomyocyte proliferation, reduce apoptosis, and improve the overall cardiac functions at 4 weeks post-MI. The results also reveal the SERT gene as a novel miR-411 target and elucidate the crossover between serotonin signalling and the Hippo pathway via ROCK1-LATS1-YAP axis. In conclusion, the modulation of the Hippo pathway using miR-411 could become a new therapeutic modality to treat cardiovascular diseases.

References

Adamec, R., Burton, P., Blundell, J., Murphy, D. L. & Holmes, A. (2006). 'Vulnerability to mild predator stress in serotonin transporter knockout mice', *Behav Brain Res,* 170(1), pp. 126-40.

Adamowicz, M., Morgan, C. C., Haubner, B. J., Noseda, M., Collins, M. J., Paiva, M. A., Srivastava, P. K., Gellert, P., Razzaghi, B., O'Gara, P., Raina, P., Game, L., Bottolo, L., Schneider, M. D., Harding, S. E., Penninger, J. & Aitman, T. J. (2018). 'Functionally Conserved Noncoding Regulators of Cardiomyocyte Proliferation and Regeneration in Mouse and Human', *Circulation: Genomic and Precision Medicine,* 11(2), p. e001805.

Agarwal, V., Bell, G. W., Nam, J. W. & Bartel, D. P. (2015). 'Predicting effective microRNA target sites in mammalian mRNAs', *Elife,* 4.

Ahuja, P., Sdek, P. & MacLellan, W. R. (2007). 'Cardiac myocyte cell cycle control in development, disease, and regeneration', *Physiological reviews,* 87(2), pp. 521-544.

Ai, P., Shen, B., Pan, H., Chen, K., Zheng, J. & Liu, F. (2018). 'MiR-411 suppressed vein wall fibrosis by downregulating MMP-2 via targeting HIF-1alpha', *J Thromb Thrombolysis,* 45(2), pp. 264-273.

Alarcon, V. B. (2010). 'Cell polarity regulator PARD6B is essential for trophectoderm formation in the preimplantation mouse embryo', *Biol Reprod,* 83(3), pp. 347-58.

Ali, S. R., Hippenmeyer, S., Saadat, L. V., Luo, L., Weissman, I. L. & Ardehali, R. (2014). 'Existing cardiomyocytes generate cardiomyocytes at a low rate after birth in mice', *Proceedings of the National Academy of Sciences,* 111(24), pp. 8850-8855.

Amano, M., Nakayama, M. & Kaibuchi, K. (2010). 'Rho-kinase/ROCK: A key regulator of the cytoskeleton and cell polarity', *Cytoskeleton (Hoboken),* 67(9), pp. 545-54.

Anderson, J. L. & Morrow, D. A. (2017). 'Acute Myocardial Infarction', *The New England journal of medicine,* 376(21), pp. 2053-2064.

Ang, K. L., Shenje, L. T., Reuter, S., Soonpaa, M. H., Rubart, M., Field, L. J. & Galiñanes, M. (2010). 'Limitations of conventional approaches to identify myocyte nuclei in histologic sections of the heart', *Am J Physiol Cell Physiol,* 298(6), pp. C1603-9.

Aylon, Y., Ofir-Rosenfeld, Y., Yabuta, N., Lapi, E., Nojima, H., Lu, X. & Oren, M. (2010). 'The Lats2 tumor suppressor augments p53-mediated apoptosis by promoting the nuclear proapoptotic function of ASPP1', *Genes & development,* 24(21), pp. 2420-2429.

Bai, T. L., Liu, Y. B. & Li, B. H. (2019). 'MiR-411 inhibits gastric cancer proliferation and migration through targeting SETD6', *Eur Rev Med Pharmacol Sci,* 23(8), pp. 3344-3350.

Balsam, L. B., Wagers, A. J., Christensen, J. L., Kofidis, T., Weissman, I. L. & Robbins, R. C. (2004). 'Haematopoietic stem cells adopt mature haematopoietic fates in ischaemic myocardium', *Nature,* 428(6983), pp. 668-673.

Bang, C., Batkai, S., Dangwal, S., Gupta, S. K., Foinquinos, A., Holzmann, A., Just, A., Remke, J., Zimmer, K., Zeug, A., Ponimaskin, E., Schmiedl, A., Yin, X., Mayr, M., Halder, R., Fischer, A., Engelhardt, S., Wei, Y., Schober, A., Fiedler, J. & Thum, T. (2014). 'Cardiac fibroblast-derived microRNA passenger strand-enriched exosomes mediate cardiomyocyte hypertrophy', *J Clin Invest,* 124(5), pp. 2136-46.

Bardy, G. H., Lee, K. L., Mark, D. B., Poole, J. E., Packer, D. L., Boineau, R., Domanski, M., Troutman, C., Anderson, J., Johnson, G., McNulty, S. E., Clapp-Channing, N., Davidson-Ray, L. D., Fraulo, E. S., Fishbein, D. P., Luceri, R. M., Ip, J. H. & Sudden Cardiac Death in Heart Failure Trial, I. (2005). 'Amiodarone or an implantable cardioverter-defibrillator for congestive heart failure', *The New England journal of medicine,* 352(3), pp. 225-237.

Bartel, D. P. (2004). 'MicroRNAs: genomics, biogenesis, mechanism, and function', *Cell,* 116(2), pp. 281-97.

Bartel, D. P. (2009). 'MicroRNAs: target recognition and regulatory functions', *Cell,* 136(2), pp. 215-33.

Bassat, E., Mutlak, Y. E., Genzelinakh, A., Shadrin, I. Y., Baruch Umansky, K., Yifa, O., Kain, D., Rajchman, D., Leach, J., Riabov Bassat, D., Udi, Y., Sarig, R., Sagi, I., Martin, J. F., Bursac, N., Cohen, S. & Tzahor, E. (2017). 'The extracellular matrix protein agrin promotes heart regeneration in mice', *Nature,* 547(7662), pp. 179-184.

Belandia, B. & Parker, M. G. (2000). 'Functional interaction between the p160 coactivator proteins and the transcriptional enhancer factor family of transcription factors', *J Biol Chem,* 275(40), pp. 30801-5.

Bergmann, O., Bhardwaj, R. D., Bernard, S., Zdunek, S., Barnabe-Heider, F., Walsh, S., Zupicich, J., Alkass, K., Buchholz, B. A., Druid, H., Jovinge, S. & Frisen, J. (2009). 'Evidence for cardiomyocyte renewal in humans', *Science,* 324(5923), pp. 98-102.

Bergmann, O., Zdunek, S., Felker, A., Salehpour, M., Alkass, K., Bernard, S., Sjostrom, S. L., Szewczykowska, M., Jackowska, T., Dos Remedios, C., Malm, T., Andra, M., Jashari, R., Nyengaard, J. R., Possnert, G., Jovinge, S., Druid, H. & Frisen, J. (2015). 'Dynamics of Cell Generation and Turnover in the Human Heart', *Cell,* 161(7), pp. 1566-75.

Bernstein, E., Kim, S. Y., Carmell, M. A., Murchison, E. P., Alcorn, H., Li, M. Z., Mills, A. A., Elledge, S. J., Anderson, K. V. & Hannon, G. J. (2003). 'Dicer is essential for mouse development', *Nat Genet,* 35(3), pp. 215-217.

Bersell, K., Arab, S., Haring, B. & Kühn, B. (2009). 'Neuregulin1/ErbB4 signaling induces cardiomyocyte proliferation and repair of heart injury', *Cell,* 138(2), pp. 257-270.

Bettencourt-Dias, M., Mittnacht, S. & Brockes, J. P. (2003). 'Heterogeneous proliferative potential in regenerative adult newt cardiomyocytes', *J Cell Sci,* 116(Pt 19), pp. 4001-9.

Bhatt, A. S., Ambrosy, A. P. & Velazquez, E. J. (2017). 'Adverse Remodeling and Reverse Remodeling After Myocardial Infarction', *Current cardiology reports,* 19(8), pp. 71-71.

Bish, L. T., Morine, K., Sleeper, M. M., Sanmiguel, J., Wu, D., Gao, G., Wilson, J. M. & Sweeney, H. L. (2008). 'Adeno-associated virus (AAV) serotype 9 provides global cardiac gene transfer superior to AAV1, AAV6, AAV7, and AAV8 in the mouse and rat', *Hum Gene Ther,* 19(12), pp. 1359-68.

Bleakley, S. (2013). 'Review of the choice and use of antidepressant drugs', *Progress in Neurology and Psychiatry,* 17(6), pp. 18-26.

Böhm, M., Ettelbrück, S., Flesch, M., van Gilst, W. H., Knorr, A., Maack, C., Pinto, Y. M., Paul, M., Teisman, A. C. & Zolk, O. (1998). 'Beta-adrenergic signal transduction following carvedilol treatment in hypertensive cardiac hypertrophy', *Cardiovascular research,* 40(1), pp. 146-155.

Bonneau, E., Neveu, B., Kostantin, E., Tsongalis, G. J. & De Guire, V. (2019). 'How close are miRNAs from clinical practice? A perspective on the diagnostic and therapeutic market', *EJIFCC,* 30(2), pp. 114-127.

Borchert, G. M., Lanier, W. & Davidson, B. L. (2006). 'RNA polymerase III transcribes human microRNAs', *Nat Struct Mol Biol,* 13(12), pp. 1097-1101.

Borden, A., Kurian, J., Nickoloff, E., Yang, Y., Troupes, C. D., Ibetti, J., Lucchese, A. M., Gao, E., Mohsin, S., Koch, W. J., Houser, S. R., Kishore, R. & Khan, M. (2019). 'Transient Introduction of miR-294 in the Heart Promotes Cardiomyocyte Cell Cycle Reentry After Injury', *Circ Res,* 125(1), pp. 14-25.

Brennecke, J., Stark, A., Russell, R. B. & Cohen, S. M. (2005). 'Principles of MicroRNA–Target Recognition', *PLoS Biol,* 3(3).

Briffa, T., Hickling, S., Knuiman, M., Hobbs, M., Hung, J., Sanfilippo, F. M., Jamrozik, K. & Thompson, P. L. (2009). 'Long term survival after evidence based treatment of acute myocardial infarction and revascularisation: follow-up of population based Perth MONICA cohort, 1984-2005', *BMJ (Clinical research ed.),* 338, pp. b36-b36.

Broderick, J. & Zamore, P. (2011). 'microRNA Therapeutics', *Gene Ther,* 18(12), pp. 1104-10.

Broer, S. & Gether, U. (2012). 'The solute carrier 6 family of transporters', *Br J Pharmacol,* 167(2), pp. 256-78.

Burgess, R. W., Skarnes, W. C. & Sanes, J. R. (2000). 'Agrin Isoforms with Distinct Amino Termini: Differential Expression, Localization, and Function', *Journal of Cell Biology,* 151(1), pp. 41-52.

Butler, M. T. & Wallingford, J. B. (2017). 'Planar cell polarity in development and disease', *Nature Reviews Molecular Cell Biology,* 18(6), pp. 375-388.

Bywater, M. J., Burkhart, D. L., Straube, J., Sabò, A., Pendino, V., Hudson, J. E., Quaife-Ryan, G. A., Porrello, E. R., Rae, J., Parton, R. G., Kress, T. R., Amati, B., Littlewood, T. D., Evan, G. I. & Wilson, C. H. (2020). 'Reactivation of Myc transcription in the mouse heart unlocks its proliferative capacity', *Nature Communications,* 11(1), p. 1827.

Cahill, T. J. & Kharbanda, R. K. (2017). 'Heart failure after myocardial infarction in the era of primary percutaneous coronary intervention: Mechanisms, incidence and identification of patients at risk', *World journal of cardiology,* 9(5), pp. 407-415.

Cai, C.-L., Zhou, W., Yang, L., Bu, L., Qyang, Y., Zhang, X., Li, X., Rosenfeld, M. G., Chen, J. & Evans, S. (2005). 'T-box genes coordinate regional rates of proliferation and regional specification during cardiogenesis', *Development (Cambridge, England),* 132(10), pp. 2475-2487.

Camargo, F. D., Gokhale, S., Johnnidis, J. B., Fu, D., Bell, G. W., Jaenisch, R. & Brummelkamp, T. R. (2007). 'YAP1 increases organ size and expands undifferentiated progenitor cells', *Curr Biol,* 17(23), pp. 2054-60.

Camelliti, P., Borg, T. K. & Kohl, P. (2005). 'Structural and functional characterisation of cardiac fibroblasts', *Cardiovasc Res,* 65(1), pp. 40-51.

Cao, J. & Poss, K. D. (2018). 'The epicardium as a hub for heart regeneration', *Nature Reviews Cardiology,* 15(10), pp. 631-647.

Care, A., Catalucci, D., Felicetti, F., Bonci, D., Addario, A., Gallo, P., Bang, M. L., Segnalini, P., Gu, Y., Dalton, N. D., Elia, L., Latronico, M. V., Hoydal, M., Autore, C., Russo, M. A., Dorn, G. W., 2nd, Ellingsen, O., Ruiz-Lozano, P., Peterson, K. L., Croce, C. M., Peschle, C. & Condorelli, G. (2007). 'MicroRNA-133 controls cardiac hypertrophy', *Nat Med,* 13(5), pp. 613-8.

Carroll, J. C., Boyce-Rustay, J. M., Millstein, R., Yang, R., Wiedholz, L. M., Murphy, D. L. & Holmes, A. (2007). 'Effects of mild early life stress on abnormal emotion-related behaviors in 5-HTT knockout mice', *Behav Genet,* 37(1), pp. 214-22.

Castaldi, A., Zaglia, T., Di Mauro, V., Carullo, P., Viggiani, G., Borile, G., Di Stefano, B., Schiattarella, G. G., Gualazzi, M. G., Elia, L., Stirparo, G. G., Colorito, M. L., Pironti, G., Kunderfranco, P., Esposito, G., Bang, M. L., Mongillo, M., Condorelli, G. & Catalucci, D. (2014). 'MicroRNA-133 modulates the beta1-adrenergic receptor transduction cascade', *Circ Res,* 115(2), pp. 273-83.

Chakraborty, S., Lakshmanan, M., Swa, H. L. F., Chen, J., Zhang, X., Ong, Y. S., Loo, L. S., Akıncılar, S. C., Gunaratne, J., Tergaonkar, V., Hui, K. M. & Hong, W. (2015). 'An oncogenic role of Agrin in regulating focal adhesion integrity in hepatocellular carcinoma', *Nature Communications,* 6(1), p. 6184.

Chakraborty, S., Njah, K., Pobbati, A. V., Lim, Y. B., Raju, A., Lakshmanan, M., Tergaonkar, V., Lim, C. T. & Hong, W. (2017). 'Agrin as a Mechanotransduction Signal Regulating YAP through the Hippo Pathway', *Cell Reports,* 18(10), pp. 2464-2479.

Chakraborty, S. & Yutzey, K. E. (2012). 'Tbx20 regulation of cardiac cell proliferation and lineage specialization during embryonic and fetal development in vivo', *Developmental biology,* 363(1), pp. 234-246.

Chan, S. W., Lim, C. J., Chong, Y. F., Pobbati, A. V., Huang, C. & Hong, W. (2011). 'Hippo Pathway-independent Restriction of TAZ and YAP by Angiomotin', *Journal of Biological Chemistry,* 286(9), pp. 7018-7026.

Chaudhry, H. W., Dashoush, N. H., Tang, H., Zhang, L., Wang, X., Wu, E. X. & Wolgemuth, D. J. (2004). 'Cyclin A2 mediates cardiomyocyte mitosis in the postmitotic myocardium', *The Journal of biological chemistry,* 279(34), pp. 35858-35866.

Chen, Y. & Wang, X. (2019). 'miRDB: an online database for prediction of functional microRNA targets', *Nucleic Acids Research,* 48(D1), pp. D127-D131.

Chendrimada, T. P., Gregory, R. I., Kumaraswamy, E., Norman, J., Cooch, N., Nishikura, K. & Shiekhattar, R. (2005). 'TRBP recruits the Dicer complex to Ago2 for microRNA processing and gene silencing', *Nature,* 436(7051), pp. 740-744.

Cheng, R. K., Asai, T., Tang, H., Dashoush, N. H., Kara, R. J., Costa, K. D., Naka, Y., Wu, E. X., Wolgemuth, D. J. & Chaudhry, H. W. (2007). 'Cyclin A2 induces cardiac regeneration after myocardial infarction and prevents heart failure', *Circulation research,* 100(12), pp. 1741-1748.

Cheng, W. L., Kao, Y. H., Chao, T. F., Lin, Y. K., Chen, S. A. & Chen, Y. J. (2019). 'MicroRNA-133 suppresses ZFHX3-dependent atrial remodelling and arrhythmia', *Acta Physiol (Oxf),* 227(3), p. e13322.

Chi, S. W., Zang, J. B., Mele, A. & Darnell, R. B. (2009). 'Argonaute HITS-CLIP decodes microRNA-mRNA interaction maps', *Nature,* 460(7254), pp. 479-86.

Chiavacci, E., Dolfi, L., Verduci, L., Meghini, F., Gestri, G., Evangelista, A. M., Wilson, S. W., Cremisi, F. & Pitto, L. (2012). 'MicroRNA 218 mediates the effects of Tbx5a over-expression on zebrafish heart development', *PLoS One,* 7(11), p. e50536.

Choi, D. S. & Maroteaux, L. (1996). 'Immunohistochemical localisation of the serotonin 5-HT2B receptor in mouse gut, cardiovascular system, and brain', *FEBS Lett,* 391(1-2), pp. 45-51.

Choi, D. S., Ward, S. J., Messaddeq, N., Launay, J. M. & Maroteaux, L. (1997). '5-HT2B receptor-mediated serotonin morphogenetic functions in mouse cranial neural crest and myocardiac cells', *Development,* 124(9), pp. 1745-55.

Chugh, P. & Dittmer, D. P. (2012). 'Potential pitfalls in microRNA profiling', *Wiley Interdiscip Rev RNA,* 3(5), pp. 601-16.

Chugh, P., Tamburro, K. & Dittmer, D. P. (2010). 'Profiling of pre-micro RNAs and microRNAs using quantitative real-time PCR (qPCR) arrays', *J Vis Exp,* (46).

Citri, A. & Yarden, Y. (2006). 'EGF-ERBB signalling: towards the systems level', *Nature reviews. Molecular cell biology,* 7(7), pp. 505-516.

Clark, K., Langeslag, M., Figdor, C. G. & van Leeuwen, F. N. (2007). 'Myosin II and mechanotransduction: a balancing act', *Trends in cell biology,* 17(4), pp. 178-186.

Cockburn, K. & Rossant, J. (2010). 'Making the blastocyst: lessons from the mouse', *J Clin Invest,* 120(4), pp. 995-1003.

Cordenonsi, M., Zanconato, F., Azzolin, L., Forcato, M., Rosato, A., Frasson, C., Inui, M., Montagner, M., Parenti, Anna R., Poletti, A., Daidone, Maria G., Dupont, S., Basso, G., Bicciato, S. & Piccolo, S. (2011). 'The Hippo Transducer TAZ Confers Cancer Stem Cell-Related Traits on Breast Cancer Cells', *Cell,* 147(4), pp. 759-772.

Cote, F., Fligny, C., Fromes, Y., Mallet, J. & Vodjdani, G. (2004). 'Recent advances in understanding serotonin regulation of cardiovascular function', *Trends Mol Med,* 10(5), pp. 232-8.

Coupland, C., Hill, T., Morriss, R., Moore, M., Arthur, A. & Hippisley-Cox, J. (2016). 'Antidepressant use and risk of cardiovascular outcomes in people aged 20 to 64: cohort study using primary care database', *Bmj,* 352, p. i1350.

D'Uva, G., Aharonov, A., Lauriola, M., Kain, D., Yahalom-Ronen, Y., Carvalho, S., Weisinger, K., Bassat, E., Rajchman, D., Yifa, O., Lysenko, M., Konfino, T., Hegesh, J., Brenner, O., Neeman, M., Yarden, Y., Leor, J., Sarig, R., Harvey, R. P. & Tzahor, E. (2015). 'ERBB2 triggers mammalian heart regeneration by promoting cardiomyocyte dedifferentiation and proliferation', *Nature Cell Biology,* 17(5), pp. 627-638.

Dangwal, S. & Thum, T. (2014). 'microRNA therapeutics in cardiovascular disease models', *Annu Rev Pharmacol Toxicol,* 54, pp. 185-203.

De Hert, M., Detraux, J. & Vancampfort, D. (2018). 'The intriguing relationship between coronary heart disease and mental disorders', *Dialogues Clin Neurosci,* 20(1), pp. 31-40.

De Ponti, F. (2004). 'Pharmacology of serotonin: what a clinician should know', *Gut,* 53(10), pp. 1520-35.

Del Re, D. P., Matsuda, T., Zhai, P., Gao, S., Clark, G. J., Van Der Weyden, L. & Sadoshima, J. (2010). 'Proapoptotic Rassf1A/Mst1 signaling in cardiac fibroblasts is protective against pressure overload in mice', *The Journal of clinical investigation,* 120(10), pp. 3555-3567.

Del Re, D. P., Yang, Y., Nakano, N., Cho, J., Zhai, P., Yamamoto, T., Zhang, N., Yabuta, N., Nojima, H., Pan, D. & Sadoshima, J. (2013). 'Yes-associated protein isoform 1 (Yap1) promotes cardiomyocyte survival and growth to protect against myocardial ischemic injury', *J Biol Chem,* 288(6), pp. 3977-88.

Deng, S., Zhao, Q., Zhen, L., Zhang, C., Liu, C., Wang, G., Zhang, L., Bao, L., Lu, Y., Meng, L., Lu, J., Yu, P., Lin, X., Zhang, Y., Chen, Y. H., Fan, H., Cho, W. C., Liu, Z. & Yu, Z. (2017). 'Neonatal Heart-Enriched miR-708 Promotes Proliferation and Stress Resistance of Cardiomyocytes in Rodents', *Theranostics,* 7(7), pp. 1953-1965.

DeRan, M., Yang, J., Shen, C.-H., Peters, E. C., Fitamant, J., Chan, P., Hsieh, M., Zhu, S., Asara, J. M., Zheng, B., Bardeesy, N., Liu, J. & Wu, X. (2014). 'Energy stress regulates hippo-YAP signaling involving AMPK-mediated regulation of angiomotin-like 1 protein', *Cell reports,* 9(2), pp. 495-503.

Diez-Cunado, M., Wei, K., Bushway, P. J., Maurya, M. R., Perera, R., Subramaniam, S., Ruiz-Lozano, P. & Mercola, M. (2018). 'miRNAs that Induce Human Cardiomyocyte Proliferation Converge on the Hippo Pathway', *Cell Rep,* 23(7), pp. 2168-2174.

Diwan, A. & Dorn, G. W., 2nd (2007). 'Decompensation of cardiac hypertrophy: cellular mechanisms and novel therapeutic targets', *Physiology (Bethesda, Md.),* 22, pp. 56-64.

Dobaczewski, M., Bujak, M., Li, N., Gonzalez-Quesada, C., Mendoza, L. H., Wang, X.-F. & Frangogiannis, N. G. (2010). 'Smad3 signaling critically regulates fibroblast phenotype and function in healing myocardial infarction', *Circulation research,* 107(3), pp. 418-428.

Dodson, B. P. & Levine, A. D. (2015). 'Challenges in the translation and commercialization of cell therapies', *BMC biotechnology,* 15, pp. 70-70.

Doggett, K., Grusche, F. A., Richardson, H. E. & Brumby, A. M. (2011). 'Loss of the Drosophila cell polarity regulator Scribbled promotes epithelial tissue overgrowth and cooperation with oncogenic Ras-Raf through impaired Hippo pathway signaling', *BMC Developmental Biology,* 11(1), pp. 1-20.

Dong, J., Feldmann, G., Huang, J., Wu, S., Zhang, N., Comerford, S. A., Gayyed, M. F., Anders, R. A., Maitra, A. & Pan, D. (2007). 'Elucidation of a universal size-control mechanism in Drosophila and mammals', *Cell,* 130(6), pp. 1120-33.

Dorn, G. W., 2nd & Brown, J. H. (1999). 'Gq signaling in cardiac adaptation and maladaptation', *Trends in cardiovascular medicine,* 9(1-2), pp. 26-34.

Dorn II, G. W. (2016). 'Parkin-dependent mitophagy in the heart', *Journal of molecular and cellular cardiology,* 95, pp. 42-49.

Ebelt, H., Zhang, Y., Kampke, A., Xu, J., Schlitt, A., Buerke, M., Müller-Werdan, U., Werdan, K. & Braun, T. (2008). 'E2F2 expression induces proliferation of terminally differentiated cardiomyocytes in vivo', *Cardiovascular Research,* 80(2), pp. 219-226.

Eddahibi, S., Chaouat, A., Morrell, N., Fadel, E., Fuhrman, C., Bugnet, A. S., Dartevelle, P., Housset, B., Hamon, M., Weitzenblum, E. & Adnot, S. (2003). 'Polymorphism of the serotonin transporter gene and pulmonary hypertension in chronic obstructive pulmonary disease', *Circulation,* 108(15), pp. 1839-44.

Eddahibi, S., Hanoun, N., Lanfumey, L., Lesch, K. P., Raffestin, B., Hamon, M. & Adnot, S. (2000). 'Attenuated hypoxic pulmonary hypertension in mice lacking the 5-hydroxytryptamine transporter gene', *J Clin Invest,* 105(11), pp. 1555-62.

Eisenberg, L. M. & Eisenberg, C. A. (2006). 'Wnt signal transduction and the formation of the myocardium', *Developmental Biology,* 293(2), pp. 305-315.

Ellen Kreipke, R., Wang, Y., Miklas, J. W., Mathieu, J. & Ruohola-Baker, H. (2016). 'Metabolic remodeling in early development and cardiomyocyte maturation', *Seminars in cell & developmental biology,* 52, pp. 84-92.

Ellison, G. M., Vicinanza, C., Smith, A. J., Aquila, I., Leone, A., Waring, C. D., Henning, B. J., Stirparo, G. G., Papait, R., Scarfo, M., Agosti, V., Viglietto, G., Condorelli, G., Indolfi, C., Ottolenghi, S., Torella, D. & Nadal-Ginard, B. (2013). 'Adult c-kit(pos) cardiac stem cells are necessary and sufficient for functional cardiac regeneration and repair', *Cell,* 154(4), pp. 827-42.

Engel, F. B., Schebesta, M. & Keating, M. T. (2006). 'Anillin localization defect in cardiomyocyte binucleation', *J Mol Cell Cardiol,* 41(4), pp. 601-12.

Eschenhagen, T., Bolli, R., Braun, T., Field, L. J., Fleischmann, B. K., Frisén, J., Giacca, M., Hare, J. M., Houser, S., Lee, R. T., Marbán, E., Martin, J. F., Molkentin, J. D., Murry, C. E., Riley, P. R., Ruiz-Lozano, P., Sadek, H. A., Sussman, M. A. & Hill, J. A. (2017). 'Cardiomyocyte Regeneration: A Consensus Statement', *Circulation,* 136(7), pp. 680-686.

Eulalio, A. & Mano, M. (2015). 'MicroRNA Screening and the Quest for Biologically Relevant Targets', *J Biomol Screen,* 20(8), pp. 1003-17.

Eulalio, A., Mano, M., Dal Ferro, M., Zentilin, L., Sinagra, G., Zacchigna, S. & Giacca, M. (2012). 'Functional screening identifies miRNAs inducing cardiac regeneration', *Nature,* 492(7429), pp. 376-81.

Evans-Anderson, H. J., Alfieri, C. M. & Yutzey, K. E. (2008). 'Regulation of cardiomyocyte proliferation and myocardial growth during development by FOXO transcription factors', *Circulation research,* 102(6), pp. 686-694.

Fang, J. C. (2005). 'Angiotensin-converting enzyme inhibitors or beta-blockers in heart failure: does it matter who goes first?', *Circulation,* 112(16), pp. 2380-2382.

Foinquinos, A., Batkai, S., Genschel, C., Viereck, J., Rump, S., Gyöngyösi, M., Traxler, D., Riesenhuber, M., Spannbauer, A., Lukovic, D., Weber, N., Zlabinger, K., Hašimbegović, E., Winkler, J., Fiedler, J., Dangwal, S., Fischer, M., de la Roche, J., Wojciechowski, D., Kraft, T., Garamvölgyi, R., Neitzel, S., Chatterjee, S., Yin, X., Bär, C., Mayr, M., Xiao, K. & Thum, T. (2020). 'Preclinical development of a miR-132 inhibitor for heart failure treatment', *Nature Communications,* 11(1), p. 633.

French, B. A. & Kramer, C. M. (2007). 'Mechanisms of Post-Infarct Left Ventricular Remodeling', *Drug discovery today. Disease mechanisms,* 4(3), pp. 185-196.

Friedman, R. C., Farh, K. K., Burge, C. B. & Bartel, D. P. (2009). 'Most mammalian mRNAs are conserved targets of microRNAs', *Genome Res,* 19(1), pp. 92-105.

Fukazawa, R., Miller, T. A., Kuramochi, Y., Frantz, S., Kim, Y. D., Marchionni, M. A., Kelly, R. A. & Sawyer, D. B. (2003). 'Neuregulin-1 protects ventricular myocytes from anthracycline-induced apoptosis via erbB4-dependent activation of PI3-kinase/Akt', *Journal of molecular and cellular cardiology,* 35(12), pp. 1473-1479.

Fumeron, F., Betoulle, D., Nicaud, V., Evans, A., Kee, F., Ruidavets, J.-B., Arveiler, D., Luc, G. & Cambien, F. (2002). 'Serotonin Transporter Gene Polymorphism and Myocardial Infarction', *Circulation,* 105(25), pp. 2943-2945.

Gabisonia, K., Prosdocimo, G., Aquaro, G. D., Carlucci, L., Zentilin, L., Secco, I., Ali, H., Braga, L., Gorgodze, N., Bernini, F., Burchielli, S., Collesi, C., Zandona, L., Sinagra, G., Piacenti, M., Zacchigna, S., Bussani, R., Recchia, F. A. & Giacca, M. (2019). 'MicroRNA therapy stimulates uncontrolled cardiac repair after myocardial infarction in pigs', *Nature,* 569(7756), pp. 418-422.

Galdos, F. X., Guo, Y., Paige, S. L., VanDusen, N. J., Wu, S. M. & Pu, W. T. (2017). 'Cardiac Regeneration: Lessons From Development', *Circulation research,* 120(6), pp. 941-959.

Gallant-Behm, C. L., Piper, J., Dickinson, B. A., Dalby, C. M., Pestano, L. A. & Jackson, A. L. (2018). 'A synthetic microRNA-92a inhibitor (MRG-110) accelerates angiogenesis and wound healing in diabetic and nondiabetic wounds', *Wound Repair Regen,* 26(4), pp. 311-323.

Gao, F., Kataoka, M., Liu, N., Liang, T., Huang, Z.-P., Gu, F., Ding, J., Liu, J., Zhang, F., Ma, Q., Wang, Y., Zhang, M., Hu, X., Kyselovic, J., Hu, X., Pu, W. T., Wang, J. a., Chen, J. & Wang, D.-Z. (2019). 'Therapeutic role of miR-19a/19b in cardiac regeneration and protection from myocardial infarction', *Nature Communications,* 10(1), p. 1802.

Gao, Y.-H., Qian, J.-Y., Chen, Z.-W., Fu, M.-Q., Xu, J.-F., Xia, Y., Ding, X.-F., Yang, X.-D., Cao, Y.-Y., Zou, Y.-Z., Ren, J., Sun, A.-J. & Ge, J.-B. (2016). 'Suppression of Bim by microRNA-19a may protect cardiomyocytes against hypoxia-induced cell death via autophagy activation', *Toxicology letters,* 257, pp. 72-83.

Gee, H. E., Buffa, F. M., Camps, C., Ramachandran, A., Leek, R., Taylor, M., Patil, M., Sheldon, H., Betts, G., Homer, J., West, C., Ragoussis, J. & Harris, A. L. (2011). 'The small-nucleolar RNAs commonly used for microRNA normalisation correlate with tumour pathology and prognosis', *Br J Cancer,* 104(7), pp. 1168-77.

Gheorghiade, M. & Goldstein, S. (2002). 'Beta-blockers in the post-myocardial infarction patient', *Circulation,* 106(4), pp. 394-398.

Gong, Z. M., Tang, Z. Y. & Sun, X. L. (2018). 'miR-411 suppresses acute spinal cord injury via downregulation of Fas ligand in rats', *Biochem Biophys Res Commun,* 501(2), pp. 501-506.

Gonzalez-Rosa, J. M., Sharpe, M., Field, D., Soonpaa, M. H., Field, L. J., Burns, C. E. & Burns, C. G. (2018). 'Myocardial Polyploidization Creates a Barrier to Heart Regeneration in Zebrafish', *Dev Cell,* 44(4), pp. 433-446.e7.

Gregory, R. I., Yan, K.-p., Amuthan, G., Chendrimada, T., Doratotaj, B., Cooch, N. & Shiekhattar, R. (2004). 'The Microprocessor complex mediates the genesis of microRNAs', *Nature,* 432(7014), pp. 235-240.

Greulich, F., Rudat, C. & Kispert, A. (2011). 'Mechanisms of T-box gene function in the developing heart', *Cardiovascular research,* 91(2), pp. 212-222.

Griffiths-Jones, S. (2004). 'The microRNA Registry', *Nucleic Acids Res,* 32(Database issue), pp. D109-11.

Griffiths-Jones, S., Grocock, R. J., van Dongen, S., Bateman, A. & Enright, A. J. (2006). 'miRBase: microRNA sequences, targets and gene nomenclature', *Nucleic Acids Res,* 34(Database issue), pp. D140-4.

Grzeschik, N. A., Amin, N., Secombe, J., Brumby, A. M. & Richardson, H. E. (2007). 'Abnormalities in cell proliferation and apico-basal cell polarity are separable in Drosophila lgl mutant clones in the developing eye', *Dev Biol,* 311.

Grzeschik, N. A., Parsons, L. M., Allott, M. L., Harvey, K. F. & Richardson, H. E. (2010). 'Lgl, aPKC, and Crumbs regulate the Salvador/Warts/Hippo pathway through two distinct mechanisms', *Curr Biol,* 20.

Guo, H., Ingolia, N. T., Weissman, J. S. & Bartel, D. P. (2010). 'Mammalian microRNAs predominantly act to decrease target mRNA levels', *Nature,* 466(7308), pp. 835-40.

Guo, L., Yuan, J., Xie, N., Wu, H., Chen, W., Song, S. & Wang, X. (2016). 'miRNA-411 acts as a potential tumor suppressor miRNA via the downregulation of specificity protein 1 in breast cancer', *Mol Med Rep,* 14(4), pp. 2975-82.

Guo, Z., Maki, M., Ding, R., Yang, Y., Zhang, B. & Xiong, L. (2014). 'Genome-wide survey of tissue-specific microRNA and transcription factor regulatory networks in 12 tissues', *Sci Rep,* 4, p. 5150.

Hahn, M. K. & Blakely, R. D. (2007). 'The functional impact of SLC6 transporter genetic variation', *Annu Rev Pharmacol Toxicol,* 47, pp. 401-41.

Halder, G. & Johnson, R. L. (2011). 'Hippo signaling: growth control and beyond', *Development,* 138(1), pp. 9-22.

Halperin, D. & Reber, G. (2007). 'Influence of antidepressants on hemostasis', *Dialogues Clin Neurosci,* 9(1), pp. 47-59.

Hamaratoglu, F., Willecke, M., Kango-Singh, M., Nolo, R., Hyun, E., Tao, C., Jafar-Nejad, H. & Halder, G. (2006). 'The tumour-suppressor genes NF2/Merlin and Expanded act through Hippo signalling to regulate cell proliferation and apoptosis', *Nat Cell Biol,* 8(1), pp. 27-36.

Hammond, S. M., Boettcher, S., Caudy, A. A., Kobayashi, R. & Hannon, G. J. (2001). 'Argonaute2, a Link Between Genetic and Biochemical Analyses of RNAi', *Science,* 293(5532), pp. 1146-1150.

Hanna, J., Hossain, G. S. & Kocerha, J. (2019). 'The Potential for microRNA Therapeutics and Clinical Research', *Frontiers in genetics,* 10, pp. 478-478.

Hara, H., Takeda, N., Kondo, M., Kubota, M., Saito, T., Maruyama, J., Fujiwara, T., Maemura, S., Ito, M., Naito, A. T., Harada, M., Toko, H., Nomura, S., Kumagai, H., Ikeda, Y., Ueno, H., Takimoto, E., Akazawa, H., Morita, H., Aburatani, H., Hata, Y., Uchiyama, M. & Komuro, I. (2018). 'Discovery of a Small Molecule to Increase Cardiomyocytes and Protect the Heart After Ischemic Injury', *JACC: Basic to Translational Science,* 3(5), pp. 639-653.

Harris, I. S., Zhang, S., Treskov, I., Kovacs, A., Weinheimer, C. & Muslin, A. J. (2004). 'Raf-1 kinase is required for cardiac hypertrophy and cardiomyocyte survival in response to pressure overload', *Circulation,* 110(6), pp. 718-723.

Hartupee, J. & Mann, D. L. (2017). 'Neurohormonal activation in heart failure with reduced ejection fraction', *Nature reviews. Cardiology,* 14(1), pp. 30-38.

Harvey, K. & Tapon, N. (2007). 'The Salvador-Warts-Hippo pathway - an emerging tumor-suppressor network', *Nat Rev Cancer,* 7.

Harvey, K. F., Pfleger, C. M. & Hariharan, I. K. (2003). 'The Drosophila Mst ortholog, hippo, restricts growth and cell proliferation and promotes apoptosis', *Cell,* 114(4), pp. 457-67.

Haskins, J. W., Nguyen, D. X. & Stern, D. F. (2014). 'Neuregulin 1-activated ERBB4 interacts with YAP to induce Hippo pathway target genes and promote cell migration', *Science signaling,* 7(355), pp. ra116-ra116.

Haubner, B. J., Schneider, J., Schweigmann, U., Schuetz, T., Dichtl, W., Velik-Salchner, C., Stein, J. I. & Penninger, J. M. (2016). 'Functional Recovery of a Human Neonatal Heart After Severe Myocardial Infarction', *Circ Res,* 118(2), pp. 216-21.

Heallen, T., Morikawa, Y., Leach, J., Tao, G., Willerson, J. T., Johnson, R. L. & Martin, J. F. (2013). 'Hippo signaling impedes adult heart regeneration', *Development,* 140(23), pp. 4683-90.

Heallen, T., Zhang, M., Wang, J., Bonilla-Claudio, M., Klysik, E., Johnson, R. L. & Martin, J. F. (2011). 'Hippo Pathway Inhibits Wnt Signaling to Restrain Cardiomyocyte Proliferation and Heart Size', *Science,* 332(6028), pp. 458-461.

Heallen, T. R., Kadow, Z. A., Kim, J. H., Wang, J. & Martin, J. F. (2019). 'Stimulating Cardiogenesis as a Treatment for Heart Failure', *Circulation Research,* 124(11), pp. 1647-1657.

Herget, G. W., Neuburger, M., Plagwitz, R. & Adler, C. P. (1997). 'DNA content, ploidy level and number of nuclei in the human heart after myocardial infarction', *Cardiovasc Res,* 36(1), pp. 45-51.

Hertig, C. M., Kubalak, S. W., Wang, Y. & Chien, K. R. (1999). 'Synergistic roles of neuregulin-1 and insulin-like growth factor-I in activation of the phosphatidylinositol 3-kinase pathway and cardiac chamber morphogenesis', *Journal of Biological Chemistry,* 274(52), pp. 37362-37369.

Hesse, M., Doengi, M., Becker, A., Kimura, K., Voeltz, N., Stein, V. & Fleischmann, B. K. (2018). 'Midbody Positioning and Distance Between Daughter Nuclei Enable Unequivocal Identification of Cardiomyocyte Cell Division in Mice', *Circ Res,* 123(9), pp. 1039-1052.

Heusch, G. & Gersh, B. J. (2017). 'The pathophysiology of acute myocardial infarction and strategies of protection beyond reperfusion: a continual challenge', *European heart journal,* 38(11), pp. 774-784.

Hinkel, R., Penzkofer, D., Zühlke, S., Fischer, A., Husada, W., Xu, Q. F., Baloch, E., van Rooij, E., Zeiher, A. M., Kupatt, C. & Dimmeler, S. (2013). 'Inhibition of microRNA-92a protects against ischemia/reperfusion injury in a large-animal model', *Circulation,* 128(10), pp. 1066-75.

Hirabayashi, S., Nakagawa, K., Sumita, K., Hidaka, S., Kawai, T., Ikeda, M., Kawata, A., Ohno, K. & Hata, Y. (2008). 'Threonine 74 of MOB1 is a putative key phosphorylation site by MST2 to form the scaffold to activate nuclear Dbf2-related kinase 1', *Oncogene,* 27(31), pp. 4281-92.

Ho, K. C., Zhou, Z., She, Y. M., Chun, A., Cyr, T. D. & Yang, X. (2011). 'Itch E3 ubiquitin ligase regulates large tumor suppressor 1 stability [corrected]', *Proc Natl Acad Sci U S A,* 108(12), pp. 4870-5.

Hodgkinson, C. P., Kang, M. H., Dal-Pra, S., Mirotsou, M. & Dzau, V. J. (2015). 'MicroRNAs and Cardiac Regeneration', *Circulation Research,* 116(10), pp. 1700-1711.

Home, P., Ray, S., Dutta, D., Bronshteyn, I., Larson, M. & Paul, S. (2009). 'GATA3 is selectively expressed in the trophectoderm of peri-implantation embryo and directly regulates Cdx2 gene expression', *J Biol Chem,* 284(42), pp. 28729-37.

Home, P., Saha, B., Ray, S., Dutta, D., Gunewardena, S., Yoo, B., Pal, A., Vivian, J. L., Larson, M., Petroff, M., Gallagher, P. G., Schulz, V. P., White, K. L., Golos, T. G., Behr, B. & Paul, S. (2012). 'Altered subcellular localization of transcription factor TEAD4 regulates first mammalian cell lineage commitment', *Proceedings of the National Academy of Sciences,* 109(19), pp. 7362-7367.

Hoyer, D., Clarke, D. E., Fozard, J. R., Hartig, P. R., Martin, G. R., Mylecharane, E. J., Saxena, P. R. & Humphrey, P. P. (1994). 'International Union of Pharmacology classification of receptors for 5-hydroxytryptamine (Serotonin)', *Pharmacol Rev,* 46(2), pp. 157-203.

Hsieh, P. C., Segers, V. F., Davis, M. E., MacGillivray, C., Gannon, J., Molkentin, J. D., Robbins, J. & Lee, R. T. (2007). 'Evidence from a genetic fate-mapping study that stem cells refresh adult mammalian cardiomyocytes after injury', *Nat Med,* 13(8), pp. 970-4.

Huang, C. K., Kafert-Kasting, S. & Thum, T. (2020). 'Preclinical and Clinical Development of Noncoding RNA Therapeutics for Cardiovascular Disease', *Circ Res,* 126(5), pp. 663-678.

Huang, W., Feng, Y., Liang, J., Yu, H., Wang, C., Wang, B., Wang, M., Jiang, L., Meng, W., Cai, W., Medvedovic, M., Chen, J., Paul, C., Davidson, W. S., Sadayappan, S., Stambrook, P. J., Yu, X. Y. & Wang, Y. (2018). 'Loss of microRNA-128 promotes cardiomyocyte proliferation and heart regeneration', *Nat Commun,* 9(1), p. 700.

Hydbring, P. & Badalian-Very, G. (2013). 'Clinical applications of microRNAs', *F1000Res,* 2.

Ikeda, K., Tojo, K., Otsubo, C., Udagawa, T., Kumazawa, K., Ishikawa, M., Tokudome, G., Hosoya, T., Tajima, N., Claycomb, W. C., Nakao, K. & Kawamura, M. (2005). '5-Hydroxytryptamine synthesis in HL-1 cells and neonatal rat cardiocytes', *Biochemical and Biophysical Research Communications,* 328(2), pp. 522-525.

Ikeda, S., He, A., Kong, S. W., Lu, J., Bejar, R., Bodyak, N., Lee, K. H., Ma, Q., Kang, P. M., Golub, T. R. & Pu, W. T. (2009). 'MicroRNA-1 negatively regulates expression of the hypertrophy-associated calmodulin and Mef2a genes', *Mol Cell Biol,* 29(8), pp. 2193-204.

Ikeda, S., Mizushima, W., Sciarretta, S., Abdellatif, M., Zhai, P., Mukai, R., Fefelova, N., Oka, S. I., Nakamura, M., Del Re, D. P., Farrance, I., Park, J. Y., Tian, B., Xie, L. H., Kumar, M., Hsu, C. P., Sadayappan, S., Shimokawa, H., Lim, D. S. & Sadoshima, J. (2019). 'Hippo Deficiency Leads to Cardiac Dysfunction Accompanied by Cardiomyocyte Dedifferentiation During Pressure Overload', *Circ Res,* 124(2), pp. 292-305.

Jacot, J. G., McCulloch, A. D. & Omens, J. H. (2008). 'Substrate stiffness affects the functional maturation of neonatal rat ventricular myocytes', *Biophysical journal,* 95(7), pp. 3479-3487.

Janssen, H. L., Reesink, H. W., Lawitz, E. J., Zeuzem, S., Rodriguez-Torres, M., Patel, K., van der Meer, A. J., Patick, A. K., Chen, A., Zhou, Y., Persson, R., King, B. D., Kauppinen, S., Levin, A. A. & Hodges, M. R. (2013). 'Treatment of HCV infection by targeting microRNA', *N Engl J Med,* 368(18), pp. 1685-94.

Jentzsch, C., Leierseder, S., Loyer, X., Flohrschutz, I., Sassi, Y., Hartmann, D., Thum, T., Laggerbauer, B. & Engelhardt, S. (2012). 'A phenotypic screen to identify hypertrophy-modulating microRNAs in primary cardiomyocytes', *J Mol Cell Cardiol,* 52(1), pp. 13-20.

Jia, J., Zhang, W., Wang, B., Trinko, R. & Jiang, J. (2003). 'The Drosophila Ste20 family kinase dMST functions as a tumor suppressor by restricting cell proliferation and promoting apoptosis', *Genes Dev,* 17(20), pp. 2514-9.

Jin, H., Sun, W., Zhang, Y., Yan, H., Liufu, H., Wang, S., Chen, C., Gu, J., Hua, X., Zhou, L., Jiang, G., Rao, D., Xie, Q., Huang, H. & Huang, C. (2018). 'MicroRNA-411 Downregulation Enhances Tumor Growth by Upregulating MLLT11 Expression in Human Bladder Cancer', *Mol Ther Nucleic Acids,* 11, pp. 312-322.

Johnson, R. & Halder, G. (2014). 'The two faces of Hippo: targeting the Hippo pathway for regenerative medicine and cancer treatment', *Nat Rev Drug Discov,* 13(1), pp. 63-79.

Jopling, C., Sleep, E., Raya, M., Martí, M., Raya, A. & Belmonte, J. C. I. (2010). 'Zebrafish heart regeneration occurs by cardiomyocyte dedifferentiation and proliferation', *Nature,* 464(7288), pp. 606-609.

Justice, R. W., Zilian, O., Woods, D. F., Noll, M. & Bryant, P. J. (1995). 'The Drosophila tumor suppressor gene warts encodes a homolog of human myotonic dystrophy kinase and is required for the control of cell shape and proliferation', *Genes Dev,* 9(5), pp. 534-46.

Kajstura, J., Urbanek, K., Perl, S., Hosoda, T., Zheng, H., Ogorek, B., Ferreira-Martins, J., Goichberg, P., Rondon-Clavo, C., Sanada, F., D'Amario, D., Rota, M., Del Monte, F., Orlic, D., Tisdale, J., Leri, A. & Anversa, P. (2010). 'Cardiomyogenesis in the adult human heart', *Circ Res,* 107(2), pp. 305-15.

Kanai, F., Marignani, P. A., Sarbassova, D., Yagi, R., Hall, R. A., Donowitz, M., Hisaminato, A., Fujiwara, T., Ito, Y., Cantley, L. C. & Yaffe, M. B. (2000). 'TAZ: a novel transcriptional co-activator regulated by interactions with 14-3-3 and PDZ domain proteins', *Embo j,* 19(24), pp. 6778-91.

Ketting, R. F., Fischer, S. E., Bernstein, E., Sijen, T., Hannon, G. J. & Plasterk, R. H. (2001). 'Dicer functions in RNA interference and in synthesis of small RNA involved in developmental timing in C. elegans', *Genes Dev,* 15(20), pp. 2654-9.

Khandaker, G. M., Zuber, V., Rees, J. M. B., Carvalho, L., Mason, A. M., Foley, C. N., Gkatzionis, A., Jones, P. B. & Burgess, S. (2019). 'Shared mechanisms between coronary heart disease and depression: findings from a large UK general population-based cohort', *Molecular Psychiatry*.

Khvorova, A., Reynolds, A. & Jayasena, S. D. (2003). 'Functional siRNAs and miRNAs exhibit strand bias', *Cell,* 115(2), pp. 209-16.

Kikuchi, K., Holdway, J. E., Werdich, A. A., Anderson, R. M., Fang, Y., Egnaczyk, G. F., Evans, T., Macrae, C. A., Stainier, D. Y. & Poss, K. D. (2010). 'Primary contribution to zebrafish heart regeneration by gata4(+) cardiomyocytes', *Nature,* 464(7288), pp. 601-5.

Kim, N. G., Koh, E., Chen, X. & Gumbiner, B. M. (2011). 'E-cadherin mediates contact inhibition of proliferation through Hippo signaling-pathway components', *Proc Natl Acad Sci U S A,* 108(29), pp. 11930-5.

Kitchen, R. R., Kubista, M. & Tichopad, A. (2010). 'Statistical aspects of quantitative real-time PCR experiment design', *Methods,* 50(4), pp. 231-6.

Klocke, R., Tian, W., Kuhlmann, M. T. & Nikol, S. (2007). 'Surgical animal models of heart failure related to coronary heart disease', *Cardiovasc Res,* 74(1), pp. 29-38.

Koudstaal, S., Bastings, M. M. C., Feyen, D. A. M., Waring, C. D., van Slochteren, F. J., Dankers, P. Y. W., Torella, D., Sluijter, J. P. G., Nadal-Ginard, B., Doevendans, P. A., Ellison, G. M. & Chamuleau, S. A. J. (2014). 'Sustained delivery of insulin-like growth factor-1/hepatocyte growth factor stimulates endogenous cardiac repair in the chronic infarcted pig heart', *Journal of cardiovascular translational research,* 7(2), pp. 232-241.

Kozomara, A., Birgaoanu, M. & Griffiths-Jones, S. (2019). 'miRBase: from microRNA sequences to function', *Nucleic Acids Res,* 47(D1), pp. D155-d162.

Kozomara, A. & Griffiths-Jones, S. (2011). 'miRBase: integrating microRNA annotation and deep-sequencing data', *Nucleic Acids Res,* 39(Database issue), pp. D152-7.

Krum, H. & Driscoll, A. (2013). 'Management of heart failure', *The Medical journal of Australia,* 199(5), pp. 334-339.

Krutzfeldt, J., Rajewsky, N., Braich, R., Rajeev, K. G., Tuschl, T., Manoharan, M. & Stoffel, M. (2005). 'Silencing of microRNAs in vivo with 'antagomirs'', *Nature,* 438(7068), pp. 685-9.

Kubin, T., Pöling, J., Kostin, S., Gajawada, P., Hein, S., Rees, W., Wietelmann, A., Tanaka, M., Lörchner, H., Schimanski, S., Szibor, M., Warnecke, H. & Braun, T. (2011). 'Oncostatin M Is a Major Mediator of Cardiomyocyte Dedifferentiation and Remodeling', *Cell Stem Cell,* 9(5), pp. 420-432.

Lamar, J. M., Stern, P., Liu, H., Schindler, J. W., Jiang, Z. G. & Hynes, R. O. (2012). 'The Hippo pathway target, YAP, promotes metastasis through its TEAD-interaction domain', *Proc Natl Acad Sci U S A,* 109(37), pp. E2441-50.

Lamba, V., Ghodke-Puranik, Y., Guan, W. & Lamba, J. K. (2014). 'Identification of suitable reference genes for hepatic microRNA quantitation', *BMC Res Notes,* 7, p. 129.

Laube, F., Heister, M., Scholz, C., Borchardt, T. & Braun, T. (2006). 'Re-programming of newt cardiomyocytes is induced by tissue regeneration', *J Cell Sci,* 119(Pt 22), pp. 4719-29.

Lauder, J. M., Wilkie, M. B., Wu, C. & Singh, S. (2000). 'Expression of 5-HT(2A), 5-HT(2B) and 5-HT(2C) receptors in the mouse embryo', *Int J Dev Neurosci,* 18(7), pp. 653-62.

Leach, J. P., Heallen, T., Zhang, M., Rahmani, M., Morikawa, Y., Hill, M. C., Segura, A., Willerson, J. T. & Martin, J. F. (2017). 'Hippo pathway deficiency reverses systolic heart failure after infarction', *Nature,* 550(7675), pp. 260-264.

Lee, J. H., Kim, T. S., Yang, T. H., Koo, B. K., Oh, S. P., Lee, K. P., Oh, H. J., Lee, S. H., Kong, Y. Y., Kim, J. M. & Lim, D. S. (2008). 'A crucial role of WW45 in developing epithelial tissues in the mouse', *Embo j,* 27(8), pp. 1231-42.

Lee, L. W., Zhang, S., Etheridge, A., Ma, L., Martin, D., Galas, D. & Wang, K. (2010). 'Complexity of the microRNA repertoire revealed by next-generation sequencing', *Rna,* 16(11), pp. 2170-80.

Lee, Y. S. & Dutta, A. (2009). 'MicroRNAs in cancer', *Annual review of pathology,* 4, pp. 199-227.

Lehtinen, M. K., Yuan, Z., Boag, P. R., Yang, Y., Villén, J., Becker, E. B. E., DiBacco, S., de la Iglesia, N., Gygi, S., Blackwell, T. K. & Bonni, A. (2006). 'A conserved MST-FOXO signaling pathway mediates oxidative-stress responses and extends life span', *Cell,* 125(5), pp. 987-1001.

Lesizza, P., Prosdocimo, G., Martinelli, V., Sinagra, G., Zacchigna, S. & Giacca, M. (2017). 'Single-Dose Intracardiac Injection of Pro-Regenerative MicroRNAs Improves Cardiac Function After Myocardial Infarction', *Circ Res,* 120(8), pp. 1298-1304.

Li, F., Wang, X., Capasso, J. M. & Gerdes, A. M. (1996). 'Rapid Transition of Cardiac Myocytes from Hyperplasia to Hypertrophy During Postnatal Development', *Journal of Molecular and Cellular Cardiology,* 28(8), pp. 1737-1746.

Lian, I., Kim, J., Okazawa, H., Zhao, J., Zhao, B., Yu, J., Chinnaiyan, A., Israel, M. A., Goldstein, L. S., Abujarour, R., Ding, S. & Guan, K. L. (2010). 'The role of YAP transcription coactivator in regulating stem cell self-renewal and differentiation', *Genes Dev,* 24(11), pp. 1106-18.

Liao, J. K., Seto, M. & Noma, K. (2007). 'Rho kinase (ROCK) inhibitors', *J Cardiovasc Pharmacol,* 50(1), pp. 17-24.

Lin, C. W., Chang, Y. L., Chang, Y. C., Lin, J. C., Chen, C. C., Pan, S. H., Wu, C. T., Chen, H. Y., Yang, S. C., Hong, T. M. & Yang, P. C. (2013). 'MicroRNA-135b promotes lung cancer metastasis by regulating multiple targets in the Hippo pathway and LZTS1', *Nat Commun,* 4, p. 1877.

Lin, Z., Murtaza, I., Wang, K., Jiao, J., Gao, J. & Li, P. F. (2009). 'miR-23a functions downstream of NFATc3 to regulate cardiac hypertrophy', *Proc Natl Acad Sci U S A,* 106(29), pp. 12103-8.

Lin, Z. & Pu, W. T. (2014). 'Strategies for cardiac regeneration and repair', *Science translational medicine,* 6(239), pp. 239rv1-239rv1.

Lin, Z., von Gise, A., Zhou, P., Gu, F., Ma, Q., Jiang, J., Yau, A. L., Buck, J. N., Gouin, K. A., van Gorp, P. R., Zhou, B., Chen, J., Seidman, J. G., Wang, D. Z. & Pu, W. T. (2014). 'Cardiac-specific YAP activation improves cardiac function and survival in an experimental murine MI model', *Circ Res,* 115(3), pp. 354-63.

Lin, Z., Zhou, P., Von Gise, A., Gu, F., Ma, Q., Chen, J., Guo, H., Van Gorp, P. R. R., Wang, D. Z. & Pu, W. T. (2015). 'Pi3kcb links Hippo-YAP and PI3K-AKT signaling pathways to promote cardiomyocyte proliferation and survival', *Circulation Research,* 116(1), pp. 35-45.

Liu, B., Li, J. & Cairns, M. J. (2012). 'Identifying miRNAs, targets and functions', *Briefings in Bioinformatics*.

Liu, S. & Martin, J. F. (2019). 'The regulation and function of the Hippo pathway in heart regeneration', *Wiley Interdiscip Rev Dev Biol,* 8(1), p. e335.

Liu, S., Miao, R., Zhai, M., Pang, Q., Deng, Y., Liu, S., Qu, K., Liu, C. & Zhang, J. (2017). 'Effects and related mechanisms of serotonin on malignant biological behavior of hepatocellular carcinoma via regulation of Yap', *Oncotarget,* 8(29), pp. 47412-47424.

Liu, Y., Liu, T., Jin, H., Yin, L., Yu, H. & Bi, J. (2018). 'MiR-411 suppresses the development of bladder cancer by regulating ZnT1', *Onco Targets Ther,* 11, pp. 8695-8704.

Lorthongpanich, C., Messerschmidt, D. M., Chan, S. W., Hong, W., Knowles, B. B. & Solter, D. (2013). 'Temporal reduction of LATS kinases in the early preimplantation embryo prevents ICM lineage differentiation', *Genes & Development,* 27(13), pp. 1441-1446.

Lovric, J., Mano, M., Zentilin, L., Eulalio, A., Zacchigna, S. & Giacca, M. (2012). 'Terminal Differentiation of Cardiac and Skeletal Myocytes Induces Permissivity to AAV Transduction by Relieving Inhibition Imposed by DNA Damage Response Proteins', *Molecular Therapy,* 20(11), pp. 2087-2097.

Lu, Y., Zhang, Y., Wang, N., Pan, Z., Gao, X., Zhang, F., Zhang, Y., Shan, H., Luo, X., Bai, Y., Sun, L., Song, W., Xu, C., Wang, Z. & Yang, B. (2010). 'MicroRNA-328 contributes to adverse electrical remodeling in atrial fibrillation', *Circulation,* 122(23), pp. 2378-87.

Lymperopoulos, A., Rengo, G. & Koch, W. J. (2013). 'Adrenergic nervous system in heart failure: pathophysiology and therapy', *Circulation research,* 113(6), pp. 739-753.

Mahmoud, A. I., Kocabas, F., Muralidhar, S. A., Kimura, W., Koura, A. S., Thet, S., Porrello, E. R. & Sadek, H. A. (2013). 'Meis1 regulates postnatal cardiomyocyte cell cycle arrest', *Nature,* 497(7448), pp. 249-253.

Mair, K. M., MacLean, M. R., Morecroft, I., Dempsie, Y. & Palmer, T. M. (2008). 'Novel interactions between the 5-HT transporter, 5-HT1B receptors and Rho kinase in vivo and in pulmonary fibroblasts', *British Journal of Pharmacology,* 155(4), pp. 606-616.

Marazziti, D. (2017). 'Understanding the role of serotonin in psychiatric diseases', *F1000Res,* 6, p. 180.

Masè, M., Grasso, M., Avogaro, L., D'Amato, E., Tessarolo, F., Graffigna, A., Denti, M. A. & Ravelli, F. (2017). 'Selection of reference genes is critical for miRNA expression analysis in human cardiac tissue. A focus on atrial fibrillation', *Sci Rep,* 7, p. 41127.

Maskell, L. J., Qamar, K., Babakr, A. A., Hawkins, T. A., Heads, R. J. & Budhram-Mahadeo, V. S. (2017). 'Essential but partially redundant roles for POU4F1/Brn-3a and POU4F2/Brn-3b transcription factors in the developing heart', *Cell Death Dis,* 8(6), p. e2861.

Masson, J., Emerit, M. B., Hamon, M. & Darmon, M. (2012). 'Serotonergic signaling: multiple effectors and pleiotropic effects', *Wiley Interdisciplinary Reviews: Membrane Transport and Signaling,* 1(6), pp. 685-713.

Matsui, Y., Nakano, N., Shao, D., Gao, S., Luo, W., Hong, C., Zhai, P., Holle, E., Yu, X., Yabuta, N., Tao, W., Wagner, T., Nojima, H. & Sadoshima, J. (2008). 'Lats2 is a negative regulator of myocyte size in the heart', *Circulation research,* 103(11), pp. 1309-1318.

Mavrakis, K. J., Wolfe, A. L., Oricchio, E., Palomero, T., de Keersmaecker, K., McJunkin, K., Zuber, J., James, T., Khan, A. A., Leslie, C. S., Parker, J. S., Paddison, P. J., Tam, W., Ferrando, A. & Wendel, H.-G. (2010). 'Genome-wide RNA-mediated interference screen identifies miR-19 targets in Notch-induced T-cell acute lymphoblastic leukaemia', *Nature cell biology,* 12(4), pp. 372-379.

Mekontso-Dessap, A., Brouri, F., Pascal, O., Lechat, P., Hanoun, N., Lanfumey, L., Seif, I., Benhaiem-Sigaux, N., Kirsch, M., Hamon, M., Adnot, S. & Eddahibi, S. (2006). 'Deficiency of the 5-hydroxytryptamine transporter gene leads to cardiac fibrosis and valvulopathy in mice', *Circulation,* 113(1), pp. 81-9.

Melke, J. (2003). 'Serotonin transporter gene polymorphisms and mental health', *Current Opinion in Psychiatry,* 16(2), pp. 215-220.

Meng, Z., Moroishi, T. & Guan, K.-L. (2016). 'Mechanisms of Hippo pathway regulation', *Genes & development,* 30(1), pp. 1-17.

Mensah, G. A., Roth, G. A. & Fuster, V. (2019). 'The Global Burden of Cardiovascular Diseases and Risk Factors', *Journal of the American College of Cardiology,* 74(20), p. 2529.

Millan, M. J., Marin, P., Bockaert, J. & Mannoury la Cour, C. (2008). 'Signaling at G-protein-coupled serotonin receptors: recent advances and future research directions', *Trends Pharmacol Sci,* 29(9), pp. 454-64.

Miller, E., Yang, J., DeRan, M., Wu, C., Su, A. I., Bonamy, G. M., Liu, J., Peters, E. C. & Wu, X. (2012). 'Identification of serum-derived sphingosine-1-phosphate as a small molecule regulator of YAP', *Chem Biol,* 19(8), pp. 955-62.

Miranda, K. C., Huynh, T., Tay, Y., Ang, Y. S., Tam, W. L., Thomson, A. M., Lim, B. & Rigoutsos, I. (2006). 'A pattern-based method for the identification of MicroRNA binding sites and their corresponding heteroduplexes', *Cell,* 126(6), pp. 1203-17.

Miyawaki, A., Obana, M., Mitsuhara, Y., Orimoto, A., Nakayasu, Y., Yamashita, T., Fukada, S.-i., Maeda, M., Nakayama, H. & Fujio, Y. (2017). 'Adult murine cardiomyocytes exhibit regenerative activity with cell cycle reentry through STAT3 in the healing process of myocarditis', *Scientific Reports,* 7(1), p. 1407.

Mohamed, T. M., Ang, Y.-S., Radzinsky, E., Zhou, P., Huang, Y., Elfenbein, A., Foley, A., Magnitsky, S. & Srivastava, D. (2018). 'Regulation of cell cycle to stimulate adult cardiomyocyte proliferation and cardiac regeneration', *Cell,* 173(1), pp. 104-116. e12.

Morikawa, Y., Zhang, M., Heallen, T., Leach, J., Tao, G., Xiao, Y., Bai, Y., Li, W., Willerson, J. T. & Martin, J. F. (2015). 'Actin cytoskeletal remodeling with protrusion formation is essential for heart regeneration in Hippo-deficient mice', *Science signaling,* 8(375), pp. ra41-ra41.

Morin-Kensicki, E. M., Boone, B. N., Howell, M., Stonebraker, J. R., Teed, J., Alb, J. G., Magnuson, T. R., O'Neal, W. & Milgram, S. L. (2006). 'Defects in yolk sac vasculogenesis, chorioallantoic fusion, and embryonic axis elongation in mice with targeted disruption of Yap65', *Mol Cell Biol,* 26(1), pp. 77-87.

Moses, K. A., DeMayo, F., Braun, R. M., Reecy, J. L. & Schwartz, R. J. (2001). 'Embryonic expression of an Nkx2-5/Cre gene using ROSA26 reporter mice', *Genesis,* 31(4), pp. 176-80.

Moss, A. J., Hall, W. J., Cannom, D. S., Klein, H., Brown, M. W., Daubert, J. P., Estes, N. A. M., 3rd, Foster, E., Greenberg, H., Higgins, S. L., Pfeffer, M. A., Solomon, S. D., Wilber, D., Zareba, W. & Investigators, M.-C. T. (2009). 'Cardiac-resynchronization therapy for the prevention of heart-failure events', *The New England journal of medicine,* 361(14), pp. 1329-1338.

Murakami, H., Mizuno, T., Taniguchi, T., Fujii, M., Ishiguro, F., Fukui, T., Akatsuka, S., Horio, Y., Hida, T., Kondo, Y., Toyokuni, S., Osada, H. & Sekido, Y. (2011). 'LATS2 is a tumor suppressor gene of malignant mesothelioma', *Cancer Res,* 71(3), pp. 873-83.

Murphy, D. L., Fox, M. A., Timpano, K. R., Moya, P. R., Ren-Patterson, R., Andrews, A. M., Holmes, A., Lesch, K. P. & Wendland, J. R. (2008). 'How the serotonin story is being rewritten by new gene-based discoveries principally related to SLC6A4, the serotonin transporter gene, which functions to influence all cellular serotonin systems', *Neuropharmacology,* 55(6), pp. 932-60.

Murrell, M., Oakes, P. W., Lenz, M. & Gardel, M. L. (2015). 'Forcing cells into shape: the mechanics of actomyosin contractility', *Nature reviews. Molecular cell biology,* 16(8), pp. 486-498.

Muthusamy, S., DeMartino, A. M., Watson, L. J., Brittian, K. R., Zafir, A., Dassanayaka, S., Hong, K. U. & Jones, S. P. (2014). 'MicroRNA-539 is up-regulated in failing heart, and suppresses O-GlcNAcase expression', *J Biol Chem,* 289(43), pp. 29665-76.

Nakamura, M. & Sadoshima, J. (2018). 'Mechanisms of physiological and pathological cardiac hypertrophy', *Nature reviews. Cardiology,* 15(7), pp. 387-407.

Nam, J. W., Rissland, O. S., Koppstein, D., Abreu-Goodger, C., Jan, C. H., Agarwal, V., Yildirim, M. A., Rodriguez, A. & Bartel, D. P. (2014). 'Global analyses of the effect of different cellular contexts on microRNA targeting', *Mol Cell,* 53(6), pp. 1031-1043.

Nebigil, C. G., Choi, D. S., Dierich, A., Hickel, P., Le Meur, M., Messaddeq, N., Launay, J. M. & Maroteaux, L. (2000). 'Serotonin 2B receptor is required for heart development', *Proc Natl Acad Sci U S A,* 97(17), pp. 9508-13.

Nebigil, C. G., Etienne, N., Messaddeq, N. & Maroteaux, L. (2003a). 'Serotonin is a novel survival factor of cardiomyocytes: mitochondria as a target of 5-HT2B receptor signaling', *Faseb j,* 17(10), pp. 1373-5.

Nebigil, C. G., Hickel, P., Messaddeq, N., Vonesch, J. L., Douchet, M. P., Monassier, L., Gyorgy, K., Matz, R., Andriantsitohaina, R., Manivet, P., Launay, J. M. & Maroteaux, L. (2001). 'Ablation of serotonin 5-HT(2B) receptors in mice leads to abnormal cardiac structure and function', *Circulation,* 103(24), pp. 2973-9.

Nebigil, C. G., Jaffre, F., Messaddeq, N., Hickel, P., Monassier, L., Launay, J. M. & Maroteaux, L. (2003b). 'Overexpression of the serotonin 5-HT2B receptor in heart leads to abnormal mitochondrial function and cardiac hypertrophy', *Circulation,* 107(25), pp. 3223-9.

Nishioka, N., Inoue, K., Adachi, K., Kiyonari, H., Ota, M., Ralston, A., Yabuta, N., Hirahara, S., Stephenson, R. O., Ogonuki, N., Makita, R., Kurihara, H., Morin-Kensicki, E. M., Nojima, H., Rossant, J., Nakao, K., Niwa, H. & Sasaki, H. (2009). 'The Hippo signaling pathway components Lats and Yap pattern Tead4 activity to distinguish mouse trophectoderm from inner cell mass', *Dev Cell,* 16(3), pp. 398-410.

Nolo, R., Morrison, C. M., Tao, C., Zhang, X. & Halder, G. (2006). 'The bantam microRNA is a target of the hippo tumor-suppressor pathway', *Curr Biol,* 16(19), pp. 1895-904.

Noorlander, C. W., Ververs, F. F., Nikkels, P. G., van Echteld, C. J., Visser, G. H. & Smidt, M. P. (2008). 'Modulation of serotonin transporter function during fetal development causes dilated heart cardiomyopathy and lifelong behavioral abnormalities', *PLoS One,* 3(7), p. e2782.

Nygren, J. M., Jovinge, S., Breitbach, M., Säwén, P., Röll, W., Hescheler, J., Taneera, J., Fleischmann, B. K. & Jacobsen, S. E. W. (2004). 'Bone marrow-derived hematopoietic cells generate cardiomyocytes at a low frequency through cell fusion, but not transdifferentiation', *Nature medicine,* 10(5), pp. 494-501.

O'Connor, C. M., Jiang, W., Kuchibhatla, M., Silva, S. G., Cuffe, M. S., Callwood, D. D., Zakhary, B., Stough, W. G., Arias, R. M., Rivelli, S. K. & Krishnan, R. (2010). 'Safety and efficacy of sertraline for depression in patients with heart failure: results of the SADHART-CHF (Sertraline Against Depression and Heart Disease in Chronic Heart Failure) trial', *J Am Coll Cardiol,* 56(9), pp. 692-9.

Oberpriller, J. O. & Oberpriller, J. C. (1974). 'Response of the adult newt ventricle to injury', *J Exp Zool,* 187(2), pp. 249-53.

Odashima, M., Usui, S., Takagi, H., Hong, C., Liu, J., Yokota, M. & Sadoshima, J. (2007). 'Inhibition of endogenous Mst1 prevents apoptosis and cardiac dysfunction without affecting cardiac hypertrophy after myocardial infarction', *Circ Res,* 100(9), pp. 1344-52.

Osadchii, O. E., Norton, G. R., McKechnie, R., Deftereos, D. & Woodiwiss, A. J. (2007). 'Cardiac dilatation and pump dysfunction without intrinsic myocardial systolic failure following chronic beta-adrenoreceptor activation', *American journal of physiology. Heart and circulatory physiology,* 292(4), pp. H1898-H1905.

Osorio, K. M., Lilja, K. C. & Tumbar, T. (2011). 'Runx1 modulates adult hair follicle stem cell emergence and maintenance from distinct embryonic skin compartments', *Journal of Cell Biology,* 193(1), pp. 235-250.

Pacak, C. A., Sakai, Y., Thattaliyath, B. D., Mah, C. S. & Byrne, B. J. (2008). 'Tissue specific promoters improve specificity of AAV9 mediated transgene expression following intra-vascular gene delivery in neonatal mice', *Genetic Vaccines and Therapy,* 6(1), p. 13.

Pantalacci, S., Tapon, N. & Leopold, P. (2003). 'The Salvador partner Hippo promotes apoptosis and cell-cycle exit in Drosophila', *Nat Cell Biol,* 5(10), pp. 921-7.

Paramasivam, M., Sarkeshik, A., Yates, J. R., 3rd, Fernandes, M. J. & McCollum, D. (2011). 'Angiomotin family proteins are novel activators of the LATS2 kinase tumor suppressor', *Mol Biol Cell,* 22(19), pp. 3725-33.

Pasumarthi, K. B., Nakajima, H., Nakajima, H. O., Soonpaa, M. H. & Field, L. J. (2005). 'Targeted expression of cyclin D2 results in cardiomyocyte DNA synthesis and infarct regression in transgenic mice', *Circulation research,* 96(1), pp. 110-118.

Pavone, L. M., Mithbaokar, P., Mastellone, V., Lo Muto, R., Spina, A., Maharajan, V., Paino, G. & Avallone, L. (2008). 'Expression of the serotonin transporter (SERT) gene during mouse development', *Vet Res Commun,* 32 Suppl 1, pp. S167-9.

Pavone, L. M., Spina, A., Rea, S., Santoro, D., Mastellone, V., Lombardi, P. & Avallone, L. (2009). 'Serotonin transporter gene deficiency is associated with sudden death of newborn mice through activation of TGF-beta1 signalling', *J Mol Cell Cardiol,* 47(5), pp. 691-7.

Peroutka, S. J. (1991). 'Serotonin receptor subtypes: Basic and clinical aspects', *New York*.

Pobbati, A. V., Chan, S. W., Lee, I., Song, H. & Hong, W. (2012). 'Structural and functional similarity between the Vgll1-TEAD and the YAP-TEAD complexes', *Structure,* 20(7), pp. 1135-40.

Pönicke, K., Gergs, U., Buchwalow, I. B., Hauptmann, S. & Neumann, J. (2012). 'On the presence of serotonin in mammalian cardiomyocytes', *Molecular and Cellular Biochemistry,* 365(1), pp. 301-312.

Poolman, R. A. & Brooks, G. (1998). 'Expressions and activities of cell cycle regulatory molecules during the transition from myocyte hyperplasia to hypertrophy', *J Mol Cell Cardiol,* 30(10), pp. 2121-35.

Porrello, E. R., Johnson, B. A., Aurora, A. B., Simpson, E., Nam, Y. J., Matkovich, S. J., Dorn, G. W., 2nd, van Rooij, E. & Olson, E. N. (2011a). 'MiR-15 family regulates postnatal mitotic arrest of cardiomyocytes', *Circ Res,* 109(6), pp. 670-9.

Porrello, E. R., Mahmoud, A. I., Simpson, E., Hill, J. A., Richardson, J. A., Olson, E. N. & Sadek, H. A. (2011b). 'Transient regenerative potential of the neonatal mouse heart', *Science,* 331(6020), pp. 1078-80.

Porrello, E. R., Mahmoud, A. I., Simpson, E., Johnson, B. A., Grinsfelder, D., Canseco, D., Mammen, P. P., Rothermel, B. A., Olson, E. N. & Sadek, H. A. (2013). 'Regulation of neonatal and adult mammalian heart regeneration by the miR-15 family', *Proceedings of the National Academy of Sciences,* 110(1), pp. 187-192.

Posch, M. G., Gramlich, M., Sunde, M., Schmitt, K. R., Lee, S. H. Y., Richter, S., Kersten, A., Perrot, A., Panek, A. N., Al Khatib, I. H., Nemer, G., Mégarbané, A., Dietz, R., Stiller, B., Berger, F., Harvey, R. P. & Ozcelik, C. (2010). 'A gain-of-function TBX20 mutation causes congenital atrial septal defects, patent foramen ovale and cardiac valve defects', *Journal of medical genetics,* 47(4), pp. 230-235.

Poss, K. D., Wilson, L. G. & Keating, M. T. (2002). 'Heart Regeneration in Zebrafish', *Science,* 298(5601), pp. 2188-2190.

Pritchard, C. C., Cheng, H. H. & Tewari, M. (2012). 'MicroRNA profiling: approaches and considerations', *Nat Rev Genet,* 13(5), pp. 358-69.

Puthanveetil, P., Wan, A. & Rodrigues, B. (2013). 'FoxO1 is crucial for sustaining cardiomyocyte metabolism and cell survival', *Cardiovasc Res,* 97(3), pp. 393-403.

Qin, H., Blaschke, K., Wei, G., Ohi, Y., Blouin, L., Qi, Z., Yu, J., Yeh, R.-F., Hebrok, M. & Ramalho-Santos, M. (2012). 'Transcriptional analysis of pluripotency reveals the Hippo pathway as a barrier to reprogramming', *Human Molecular Genetics*.

Quaife-Ryan, G. A., Sim, C. B., Ziemann, M., Kaspi, A., Rafehi, H., Ramialison, M., El-Osta, A., Hudson, J. E. & Porrello, E. R. (2017). 'Multicellular Transcriptional Analysis of Mammalian Heart Regeneration', *Circulation,* 136(12), pp. 1123-1139.

Ralston, A., Cox, B. J., Nishioka, N., Sasaki, H., Chea, E., Rugg-Gunn, P., Guo, G., Robson, P., Draper, J. S. & Rossant, J. (2010). 'Gata3 regulates trophoblast development downstream of Tead4 and in parallel to Cdx2', *Development,* 137(3), pp. 395-403.

Ramage, A. G. & Villalon, C. M. (2008). '5-hydroxytryptamine and cardiovascular regulation', *Trends Pharmacol Sci,* 29(9), pp. 472-81.

Ramamoorthy, S., Shippenberg, T. S. & Jayanthi, L. D. (2011). 'Regulation of monoamine transporters: Role of transporter phosphorylation', *Pharmacol Ther,* 129(2), pp. 220-38.

Rao, P. K., Toyama, Y., Chiang, H. R., Gupta, S., Bauer, M., Medvid, R., Reinhardt, F., Liao, R., Krieger, M., Jaenisch, R., Lodish, H. F. & Blelloch, R. (2009). 'Loss of Cardiac microRNA-Mediated Regulation Leads to Dilated Cardiomyopathy and Heart Failure', *Circulation Research,* 105(6), pp. 585-594.

Robertson, A., Mohamed, T. M. A., El Maadawi, Z., Stafford, N., Bui, T., Lim, D.-S., Cartwright, E. J. & Oceandy, D. (2017). 'Genetic ablation of the mammalian sterile-20 like kinase 1 (Mst1) improves cell reprogramming efficiency and increases induced pluripotent stem cell proliferation and survival', *Stem Cell Research,* 20, pp. 42-49.

Ronnebaum, S. M. & Patterson, C. (2010). 'The FoxO family in cardiac function and dysfunction', *Annual review of physiology,* 72, pp. 81-94.

Rouleau, J. L., de Champlain, J., Klein, M., Bichet, D., Moyé, L., Packer, M., Dagenais, G. R., Sussex, B., Arnold, J. M., Sestier, F. & et al. (1993). 'Activation of neurohumoral systems in postinfarction left ventricular dysfunction', *Journal of the American College of Cardiology,* 22(2), pp. 390-398.

Rudnick, G. (2006). 'Serotonin transporters--structure and function', *J Membr Biol,* 213(2), pp. 101-10.

Rumiantsev, P. P. & Shmantsar, I. A. (1968). '[Submicroscopic patterns of reactive changes in frog heart muscle cells during regeneration]', *Tsitologiia,* 10(10), pp. 1234-47.

Rumyantsev, P. P. (1977). 'Interrelations of the proliferation and differentiation processes during cardiact myogenesis and regeneration', *Int Rev Cytol,* 51, pp. 186-273.

Sabirzhanova, I., Sabirzhanov, B., Bjordahl, J., Brandt, J., Jay, P. Y. & Clark, T. G. (2009). 'Activation of Tolloid-like 1 gene expression by the cardiac specific homeobox gene Nkx2-5', *Dev Growth Differ,* 51(4), pp. 403-10.

Salah, Z., Melino, G. & Aqeilan, R. I. (2011). 'Negative regulation of the Hippo pathway by E3 ubiquitin ligase ITCH is sufficient to promote tumorigenicity', *Cancer Res,* 71(5), pp. 2010-20.

Salic, A. & Mitchison, T. J. (2008). 'A chemical method for fast and sensitive detection of DNA synthesis in vivo', *Proceedings of the National Academy of Sciences,* 105(7), pp. 2415-2420.

Salto-Tellez, M., Yung Lim, S., El-Oakley, R. M., Tang, T. P., ZA, A. L. & Lim, S. K. (2004). 'Myocardial infarction in the C57BL/6J mouse: a quantifiable and highly reproducible experimental model', *Cardiovasc Pathol,* 13(2), pp. 91-7.

Sanganalmath, S. K. & Bolli, R. (2013). 'Cell therapy for heart failure: a comprehensive overview of experimental and clinical studies, current challenges, and future directions', *Circulation research,* 113(6), pp. 810-834.

Sansores-Garcia, L., Bossuyt, W., Wada, K.-I., Yonemura, S., Tao, C., Sasaki, H. & Halder, G. (2011). 'Modulating F-actin organization induces organ growth by affecting the Hippo pathway', *The EMBO journal,* 30(12), pp. 2325-2335.

Sari, Y. & Zhou, F. C. (2003). 'Serotonin and its transporter on proliferation of fetal heart cells', *Int J Dev Neurosci,* 21(8), pp. 417-24.

Sauer, W. H., Berlin, J. A. & Kimmel, S. E. (2003). 'Effect of antidepressants and their relative affinity for the serotonin transporter on the risk of myocardial infarction', *Circulation,* 108(1), pp. 32-6.

Scarabelli, T. M., Knight, R. A., Rayment, N. B., Cooper, T. J., Stephanou, A., Brar, B. K., Lawrence, K. M., Santilli, G., Latchman, D. S., Baxter, G. F. & Yellon, D. M. (1999). 'Quantitative assessment of cardiac myocyte apoptosis in tissue sections using the fluorescence-based tunel technique enhanced with counterstains', *J Immunol Methods,* 228(1-2), pp. 23-8.

Schiaffino, S., Gorza, L. & Ausoni, S. (1993). 'Troponin isoform switching in the developing heart and its functional consequences', *Trends in cardiovascular medicine,* 3(1), pp. 12-17.

Schlegelmilch, K., Mohseni, M., Kirak, O., Pruszak, J., Rodriguez, J. R., Zhou, D., Kreger, B. T., Vasioukhin, V., Avruch, J., Brummelkamp, T. R. & Camargo, F. D. (2011). 'Yap1 acts downstream of alpha-catenin to control epidermal proliferation', *Cell,* 144(5), pp. 782-95.

Schlosser, K., Taha, M., Deng, Y. & Stewart, D. J. (2018). 'Systemic delivery of MicroRNA mimics with polyethylenimine elevates pulmonary microRNA levels, but lacks pulmonary selectivity', *Pulm Circ,* 8(1), p. 2045893217750613.

Scholzen, T. & Gerdes, J. (2000). 'The Ki-67 protein: from the known and the unknown', *J Cell Physiol,* 182(3), pp. 311-22.

Schroeder, M. C. & Halder, G. (2012). 'Regulation of the Hippo pathway by cell architecture and mechanical signals', *Seminars in Cell & Developmental Biology,* 23(7), pp. 803-811.

Schultz, J. E. J., Witt, S. A., Glascock, B. J., Nieman, M. L., Reiser, P. J., Nix, S. L., Kimball, T. R. & Doetschman, T. (2002). 'TGF-beta1 mediates the hypertrophic cardiomyocyte growth induced by angiotensin II', *The Journal of clinical investigation,* 109(6), pp. 787-796.

Schwarzenbach, H., da Silva, A. M., Calin, G. & Pantel, K. (2015). 'Data Normalization Strategies for MicroRNA Quantification', *Clin Chem,* 61(11), pp. 1333-42.

Senyo, S. E., Steinhauser, M. L., Pizzimenti, C. L., Yang, V. K., Cai, L., Wang, M., Wu, T. D., Guerquin-Kern, J. L., Lechene, C. P. & Lee, R. T. (2013). 'Mammalian heart renewal by pre-existing cardiomyocytes', *Nature,* 493(7432), pp. 433-6.

Sepramaniam, S., Armugam, A., Lim, K. Y., Karolina, D. S., Swaminathan, P., Tan, J. R. & Jeyaseelan, K. (2010). 'MicroRNA 320a functions as a novel endogenous modulator of aquaporins 1 and 4 as well as a potential therapeutic target in cerebral ischemia', *J Biol Chem,* 285(38), pp. 29223-30.

Serebruany, V. L., Suckow, R. F., Cooper, T. B., O'Connor, C. M., Malinin, A. I., Krishnan, K. R., van Zyl, L. T., Lekht, V. & Glassman, A. H. (2005). 'Relationship between release of platelet/endothelial biomarkers and plasma levels of sertraline and N-desmethylsertraline in acute coronary syndrome patients receiving SSRI treatment for depression', *Am J Psychiatry,* 162(6), pp. 1165-70.

Shan, D., Shang, Y. & Hu, T. (2019). 'MicroRNA-411 Inhibits Cervical Cancer Progression by Directly Targeting STAT3', *Oncol Res,* 27(3), pp. 349-358.

Shao, D., Zhai, P., Del Re, D. P., Sciarretta, S., Yabuta, N., Nojima, H., Lim, D. S., Pan, D. & Sadoshima, J. (2014). 'A functional interaction between Hippo-YAP signalling and FoxO1 mediates the oxidative stress response', *Nat Commun,* 5, p. 3315.

Shapiro, S. D., Ranjan, A. K., Kawase, Y., Cheng, R. K., Kara, R. J., Bhattacharya, R., Guzman-Martinez, G., Sanz, J., Garcia, M. J. & Chaudhry, H. W. (2014). 'Cyclin A2 induces cardiac regeneration after myocardial infarction through cytokinesis of adult cardiomyocytes', *Science translational medicine,* 6(224), pp. 224ra27-224ra27.

Shearman, L. P., McReynolds, A. M., Zhou, F. C. & Meyer, J. S. (1998). 'Relationship between [125I]RTI-55-labeled cocaine binding sites and the serotonin transporter in rat placenta', *Am J Physiol,* 275(6), pp. C1621-9.

Shin, C., Nam, J. W., Farh, K. K., Chiang, H. R., Shkumatava, A. & Bartel, D. P. (2010). 'Expanding the microRNA targeting code: functional sites with centered pairing', *Mol Cell,* 38(6), pp. 789-802.

Small, E. M., Frost, R. J. & Olson, E. N. (2010). 'MicroRNAs add a new dimension to cardiovascular disease', *Circulation,* 121(8), pp. 1022-32.

Song, H., Mak, K. K., Topol, L., Yun, K., Hu, J., Garrett, L., Chen, Y., Park, O., Chang, J., Simpson, R. M., Wang, C. Y., Gao, B., Jiang, J. & Yang, Y. (2010). 'Mammalian Mst1 and Mst2 kinases play essential roles in organ size control and tumor suppression', *Proc Natl Acad Sci U S A,* 107(4), pp. 1431-6.

Song, H., Song, J., Lu, L. & Li, S. (2019). 'SNHG8 is upregulated in esophageal squamous cell carcinoma and directly sponges microRNA-411 to increase oncogenicity by upregulating KPNA2', *Onco Targets Ther,* 12, pp. 6991-7004.

Soonpaa, M. H. & Field, L. J. (1997). 'Assessment of cardiomyocyte DNA synthesis in normal and injured adult mouse hearts', *Am J Physiol,* 272(1 Pt 2), pp. H220-6.

Soonpaa, M. H., Rubart, M. & Field, L. J. (2013). 'Challenges measuring cardiomyocyte renewal', *Biochim Biophys Acta,* 1833(4), pp. 799-803.

Sorrentino, G., Ruggeri, N., Specchia, V., Cordenonsi, M., Mano, M., Dupont, S., Manfrin, A., Ingallina, E., Sommaggio, R., Piazza, S., Rosato, A., Piccolo, S. & Del Sal, G. (2014). 'Metabolic control of YAP and TAZ by the mevalonate pathway', *Nature cell biology,* 16(4), pp. 357-366.

Ståhlberg, A., Kubista, M. & Pfaffl, M. (2004). 'Comparison of reverse transcriptases in gene expression analysis', *Clin Chem,* 50(9), pp. 1678-80.

Stanley, E. G., Biben, C., Elefanty, A., Barnett, L., Koentgen, F., Robb, L. & Harvey, R. P. (2002). 'Efficient Cre-mediated deletion in cardiac progenitor cells conferred by a 3'UTR-ires-Cre allele of the homeobox gene Nkx2-5', *Int J Dev Biol,* 46(4), pp. 431-9.

Struthers, A. D. (2005). 'Pathophysiology of heart failure following myocardial infarction', *Heart,* 91 Suppl 2(Suppl 2), pp. ii14-6; discussion ii31, ii43-8.

Sun, M., Huang, F., Yu, D., Zhang, Y., Xu, H., Zhang, L., Li, L., Dong, L., Guo, L. & Wang, S. (2015). 'Autoregulatory loop between TGF-beta1/miR-411-5p/SPRY4 and MAPK pathway in rhabdomyosarcoma modulates proliferation and differentiation', *Cell Death Dis,* 6, p. e1859.

Sutton, M. G. & Sharpe, N. (2000). 'Left ventricular remodeling after myocardial infarction: pathophysiology and therapy', *Circulation,* 101(25), pp. 2981-2988.

Sweitzer, N. K. (2003). 'Cardiology patient page. What is an angiotensin converting enzyme inhibitor?', *Circulation,* 108(3), pp. e16-e18.

Takagawa, J., Zhang, Y., Wong, M. L., Sievers, R. E., Kapasi, N. K., Wang, Y., Yeghiazarians, Y., Lee, R. J., Grossman, W. & Springer, M. L. (2007). 'Myocardial infarct size measurement in the mouse chronic infarction model: comparison of area- and length-based approaches', *Journal of applied physiology (Bethesda, Md. : 1985),* 102(6), pp. 2104-2111.

Tamm, C., Böwer, N. & Annerén, C. (2011). 'Regulation of mouse embryonic stem cell self-renewal by a Yes–YAP–TEAD2 signaling pathway downstream of LIF', *Journal of Cell Science,* 124(7), pp. 1136-1144.

Tane, S., Ikenishi, A., Okayama, H., Iwamoto, N., Nakayama, K. I. & Takeuchi, T. (2014). 'CDK inhibitors, p21(Cip1) and p27(Kip1), participate in cell cycle exit of mammalian cardiomyocytes', *Biochem Biophys Res Commun,* 443(3), pp. 1105-9.

Tang, A. S. L., Wells, G. A., Talajic, M., Arnold, M. O., Sheldon, R., Connolly, S., Hohnloser, S. H., Nichol, G., Birnie, D. H., Sapp, J. L., Yee, R., Healey, J. S., Rouleau, J. L. & Resynchronization-Defibrillation for Ambulatory Heart Failure Trial, I. (2010). 'Cardiac-resynchronization therapy for mild-to-moderate heart failure', *The New England journal of medicine,* 363(25), pp. 2385-2395.

Tapon, N., Harvey, K. F., Bell, D. W., Wahrer, D. C., Schiripo, T. A., Haber, D. & Hariharan, I. K. (2002). 'salvador Promotes both cell cycle exit and apoptosis in Drosophila and is mutated in human cancer cell lines', *Cell,* 110(4), pp. 467-78.

Tarang, S. & Weston, M. D. (2014). 'Macros in microRNA target identification: a comparative analysis of in silico, in vitro, and in vivo approaches to microRNA target identification', *RNA Biol,* 11(4), pp. 324-33.

Terrados, G., Finkernagel, F., Stielow, B., Sadic, D., Neubert, J., Herdt, O., Krause, M., Scharfe, M., Jarek, M. & Suske, G. (2012). 'Genome-wide localization and expression profiling establish Sp2 as a sequence-specific transcription factor regulating vitally important genes', *Nucleic Acids Research,* 40(16), pp. 7844-7857.

Thum, T., Galuppo, P., Wolf, C., Fiedler, J., Kneitz, S., van Laake, L. W., Doevendans, P. A., Mummery, C. L., Borlak, J., Haverich, A., Gross, C., Engelhardt, S., Ertl, G. & Bauersachs, J. (2007). 'MicroRNAs in the human heart: a clue to fetal gene reprogramming in heart failure', *Circulation,* 116(3), pp. 258-67.

Thum, T., Gross, C., Fiedler, J., Fischer, T., Kissler, S., Bussen, M., Galuppo, P., Just, S., Rottbauer, W., Frantz, S., Castoldi, M., Soutschek, J., Koteliansky, V., Rosenwald, A., Basson, M. A., Licht, J. D., Pena, J. T., Rouhanifard, S. H., Muckenthaler, M. U., Tuschl, T., Martin, G. R., Bauersachs, J. & Engelhardt, S. (2008). 'MicroRNA-21 contributes to myocardial disease by stimulating MAP kinase signalling in fibroblasts', *Nature,* 456(7224), pp. 980-4.

Tian, W., Yu, J., Tomchick, D. R., Pan, D. & Luo, X. (2010). 'Structural and functional analysis of the YAP-binding domain of human TEAD2', *Proc Natl Acad Sci U S A,* 107(16), pp. 7293-8.

Tian, Y., Liu, Y., Wang, T., Zhou, N., Kong, J., Chen, L., Snitow, M., Morley, M., Li, D., Petrenko, N., Zhou, S., Lu, M., Gao, E., Koch, W. J., Stewart, K. M. & Morrisey, E. E. (2015). 'A microRNA-Hippo pathway that promotes cardiomyocyte proliferation and cardiac regeneration in mice', *Sci Transl Med,* 7(279), p. 279ra38.

Tomari, Y., Du, T. & Zamore, P. D. (2007). 'Sorting of Drosophila small silencing RNAs', *Cell,* 130(2), pp. 299-308.

Torres, A., Torres, K., Wdowiak, P., Paszkowski, T. & Maciejewski, R. (2013). 'Selection and validation of endogenous controls for microRNA expression studies in endometrioid endometrial cancer tissues', *Gynecologic Oncology,* 130(3), pp. 588-594.

Torrini, C., Cubero, R. J., Dirkx, E., Braga, L., Ali, H., Prosdocimo, G., Gutierrez, M. I., Collesi, C., Licastro, D., Zentilin, L., Mano, M., Zacchigna, S., Vendruscolo, M., Marsili, M., Samal, A. & Giacca, M. (2019). 'Common Regulatory Pathways Mediate Activity of MicroRNAs Inducing Cardiomyocyte Proliferation', *Cell Rep,* 27(9), pp. 2759-2771.e5.

Toulouse, A. & Nolan, Y. M. (2015). 'A role for mitogen-activated protein kinase phosphatase 1 (MKP1) in neural cell development and survival', *Neural Regen Res,* 10(11), pp. 1748-9.

Triastuti, E., Nugroho, A. B., Zi, M., Prehar, S., Kohar, Y. S., Bui, T. A., Stafford, N., Cartwright, E. J., Abraham, S. & Oceandy, D. (2019). 'Pharmacological inhibition of Hippo pathway, with the novel kinase inhibitor XMU-MP-1, protects the heart against adverse effects during pressure overload', *Br J Pharmacol,* 176(20), pp. 3956-3971.

Tseng, Y. S., You, M. Y., Hsu, Y. C. & Yang, K. C. (2019). 'P5388N-cadherin promotes cardiac regeneration by stabilizing beta-catenin', *European Heart Journal,* 40(Supplement_1).

Ucar, A., Gupta, S. K., Fiedler, J., Erikci, E., Kardasinski, M., Batkai, S., Dangwal, S., Kumarswamy, R., Bang, C., Holzmann, A., Remke, J., Caprio, M., Jentzsch, C., Engelhardt, S., Geisendorf, S., Glas, C., Hofmann, T. G., Nessling, M., Richter, K., Schiffer, M., Carrier, L., Napp, L. C., Bauersachs, J., Chowdhury, K. & Thum, T. (2012). 'The miRNA-212/132 family regulates both cardiac hypertrophy and cardiomyocyte autophagy', *Nat Commun,* 3, p. 1078.

Udan, R. S., Kango-Singh, M., Nolo, R., Tao, C. & Halder, G. (2003). 'Hippo promotes proliferation arrest and apoptosis in the Salvador/Warts pathway', *Nat Cell Biol,* 5(10), pp. 914-20.

van Berlo, J. H., Kanisicak, O., Maillet, M., Vagnozzi, R. J., Karch, J., Lin, S. C., Middleton, R. C., Marban, E. & Molkentin, J. D. (2014). 'c-kit+ cells minimally contribute cardiomyocytes to the heart', *Nature,* 509(7500), pp. 337-41.

van Rooij, E. & Olson, E. N. (2012). 'MicroRNA therapeutics for cardiovascular disease: opportunities and obstacles', *Nat Rev Drug Discov,* 11(11), pp. 860-872.

van Rooij, E., Sutherland, L. B., Liu, N., Williams, A. H., McAnally, J., Gerard, R. D., Richardson, J. A. & Olson, E. N. (2006). 'A signature pattern of stress-responsive microRNAs that can evoke cardiac hypertrophy and heart failure', *Proc Natl Acad Sci U S A,* 103(48), pp. 18255-60.

Varelas, X. (2014). 'The Hippo pathway effectors TAZ and YAP in development, homeostasis and disease', *Development,* 141(8), pp. 1614-1626.

Varelas, X., Miller, B. W., Sopko, R., Song, S., Gregorieff, A., Fellouse, F. A., Sakuma, R., Pawson, T., Hunziker, W., McNeill, H., Wrana, J. L. & Attisano, L. (2010). 'The Hippo Pathway Regulates Wnt/β-Catenin Signaling', *Developmental Cell,* 18(4), pp. 579-591.

Vassilev, A., Kaneko, K. J., Shu, H., Zhao, Y. & DePamphilis, M. L. (2001). 'TEAD/TEF transcription factors utilize the activation domain of YAP65, a Src/Yes-associated protein localized in the cytoplasm', *Genes Dev,* 15(10), pp. 1229-41.

Vaudin, P., Delanoue, R., Davidson, I., Silber, J. & Zider, A. (1999). 'TONDU (TDU), a novel human protein related to the product of vestigial (vg) gene of Drosophila melanogaster interacts with vertebrate TEF factors and substitutes for Vg function in wing formation', *Development,* 126(21), pp. 4807-16.

Verghese, S., Bedi, S. & Kango-Singh, M. (2012). 'Hippo signalling controls Dronc activity to regulate organ size in Drosophila', *Cell Death Differ,* 19(10), pp. 1664-76.

von Gise, A., Lin, Z., Schlegelmilch, K., Honor, L. B., Pan, G. M., Buck, J. N., Ma, Q., Ishiwata, T., Zhou, B., Camargo, F. D. & Pu, W. T. (2012). 'YAP1, the nuclear target of Hippo signaling, stimulates heart growth through cardiomyocyte proliferation but not hypertrophy', *Proceedings of the National Academy of Sciences of the United States of America,* 109(7), pp. 2394-2399.

Wahlquist, C., Jeong, D., Rojas-Munoz, A., Kho, C., Lee, A., Mitsuyama, S., van Mil, A., Park, W. J., Sluijter, J. P., Doevendans, P. A., Hajjar, R. J. & Mercola, M. (2014). 'Inhibition of miR-25 improves cardiac contractility in the failing heart', *Nature,* 508(7497), pp. 531-5.

Walsh, S., Ponten, A., Fleischmann, B. K. & Jovinge, S. (2010). 'Cardiomyocyte cell cycle control and growth estimation in vivo--an analysis based on cardiomyocyte nuclei', *Cardiovasc Res,* 86(3), pp. 365-73.

Wang, G., Zhang, Y., Zhao, X., Meng, C., Ma, L. & Kong, Y. (2015). 'MicroRNA-411 inhibited matrix metalloproteinase 13 expression in human chondrocytes', *Am J Transl Res,* 7(10), pp. 2000-6.

Wang, J., Faust, S. M. & Rabinowitz, J. E. (2011). 'The next step in gene delivery: molecular engineering of adeno-associated virus serotypes', *J Mol Cell Cardiol,* 50(5), pp. 793-802.

Wang, W., Xiao, Z.-D., Li, X., Aziz, K. E., Gan, B., Johnson, R. L. & Chen, J. (2015). 'AMPK modulates Hippo pathway activity to regulate energy homeostasis', *Nature cell biology,* 17(4), pp. 490-499.

Wang, W. E., Li, L., Xia, X., Fu, W., Liao, Q., Lan, C., Yang, D., Chen, H., Yue, R., Zeng, C., Zhou, L., Zhou, B., Duan, D. D., Chen, X., Houser, S. R. & Zeng, C. (2017). 'Dedifferentiation, proliferation, and redifferentiation of adult mammalian cardiomyocytes after ischemic injury', *Circulation,* 136(9), pp. 834-848.

Wang, X. (2014). 'Composition of seed sequence is a major determinant of microRNA targeting patterns', *Bioinformatics,* 30(10), pp. 1377-83.

Wang, Z., Cui, M., Shah, A. M., Ye, W., Tan, W., Min, Y. L., Botten, G. A., Shelton, J. M., Liu, N., Bassel-Duby, R. & Olson, E. N. (2019). 'Mechanistic basis of neonatal heart regeneration revealed by transcriptome and histone modification profiling', *Proc Natl Acad Sci U S A,* 116(37), pp. 18455-18465.

Webb, C., Upadhyay, A., Giuntini, F., Eggleston, I., Furutani-Seiki, M., Ishima, R. & Bagby, S. (2011). 'Structural features and ligand binding properties of tandem WW domains from YAP and TAZ, nuclear effectors of the Hippo pathway', *Biochemistry,* 50(16), pp. 3300-9.

Wei, K., Serpooshan, V., Hurtado, C., Diez-Cuñado, M., Zhao, M., Maruyama, S., Zhu, W., Fajardo, G., Noseda, M., Nakamura, K., Tian, X., Liu, Q., Wang, A., Matsuura, Y., Bushway, P., Cai, W., Savchenko, A., Mahmoudi, M., Schneider, M. D., van den Hoff, M. J. B., Butte, M. J., Yang, P. C., Walsh, K., Zhou, B., Bernstein, D., Mercola, M. & Ruiz-Lozano, P. (2015). 'Epicardial FSTL1 reconstitution regenerates the adult mammalian heart', *Nature,* 525(7570), pp. 479-485.

Weisman, H. F. & Healy, B. (1987). 'Myocardial infarct expansion, infarct extension, and reinfarction: pathophysiologic concepts', *Progress in cardiovascular diseases,* 30(2), pp. 73-110.

Wong, N. & Wang, X. (2015). 'miRDB: an online resource for microRNA target prediction and functional annotations', *Nucleic Acids Res,* 43(Database issue), pp. D146-52.

Woo, Y. J., Panlilio, C. M., Cheng, R. K., Liao, G. P., Atluri, P., Hsu, V. M., Cohen, J. E. & Chaudhry, H. W. (2006). 'Therapeutic delivery of cyclin A2 induces myocardial regeneration and enhances cardiac function in ischemic heart failure', *Circulation,* 114(1_supplement), pp. I-206-I-213.

Wu, S., Huang, J., Dong, J. & Pan, D. (2003). 'hippo encodes a Ste-20 family protein kinase that restricts cell proliferation and promotes apoptosis in conjunction with salvador and warts', *Cell,* 114(4), pp. 445-56.

Xia, K., Zhang, Y., Cao, S., Wu, Y., Guo, W., Yuan, W. & Zhang, S. (2015). 'miR-411 regulated ITCH expression and promoted cell proliferation in human hepatocellular carcinoma cells', *Biomed Pharmacother,* 70, pp. 158-63.

Xiang, F.-l., Guo, M. & Yutzey, K. E. (2016). 'Overexpression of Tbx20 in adult cardiomyocytes promotes proliferation and improves cardiac function after myocardial infarction', *Circulation,* 133(11), pp. 1081-1092.

Xin, M., Kim, Y., Sutherland, L. B., Murakami, M., Qi, X., McAnally, J., Porrello, E. R., Mahmoud, A. I., Tan, W., Shelton, J. M., Richardson, J. A., Sadek, H. A., Bassel-Duby, R. & Olson, E. N. (2013). 'Hippo pathway effector Yap promotes cardiac regeneration', *Proceedings of the National Academy of Sciences of the United States of America,* 110(34), pp. 13839-13844.

Xin, M., Kim, Y., Sutherland, L. B., Qi, X., McAnally, J., Schwartz, R. J., Richardson, J. A., Bassel-Duby, R. & Olson, E. N. (2011). 'Regulation of insulin-like growth factor signaling by Yap governs cardiomyocyte proliferation and embryonic heart size', *Science signaling,* 4(196), pp. ra70-ra70.

Xu, M. Z., Yao, T. J., Lee, N. P., Ng, I. O., Chan, Y. T., Zender, L., Lowe, S. W., Poon, R. T. & Luk, J. M. (2009). 'Yes-associated protein is an independent prognostic marker in hepatocellular carcinoma', *Cancer,* 115(19), pp. 4576-85.

Xu, N., Yang, W., Liu, Y., Yan, F. & Yu, Z. (2018). 'MicroRNA-411 promoted the osteosarcoma progression by suppressing MTSS1 expression', *Environ Sci Pollut Res Int,* 25(12), pp. 12064-12071.

Yamada, Y., Izawa, H., Ichihara, S., Takatsu, F., Ishihara, H., Hirayama, H., Sone, T., Tanaka, M. & Yokota, M. (2002). 'Prediction of the risk of myocardial infarction from polymorphisms in candidate genes', *The New England journal of medicine,* 347(24), pp. 1916-1923.

Yamamoto, K., Seike, M., Takeuchi, S., Soeno, C., Miyanaga, A., Noro, R., Minegishi, Y., Kubota, K. & Gemma, A. (2014). 'MiR-379/411 cluster regulates IL-18 and contributes to drug resistance in malignant pleural mesothelioma', *Oncol Rep,* 32(6), pp. 2365-72.

Yamamoto, S., Yang, G., Zablocki, D., Liu, J., Hong, C., Kim, S. J., Soler, S., Odashima, M., Thaisz, J., Yehia, G., Molina, C. A., Yatani, A., Vatner, D. E., Vatner, S. F. & Sadoshima, J. (2003). 'Activation of Mst1 causes dilated cardiomyopathy by stimulating apoptosis without compensatory ventricular myocyte hypertrophy', *J Clin Invest,* 111(10), pp. 1463-74.

Yang, H., Qin, X., Wang, H., Zhao, X., Liu, Y., Wo, H. T., Liu, C., Nishiga, M., Chen, H., Ge, J., Sayed, N., Abilez, O. J., Ding, D., Heilshorn, S. C. & Li, K. (2019). 'An in Vivo miRNA Delivery System for Restoring Infarcted Myocardium', *ACS Nano,* 13(9), pp. 9880-9894.

Yang, W. J., Yang, D. D., Na, S., Sandusky, G. E., Zhang, Q. & Zhao, G. (2005). 'Dicer Is Required for Embryonic Angiogenesis during Mouse Development', *Journal of Biological Chemistry,* 280(10), pp. 9330-9335.

Yang, Y., Cheng, H.-W., Qiu, Y., Dupee, D., Noonan, M., Lin, Y.-D., Fisch, S., Unno, K., Sereti, K.-I. & Liao, R. (2015a). 'MicroRNA-34a Plays a Key Role in Cardiac Repair and Regeneration Following Myocardial Infarction', *Circulation research,* 117(5), pp. 450-459.

Yang, Y., Del Re, D. P., Nakano, N., Sciarretta, S., Zhai, P., Park, J., Sayed, D., Shirakabe, A., Matsushima, S., Park, Y., Tian, B., Abdellatif, M. & Sadoshima, J. (2015b). 'miR-206 Mediates YAP-Induced Cardiac Hypertrophy and Survival', *Circ Res,* 117(10), pp. 891-904.

Yavarone, M. S., Shuey, D. L., Tamir, H., Sadler, T. W. & Lauder, J. M. (1993). 'Serotonin and cardiac morphogenesis in the mouse embryo', *Teratology,* 47(6), pp. 573-84.

Yi, R., Qin, Y., Macara, I. G. & Cullen, B. R. (2003). 'Exportin-5 mediates the nuclear export of pre-microRNAs and short hairpin RNAs', *Genes Dev,* 17(24), pp. 3011-6.

Yin, H., Kanasty, R. L., Eltoukhy, A. A., Vegas, A. J., Dorkin, J. R. & Anderson, D. G. (2014). 'Non-viral vectors for gene-based therapy', *Nature Reviews Genetics,* 15(8), pp. 541-555.

Yu, F.-X. & Guan, K.-L. (2013). 'The Hippo pathway: regulators and regulations', *Genes & development,* 27(4), pp. 355-371.

Yu, F.-X., Luo, J., Mo, J.-S., Liu, G., Kim, Y. C., Meng, Z., Zhao, L., Peyman, G., Ouyang, H., Jiang, W., Zhao, J., Chen, X., Zhang, L., Wang, C.-Y., Bastian, B. C., Zhang, K. & Guan, K.-L. (2014). 'Mutant Gq/11 promote uveal melanoma tumorigenesis by activating YAP', *Cancer cell,* 25(6), pp. 822-830.

Yu, F. X., Zhang, Y., Park, H. W., Jewell, J. L., Chen, Q., Deng, Y., Pan, D., Taylor, S. S., Lai, Z. C. & Guan, K. L. (2013). 'Protein kinase A activates the Hippo pathway to modulate cell proliferation and differentiation', *Genes Dev,* 27(11), pp. 1223-32.

Yu, F. X., Zhao, B., Panupinthu, N., Jewell, J. L., Lian, I., Wang, L. H., Zhao, J., Yuan, H., Tumaneng, K., Li, H., Fu, X. D., Mills, G. B. & Guan, K. L. (2012). 'Regulation of the Hippo-YAP pathway by G-protein-coupled receptor signaling', *Cell,* 150(4), pp. 780-91.

Yu, J., Zheng, Y., Dong, J., Klusza, S., Deng, W. M. & Pan, D. (2010). 'Kibra functions as a tumor suppressor protein that regulates Hippo signaling in conjunction with Merlin and Expanded', *Dev Cell,* 18(2), pp. 288-99.

Zacchigna, S., Zentilin, L. & Giacca, M. (2014). 'Adeno-associated virus vectors as therapeutic and investigational tools in the cardiovascular system', *Circulation research,* 114(11), pp. 1827-1846.

Zaiss, A.-K., Liu, Q., Bowen, G. P., Wong, N. C. W., Bartlett, J. S. & Muruve, D. A. (2002). 'Differential Activation of Innate Immune Responses by Adenovirus and Adeno-Associated Virus Vectors', *Journal of Virology,* 76(9), pp. 4580-4590.

Zhang, C., Wang, H., Liu, X., Hu, Y., Ding, L., Zhang, X., Sun, Q. & Li, Y. (2019). 'Oncogenic microRNA-411 promotes lung carcinogenesis by directly targeting suppressor genes SPRY4 and TXNIP', *Oncogene,* 38(11), pp. 1892-1904.

Zhang, D., Yang, X. J., Luo, Q. D., Fu, D. L., Li, Z. L., Zhang, P. & Chong, T. (2019). 'Down-Regulation of Circular RNA_000926 Attenuates Renal Cell Carcinoma Progression through miRNA-411-Dependent CDH2 Inhibition', *Am J Pathol*.

Zhang, J., Smolen, G. A. & Haber, D. A. (2008). 'Negative Regulation of YAP by LATS1 Underscores Evolutionary Conservation of the Drosophila Hippo Pathway', *Cancer Research,* 68(8), pp. 2789-2794.

Zhang, L., Ren, F., Zhang, Q., Chen, Y., Wang, B. & Jiang, J. (2008). 'The TEAD/TEF family of transcription factor Scalloped mediates Hippo signaling in organ size control', *Dev Cell,* 14.

Zhang, N., Bai, H., David, K. K., Dong, J., Zheng, Y., Cai, J., Giovannini, M., Liu, P., Anders, R. A. & Pan, D. (2010). 'The Merlin/NF2 tumor suppressor functions through the YAP oncoprotein to regulate tissue homeostasis in mammals', *Dev Cell,* 19(1), pp. 27-38.

Zhang, Y., Gago-Lopez, N., Li, N., Zhang, Z., Alver, N., Liu, Y., Martinson, A. M., Mehri, A. & MacLellan, W. R. (2019). 'Single-cell imaging and transcriptomic analyses of endogenous cardiomyocyte dedifferentiation and cycling', *Cell Discov,* 5, p. 30.

Zhang, Y., Li, T. S., Lee, S. T., Wawrowsky, K. A., Cheng, K., Galang, G., Malliaras, K., Abraham, M. R., Wang, C. & Marbán, E. (2010). 'Dedifferentiation and proliferation of mammalian cardiomyocytes', *PLoS One,* 5(9), p. e12559.

Zhang, Y., Wang, Z. & Gemeinhart, R. A. (2013). 'Progress in microRNA delivery', *J Control Release,* 172(3), pp. 962-74.

Zhang, Y., Xu, G., Liu, G., Ye, Y., Zhang, C., Fan, C., Wang, H., Cai, H., Xiao, R., Huang, Z. & Luo, Q. (2016). 'miR-411-5p inhibits proliferation and metastasis of breast cancer cell via targeting GRB2', *Biochem Biophys Res Commun,* 476(4), pp. 607-613.

Zhao, B., Li, L., Lu, Q., Wang, L. H., Liu, C. Y., Lei, Q. & Guan, K. L. (2011). 'Angiomotin is a novel Hippo pathway component that inhibits YAP oncoprotein', *Genes Dev,* 25(1), pp. 51-63.

Zhao, B., Li, L., Tumaneng, K., Wang, C. Y. & Guan, K. L. (2010). 'A coordinated phosphorylation by Lats and CK1 regulates YAP stability through SCF(beta-TRCP)', *Genes Dev,* 24(1), pp. 72-85.

Zhao, B., Li, L., Wang, L., Wang, C.-Y., Yu, J. & Guan, K.-L. (2012). 'Cell detachment activates the Hippo pathway via cytoskeleton reorganization to induce anoikis', *Genes & development,* 26(1), pp. 54-68.

Zhao, B., Wei, X., Li, W., Udan, R. S., Yang, Q., Kim, J., Xie, J., Ikenoue, T., Yu, J., Li, L., Zheng, P., Ye, K., Chinnaiyan, A., Halder, G., Lai, Z.-C. & Guan, K.-L. (2007). 'Inactivation of YAP oncoprotein by the Hippo pathway is involved in cell contact inhibition and tissue growth control', *Genes & development,* 21(21), pp. 2747-2761.

Zhao, B., Ye, X., Yu, J., Li, L., Li, W., Li, S., Yu, J., Lin, J. D., Wang, C. Y., Chinnaiyan, A. M., Lai, Z. C. & Guan, K. L. (2008). 'TEAD mediates YAP-dependent gene induction and growth control', *Genes Dev,* 22(14), pp. 1962-71.

Zhao, J., Xu, J. & Zhang, R. (2018). 'MicroRNA-411 inhibits malignant biological behaviours of colorectal cancer cells by directly targeting PIK3R3', *Oncol Rep,* 39(2), pp. 633-642.

Zhao, L., Borikova, A. L., Ben-Yair, R., Guner-Ataman, B., MacRae, C. A., Lee, R. T., Burns, C. G. & Burns, C. E. (2014). 'Notch signaling regulates cardiomyocyte proliferation during zebrafish heart regeneration', *Proceedings of the National Academy of Sciences,* 111(4), pp. 1403-1408.

Zhao, Y., Ransom, J. F., Li, A., Vedantham, V., von Drehle, M., Muth, A. N., Tsuchihashi, T., McManus, M. T., Schwartz, R. J. & Srivastava, D. (2007). 'Dysregulation of cardiogenesis, cardiac conduction, and cell cycle in mice lacking miRNA-1-2', *Cell,* 129(2), pp. 303-17.

Zhao, Z., Qin, L. & Li, S. (2016). 'miR-411 contributes the cell proliferation of lung cancer by targeting FOXO1', *Tumour Biol,* 37(4), pp. 5551-60.

Zhou, J., Dong, X., Zhou, Q., Wang, H., Qian, Y., Tian, W., Ma, D. & Li, X. (2014). 'microRNA expression profiling of heart tissue during fetal development', *Int J Mol Med,* 33(5), pp. 1250-60.

Zhou, X., Wang, S., Wang, Z., Feng, X., Liu, P., Lv, X.-B., Li, F., Yu, F.-X., Sun, Y., Yuan, H., Zhu, H., Xiong, Y., Lei, Q.-Y. & Guan, K.-L. (2015). 'Estrogen regulates Hippo signaling via GPER in breast cancer', *The Journal of clinical investigation,* 125(5), pp. 2123-2135.

Zi, M., Maqsood, A., Prehar, S., Mohamed, T. M. A., Abou-Leisa, R., Robertson, A., Cartwright, E. J., Ray, S. G., Oh, S., Lim, D.-S., Neyses, L. & Oceandy, D. (2014). 'The mammalian Ste20-like kinase 2 (Mst2) modulates stress-induced cardiac hypertrophy', *The Journal of biological chemistry,* 289(35), pp. 24275-24288.